T.C.
IŞIK UNIVERSTIY
SCHOOL OF GRADUATE STUDIES

MASTER THESIS
DEPARTMENT OF CIVIL ENGINEERING PROGRAM
CIVIL ENGINEERING PROGRAM

Eren DURMAZ

A CASE STUDY OF INVESTIGATION OF THE LATERAL EARTH PRESSURE UNDER GROUP EFFECTS OF JET GROUT COLUMNS

SUPERVISOR
Asst. Prof. Dr. Ehsan ETMİNAN

İSTANBUL, September 2025

T.C.
IŞIK UNIVERSTIY
SCHOOL OF GRADUATE STUDIES

MASTER THESIS
DEPARTMENT OF CIVIL ENGINEERING PROGRAM
CIVIL ENGINEERING PROGRAM

Eren DURMAZ
(22CIVL5001)

A CASE STUDY OF INVESTIGATION OF THE LATERAL EARTH PRESSURE UNDER GROUP EFFECTS OF JET GROUT COLUMNS

SUPERVISOR
Asst. Prof. Dr. Ehsan ETMİNAN

İSTANBUL, September 2025

T.C.
IŞIK UNIVERSTIY
SCHOOL OF GRADUATE STUDIES

MASTER THESIS
DEPARTMENT OF CIVIL ENGINEERING PROGRAM
CIVIL ENGINEERING PROGRAM

Eren DURMAZ

(22CIVL5001)

A CASE STUDY OF INVESTIGATION OF THE LATERAL EARTH PRESSURE UNDER GROUP EFFECTS OF JET GROUT COLUMNS

Date of Thesis Defense: 16-09-2025

Thesis Supervisor :Asst. Prof. Dr. Ehsan ETMINAN / Işık University

Jury Members :Asst. Prof. Dr. Önder UMUT/ Işık University

:Asst. Prof. Dr. Kaveh DEHGHANIAN / Aydın University

İSTANBUL, September 2025

ABSTRACT

This thesis offers a detailed numerical case study on the impact of group effects from jet grout columns on lateral earth pressure behavior. Jet grouting, a sophisticated ground improvement technology, is extensively utilized to augment the strength and stability of poor soils. In seismically active nations like Türkiye, mitigating lateral earth stresses on retaining structures is essential for preserving structural integrity. A series of finite element calculations were performed in PLAXIS 2D to assess the lateral earth pressure distribution in a cohesive soil mass enhanced by clustered jet grout columns. To examine group effects, column spacing and layout were modified, while column length remained unchanged. The soil model was constructed using site-specific geotechnical data and simulated with suitable constitutive models to depict soft clay behavior.

The results demonstrate that diminishing column spacing markedly reduces the lateral earth pressures exerted on the diaphragm wall and enhances positive group interactions among the jet grout columns. Furthermore, an optimal column arrangement improves slope stability and diminishes structural requirements on the diaphragm wall. The study highlights the necessity of considering group interactions in the design of jet grout column systems, especially in seismically active areas, and provides practical guidance for geotechnical engineers involved in urban excavations and retaining structures subjected to seismic conditions.

Keywords: Jet grouting, Lateral Earth Pressure, Group Effect, PLAXIS Analysis, Ground Improvement

ÖZET

JET GROUT KOLONLARININ GRUP ETKİSİ ALTINDA YANAL TOPRAK BASINCININ İNCELENMESİNE YÖNELİK VAKA ÇALIŞMASI

Bu tez, sayısal bir vaka çalışması aracılığıyla jet grout kolonlarının grup etkilerinin yatay zemin basıncı davranışı üzerindeki davranışlarını kapsamlı biçimde incelemektedir. İleri bir zemin iyileştirme yöntemi olan jet grouting, zayıf zeminlerin dayanım ve stabilitesini artırmak amacıyla yaygın olarak kullanılmaktadır. Deprem tehlikesinin süreklilik gösterdiği Türkiye gibi sismik açıdan etkin ülkelerde, istinat yapılarına etki eden yatay zemin basınçlarının azaltılması, yapısal bütünlüğün korunması için kritik önemdedir. Bu kapsamda, grup hâlindeki jet grout kolonlarıyla iyileştirilmiş kohezyonlu bir zemin kütlesinde yatay zemin basıncı dağılımını değerlendirmek üzere PLAXIS 2D kullanılarak bir dizi sonlu eleman analizi gerçekleştirilmiştir. Grup etkisini irdelemek amacıyla kolon aralığı ve yerleşim düzeni değiştirilmiş; jet grout kolon uzunluğu ise sabit tutulmuştur. Zemin modeli, sahaya özgü geoteknik veriler kullanılarak oluşturulmuş ve yumuşak kil davranışını temsil eden uygun konstitutif malzeme modelleri ile simüle edilmiştir.

Bulgular, kolonlar arası aralığın azaltılmasının diyafram duvara etki eden yatay zemin basınçlarını belirgin biçimde düşürdüğünü ve jet grout kolonlarının grup etkisini artırdığını göstermektedir. Ayrıca, kolonların optimum bir konfigürasyonunun şev stabilitesini artırdığı ve diyafram duvar üzerindeki yapısal yükleri azalttığı gözlenmiştir. Bu çalışma, özellikle sismik açıdan etkin bölgelerde, jet grout kolon sistemlerinin tasarımında grup etkileşimlerinin dikkate alınmasının önemini vurgulamaktadır. Elde edilen sonuçlar, kentsel kazılar ve sismik koşullara maruz kalan istinat yapıları üzerinde çalışan geoteknik mühendislere anlamlı içgörüler sunmaktadır.

Anahtar Kelimeler: Jet Grout Uygulaması, Yanal Toprak Basıncı, Grup Etkisi, PLAXIS Analizi, Zemin İyileştirme

ACKNOWLEDGEMENTS

I would like to express my heartfelt gratitude to the faculty members of the Civil Engineering Department at Işık University, where I had the opportunity to gain valuable academic experience and knowledge throughout my master's education.

I am especially thankful to my thesis advisor, Assist. Prof. Ehsan Etminan, for his continuous guidance, support, and constructive feedback throughout every stage of this research. His expertise and encouragement were pivotal in shaping this study. I am deeply grateful to my family, whose constant support and belief in me have been a source of strength during this academic journey. I owe special thanks to my beloved wife,whose patience, love, and unwavering encouragement made even the most challenging moments more manageable and meaningful.Without the support of these wonderful individuals, this work would not have been possible.

Eren DURMAZ

TABLE OF CONTENTS

LIST OF FIGURES

LIST OF TABLE

LIST OF ABBREVIATIONS

$\boldsymbol{h_1}$: Thickness of the soft soil layer where negative skin friction may develop

$\boldsymbol{h_2}$: Depth of the competent bearing layer into which the columns are fully embedded

$\boldsymbol{A_{Jg}}$: Base area of the jet grout column

$\boldsymbol{A_f}$: area of the foundation.

$\boldsymbol{A_p}$: Cross-sectional area of the column (m²)

$\boldsymbol{D_f}$: Depth of footing embedment

$\boldsymbol{E_{JGC}}$ **:** Modulus of elasticity of the jet grout column (kN/m²)

$\boldsymbol{E_p}$: Modulus of elasticity of the column (kN/m²)

$\boldsymbol{FS_{overturning}}$: Factor of safety against overturning,

$\boldsymbol{K_0}$: Coefficient of lateral earth pressure at rest

$\boldsymbol{N_i}$: Vertical Component of The Slice Weight

$\boldsymbol{N_q}$: Bearing capacity factor

$\boldsymbol{P_{ul(grup)}}$: Bearing capacity of the jet grout column group

$\boldsymbol{P_{ul(column)}}$: Bearing capacity of a single jet grout column

$\boldsymbol{P_{ul(grup)}}$: Bearing capacity of the jet grout column group

$\boldsymbol{Q_{11(ort)}}$: Average lateral friction value at depth h_1

$\boldsymbol{Q_{12(ort)}}$: Average lateral friction value at depth h_2

$\boldsymbol{Q_b}$: Calculation of Tip (End-Bearing) Resistance

$\boldsymbol{Q_b}$: Unit tip bearing capacity at depth H

$\boldsymbol{Q_{group}}$: Total load-bearing capacity of the column group,

$\boldsymbol{Q_s}$: Skin Friction Resistance

$\boldsymbol{Q_{single}}$ = Load-bearing capacity of a single column,

$\boldsymbol{Q_{va}}$: Vertical load applied to the column (kN)

$\boldsymbol{\sum V}$ **:** Total vertical load at the base of the wall

$\boldsymbol{c'}$: Effective cohesion of the soil

$\boldsymbol{n_1, n_2}$ = Number of columns in each row and column, respectively,

s_0 : Settlement of the unimproved soil,

s_1 : Settlement of the soil improved with a group of columns.

D_{jg} : Diameter f the jet grout column

K_a Coulomb active earth pressure

K_s : Coefficient of lateral earth pressure

P_p : Total Passive Force

T_{f_i} : Shear Strength

c_u : Undrained shear strength of the soil

l_1 , l_2 : Upper and lower depth boundaries of the column (m)

z_0: Depth of the tension crack zone

γ' : Effective unit weight of the soil

σ_n : Average Normal Stress

σ'_{v0}: Effective vertical stress at the base of the column (kPa)

ΔL_i : Length of The Slice Base

Δ**h(e)** : Elastic shortening of the column (m)

$\sum Ac$ = Total cross-sectional area of all columns,

A : Cross-sectional area of the column (m^2)

AFAD : Disaster and Emergency Management Authority of Turkey

AGF : Artificial Ground Freezing

B : Width of the footing

BKS : Building usage class (TBEC-2018)

CBR : California Bearing Ratio

CJG : Column Jet Grout

CPT : Cone Penetration Testing

D : Diameter of each column,

DD-1 : Maximum expected earthquake ground motion

DD-2 : Standard design earthquake ground motion

DD-3 : Frequently expected earthquake ground motion

DD-4 : Service level earthquake ground motion

E : Elasticity Modulus

E_{50} : Static Elastic Modulus

E_{oed}: Oedometer modulus (for one-dimensional consolidation)

ERT : Electrical Resistivity Tomography

E_{ur} : Unloading-reloading modulus (for stress reversals)

FEM : Finite Element Method

FPP : Flexible PolyPropylene

G_0: Initial small-strain shear modulus (G_0)

GEI : Group Effect Index

H: Height of the wall

HDPE : High-Density Polyethylene

HS : Hardening Soil

MASW : Multichannel Analysis of Surface Waves

PA : Polyamide

PE : Polyethylene

PET : Polyester

PP : Polypropylene

PVC : Polyvinyl Chloride

PVD : Prefabricated Vertical Drains

RPM : Revolutions Per Minute

S : Center-to-center spacing between columns

SPT : Standart Penetration Testing

TAM : Tube-A-Manchette

TBDY-2018 : Turkish Building Earthquake Code

UCS : Unconfined Compressive Strength

UPV : Ultrasonic Pulse Velocity

V : Poisson's ratio

z: Depth (m)

α : Adhesion reduction factor

γ: Unit weight of the soil (kN/m³),

$\gamma sat, \gamma unsat$: Saturated and unsaturated unit weights

δ: Interface friction angle between soil and column surface

η : Number of columns in the group.

ξ: Shape factor

ϕ: Internal Friction Angle

Ψ : Dilatancy Angle

Ac : Cross-sectional area of a single jet grout column

B : Width of the block

D : Column diameter (m)

L : Length of the column (m)

St : Total elastic settlement of the jet grout column (m)

e : Eccentricity of the resultant load from the center of the footing

m : Number of columns in the vertical direction

n : Number of columns in the horizontal direction

Kp is the passive earth pressure

α : Adhesion factor between soil and column (dimensionless)

β : Backfill Surface

δ : Soil interface friction

σ : Stress acting on the column (kN/m^2)

γ : Unit weight of soil (kN/m^3)

CHAPTER 1

1. INTRODUCTION

Geotechnical engineering projects in urban environments frequently confront the challenges posed by weak or problematic soils, particularly in the design of excavations and retaining structures. As population density increases and development extends into geologically sensitive areas, ensuring the safety and stability of retaining systems becomes critically important. In this context, jet grouting is recognized as an effective ground-improvement technique that enhances soil strength, reduces permeability, and improves deformation characteristics.

Jet grouting involves the high-pressure injection of grout into the ground to form rigid columns that improve the mechanical properties of the treated soil. Depending on design requirements, columns may be installed individually or in groups. Although the behavior of single jet-grout columns has been extensively investigated in the literature, interactions among grouped columns—particularly under lateral loading—remain insufficiently understood. In practice, however, columns are often arranged in rows or grid patterns, and these interactions can markedly influence lateral earth-pressure distributions and the overall performance of retaining systems.

Turkey lies within one of the world's most seismically active belts, and its history of destructive earthquakes underscores the need for robust geotechnical design. In seismic regions, lateral earth pressure imposes significant demands on retaining structures, especially during earthquakes. Accordingly, understanding the role of the group effect of jet-grout columns on lateral earth pressure is vital for enhancing the resilience and safety of earth-retaining systems.

This thesis investigates, through numerical modeling, the influence of the group effect of jet-grout columns on lateral earth-pressure behavior. Parametric analyses conducted in PLAXIS 2D are employed to examine, in soft cohesive

soils, how variations in column spacing (intercolumn clear spacing) and layout configuration affect lateral earth-pressure distributions. Column length is treated as a fixed parameter in all analyses. The objective is to deepen understanding of group interactions in jet-grouting systems and to provide practical recommendations for geotechnical design under static and potential seismic conditions.

In sum, this study advances knowledge on the application of jet grouting in retaining structures, particularly in seismically active regions. The findings are expected to contribute to the development of safer, more economical, and technically robust ground-improvement solutions for future engineering projects.

1.1 RESEARCH PROBLEM AND RESEARCH QUESTION

In geotechnical engineering, the design of retaining structures is profoundly affected by the intensity and distribution of lateral soil pressure exerted on them. While several theoretical models for assessing lateral pressure are available, they often presume homogenous, unreinforced soils and inadequately include the impacts of soil enhancement techniques like jet grouting. Clustered jet grout columns provide a reinforced soil matrix that modifies the stress distribution in the surrounding soil. Nonetheless, the aggregate or 'collective' impact of these columns, especially concerning their interaction and effect on lateral earth pressure, is inadequately comprehended in both theoretical and practical domains.

In seismically active nations like Turkey, where earthquakes are notably intense, the inadequate comprehension of the behavior of clustered jet grout columns results in ambiguity in geotechnical design approaches. Due to the absence of a conclusive evaluation on the influence of column spacing, length, and configuration on lateral pressure, engineers may either excessively build retaining structures, resulting in superfluous expenses, or inadequately design them, posing safety hazards.

This thesis investigates the inadequate comprehension of how the arrangement of jet grout columns in a group effect influences lateral earth pressure in cohesive soils.

This investigation was executed under the auspices of the subsequent basic scientific inquiry:

What is the impact of the arrangement of jet grout columns on lateral earth pressure due to group effects, and what are the consequences for geotechnical design in seismic zones?

This study seeks to furnish essential information on the design optimization of jet grout systems, specifically for retaining structures subjected to substantial lateral loads.

1.2 OBJECTIVES AND CONTRIBUTIONS OF THE STUDY

The primary objective of this study is to investigate how the layout of jet-grout columns (i.e., column spacing and arrangement) affects the magnitude and distribution of lateral earth pressure in soft cohesive soils. The study seeks to elucidate the group-interaction mechanisms that emerge when multiple columns are installed in close proximity and to assess how these interactions are reflected in the performance of retaining structures, particularly in environments where seismic effects are pronounced, such as Turkey. The investigation is grounded in PLAXIS 2D numerical modeling; column length is held constant across all analyses, whereas column spacing and layout configuration are treated as variables.

Accordingly, the study:

(i) conducts a comprehensive literature review on theories of lateral earth pressure and on the use of jet grouting in ground improvement;

(ii) develops numerical models in PLAXIS 2D that represent column groups within cohesive soil profiles;

(iii) varies column spacing and layout configuration—with column length fixed to examine, parametrically, their influence on lateral earth-pressure response;

(iv) quantifies the group effect and stress redistribution, and derives design-oriented inferences for retaining structures;

(v) evaluates the lateral pressures of jet-grout columns subject to group effects.

The anticipated contributions are as follows:

(i) provides a quantitative characterization of the group effect of jet-grout columns on the dynamics of lateral earth pressure in soft cohesive soils;

(ii) offers design-oriented recommendations for optimizing column spacing and layout to reduce lateral demands on retaining structures;

(iii) integrates theoretical background, numerical modeling, and application-oriented analyses to bridge a significant gap in the literature;

(iv) serves as a reference for engineers and researchers seeking to enhance the performance and safety of jet-grout systems in contemporary geotechnical design.

1.3 METHODOLOGY

This thesis investigates the contribution of jet-grout columns to lateral stability under group effects by means of field-supported numerical modeling. Geotechnical parameters were first established through boreholes, laboratory tests, MASW, and pressuremeter measurements, and the as-built jet-grout geometry (column diameter, length, and layout) was transferred directly into the model. Numerical analyses were performed in PLAXIS 2D using the Mohr–Coulomb constitutive model; suitable boundary conditions were defined and local mesh refinement was applied around the columns to enhance solution accuracy. Columns were activated via staged construction, and to isolate group effects a series of scenarios was created by varying column spacing (0.75–1.00–1.50 m), diameter, and group arrangements. For each scenario, outputs for the

jet-grouted zones included horizontal stress, bending moment, shear force, and vertical displacement/settlement; to capture soil–structure interaction, the horizontal displacement of the retaining wall was also assessed. All responses were compared before and after excavation, synthesized both graphically and numerically, and interpreted against the relevant literature to derive design-oriented implications.

CHAPTER 2

2. LITERATURE REVIEW

This chapter elucidates the necessity of ground improvement and the situations in which it is relevant; delineates the aims of improvement, examines the primary criteria affecting technique selection, and categorizes the key ways based on existing research. The theoretical underpinnings and engineering concepts of techniques for altering soil behavior are delineated; the principles of implementation, key design issues, and methodologies for performance evaluation, quality assurance, and verification are succinctly assessed. This chapter seeks to establish a logical framework for method selection by critically examining the assumptions and limits of various techniques, tailored to diverse ground conditions, desired performance levels, and site constraints. This extensive framework prepares for Chapter 3, which thoroughly examines the jet-grouting method, including its historical evolution, areas of application, suitability for various soil types, benefits and drawbacks, technical variations, equipment, operational parameters, injection techniques, field and laboratory controls, and previous research.

2.1 GROUND IMPROVEMENT

With increasing population growth and rapid urbanization, the number and scale of infrastructure projects in metropolitan areas have significantly expanded. As a result, one of the most critical aspects of modern construction practice has become the improvement of weak and unconsolidated soils. In areas where the soil has not undergone sufficient consolidation or possesses poor mechanical properties, ground improvement is not optional but a necessity to ensure structural safety and serviceability. To render such soils suitable for

construction, various ground modification techniques have been developed and applied in engineering practice.

Advancements in soil mechanics have allowed engineers to better understand geotechnical problems and predict complex soil behavior under loading, leading to the development of a wide range of ground improvement methods. These techniques play an essential role in civil engineering projects, particularly in enhancing ground stability and providing support for structures ranging from shallow foundations to deep excavation systems. From stabilizing loose soils for construction purposes to mitigating the effects of soil liquefaction during seismic events, ground improvement methods are indispensable for ensuring the safety, durability, and functionality of modern infrastructure systems.

2.1.1 Objectives Of Ground Improvement Techniques

The primary objective of ground improvement techniques is to increase the bearing capacity of the soil by enhancing its stiffness, thereby reducing seismic hazards and mitigating the risk of liquefaction. In addition, such methods are known to reduce settlement values, particularly in structures located on high-risk soils. The choice of improvement method varies depending on the soil profile and the characteristics of the structure to be constructed (Kramer, 1996).

The main objectives targeted in ground improvement can be summarized as follows (Sağlamer, 2006).

- To increase the bearing capacity of the soil,
- To reduce settlements under loading and accelerate consolidation,
- To minimize soil deformations and mitigate the risk of liquefaction,
- To reduce swelling and shrinkage potential,
- To decrease soil permeability,
- To reduce compressibility,
- To prevent corrosion and erosion,
- To facilitate soil drainage.

Ground improvement methods are particularly necessary in cases where the soil is determined to be incapable of providing adequate strength under the static loads of structures. The primary objective of these methods is either to reduce the void ratio of the soil using mechanical equipment or to fill the voids with chemical admixtures such as cement, lime, or bentonite (Mitchell, 1976).

2.2 GROUND CONDITIONS THAT REQUIRE IMPROVEMENT

With the proliferation of construction projects and newly urbanized regions, locating naturally appropriate ground conditions is becoming progressively challenging. As a result, construction on sites with inadequate soil properties has become unavoidable, resulting in numerous geotechnical issues such as inadequate bearing capacity, excessive settlement, elevated groundwater levels, and an increased risk of liquefaction based on soil characteristics. In poor or problematic ground conditions, it is imperative to do comprehensive geotechnical investigations and use suitable ground improvement techniques to limit hazards and assure structural safety.

Soils with high liquefaction potential are listed below (Özdemir & Mehmet, 2006):

- Peaty and marshy soils
- Soft clays,
- Loose sands,
- Thick alluvial deposits with high groundwater levels.

The degradation of organic plant materials in peat and marshy soils, along with their incorporation into the soil matrix, can significantly affect the engineering qualities of the ground. These soil types typically exhibit minimal bearing capacity and are deemed unsuitable for use as foundation soils. Nonetheless, when construction on such soils is imperative, ground enhancement is crucial to guarantee stability and efficacy. The circumstances in soft clays remain mostly unchanged. These soils demonstrate significant compressibility and experience substantial deformations even under minimal

loads. Consequently, while constructing a foundation on soft clay, the implementation of suitable ground improvement measures is essential.

Loose sands and dense soft alluvial deposits with elevated groundwater levels may support modest loads, with deformation remaining within acceptable limits. Nevertheless, when exposed to cyclic or repeated loading over time, they are susceptible to strength deterioration, leading to diminished bearing capacity and severe deformations.

When confronted with subsoils that exhibit inadequate bearing capacity, several engineering options are available: abandoning the site in question and opting for a more appropriate location, designing deep foundations to convey loads to more competent soil strata, excavating and substituting the weak soil with a more stable material under regulated conditions, or most frequently-employing ground improvement techniques to augment the strength and stiffness of the existing soil.

2.3 FACTORS INFLUENCING THE SELECTIONS OF GROUND IMPROVEMENT TECHNIQUES

- Soil profile and properties (percentage of fines, consistency, normally consolidated/overconsolidated, etc.)
- Groundwater conditions
- Required area and depth for improvement
- Environmental factors
- Interaction with existing structures
- Construction-related factors (work schedule, accessibility, materials, constraints related to working in subsurface conditions)

2.4 CLASSIFICATION OF GROUND IMPROVEMENT TECHNIQUES

According to the Method of Application;

- Temporary improvement methods applied only during the construction phase
- Permanent improvement methods applied without adding materials to the soil
- Improvement methods involving the addition of various materials to the soil

ACCORDING TO THE DEPTH OF APLICATION

- Deep improvement methods
- Shallow (surface) improvement methods

2.5 GROUND IMPROVEMENT METHODS

The generally accepted ground improvement techniques applied in geotechnical engineering to improve the mechanical and physical characteristics of weak or problematic soils are given a summary in this part. These techniques are meant to raise bearing capacity, lower settlement, lower risk of liquefaction, and strengthen general ground stability. Various methods can be used separately or in concert depending on the type of soil, project needs, and environmental restrictions. The basic ideas, mechanics, and general application areas of the most frequently used ground improvement methods in modern engineering practice are introduced in the next subsections.

2.5.1 Vibroflotation

Vibroflotation, or vibro-compaction, is a prevalent and essential ground enhancement method in civil engineering. The process entails the utilization of high-frequency vibrations transmitted to the ground via a vibrating probe or plate, also known as a vibroflot. The vibrations induce the reconfiguration of soil particles, resulting in heightened soil density and improved bearing ability. This method is especially efficient in granular soils, where particle interlocking and frictional resistance can be markedly enhanced.

Vibroflotation has been effectively utilized in several construction endeavors, including foundational works for edifices, bridges, and roadways. It is employed in extensive reclamation initiatives, including sanitary landfills and port facilities, where ground stability is essential. The approach enhances the compaction properties of loose soils, hence regulating settlement and alleviating geotechnical hazards linked to suboptimal ground conditions. Bell, F.G. (1993).

Vibro-compaction is a meticulously designed process intended to alter the mechanical properties of granular soils. Vibratory probes fitted with eccentric weights enter the soil to specified depths and emit regulated vibrations during their systematic retraction. This dynamic contact triggers a sequence of particle rearrangements and compaction processes, leading to the densification of the soil matrix and a significant enhancement of its load-bearing capacity. This method's precision and versatility enable engineers to customize the application to particular ground conditions and project specifications, guaranteeing excellent results.

In vibroflotation, a torpedo-shaped probe, suspended by a crane, is employed to compact the soil column. These vibroflots often possess weights between 14 and 40 kN, diameters from 30 to 46 cm, and lengths approximately ranging from 3.0 to 4.9 meters. The probe features an eccentrically positioned weight powered by either electric or hydraulic means via a central shaft. Figure 2.1 The settlement caused by vibration generally ranges from 5% to 15% of the thickness of the treated soil layer. The arrangement of compaction points typically follows an equilateral triangle configuration, with center-to-center distances varying from 2.5 to 5.0 meters (Kirsch, K., & Bell, A. 2017).

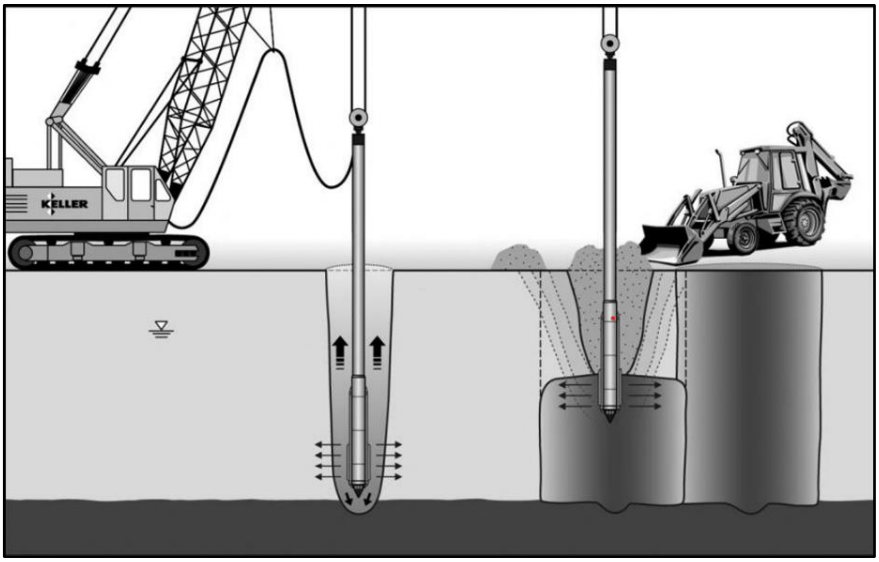

Figure 2.1 Vibro compaction method operating phases (Courtesy of Keller Group)

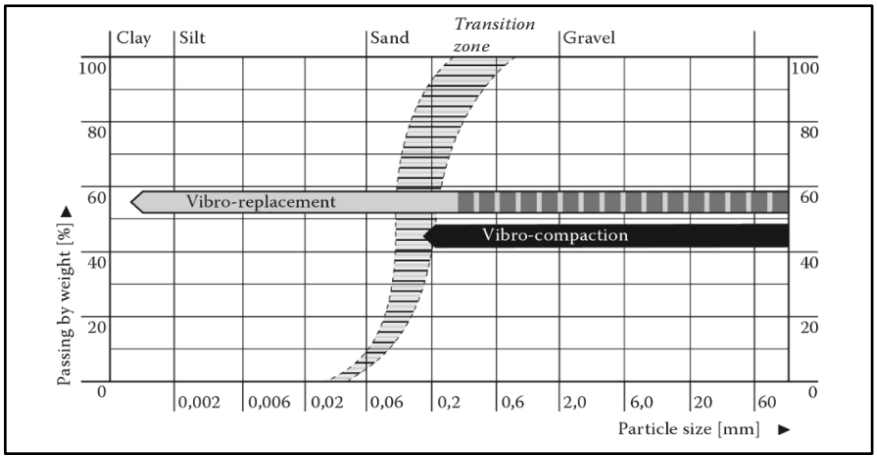

Figure 2.2 Range of soil types treatable by vibro compaction and vibro replacement (Wehr ve Sondermann, 2013)

Figure 2.2 depicts the range of grain size distribution suitable for vibro-compaction and vibro-replacement techniques. The horizontal axis indicates particle size in millimeters, spanning from clay-sized particles (<0.002 mm) to gravel-sized particles (>2 mm), and the vertical axis denotes the percentage

passing by weight. The illustration distinctly differentiates the appropriate soil conditions for each technique. Vibro-compaction is demonstrated to be successful in clean, coarse-grained soils, generally consisting of sands and gravels with negligible fines content. Conversely, vibro-replacement, or stone columns, is suitable for soils with elevated fines content, such as silty or weakly cohesive soils, where direct compaction is impractical. The transition zone signifies soil gradations where the efficacy of each method may fluctuate based on in-situ variables and vibration energy input. This classification assists engineers in choosing the suitable approach according to particle size distribution and soil behavior traits.

The benefits of vibro-compaction are notably considerable in civil engineering applications, beyond its mechanical complexities. Vibro-compaction boosts soil density and strength, hence reducing settlement, mitigating foundation instability risks, and improving the structural integrity of essential infrastructure elements. Its cost-effectiveness and operational efficiency provide a viable alternative to traditional ground improvement techniques, facilitating the optimization of project timelines and minimizing resource costs.

However, the successful implementation of vibro-compaction relies on a nuanced understanding of its complexities and associated considerations. Factors such as vibration frequency, energy output, and soil properties must be carefully evaluated and calibrated to optimize process efficiency and minimize potential risks. Additionally, environmental and regulatory considerations emphasize the need for a comprehensive approach to project planning and execution ensuring compliance with established standards and protocols while safeguarding environmental integrity.

The study conducted by Randolph and Hope (2004) provides valuable insight into the effectiveness of vibroflotation in ground improvement projects. Their research focused on the performance of vibroflotation in enhancing the bearing capacity of loose sand deposits. Through a series of field trials, they observed significant increases in relative density and improvements in load-

bearing characteristics of the soil following the vibroflotation process. The study highlights the effectiveness of vibroflotation as a ground improvement technique, particularly in loose or sandy soils.

The advantages of vibroflotation include enhanced bearing capacity, improved settlement control, and cost-effectiveness. By densifying loose or granular soils, vibroflotation significantly increases their load-bearing capacity, allowing for the construction of heavier structures without the need for expensive foundation reinforcements (Randolph & Hope, 2004). It also reduces the potential for settlement, thereby contributing to the long-term stability of structures built on treated ground. In addition, vibroflotation has been shown to mitigate liquefaction potential in saturated sands and to effectively control settlement under seismic loading conditions (De la Guardia et al., 2019). Owing to its relatively fast installation and minimal disruption to surrounding areas, vibroflotation offers a cost-effective solution, particularly for large-scale ground improvement projects.

Vibroflotation is very successful in granular soils with minimal clay concentration, but its efficacy may be constrained in cohesive soils like clays. In such soils, attaining substantial densification can be difficult and may necessitate additional procedures or alternate ground enhancement techniques. Furthermore, environmental considerations are imperative, as vibroflotation may produce noise and vibrations that could impact adjacent structures or delicate environments. The disposal of surplus materials, such as granular backfill utilized to fill voids generated during the process, may potentially pose environmental concerns if not managed appropriately. Vibroflotation necessitates a site-specific and meticulously calibrated design methodology. Soil type, groundwater conditions, and project specifications must be meticulously assessed to ascertain the appropriate treatment parameters. Additionally, synchronizing vibroflotation with other construction operations and existing subterranean utilities may present logistical difficulties necessitating meticulous preparation.

2.5.2 Dynamic Compaction

Dynamic compaction is a soil enhancement method frequently employed to augment the density and strength of soil strata, especially in anticipation of construction endeavors. It entails the regulated release of substantial weights onto the ground surface to produce high-energy shock waves that disseminate through the soil mass. These waves induce a reconfiguration of soil particles, resulting in a decreased void ratio and an enhancement in both density and load-bearing capability. Dynamic compaction is generally utilized for granular soils, including sand, gravel, or sandy gravel, where particle interlocking is little and natural compaction is inadequate. Upon exposure to repeated high-energy impacts from dynamic compaction, these loose soils demonstrate considerable enhancements in strength and stiffness, rendering them appropriate for structural foundations and infrastructure projects.

Nonetheless, the approach is typically inappropriate for cohesive soils like clays or silts, as these materials exhibit distinct responses to dynamic loading and frequently fail to attain the intended densification. In these instances, alternate techniques like soil mixing or preloading with vertical drains are frequently more efficacious. Mostafa (2010) highlights that numerical modeling of dynamic compaction in fine-grained soils exhibits minimal enhancement owing to the creation of excess pore pressure and low permeability. Alnaim et al. (2022) provided a decision-making framework utilizing CPT data, indicating that dynamic compaction is most efficacious in coarse-grained, non-cohesive soils and necessitates thorough evaluation prior to application in mixed or fine-grained profiles.

This technique was initially identified and refined in the early 20th century by French engineer Professor Louis Ménard (Ménard & Broise, 1975). Ménard also innovated the creation of exceptionally massive tampers (weighing up to 200 metric tons) and the utilization of enormous cranes and tripod towers capable of releasing these weights from heights of up to 40 meters. His

innovation was motivated by the natural occurrence of soil densification seen at meteorite impact sites, which he aimed to duplicate for engineering applications.

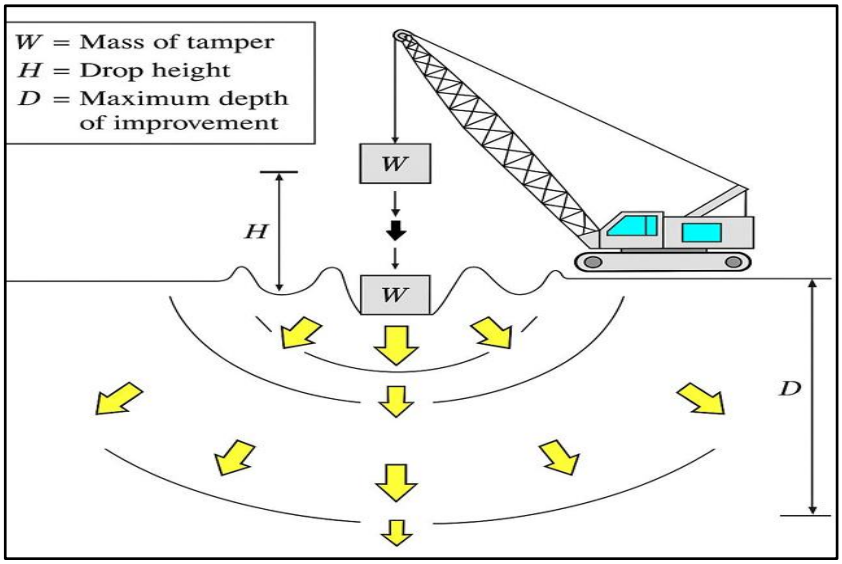

Figure 2.3 Schematic illustration of the dynamic compaction process.

Dynamic compaction commences with a site assessment to evaluate soil characteristics, encompassing soil type, moisture content, and compaction specifications. Based on this assessment, suitable equipment, often steel drop weights or steel ballast, is chosen according to the required compaction energy and treatment depth. The region designated for compaction is organized into an ordered structure, with drop locations and sequences meticulously arranged to guarantee consistent energy distribution throughout the area. Weights are elevated to a specified height using cranes or hydraulic systems and thereafter released to descend freely onto the ground surface. This procedure is methodically reiterated across the site until the desired compaction level is attained. The process is depicted in Figure 2.3.

Dynamic compaction offers several advantages, including cost-effectiveness compared to alternative ground improvement methods such as deep soil mixing or stone columns, rapid implementation suitable for projects

with tight construction schedules, and significant enhancement of soil strength and stability, making it suitable for supporting heavy structures.

However, dynamic compaction also has certain limitations, including restricted improvement depth particularly in areas with existing structures or underground utilities along with the generation of significant noise and ground vibrations that may be problematic in densely populated or sensitive areas, and the potential risk of damage to nearby structures due to the impact of heavy falling weights.

2.5.3 Controlled Blasting

Blasting for ground enhancement is a method employed to augment the engineering characteristics of particular soil types using controlled explosive detonations. This technique is frequently utilized for granular soils like sands or gravels, where conventional compaction methods may be inadequate. The explosion produces shock waves that cause particle reconfiguration and densification, thus enhancing the soil's load-bearing ability. Although blasting is successful in dry soils, its efficacy is frequently constrained in partially saturated soils due to capillary tension and the existence of gas bubbles, which can attenuate the explosion's energy. This approach is predominantly utilized in thoroughly saturated soils, where it can yield substantial enhancements in density and stiffness. Kramer (1996) asserts that blasting is most efficacious in loose sandy soils with less than 20% silt and under 5% clay content.

Blasting for ground improvement offers several advantages, including rapid soil densification within a short time frame, cost-effectiveness for large-scale projects, and high efficiency in granular soils where traditional compaction methods may be less effective; however, it also presents certain drawbacks such as environmental impacts related to noise, vibration, and air pollution, inherent safety risks associated with the use of explosives requiring strict regulatory compliance, and limited applicability in certain soil types and site conditions.

2.5.4 Drainage Of Water In Soil Improvement

In conditions where the groundwater table is high and the moisture content of the soil negatively affects its engineering properties, the removal of excess water from the ground through channels, trenches, or pumps is referred to as drainage (Şengezer, 2010). In addition to facilitating the removal of water, drainage plays a crucial role in reducing pore water pressure, enhancing the shear strength of the soil, accelerating consolidation settlements, and ultimately improving overall ground stability.

Surface drainage pertains to the regulation of water movement across the terrain to avert water accumulation and to ensure the secure evacuation of runoff from a location. The method includes the design and execution of surface channels, lateral ditches, header ditches, culverts, and grading systems to redirect surface water from structures, landscapes, and other water-sensitive zones. Alongside structural systems, pragmatic techniques like sealing surface fissures and covering slope faces are utilized. Surface drainage mitigates erosion, flooding, and soil saturation by regulating surface water movement, therefore enhancing the stability and functionality of the surrounding environment and soil conditions.

2.5.4.1 Subsurface Drainage

Subsurface water presents a considerable risk to slope stability, foundation bearing capacity, and the general deformation characteristics of soil masses. Subsurface drainage seeks to avert soil saturation to critical thresholds or to mitigate current saturation issues by lowering pore water pressures inside the soil. Efficient subsurface drainage augments soil shear strength and elevates overall geotechnical performance. Engineers systematically regulate groundwater flow to safeguard slope integrity, provide foundation stability, and reduce detrimental deformations in the constructed environment. Common subsurface drainage methods encompass vertical drains, horizontal drains, gravel trenches, geosynthetic drains, and piping systems.

2.5.4.2 Preloading

Preloading is frequently utilized as an efficient remedy when the bearing capacity of saturated cohesive soils is markedly diminished, particularly in soft clay layers that demonstrate poor shear strength and substantial consolidation settlements due to low permeability. This method entails the provisional imposition of a surcharge load on the ground surface to expedite consolidation and reduce post-construction settlement. Subsurface drainage systems are essential in dissipating excess pore water pressure and expediting consolidation. Efficient groundwater management improves the efficacy of the preloading technique, resulting in superior soil stabilization and minimizing settlement hazards in clay soils. Preloading functions as a preemptive strategy, especially in regions with highly compressible soils, facilitating the majority of settlement prior to construction, thereby guaranteeing both short- and long-term structural stability. Materials like aggregate, sand, or coarse fill are typically employed as surcharge loads, deliberately positioned for facile removal post-treatment. Preloading induces volumetric contraction in cohesionless soils, while facilitating pore water outflow and reducing void ratio in high-moisture cohesive soils. The effects of preloading include improved stability of reinforced concrete structures, enhanced soil compaction, and increased bearing capacity, consequently increasing the overall performance and durability of construction projects.

This approach is widely supported in the literature, as studies have shown that preloading combined with vertical drains can significantly accelerate consolidation, reduce post-construction settlement, and improve the strength characteristics of soft clayey soils, particularly in fully saturated conditions (Indraratna, Balasubramaniam, & Khan, 1994).

2.5.4.3 Vacum Preloading

Vacuum preloading is a ground enhancement technology categorized as a surcharge preloading approach. It is very efficacious for the remediation of soft,

fine-grained soils. The main aim of this procedure is to expedite soil consolidation by diminishing pore water pressure inside a confined soil mass, thus enhancing effective stress without modifying total stress. In contrast to traditional surcharge techniques, vacuum preloading presents a more cost-effective and efficient solution, particularly in regions where the imposition of substantial fill loads is unfeasible or financially burdensome.

The vacuum preloading system comprises three primary components: a surface sealing system, a drainage network, and a vacuum pumping mechanism. This configuration employs vacuum pressure on the soil mass via vertical and horizontal drains, facilitating the dissipation of surplus pore water pressure. Consequently, the effective stress inside the soil progressively escalates. A sand blanket is frequently employed on the surface to function as a drainage layer and to disseminate the vacuum pressure from the horizontal collecting pipes to the vertical drains. This technique is frequently employed alongside prefabricated vertical drains (PVDs) or sand drains, which accelerate the drainage process and guarantee consistent pressure distribution inside the soil mass. The principle of operation is shown in Figure 2.4.

Prefabricated vertical drains are particularly advantageous in vacuum preloading systems as they enhance installation speed and improve cost-efficiency. Additionally, the drains function as a barrier against air intrusion, maintaining the vacuum seal within the soil mass. The combination of controlled vacuum pressure and an effective drainage network allows for rapid consolidation, reduction of long-term settlements, and improved soil strength within a significantly shorter time frame compared to traditional preloading methods.

2.5.4.4 Drains

Employing good drainage techniques is crucial for diminishing pore water pressure and improving soil characteristics, especially in fine-grained soils where elevated water content can undermine strength and load-bearing capacity. Implementing a strong drainage system on-site is essential to reduce water

infiltration and preserve ideal ground conditions. Deep drainage systems and the methodical extraction of surplus water from the site are crucial in attaining this objective. Additionally, for structures erected on low-permeability soils, the installation of drainage systems during both construction and post-construction phases is essential to avert consolidation-related settlements and reduce potential loss in bearing capacity. Vertical drains, sand drains, and prefabricated drainage systems have proven to be beneficial in promoting efficient water discharge, expediting consolidation settlement rates, and guaranteeing the long-term stability and performance of construction projects.

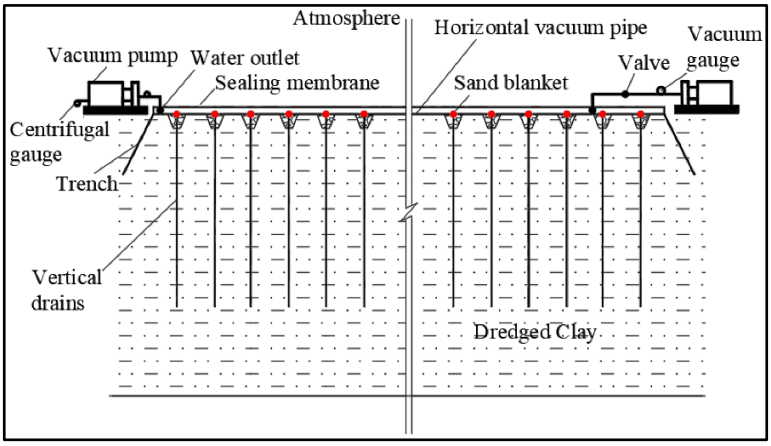

Figure 2.4 Vacuum Preloading System

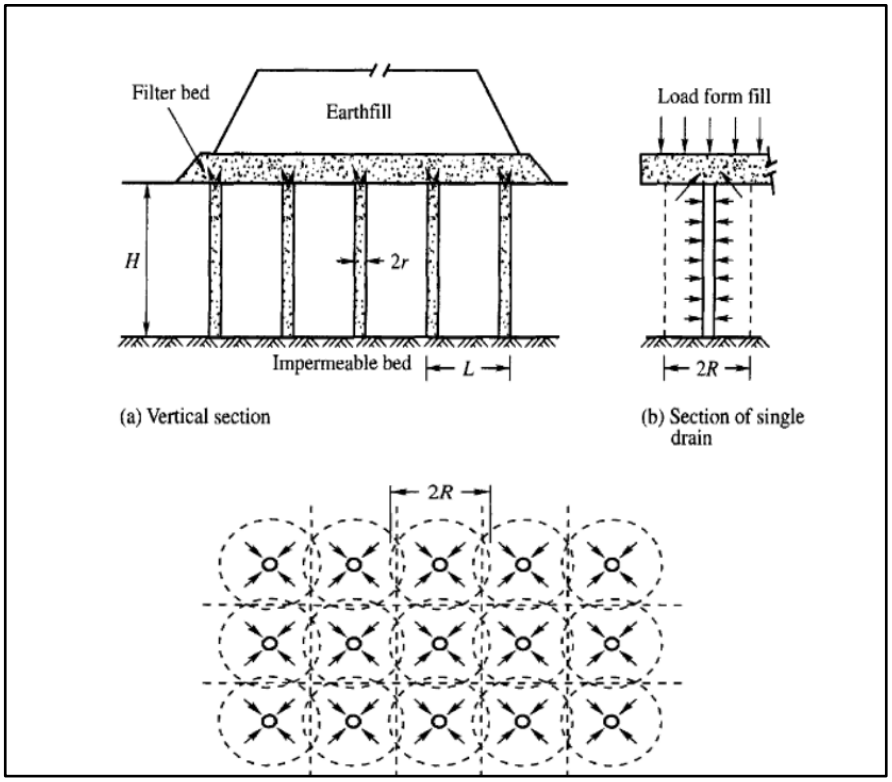

Figure 2.5 Consolidation of Soil Using Sand Drains (V.N.S. Murthy)

2.5.4.4.i Prefabricated Vertical Drains

Vertical drains are extensively employed as a ground enhancement technique to expedite consolidation, alleviate the impacts of surcharge loading, enhance settlement rates, diminish preloading duration, shorten drainage pathways, and promote the swift dissipation of surplus pore water pressures. Although conventional sand drains have been utilized historically, prefabricated vertical drains (PVDs), including plastic strip drains, have surfaced in the last thirty years as viable alternatives. Nonetheless, caution is essential during their production and installation to prevent disruption, which may diminish their permeability and drainage efficacy.

In practical applications, preloading is generally executed prior to construction by imposing a temporary surcharge load, typically consisting of sand or gravel fill, that is equal to or exceeds the anticipated structural load. This

surcharge exerts pressure on the underlying soil, facilitating the formation of the clay strata. Upon achieving the desired settlement or level of consolidation, the temporary fill is eliminated before structural building commences. The preconsolidation of soft clays mitigates long-term settlements and enhances foundation performance. In this preloading phase, vertical drains function as pathways for the dissipation of excess pore pressures from the soil's voids, directing water horizontally towards the drains and vertically to the ground surface.

Nonetheless, complications such as smear zones resulting from disturbances or deformation of drain walls during installation can considerably diminish the drain's permeability. In highly compressible soils, installation-induced lateral displacement and shear deformation surrounding the drain may result.

According to Yee and Aun (2010), the installation of horizontal drainage systems over an area of 100,000 m^2 results in an average emission of approximately 13.6 kg of CO_2 per square meter into the environment.in a decrease in both the soil's permeability and undrained shear strength.

2.5.4.4.ii Sand Drains

Sand drains are a traditional ground enhancement technique employed to expedite the consolidation of saturated, low-permeability cohesive soils, especially soft clays. The method entails the insertion of vertical columns loaded with well-graded sand into the soil to function as artificial drainage conduits. Vertical drains are generally created by drilling into the soil with a mandrel or auger, subsequently backfilling the boreholes with sand, and ultimately providing a surcharge load to facilitate consolidation. The arrangement of sand drains typically follows a systematic grid design to guarantee consistent settlement and efficient dissipation of pore water pressure (Mesri et al., 1997).

Sand drains have been extensively utilized since the 1930s and constitute one of the earliest methods of vertical drainage. Nonetheless, limitations in equipment and material placement control have led to a drop in their popularity

following the advent of prefabricated vertical drains (PVDs), which provide enhanced installation efficiency and quality assurance. Nonetheless, sand drains are effective for projects necessitating high permeability drainage materials and are especially appropriate in regions where geosynthetic materials may be inaccessible or prohibitively expensive (Bo, 2011).

The principal purpose of sand drains is to reduce the drainage distance and so expedite the process of primary consolidation. The rapid relief of extra pore water pressure enhances soil shear strength, accelerates settlement, and diminishes the likelihood of post-construction deformation. This procedure markedly improves the load-bearing capability of foundation soils, rendering them appropriate for sustaining infrastructure including embankments, storage tanks, and highways. Mitchell and Soga (2005) assert that sand drains can diminish the consolidation duration by 50–70% relative to natural vertical drainage alone.

Correct installation is essential for the efficacy of sand drains. Soil disturbance, smearing effects from drilling, and irregular backfilling can reduce the effectiveness of drains by decreasing permeability and increasing resistance to water flow. Hird et al. (1992) emphasized the necessity of carefully selecting installation methods to minimize shear-induced smearing of clay walls, as such effects may hinder the consolidation process.

2.5.4.4.iii Prefabricated Vertical Drains

Prefabricated Vertical Drains (PVDs), sometimes referred to as plastic drains or wick drains, have predominantly supplanted conventional sand drains owing to their straightforward installation, reliable performance, and efficacy in expediting the consolidation of saturated fine-grained soils. These drains often consist of a plastic core encased in a geotextile filter, facilitating water passage but obstructing soil particle infiltration. PVDs provide an effective remedy for ground enhancement, especially in soft clayey soils characterized by limited permeability, where pore water cannot rapidly disperse under natural circumstances (Indraratna et al., 2005).

The drains are installed utilizing a mandrel, a steel installation rod affixed to specialized apparatus that drives the drain vertically into the soil. The installation procedure is swift; depths of up to 20 meters can be attained in roughly three minutes. The distance between the drains is often established at 1.5 to 2.5 meters, contingent upon the necessary consolidation rate and soil properties. The typical cross-sectional dimensions of PVDs are roughly 100 mm by 4 mm, and they can be deployed to depths of up to 65 meters (Bergado et al., 1991). PVDs expedite the consolidation process, diminish post-construction settling, and improve structural stability by minimizing the drainage path and promoting the radial flow of pore water.

Notwithstanding their benefits, the efficacy of PVDs may be compromised by installation-induced smear zones, which diminish the permeability of adjacent soil and obstruct drainage. Hansbo (1987) asserts that precise regulation of mandrel dimensions and penetration methods is crucial to reduce shear-induced smearing and enhance drain efficacy. Moreover, project-specific criteria, including intended settlement period and the depth of soft strata, must be taken into account while establishing the spacing and configuration of the drains (Indraratna et al., 2005). The incorporation of PVDs in ground improvement initiatives not only diminishes construction duration but also enhances soil performance under load, especially when utilized alongside preloading methods.

2.5.4.5 Electro-Osmosis

Conventional preloading and vacuum preloading techniques are frequently employed for the enhancement of soft fine-grained soils, including silts and silty clays. Nonetheless, the exceedingly low permeability of clayey soils renders these procedures time-consuming and may still lead to considerable post-treatment settling. Conversely, electro-osmosis has proven to be an efficient technique for reinforcing saturated cohesive soils and improving drainage. Moreover, electro-osmosis has been utilized in mineral processing and filtration systems (Estabragh et al., 2015).

Applying a direct electric potential across a saturated clay mass from anode to cathode initiates electro-osmotic flow, resulting in the migration of water through the soil. In this electric field, cations advance toward the cathode, accompanied by water molecules, whereas anions proceed toward the anode. In practical configurations like square or hexagonal electrode patterns, point wells or analogous drains function as cathodes, whereas inserted metal rods serve as anodes. This promotes water flow towards the cathode, improving drainage and alleviating excess pore water pressure. For instance, the utilization of a cathodic well facilitates the collection and release of water, hence augmenting the effective stress and load-bearing capacity of the soil mass situated between the electrodes (Gan et al., 2022; Tao et al., 2022).

Numerous investigations have demonstrated that electro-osmosis enhances the consolidation process in low-permeability clays more efficiently than surcharge or vacuum methods alone. Furthermore, the application of electro-osmosis in conjunction with preloading techniques, whether through surcharge or vacuum, has been shown to markedly improve both the pace of consolidation and strength development (Tao et al., 2022). Laboratory-scale investigations shown that the integration of EO with surcharge preloading augmented overall settlement by 34.5% and cumulative drainage by 20.8% relative to the application of EO in isolation (Tao et al., 2022). A combination of vacuum preloading and electro-osmosis enhanced the undrained shear strength of marine clay by around 60% relative to vacuum alone, with negligible additional settlement (Wang et al., 2016).

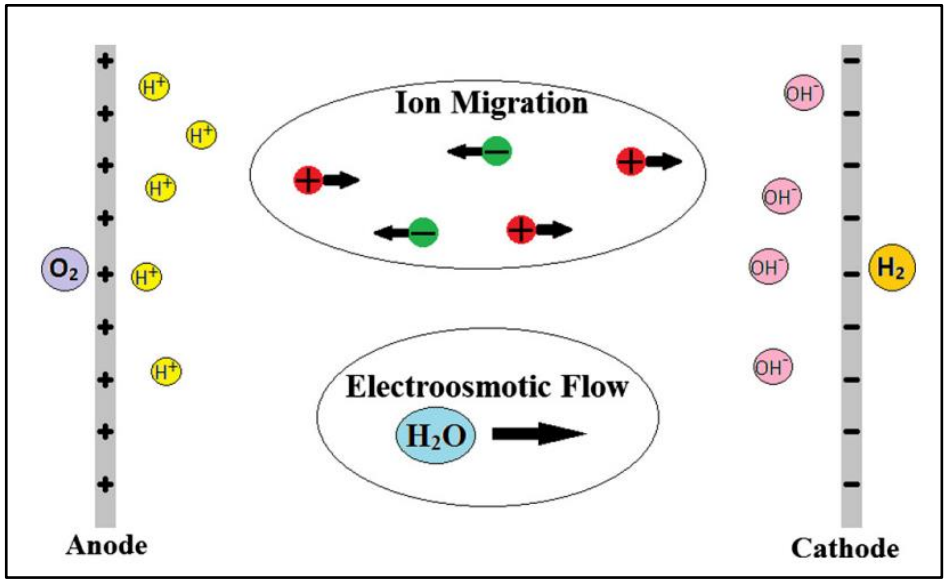

Figure 2.6 Electro-Osmosis Process In Clayey Soils (Martin, L., Alizadeh, V., & Meegoda, J. (2019)

2.5.5 Grouting Techniques

Grouting, or ground injection, is a well-established soil improvement technique used to increase the strength and reduce the permeability of soil or rock masses by injecting fluid, semi-fluid, or solidifying materials under pressure into the ground. The primary aim of this method is to fill voids within the soil structure, thereby improving its engineering behavior, such as load-bearing capacity and resistance to seepage (Karol, 2003; Warner et al., 2007).

The technique is commonly applied to prevent excessive settlement, control lateral earth pressure, fill underground voids, reduce the risk of liquefaction, improve slope stability, increase the bearing capacity of neighboring foundations, minimize shrinkage and swelling behavior in expansive soils, and control seepage in hydraulic structures (Akbulut & Saglamer, 2002; Aydin, 2011).

The injection process typically involves the use of grout mixtures containing materials such as cement, bentonite, lime, clay, and various chemical additives. Among these, cement-based grouts are the most widely used,

particularly for treating coarse-grained and loose soils, as they offer high strength gain and cost-efficiency (Bruce, 2005; Cristelo et al., 2011). The water-cement grout mix is especially effective in sandy or gravelly soils where the pore spaces allow for permeation or compaction grouting.

Grouting parameters such as injection rate and pressure are selected based on the intended improvement objective and the soil's geotechnical characteristics, including relative density and particle size distribution. Proper adjustment of these parameters is crucial to ensure the effectiveness and uniformity of the treatment (Jefferis, 2016). As illustrated in Figure (2.7)., various types of grouting techniques are used in practice, including fracture grouting, compaction grouting, permeation grouting, and jet grouting each suited to different ground conditions and improvement needs.

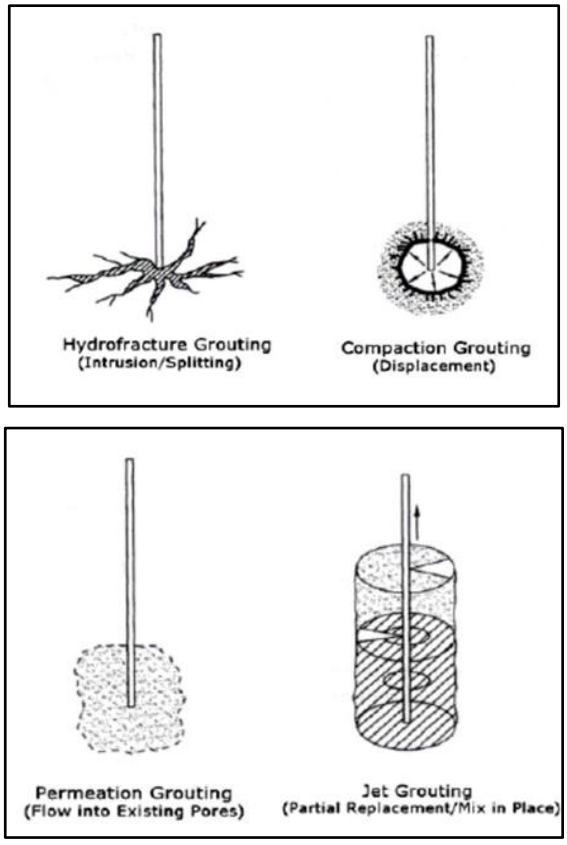

Figure 2.7 Grouting Techniques CIRIA, 2000.

2.5.5.1 Permeation Grouting

Permeation grouting is a soil improvement method wherein low-viscosity grout is injected at low pressures into the interstices of soil particles, minimally disrupting the existing soil structure. The injected grout progressively solidifies, enhancing the soil's mechanical and hydrogeological characteristics (Karol, 2003). This technique is especially efficacious in cohesionless soils like clean sands and gravels, where the permeability sufficiently allows grout infiltration.

As soil permeability decreases, the technical and economic feasibility of permeation grouting becomes more challenging. The particle size of the soil must be sufficiently larger than the solid particles in the grout to avoid clogging and ensure successful injection. For example, the use of particulate-based grouts such as cement requires that the mean particle size of the soil be significantly greater than the largest particles in the grout (Bruce & Sterling, 2002).

In superficial applications, permeation grouting can be executed in a singular phase by placing a grout pipe and injecting in an upward direction. Alternatively, grouting may be performed during or immediately following borehole drilling. In deeper soil profiles, where elevated injection pressures are required, a sequential injection process is implemented. This approach involves the sequential application of grouting at varying depths, permitting each phase to cure prior to advancement. This enhances the attainable injection depth and the regulation of grout dispersion, while concurrently reducing surface loss of grout material (Warner et al., 2007).

Permeation grouting is often applicable in sandy soils containing less than 12% fines (silt and clay), however soils with over 20% fines are frequently deemed unsuitable due to their low permeability (Karol, 2003; Bruce, 2005).

2.5.5.2 Compaction Grouting

Compaction grouting is frequently employed in soils with significant liquefaction potential. This approach prevents grout from mixing with soil or permeating between soil particles; rather, it displaces adjacent particles,

resulting in densification. The injected grout remains confined to the vicinity of the injection point and does not disperse much. It is a low-mobility, rigid grout utilized to consolidate the adjacent loose soils.

This approach is generally employed with grout materials containing aggregate sizes under 25 mm and utilized in loose or cohesionless soils. Injection pressures may attain levels of up to 4 MPa. The grout utilized in compaction grouting typically comprises a cementitious mixture with fine particles. A combination of cement and sand is frequently utilized, with the occasional inclusion of fly ash in the mixture. Densification occurs during injection as the grout fills the voids and exerts pressure exceeding the strength of the surrounding soil.

A significant benefit of this approach is its generation of minimum vibration and noise during application, rendering it appropriate for proximity to existing structures. Moreover, the columns created by this method exhibit exceptional durability and enhance ground performance (Chun et al., 2005). The application of compaxial grouting in very soft clay soils may lead to additional pore water pressures and subsequent settlement.

2.5.5.3 Fracture Grouting

Fracture grouting is a novel ground improvement method that has been predominantly developed and implemented in Europe. This method is specifically engineered for low-permeability, fine-grained soils, where traditional injection techniques typically prove ineffectual.

This approach involves the intentional fracturing of soil through the injection of a stable, low-viscosity, cement-based grout at high pressures, typically about 4 MPa. The grout creates regulated fissures in the soil mass, resulting in hardened cementitious channels and microcracks upon curing. These created cracks improve the soil's structural integrity and provide access to voids and areas that would otherwise be inaccessible using conventional permeation or compaction grouting methods.

The grout infiltrates and swells within the fissures, resulting in a limited displacement of the adjacent earth. The infilling and reinforcement of these voids lead to greater soil stability, less deformability, and improved overall ground performance.

2.5.6 Geosynthetics

Diverse methodologies are presently utilized in ground enhancement and reinforcing applications. When choosing these methods, it is crucial to verify that the designs are secure, cost-effective, and useful in alignment with engineering principles. Geosynthetic materials, synthetic engineering goods, are frequently employed as substitutes for more expensive conventional soil enhancement techniques or in conjunction with them. Geosynthetics, composed of polymers, are extensively employed in geotechnical engineering for reinforcement, drainage, separation, and filtration. The term "polymer" derives from the Greek words "poli" (many) and "meros" (part), and the strength and performance of geosynthetic materials enhance proportionately with the polymer content. Geotextiles, a prevalent category of geosynthetics, can be categorized according to their function and thickness. Thin geotextiles are primarily utilized for filtration and separation, whilst thicker geotextiles are predominantly used for cushioning and drainage purposes. Their introduction into soil improvement has allowed engineers to design more stable and cost-effective structures on problematic ground, which is a key reason these materials are now standard in many civil engineering applications (Holtz et al., 2008)

Geosynthetics are produced from diverse source materials that exhibit distinct features and qualities. The raw ingredients comprise:

- polypropylene (PP)
- polyethylene (PE)
- polyester (PET)
- polyvinyl chloride (PVC)
- polyamide (PA)

Geotextiles are flexible, planar, permeable fabrics composed of polymers. They are predominantly created by amalgamating yarns, filaments, or fibers using diverse manufacturing methods. Geotextiles are categorized into two primary types based on their production method: woven and nonwoven geotextiles.

- Woven geotextiles are manufactured by interlacing threads by weaving methods, distinguished by their high tensile strength and low permeability. Owing to these characteristics, they are frequently employed in applications related to soil reinforcement, separation, and protection.
- Nonwoven geotextiles are textile fabrics formed from fibers that are interconnected via mechanical (needlepunching), thermal, or chemical methods. These materials possess a fibrous structure characterized by high permeability and are extensively utilized for drainage, filtration, and separation purposes.
- Geotextiles are frequently employed for the following applications:
- Separation: To avert the intermingling of soil strata with varying grain size distributions.
- Filtration: To facilitate regulated water passage through the soil while retaining small particles.
- Drainage: To enable the expulsion of surplus water from the soil.
- Reinforcement: To enhance the load-bearing capacity of the substrate.
- Protection: To safeguard underlying structures from mechanical harm.
- Barrier/Sealing: To serve as an impermeable barrier that obstructs the transmission of water or other fluids, particularly in asphalt pavemen

2.5.6.1 Geogrid

Geogrids are net-structured products obtained by intersecting synthetic materials with high tensile strength at certain intervals or by stretching perforated layers in certain directions. The large openings in the structure of geogrids penetrate into the soil material and ensure that it is effectively locked. Thus, the bearing capacity and stability of the ground is greatly increased.

The usage areas of geogrids are quite diverse:

- In the substrate of unpaved roads,
- Under the ballast layer of railway lines,
- Reinforcement of embankment dams and road embankments,
- Slope stabilisation and landslide areas,
- In the creation of gabion structures,
- Foundation reinforcement in soft soils,
- For reinforcement purposes in pile foundation systems,
- It is used as a reinforcement layer to increase the cracking resistance of asphalt pavements.

Figure 2.8 Example of Geogrid Utilization URL[1]

2.5.6.2 Geomembrane

Geomembranes have become vital components in geotechnical engineering applications owing to their superior tensile strength and efficient load transmission properties. These materials are polymeric or asphalt-based, flexible, impermeable, and flat synthetic liners primarily employed to inhibit fluid migration, so functioning as barriers.

The initial geomembranes were historically manufactured from synthetic rubber. Since the 1980s, thermoset polymers have been progressively supplanted by thermoplastic polymers in industrial applications. Currently, the predominant forms of geomembranes are high-density polyethylene (HDPE), flexible polypropylene (FPP), and polyvinyl chloride (PVC).

- Geomembranes are extensively utilized in the subsequent applications:
- Coating of potable water reservoirs and storage tanks,
- As barriers in solid and liquid waste containment systems,
- Ensuring impermeability in irrigation canals,
- Mitigating seepage in dams and ponds,
- Waterproofing of subterranean tunnels and constructions.
- Restricting toxic liquids in ecologically vulnerable regions to avert contamination.

Geomembranes occupy a crucial role in environmental engineering applications due to their exceptional resistance to water and hazardous compounds, coupled with their extended lifespan.

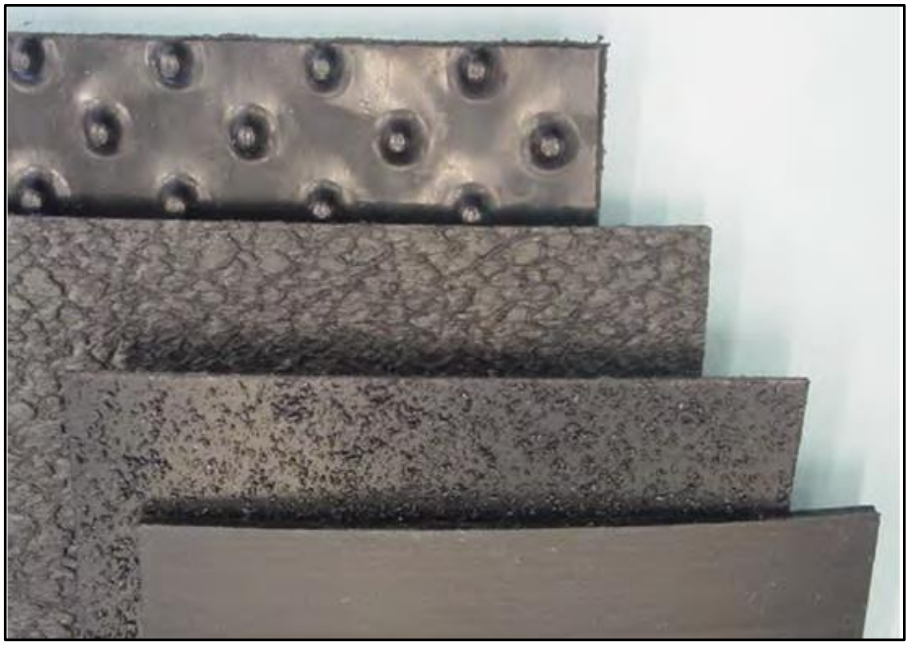

Figure 2.9 Geotextiles in Embankment Dams (April, 2008)

2.5.6.3 Geocomposite

Geocomposites are multifunctional geosynthetic materials created by amalgamating two or more distinct forms of geosynthetics, such as geotextiles, geomembranes, geonets, or geogrids, into a cohesive product (Koerner, 2012; Shukla, 2016). Through the integration of these components, a geocomposite can concurrently execute many functions such as drainage, filtration, reinforcement, or barrier protection often with greater efficacy than individual geosynthetics utilized in isolation (Müller & Saathoff, 2015; Śpitalniak et al., 2019). This synergistic design improves engineering performance by utilizing the complementary features of each component, leading to higher efficiency, such as superior drainage capacity, increased structural stability, or improved impermeability, in contrast to single-component solutions. Consequently, geocomposites often provide a cost-efficient and construction-effective option, minimizing the requirement for substantial natural aggregate layers and accelerating installation, while preserving or enhancing the long-term stability of the geotechnical system (Kiersnowska et al., 2023).

2.5.6.3.i Primary Applications Of Geocomposites

Geocomposites possess diverse uses in civil and environmental engineering. Their principal applications encompass:

- Application in Drainage Systems: Geocomposites serve as drainage layers in soils necessitating swift and regulated extraction of water and fluids, especially in road subgrades, tunnels, retaining walls, and embankment fills.
- Application in Erosion Control: They are utilized on slopes, riverbanks, and coastal regions to mitigate soil loss by enhancing surface water drainage, hence diminishing erosion.
- Application in Waste Containment Facilities: In landfills and waste storage facilities, geocomposites are utilized in conjunction with geomembranes to deliver sealing and drainage capabilities. This dual function mitigates the release of hazardous materials into the environment, hence promoting environmental conservation.
- Application in Railway and Road Infrastructure: They are situated beneath the ballast layers of railways and within road embankment fills to improve load-bearing capacity, facilitate proper drainage, and minimize long-term maintenance expenses.
- Application in Building and Foundation Systems: Geocomposites utilized beneath building foundations facilitate drainage and waterproofing, safeguarding the structure from water damage and enhancing the stability of the foundation soil.

In summary, geocomposites are advanced products that integrate the benefits of several geosynthetic materials into a unified system, providing substantial advantages in building engineering. Their broad applicability, simplicity of installation, and economical nature have resulted in their growing utilization in contemporary infrastructure projects.

2.5.7 Soil Stabilisation With Additives

Soil stabilization is the process of enhancing the engineering qualities of soils by using external materials to improve their bearing capacity and mitigate issues linked to settlement and deformation. Additive-based stabilization strategies yield enduring enhancements in the soil's physical, chemical, and mechanical qualities. These solutions are especially beneficial in situations when the native soil exhibits inadequate strength or stability, thus enhancing structural safety. The most often utilized additions include lime, cement, bitumen, fly ash, and different polymeric compounds.

2.5.7.1 Lime Stabilization

Bell (1996) illustrates that incorporating a minor proportion of lime into clay soils can markedly improve their engineering characteristics. In his research, lime treatment diminished the fluidity of clays and resulted in significant enhancements in strength and stiffness, along with an improved California Bearing Ratio (CBR) for the soil. The enhancements result from chemical reactions (cation exchange and pozzolanic activity) that generate cementitious chemicals in the soil, consequently substantiating lime stabilization as an efficacious technique for augmenting soil strength and stability.

2.5.7.2 Cement Stabilization

Croft (1967) discovered that even a modest quantity of Portland cement can significantly enhance the strength and load-bearing capability of soils. Cement serves as a binder, occupying spaces and creating a stiff matrix that enhances the soil's unconfined compressive strength. Research indicates that incorporating a little percentage of cement by weight results in significant improvements in unconfined compressive strength in clayey or loess soils. This research substantiates the efficacy of cement stabilization, as it diminishes soil fluidity and engenders a robust, cemented soil matrix that is more appropriate for construction purposes.

2.5.7.3 Bitumen Stabilization

Bituminous additives, including asphalt cement or emulsified bitumen, enhance soil by agglomerating particles and imparting water resistance to the mixture. Andavan and Kumar (2020) indicate that the incorporation of a bitumen emulsion into granular soil substantially enhanced its CBR, with an approximate rise of 50% in one instance, signifying a considerable improvement in bearing capacity. The bitumen envelops soil particles, imparting a binding and impermeable quality that improves structural integrity and diminishes moisture vulnerability. This demonstrates the efficacy of bitumen stabilization in producing more resilient road bases and subgrades, particularly in moist circumstances.

2.5.7.4 Fly Ash Stabilization

Fly ash, a fine pozzolanic by-product of coal combustion, has been effectively utilized to stabilize problematic soils. Cokca (2001) examined Class C fly ash as an addition for expansive clay and saw substantial enhancements: the modified soil exhibited less swell potential and heightened strength, allowing it to satisfy construction standards. The research found that expansive soil can be effectively stabilized with fly ash. Fly ash provides silica and alumina that react, particularly in the presence of lime or calcium in high-calcium ashes, to create cementitious compounds, so improving the soil's load-bearing capacity and alleviating problems such as excessive shrink-swell behavior. This offers compelling evidence for the efficacy of fly ash stabilization in enhancing soil performance for engineering purposes.

2.5.8 Thermal Methods

One of the techniques developed to improve the mechanical and physical properties of soils is the application of thermal methods. This approach aims to achieve temporary or permanent enhancement in soil behavior by utilizing the interaction of soils with elevated or reduced temperatures. Thermal methods are

particularly considered as alternative or complementary ground improvement techniques in soils with low bearing capacity, high compressibility, or low shear strength. Depending on the form of application, thermal stabilization methods are categorized into two main groups: stabilization by heating and stabilization by freezing.

2.5.8.1 Thermal Stabilization By Heating

The heating technique is predominantly utilized for fine-grained soils, particularly unsaturated silts and clays. The major purpose of this procedure is to remove moisture from the soil through elevated temperatures and to strengthen the interparticle connections, hence increasing the mechanical strength of the soil. Research indicates that heating soils to around 110 °C causes substantial moisture loss, hence enhancing bearing capacity and diminishing deformation behavior.

When the soil temperature attains between 400 and 600 °C, clay minerals experience silicatization. At approximately 900 °C, clays undergo phase transitions akin to those in brick production, resulting in heightened rigidity and water resistance. Nonetheless, high-temperature applications are infrequently practical or cost-effective in field settings and are typically confined to specialized engineering endeavors.

Two primary heating methods are employed: electric heating and combustion heating. In electrical systems, electrodes embedded in the ground transform electrical energy directly into thermal energy. In combustion systems, flames produced from gasoline or other fuels are laterally channeled through pipes situated in boreholes. In both methodologies, heat is meticulously transferred into the soil, with wellheads generally enclosed and insulated to reduce heat dissipation.

2.5.8.2 Ground Freezing Stabilization

Ground freezing stabilization is a method that temporarily enhances soil stability by freezing the pore water in situ at extremely low temperatures. The

development of ice in the soil pore space aggregates the particles, like to cement in concrete, markedly enhancing stiffness, shear strength, and impermeability (Sanger & Sayles, 1979; Jessberger, 1988). This technique is especially efficacious for short-term stabilization in poor or water-saturated soils when traditional methods are insufficient, including deep excavations, tunnel building, and vertical shafts (Wang et al., 2019).

The freezing procedure is generally executed with a concentric double-pipe system embedded in the soil (Jones, 2010). This device circulates a refrigerant, such as brine chilled with ammonia or carbon dioxide, through the inner pipe and extracts it from the outer pipe, leading to the gradual freezing of the surrounding ground (Sanger & Sayles, 1979). In critical situations necessitating swift freezing, liquid nitrogen can be employed, facilitating the rapid creation of an ice wall due to its exceptionally low boiling point of –196 °C (Andersland & Ladanyi, 2004).

A notable feature of frozen soils is the simultaneous presence of liquid water and ice in the pore spaces at subzero temperatures. In sandy soils, the phase transition occurs between 0 and -0.5 °C, whereas in clay soils, it varies from 0 to -5 °C, contingent upon the soil's mineral composition and moisture content (Vyalov, 1986). The strength of frozen soils is directly affected by the quantity of unfrozen water, which diminishes as the temperature decreases. Thus, frozen clays necessitate lower temperatures than sands to attain comparable strength levels owing to their elevated unfrozen water content (Wang et al., 2019).

Although successful, the efficacy of artificial ground freezing (AGF) is significantly contingent upon site-specific variables. In regions where groundwater velocities surpass around 2 m/day, heat dissipation from the soil surface is counterbalanced by the continual entry of warmer water, potentially inhibiting the construction of a complete ice wall (Chung & Carson, 2002). Furthermore, AGF is recognized for its substantial operational expenses attributed to energy usage and equipment necessities, rendering it fiscally viable solely for intricate or high-risk engineering endeavors (Jessberger, 1988; Andersland & Ladanyi, 2004).

2.5.9 Storm Columns

The stone column method is an efficient technique for enhancing the engineering qualities of soils, particularly for soft soils with limited bearing capacity. This technique is utilized in loose or water-saturated clays, silty sands, alluvial soils, and regions with liquefaction potential to enhance bearing capacity, diminish settlements, expedite consolidation, and avert soil vulnerabilities that may arise during seismic events. Stone columns are vertical, solid structures embedded in the ground and filled with granular materials like crushed stone or gravel, with a grain diameter ranging from 20 to 75 mm. The columns are formed by progressively compacting the stone materials inserted into the excavated cavities in the earth. Stone columns enhance soil performance by redistributing loads from the ground to columns with elevated bearing capacity. Simultaneously, due to their elevated permeability, they function as drainage conduits, diminishing pore water pressure and expediting consolidation (Ercan, M. (2020) - Şengezer, L. (2020).

2.5.9.1 Fields Of Application

Stone columns are efficiently employed to address the following engineering challenges:

- Enhancing the bearing capacity of soft and medium cohesive clay soils
- Decreasing consolidation duration - Mitigating liquefaction risk during seismic events
- Enhancing the stability of embankments
- Mitigation of total and differential settlement values that may arise in buildings
- Egress of water from the soil through functioning as a vertical drain

2.5.9.2 Methods Of Stone Column Fabrication

Stone columns can be produced using various manufacturing procedures based on the site's soil characteristics. The predominant methods are as follows:

Stone column treatments are executed using diverse procedures based on soil conditions. The Vibro-Replacement (Wet Method) involves generating a cavity in the soil utilizing a vibratory probe (vibroflot) alongside a water jet, subsequently filling the cavity with granular material from the surface and compacting it via vibration. This technique is depicted in Figure 2.9. It is very efficacious in extremely soft soils with elevated groundwater levels (Ceylan, 2020). Conversely, the Vibro-Displacement (Dry Method) is utilized without employing a water jet, as illustrated in Figures 2.10 and 2.11. This approach involves feeding dry granular material from the bottom and directly inserting it into the ground using the vibroflot. The cavity is maintained in a stable condition through the ongoing compression of the added material. This method is particularly appropriate for applications at depths of up to 25 meters (FHWA, 1983).

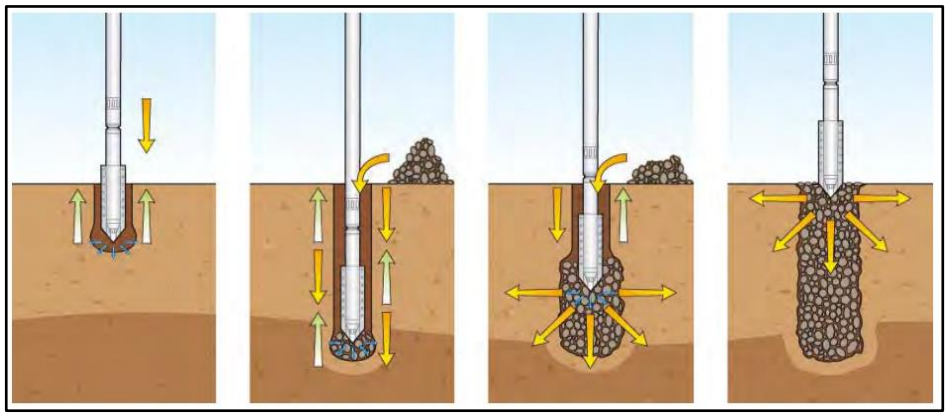

Figure 2.10 Wet - Top - Feed Method Process Schematic (Taube, 2001)

The Rammed Stone Column technique is utilized under stable ground conditions. This process entails driving a steel casing into the earth to form a hollow, subsequently filled with a sand-gravel mixture and compacted by the

impact of a large weight (Ayan, 2016). A prevalent technique in Japan is the Sand Compaction Pile (Japanese Method), which has demonstrated efficacy in clayey soils with elevated groundwater levels. This technique involves achieving the appropriate depth with a steel casing, followed by the insertion and compaction of sand layers into the soil (Ceylan, 2020).

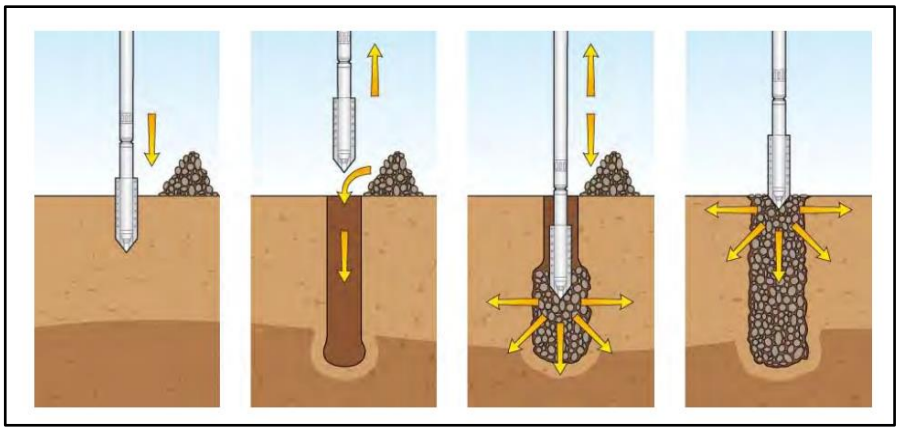

Figure 2.11 Dry – Bottom - Feed Method Process Schematic (Taube, 2001)

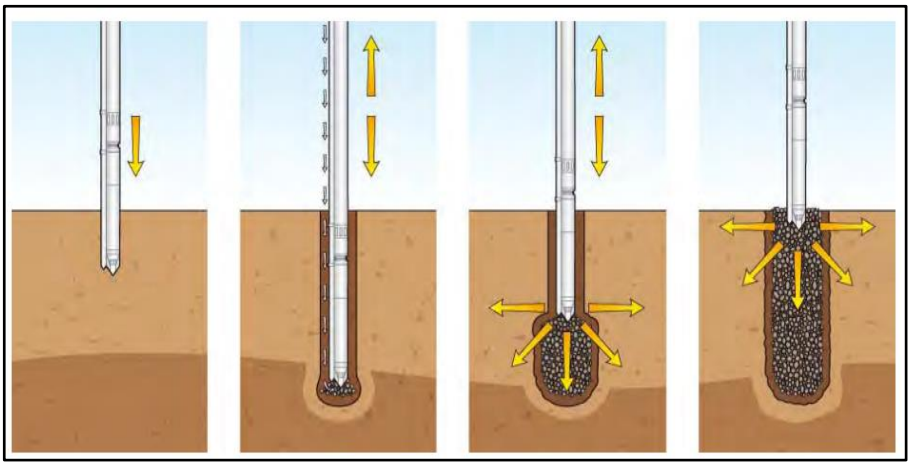

Figure 2.12 Dry – Top - Feed Method Process Schematic(Taube, 2001)

Benefits: The implementation of stone columns provides numerous geotechnical advantages. Firstly, they markedly enhance the load-bearing capability of soft and weak soils. Moreover, they mitigate settlement magnitudes

and expedite the consolidation process by facilitating vertical drainage pathways. Stone columns effectively mitigate the risk of soil liquefaction under dynamic loading situations. Furthermore, the drainage action generated by the columns facilitates a decrease in surplus pore water pressure.

Constraints: Notwithstanding their benefits, stone columns may demonstrate constraints under specific ground conditions. In highly weak, organic, or peat soils, column deformation and instability may arise from inadequate lateral support. Moreover, when the column tips cannot be anchored into a suitable bearing layer, the system's overall performance may be adversely affected.

2.5.10 Bored Pile

The bored pile technique is an efficient deep foundation approach employed to convey structural loads from weak soils to deeper, more competent soil layers. It is predominantly favored in ground enhancement applications, applicable to both new construction endeavors and the fortification of existing edifices. Bored piles are frequently utilized as shoring components in deep excavations, ensuring excavation safety and lateral support. Piles are fabricated with or without reinforcement and can be created as either reinforced concrete or steel-reinforced elements, regardless of their diameter.

The bored pile construction method typically has three primary stages: drilling, cage installation, and concrete pouring. In the preliminary stage, suitable drilling apparatus is chosen according to the geological parameters and groundwater elevation. Casing pipes or bentonite slurry may be employed to avert soil collapse during drilling. Borehole diameters generally vary from 50 cm to 200 cm.

Upon completion of drilling, the borehole is cleaned, and the pre-fabricated reinforcing cage is positioned accordingly. Ensuring that the reinforcement is fitted with adequate concrete cover is crucial to prevent corrosion. For cages over 12 meters in length, supplementary connection components such as tie wires, welding, or clamps are employed to ensure cage

stability during installation. Subsequent to the installation of the cage, ready-mix concrete is introduced into the borehole, concurrently withdrawing the casing to permit the concrete to ascend alongside it. In bored pile systems, it is advisable to do concreting on the same day as drilling. Otherwise, soil deformations may result in borehole collapse or expansion, necessitating supplementary drilling and cleaning procedures. The integrity and durability of the concrete utilized in pile fabrication must be confirmed through on-site testing. Proper concrete cover must be maintained to sustain the load-bearing capacity of the reinforcement and to avert corrosion-induced deterioration.

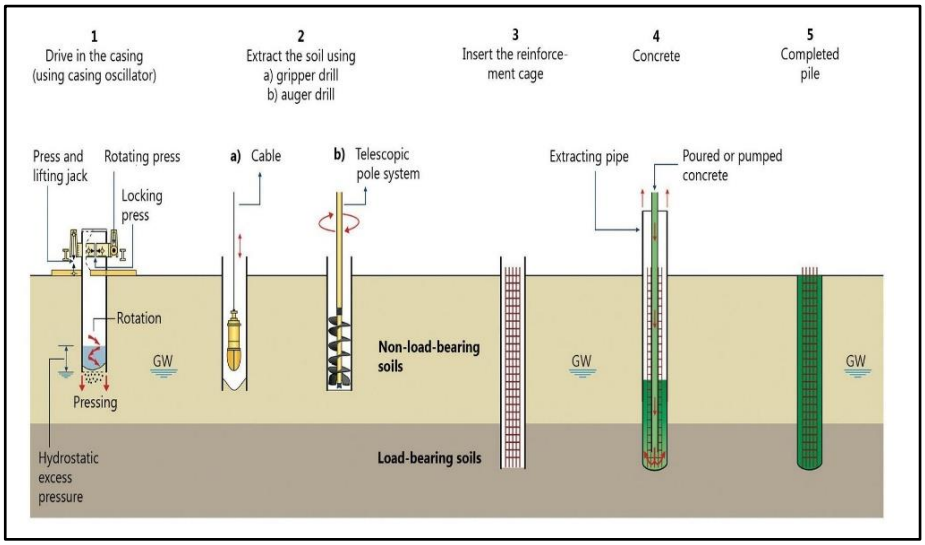

Figure 2.13 Bored Pile Construction Stages URL[2]

Figure 2.13 illustrates the phases of bored pile construction. A casing pipe is first hammered into the ground utilizing a casing oscillator. Throughout this procedure, any surplus hydrostatic pressure is regulated to maintain soil stability. During the second stage, the in-situ soil is dug utilizing drilling apparatus such as a clamp drill or auger drill. After the borehole is cleaned, a pre-fabricated reinforcement cage, constructed in accordance with the project specifications, is positioned into the hole. Maintaining sufficient concrete cover and ensuring good vertical alignment of the cage are essential for corrosion resistance and

structural integrity. During the fourth step, fresh concrete is either poured or pumped into the borehole as the casing is concurrently extracted. This facilitates uniform concrete ascent, hence minimizing segregation and guaranteeing consistent filling. Upon the completion of concreting, the pile is entirely formed, yielding a robust and resilient foundation element adept at securely transmitting structural loads to deeper, more competent soil strata.

2.5.11 Micro Pile

Micropiles are a commonly favored ground enhancement method owing to their diminutive dimension and versatile applicability. Micropiles, generally with diameters between 15 and 35 cm, are employed to augment the bearing capacity of unstable soils, reinforce the foundations of existing structures, and enable construction in places with restricted accessibility. Micropiles, constructed from reinforced and grouted concrete, can be set vertically or at an angle, allowing them to withstand diverse load types (Han, 2006; Ceylan, 2021; Babu, 2004).

The application process commences with the drilling of small-diameter boreholes into the ground. Reinforcement bars are placed into these holes, which are then filled with appropriately mixed grout or injection concrete, creating a hard pile. In situations necessitating further support, the borehole may be reinforced with steel casing. The grouting process may be conducted in one or many steps, contingent upon the soil type, groundwater level, and pile length. A supplementary grouting technique, referred to as re-injection, is occasionally utilized to improve the adhesion between the pile and the adjacent soil (Juran et al., 1999; Elkamash, 2016; Azat, 2020).

Micropiles act as rigid components in the earth, transferring loads to the surrounding soil mostly via skin friction. This characteristic enables significant enhancements in bearing capacity, particularly in suboptimal soil conditions. Furthermore, they effectively diminish settlement and significantly contribute to the enhancement of soil stability. The localized soil densification during

installation expedites consolidation and facilitates the rapid dissipation of excess pore water pressures (Han, 2006; Juran et al., 1999; Azat, 2020).

The primary advantages of micropile systems include their capacity for installation without harming nearby structures, their suitability for limited places, and their relatively silent and low-vibration installation procedure. Consequently, micropiles are frequently the favored technique in historic structures, urban locales, and other delicate settings. Moreover, micropiles provide excellent solutions in geotechnically intricate situations, as they can operate efficiently via stratified soil layers before encountering the bearing stratum (Elkamash, 2016; Ceylan, 2021; Babu, 2004).

In conclusion, micropiles are an effective ground improvement technique used to enhance the bearing capacity of soils, ensure structural safety, and improve long-term performance. Due to their ease of application, especially in areas with limited access and in sensitive projects, they are reliably preferred in geotechnical engineering practices.

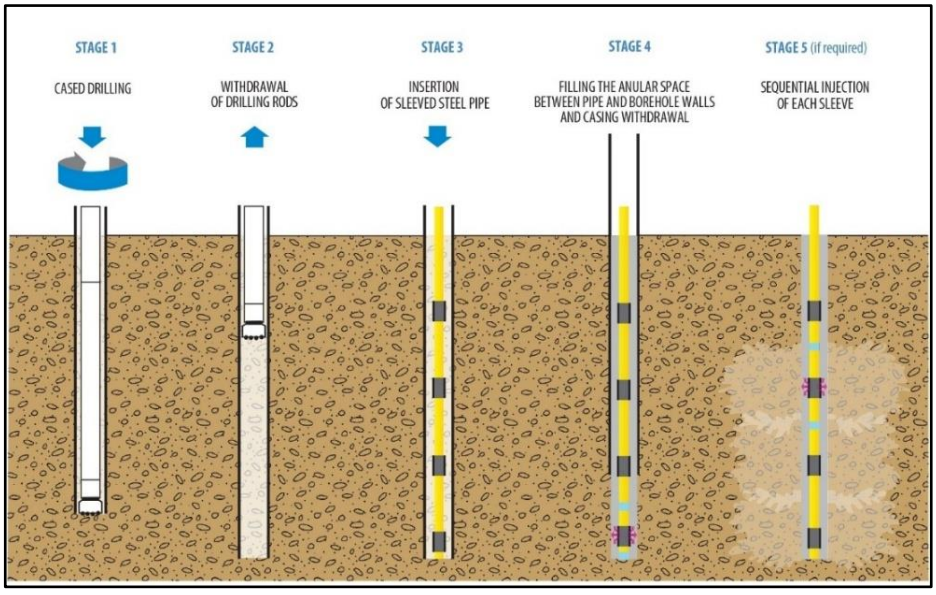

Figure 2.14 Manufacturing Process of Mini Piles [URL 3]

The construction of micropiles is carried out in a sequence of clearly defined stages to ensure structural efficiency and soil compatibility (Figure 2.14.). The process begins with Stage 1, where cased drilling is performed using appropriate rotary equipment to penetrate the subsoil while maintaining borehole stability. In Stage 2, the drilling rods are withdrawn, creating a clean and stable borehole. Following this, Stage 3 involves the insertion of a sleeved steel pipe, which is the primary structural element of the micropile and often contains grout sleeves that facilitate controlled injection. In Stage 4, the annular space between the borehole wall and the installed pipe is filled with grout, ensuring full contact between the pile and surrounding soil, while simultaneously withdrawing the casing. Finally, in Stage 5 (if required), grout is injected sequentially through the sleeves to increase load transfer efficiency and improve bonding with the adjacent soil layers. This multi-stage installation method ensures the micropile achieves its desired strength, stiffness, and performance, especially in challenging soil conditions or restricted-access areas.

2.5.12 Soil Nailing

Soil nailing is a ground reinforcement method employed to stabilize in-situ excavation slopes or natural embankments. This approach involves the insertion of steel bars (nails) into the soil at prescribed angles, enhancing the shear strength of weak soil masses and regulating deformations (Adams, 1972; Han, 2006). It offers a dependable and cost-effective solution, particularly for temporary excavation support systems and slope stabilization requirements.

Soil nails are generally put at angles between 15° and 30°, with diameters of 25 to 50 mm and lengths from 4 to 12 meters (Elkamash et al., 2016). Upon installation, the nails are grouted with a cementitious mixture to improve the bond between their heads and the adjacent soil. Anchor plates are affixed to the exposed ends of the nails, and the surface is typically strengthened with shotcrete to guarantee system integrity (Juran et al., 1999).

This method facilitates internal soil stability without inducing surface displacement. Moreover, its interoperability with staged excavation procedures

enhances time efficiency. It is extensively utilized in urban environments, especially in excavations near structures, road construction, and temporary shoring systems (Prasetya et al., 2025).

The efficacy of a soil nailing system is generally assessed via on-site pull-out tests performed during installation. Factors include soil characteristics, groundwater conditions, and grout quality directly affect the efficacy of the nails (Han, 2006; Babu, 2004). The incorporation of drainage systems during installation is essential for regulating pore water pressure.

In summary, soil nailing has emerged as a prevalent ground improvement technique in contemporary geotechnical engineering projects owing to its cost efficiency, simplicity of execution, and responsiveness to environmental factors

CHAPTER 3

3. JET GROUTING

Jet grouting is an innovative geotechnical improvement technique that utilizes high-pressure injection to enhance ground properties. In this method, a water-cement mixture is injected at very high pressure through specially designed nozzles located on a rod inserted into the ground via a narrow borehole. The high-energy jet erodes the surrounding soil, mixes with it, and subsequently hardens to form an in-situ soil-cement column (Akagi et al., 1994). These jet grout columns significantly increase the strength and stiffness of the treated ground while also drastically reducing its permeability. As a result, jet grouting has become a globally applied solution, capable of addressing a wide range of geotechnical challenges (Bruce, 2005).

3.1 HISTORICAL DEVELOPMENT OF THE JET GROUTING METHOD

The earliest known applications of jet grouting date back to the 1950s, during a dam project in Pakistan. In this project, implemented by the Cementation Company, the technique aimed to form an impermeable barrier through high-pressure injection (Mori et al., 1981).

During the 1960s, the method was further systematized in Japan. Starting in 1965, the Yamakado brothers developed a procedure based on cutting the soil using high-pressure water jets, followed by cement grout injection (Akagi et al., 1994). Around the same time, Nakanishi introduced a method named "Chemical Churning Pile (CCP)", which was later patented in Japan in 1968 (Nakanishi, 1968).

In the early 1970s, as an alternative to the CCP technique, the "jet grouting" method was developed by Yahiro and Yoshida. Their technique

involved loosening the soil with a water jet and mixing it in-situ with cement grout (Yahiro & Yoshida, 1973). Concurrently, Kajima Corporation introduced the "Column Jet Grout (CJG)" technique, which incorporated a rotary injection system to form cylindrical columns (Terashi, 2003).

Jet grouting technology was introduced to Europe in the late 1970s through licensing agreements with Japanese firms. The technique gained significant traction, particularly in Italy and Germany, where it was adopted and further improved (Bruce et al., 1987).

Throughout the 1980s, technological advancements in jet grouting included increased pump capacities and the development of triple injection systems (water + air + cement), enabling the formation of larger and more homogeneous columns (Mori et al., 1981; Akagi et al., 1994).

In recent years, advanced systems such as X-Jet have enabled the production of wider diameter columns. Additionally, computer-controlled equipment has allowed for real-time optimization of injection parameters, thereby enhancing application precision (Saito et al., 2011).

3.2 DOMAINS OF APPLICATION

The jet grouting technology has emerged as a favored solution in many contemporary geotechnical and structural engineering applications due to its multiple advantages. Particularly in challenging soil situations, it functions as an efficient means to guarantee structural integrity and uphold the sustainability of construction endeavors.

Ground Improvement: In soils with inadequate bearing capacity, jet grout columns are utilized to augment ground strength and mitigate future settlements. This use is essential for enhancing structural reliability in both new constructions and existing structures.

- Foundation Reinforcement of Existing Structures: Jet grouting is commonly employed to enhance the foundations of buildings situated near excavation sites. This technology supports foundations

from below, ensuring stability and reducing the effects of adjacent construction activity.

- Waterproofing and Seepage Control: In projects where groundwater management is essential-such as dam foundations or deep excavations-impermeable barriers can be created employing jet grouting, effectively obstructing water infiltration and seepage.
- Support for Deep Excavations: In urban settings with constrained space, jet grout columns are employed to reinforce excavation walls and foundations. This guarantees secure excavation procedures while safeguarding nearby structures from possible distortion or harm.
- Tunnels and Underground Structures: Before tunnel excavation, the adjacent soil may be prepared with jet grouting to reduce distortion and regulate groundwater ingress. This substantially enhances tunnel stability and safeguards adjacent infrastructure.
- Mitigation of Liquefaction Potential: In seismic regions, loose, water-saturated soils are treated with jet grouting to reduce the risk of liquefaction. This reinforcement improves the durability of structures during seismic events and mitigates structural damage.

The application areas clearly illustrate the adaptability of the jet grouting method and its efficacy in resolving diverse geotechnical issues faced in modern engineering projects.

Jet grouting has emerged as more than one viable solution for building projects. Figure 3.1, prepared by Croce et al. (2014), shows frequently used jet grouting aplications

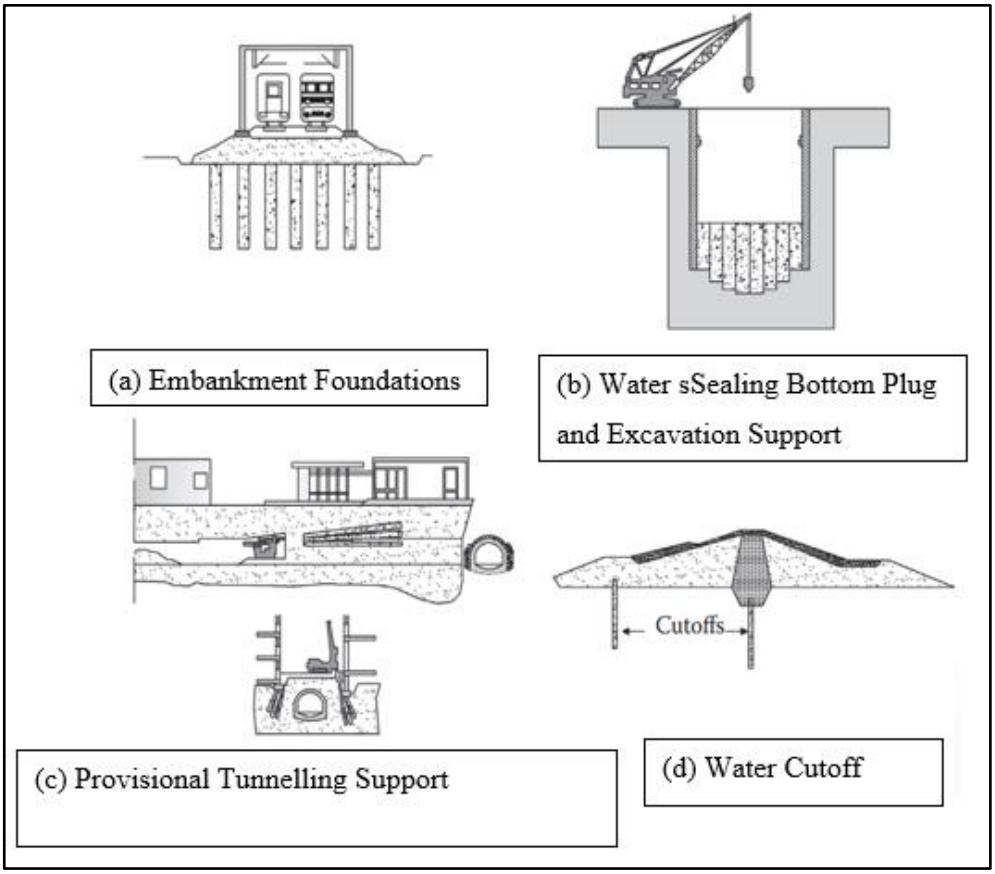

Figure 3.1 Examples of Various Applications of Jet Grouting (Croce ve ark, 2014)

3.3 APPLICABILITY OF THE JET GROUT METHOD IN DIFFERENT SOIL TYPES

3.3.1 Relevance In Fine- Grained Soils

Jet grouting in fine-grained, cohesive soils like clay and silt has distinct obstacles. The technique involves the physical disturbance of the earth and its amalgamation with injected grout. The compressive strength of the resultant column in these soils is predominantly influenced by the grout mix ratio and injection pressure. Cinar (2023) indicated that unconfined compressive strengths for columns in clayey soils often range from 4 to 15 MPa. The values are often

inferior to those observed in coarser soils, mainly because of the restricted penetrating ability of the grout in fine-grained matrices.

Regulating the return flow of excavated materials during jetting is essential in these soils. If dislodged soil particles are inadequately eliminated, ground heave or excessive internal pressure may ensue. These difficulties can frequently be alleviated by optimizing drilling velocity and injection flow rate. Furthermore, employing water or air-assisted jets can enhance the effective cutting diameter and optimize grout-soil mixing (Bauer Maschinen GmbH, 2017).

Research on heterogeneous clay deposits has demonstrated that jet grout columns may incorporate a considerable amount of unblended native material. Stark et al. (2009) noted that columns formed with triple fluid systems maintained 50–60% of the original soil content. Conversely, soil mixing columns yielded more uniform mixtures (Stark et al., 2009). Consequently, although jet grouting is theoretically viable in clay-rich environments, achieving homogeneity necessitates precise parameters and, in certain instances, alternate jetting methodologies such as dual-fluid systems.

3.3.2 Relevance In Coarse- Grained Soils

Jet grouting is typically more efficacious in granular soils, including sands and small gravels. The porous structure of these soils enables the high-pressure jet to disintegrate the particles and amalgamate the grout more effectively. Cinar (2023) documented unconfined compressive values ranging from 15 to 36 MPa in jet grout columns established in sandy soils, markedly exceeding those in clay soils. The enhancement in strength is ascribed to improved penetration and more consistent soil-grout amalgamation.

Nonetheless, in extremely coarse sands or sandy-gravel composites, material attrition may provide a problem. Nonetheless, efficient column formation can still be accomplished utilizing suitable nozzles and systems with air-assisted injection (BL process) (Bauer Maschinen GmbH, 2017). Cement-based or chemical grouting procedures are generally favored for gravels above

2 mm in diameter, as they are more suitable for bigger particle sizes (Bauer Maschinen GmbH, 2017)

3.3.3 Jet Grouting In Diverse Soil Types

In stratified or heterogeneous soils, jet grouting offers the benefit of unifying disparate layers into a cohesive composite structure. This is especially advantageous in heterogeneous deposits beneath the water table, such as alternating clay, silt, and sand profiles. Nonetheless, disparate resistance among several strata may result in inconsistent jetting and column anomalies. Stark et al. (2009) discovered that in layered clays, triple fluid jet grout columns preserved more than fifty percent of their initial soil matrix. This indicates that, notwithstanding jetting, complete integration may not be realized without meticulous process control.To mitigate such variability, several jetting techniques may be utilized. Dual-fluid systems typically exhibit greater efficacy in silty-sandy soils, resulting in broader and more uniform columns (Bauer Maschinen GmbH, 2017). It is advisable to utilize trial columns and real-time monitoring, such as acoustic logging, to guarantee uniform quality (Bogati, 2019).

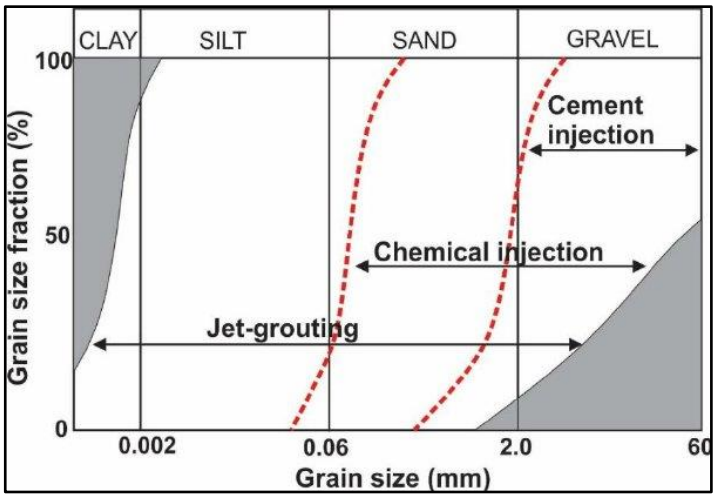

Figure 3.2 Jet Grout Application Limits For Various Soil Types (Passlick and Doerendahl, 2006)

The chart above presents, in a clear and comparative format, the effective grain size ranges for various injection techniques. The horizontal axis represents soil particle size (in millimeters), while the vertical axis shows the corresponding grain size fraction. Additionally, soil types such as clay, silt, sand, and gravel are segmented across the top axis for classification purposes.When I look at this figure, it's quite evident that jet grouting stands out as the method with the widest applicability range among all injection techniques. It can be applied effectively from extremely fine-grained soils such as clay (around 0.002 mm) up to coarse gravels in the 10–20 mm range. This broad adaptability is one of the main reasons why jet grouting has become so widely used in modern geotechnical engineering. Chemical injection is shown as most effective in silty and fine sandy soils. Because of its low viscosity, chemical grout can infiltrate between smaller particles, but its efficiency is severely limited in very fine-grained soils like clay and in coarser gravels. Cement injection, on the other hand, is more commonly applied to sandy and gravelly soils where the grout can adequately penetrate and fill the larger voids. However, its inability to be used in low-permeability soils like silt or clay illustrates the narrower scope of this method.

The reason jet grouting covers such a broad grain size range is that, unlike classical grouting methods which rely on percolation into pore spaces, it physically displaces and mixes the soil in situ through high-pressure jets. This allows the technique to be effective regardless of the soil's permeability or porosity making it applicable in both low-permeability clays and more permeable sand-gravel mixtures. In my opinion, this chart not only illustrates the technical limits of each injection method but also serves as a practical guide for evaluating which technique may be best suited for a given soil condition before field application. The versatility and adaptability offered by jet grouting make it a highly valuable method especially in complex and heterogeneous ground profiles where conventional methods often fall short.

3.4 ADVANTAGES AND DISADVANTAGE OF THE JET GROUTING METHOD

3.4.1 Advantages Of The Jet Grouting Method

Jet grouting is a modern ground enhancement method extensively employed in subterranean and geotechnical engineering. Although it has many engineering benefits that render it advantageous for different projects, it also entails specific limits that must be considered during the planning and design stages.

Relevance Jet grouting can be effectively utilized in a diverse array of soil types, including cohesive and non-cohesive soils, as well as gravelly and alluvial deposits. The procedure produces highly successful results when implemented with suitable parameters, even in difficult soil conditions.

- Geometric Flexibility: The diameter, length, and configuration of jet grout columns can be customized to satisfy project-specific criteria. This versatility enables engineers to create tailored solutions that satisfy structural requirements, such as designing columns in circular, wall-type, or grid configurations to regulate stiffness distribution.
- Enhancement of Impermeability: Jet grout columns can markedly decrease permeability by occupying cavities within the soil matrix during the injection process. This characteristic renders it an optimal selection for efforts necessitating water cut-off solutions, including dam foundations, river crossings, or tunnel excavations.
- High Strength Characteristics: When engineered with suitable mix ratios and implemented under regulated conditions, jet grout columns yield soil-cement compounds exhibiting elevated compressive strength. This provides a significant benefit in load transfer through weak or compressible soils.

- Applicability Under Existing Structures: Owing to its low-vibration characteristics, jet grouting can be securely utilized beneath sensitive infrastructures, including historical edifices, active industrial sites, and transit systems. This facilitates in-situ fortification of foundations without jeopardizing the integrity of existing structures.
- Enhancement of Liquefaction Resistance: In seismically active areas, jet grouting is commonly employed to create stiff inclusions in loose sandy or silty soils to reduce the danger of liquefaction. This greatly improves the seismic performance and stability of superimposed structures.
- Decreased Excavation and Construction Duration: The absence of pre-compaction for jet grout columns allows for expedited construction timelines. The utilization of rapid-setting grout mixtures positively impacts the entire project schedule.

3.4.2 Disadvantages Of The Jet Grouting Method

- Elevated Expenses: Jet grouting is generally more costly than several traditional ground improvement techniques owing to the need for specialist high-pressure equipment and significant cement use. Consequently, it is often advised for deployment in essential areas rather than extensive applications.
- High Cost: Jet grouting tends to be more expensive than many conventional ground improvement methods due to the need for specialized high-pressure equipment, significant cement consumption, and skilled labor. As such, it is often recommended for use in critical zones rather than large-scale applications.
- Sensitivity to Operational Parameters: The efficacy of jet grouting is significantly influenced by the meticulous regulation of operational parameters, including injection pressure, withdrawal rate, rotating speed, and mix ratio. Consistent field results need a skilled team and well calibrated equipment.

- Soil Structure Limitations: In soils characterized by a substantial presence of coarse gravel or sizable cobbles, the formation of homogeneous and continuous columns may be challenging. These particles may impede grout flow and undermine column geometry and structural integrity.
- Challenges Associated with Groundwater Conditions: In regions with elevated groundwater levels, grout dispersion may be obstructed, and the injection procedure might result in the leaking of the slurry onto adjacent soils. This may lead to localized softening or loss of structural support in neighboring regions.
- Environmental Considerations: Jet grouting may cause soil displacement and slurry overflow, possibly impacting adjacent structures and subterranean utilities. Consequently, a comprehensive environmental and geotechnical effect assessment is required before execution.
- Challenges in Quality Control and Verification: Assessing the quality of jet grout columns often necessitates coring and testing methodologies, including unconfined compressive strength tests or crosshole procedures. The heterogeneous character of the columns often hampers interpretation, since an individual core sample may not accurately reflect the overall state of the column, resulting in confusion about quality assurance.

In conclusion, while jet grouting offers excellent solutions to many geotechnical challenges due to its many benefits, it requires extensive technical expertise and precise application. Soil parameters, the physical characteristics of the site, and structural requirements must be meticulously evaluated prior to application. The approach should be properly followed to guarantee optimum performance and project success.

3.5 JET GROUT METHOD TECHNIQUES: JET1, JET2 AND JET 3

Jet grouting is a ground improvement technology that utilizes high-pressure injection to form cementitious columns inside the soil bulk. The on-site implementation of this approach necessitates the incorporation of many components, including a cement silo, mixing unit, high-pressure grout pump, air compressor, and the jet grouting rig. Figure 3.3. demonstrates that the manufacturing of jet grout columns typically comprises four primary processes. The initial phase, drilling, entails vertically entering the earth with jet grout drilling apparatus till the specified design depth is attained. Subsequently, in the jetting test phase, system parameters including injection pressure, flow rate, and soil reaction are assessed on-site. This test is essential to assess the soil's response to the jet and to implement required modifications before to full-scale production. Ultimately, in the completion phase, the drilling rod is entirely retracted, allowing the column to solidify. The equipment is thereafter relocated to the next designated site, and the procedure is reiterated in alignment with the project specifications, which delineate the quantity of columns, their classifications (Jet-1, Jet-2, or Jet-3), and their spatial configuration. Ultimately, in the completion phase, the drilling rod is entirely retracted, allowing the column to solidify. The equipment is thereafter relocated to the next designated site, and the procedure is reiterated in alignment with the project specifications, which delineate the quantity of columns, their classifications (Jet-1, Jet-2, or Jet-3), and their spatial configuration. Each column is constructed under stringent regulation of rotation and lifting velocities, which directly influence its geometry and structural integrity. Consequently, field monitoring and testing are elements of the quality assurance protocol in jet grouting operations. Figure 3.3. Schematic depiction of the jet grout column production process: from left to right drilling, jetting test, column formation, and finishing phases. Based on this general manufacturing approach, one of three jet grouting procedures may be chosen according to the soil conditions and technical specifications: Jet-1 (single fluid), Jet-2 (double fluid), and Jet-3 (triple fluid). Each method provides distinct

benefits, equipment arrangements, and applicability across various soil types. The subsequent sections will provide a detailed explanation of these systems.

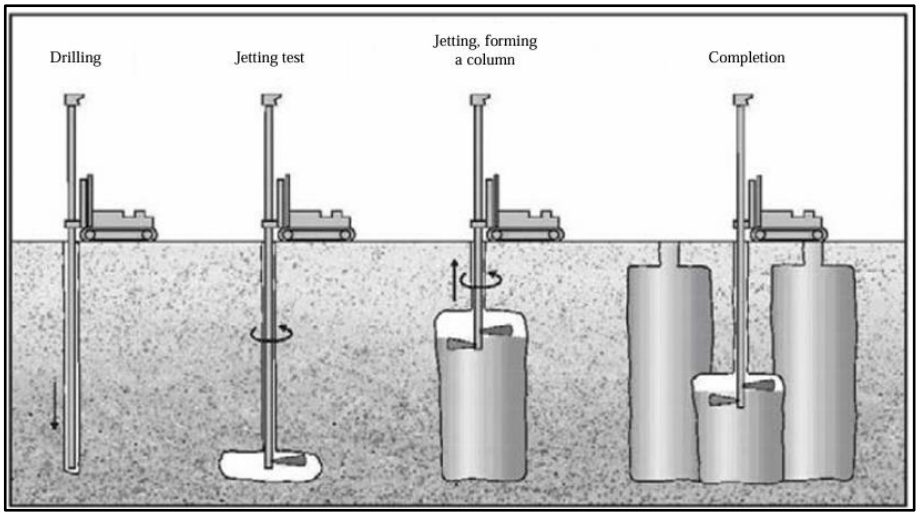

Figure 3.3 Sequence of Jet Grouting Method (Ehsanzadeh, B., & Ahangari, K. 2014.)

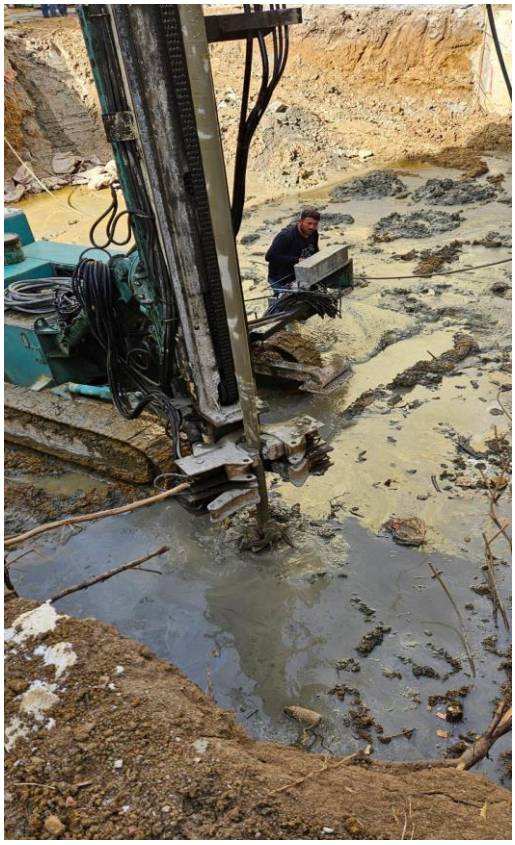

Figure 3.4 Field View of Jet Grouting Application

Figure 3.4. shows the moment when the jet grouting equipment is actively injected into the ground. Thanks to the mortar injected into the ground with high pressure from the monitor tip, mixing and in-situ improvement process is carried out on the ground. Depending on the site conditions, excess grout and fragmented soil mixture can be observed on the ground surface after injection. During the application, the operator controls the diameter, shape and continuity of the column by controlling the injection parameters. This image reflects the application phase of jet grouting column manufacturing and real field conditions.

3.5.1 Jet 1 Single Fluid Jet Grouting

The single-fluid (Jet-1) system is the most straightforward structure among jet grouting systems. This technique relies on the notion of pumping just cement-

based mortar into the ground under high pressure. The jet energy is sufficiently enough to disrupt the natural structure of the ground, with the resultant voids being filled with the same mortar, so enhancing the ground in situ. Despite the apparent simplicity of the application procedure, achieving the desired column quality may be unattainable if executed without the appropriate settings. The injection apparatus employed in the system is rather uncomplicated; typically, a single-walled drill pipe and specialized nozzles at the pipe's terminus are enough. The nozzles typically measure 2.0-2.4 mm in diameter and are arranged symmetrically around the display. The prepared cement slurry is ejected into the floor via these nozzles at a high pressure of roughly 400 bar. The high-velocity jet physically disintegrates and disperses the floor while concurrently filling the vacant space. This mechanism occurs through both shearing and mixing effects.(Figure 3.5;A)

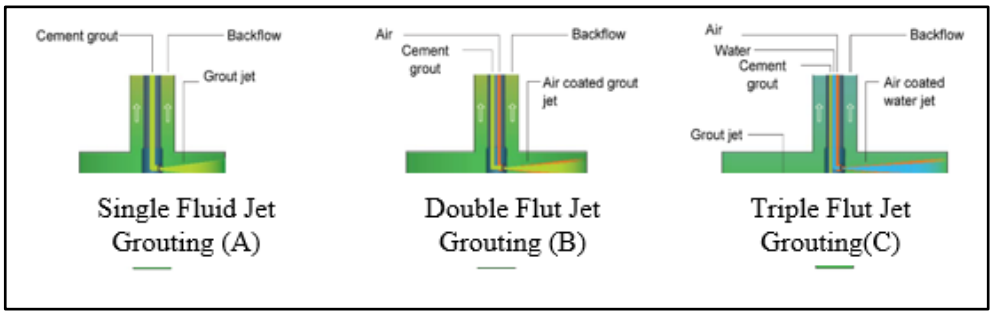

Figure 3. 5 Jet Grout Method Techniques [URL 4]

3.5.2 Jet-2 (Double Fluid) Jet Grouting System

Among the jet grouting techniques, the dual-fluid system (Jet-2) stands out for its capacity to create larger diameter columns. This approach is sometimes referred to as the 'Jumbo Special Pile' method. The main difference from Jet-1 is that a jet of compressed air is introduced into the ground simultaneously with the injection of cement mortar. The use of high pressure air significantly increases the shear energy of the jet, facilitating the creation of larger diameter columns as opposed to the single fluid technique.

The Jet-2 system's monitor (injection head) consists of two concentric tubes. The inner pipe conveys the grout, and the outside pipe transmits compressed air. The interior nozzles dispense the grout, whilst the outside nozzles emit compressed air. The air jet encases the grout jet, functioning as a protective sheath. This arrangement facilitates deeper grout penetration into the soil and enhances the volume of dirt being excavated and mixed (Figure 3.6; B).

The grout is usually injected at a pressure of 400-500 psi, while air is supplied at 7-17 bar. The air jet facilitates the mechanical breakdown of the soil and creates a buffer zone between the grout and groundwater, helping to keep the grout within the designated treatment area. Air also improves waste removal efficiency by vertically transporting dislodged soil particles.

The diameter of the columns created with Jet-2 fluctuates based on soil density and application parameters. In medium-dense soils, column diameters typically measure around 1.0 meter, although in loose, more permeable soils, diameters may extend to 1.4 to 1.8 meters. In documented applications involving sandy soils, injection pressures of around 45 MPa have produced columns up to 1.4 meters in diameter. These applications often utilized 930 kg/m³ of cement, a grout flow rate of 130 L/min, and a unit weight of 16–17 kN/m³ for the grout. This performance underscores the system's efficiency for both compactness and the assurance of comprehensive mixing and uniformity.

Jet-2 is recognized for its superior energy efficiency relative to Jet-1. The air jet aids in maintaining the kinetic energy of the grout jet by minimizing friction losses. It further mitigates turbulence generated by the cutting process, facilitating a more uniform settlement of the grout. These attributes render Jet-2 particularly efficient in silty sands, rigid clays, and diverse transitional soils, where Jet-1 may underperform.

3.5.3 Jet-3 (Triple Fluid) Jet Grout System

Among all jet grouting systems, the triple fluid system (Jet-3) is distinguished as the most intricate regarding both equipment and application methodology. This technology is explicitly engineered to get optimal outcomes

in complex and stratified soil conditions. The operational principle relies on the concurrent execution of three processes: soil disintegration via a high-energy water jet, support by compressed air, and the injection of cementitious grout into the fragmented soil. This enables Jet-3 to execute simultaneous mixing and cutting operations, offering a highly adaptable ground enhancement method.

The apparatus comprises a spray head (monitor) consisting of three concentric pipes. Each pipe conveys a distinct fluid:

- The main pipe transports high-pressure water (400–600 bar).
- The intermediate pipe carries compressed air (7–17 bar).
- The external pipe injects grout at a pressure of 20 to 80 bar into the earth.

The jets are positioned in two distinct zones within the display. The higher jets emit combined jets of water and air to disintegrate the dirt. Simultaneously, the lower nozzles introduce the grout into the created cavities, finalizing the column formation process (see to Figure 3.6;C). Due to this dual mechanism, Jet-3 is effective in both coarse and fine soils.

A key feature of the Jet-3 technology is its capacity to create large-diameter columns. With appropriate parameter regulation, column diameters may attain dimensions ranging from 1200 mm to 2000 mm, and in some loose soils, may even surpass 2 meters. The enlarged diameter results from the elevated physical energy imparted to the soil and the multifaceted characteristics of the jet stream, which improve penetration and distribution efficacy.

Drilling is often executed by rotating the apparatus within the soil. In very compacted or rigid soils, just rotation may be inadequate. In these instances, a combination of rotation and percussion is utilized to finalize the drilling phase. For certain soil types, the monitor is incapable of executing the drilling, necessitating the use of other equipment for pre-boring.

The Jet-3 system's primary benefit lies in its capacity to concurrently adjust to diverse ground conditions. In coarse and permeable soils, the mixing effect prevails, but in cohesive and fine-grained soils, the cutting effect is more pronounced. Consequently, Jet-3 is frequently the favored option for challenging

tasks, including intricate slope stabilizations, impermeable barriers for dams, deep foundation enhancements, and subterranean infrastructure endeavors.

3.6 EQUIPMENT USED IN JET GROUTING METHOD

The effective execution of the jet grouting technique relies not alone on theoretical design but also on the capability and compatibility of the on-site equipment. Jet grouting is a comprehensive procedure that encompasses drilling, high-pressure injection, and the formulation of the injection mixture. To perform this operation efficiently, diverse equipment functions in unison on-site. The following are the primary components often utilized in jet grouting applications:

3.6.1 Drilling Rig

To create jet grout columns, it is essential to bore holes into the ground to the specified depths. This procedure is often executed with rotary or percussive drilling methods. Contemporary drilling rigs may be adapted for vertical or inclined drilling, enabling the installation of columns at the specified orientation.

- Characteristics: Elevated torque capacity, capability to accommodate extended drill rods, and consistent performance.
- Selection Criteria: Must be determined by the prevailing ground conditions. More robust methods are favored for hard rock formations.
- Figure 3.6 shows the jet grout drilling machine in the field environment.

Figure 3.6 Jet Grout Drilling Machine in the Field Environment

The fundamental idea of jet grouting-involving the injection of cement grout at elevated pressure-is executed with these pumps. Various pressure levels are necessitated based on the kind of application (Jet-1, Jet-2, Jet-3). In Jet-3 applications, the injection pressure can attain levels of up to 400 bar.

- Standard Pressure Range: Functions within 200–600 bar
- Flow Capacity: Ranges from 50 to 200 liters per minute
- Figure 3.7 shows the jet grout high-pressure pump unit in the field environment.

Figure 3.7 Jet Grout High-Pressure Pump Unit

3.6.2 Mixing Apparatures

This equipment guarantees the uniform preparation of cement grout or other injection combinations. A dual-stage system is frequently employed:

- Pre-Mixer: The preliminary phase in which dry substances and water are amalgamated.
- Agitator: The phase in which the grout is blended into a uniform and consistent composition.

Inadequate mixing may result in diminished column strength and the creation of heterogeneous soilcrete. Consequently, consistent maintenance and regulation of mixing velocity are important. Figure 3.8 shows the Mixing Apparatus (Mixer) in the field environment.

Figure 3.8 Mixing Apparatus (Mixer)

3.6.3 Cement Storage Silo

Cement for jet grouting applications is typically transported to the site by tanker trucks and stored in vertical silos. The silo delivers cement constantly and reliably to the mixing equipment to guarantee ongoing operation.

- Specifications: Dustproof, often vertical silos with a capacity of 30 to 50 tons
- Equipment: Comprises screw conveyors, pneumatic systems, or vacuum-based feeders.

3.6.4 Water Reservoir With Air Compressor

Water is essential for grout formulation and jetting procedures. In Jet-2 and Jet-3 systems, pressurized air is utilized to facilitate soil decomposition. Consequently, high-pressure air compressors are indispensable.

- Water Tank Capacity: 5 to 10 cubic meters

- Compressor Capacity: A working pressure of 7–10 bar and an air flow rate of roughly 10 m^3/min are adequate.

3.6.5 Control Panel and Automation Systems

Contemporary jet grouting systems are often outfitted with automated injection mechanisms. The control panel allows real-time surveillance of essential parameters:

- Injection Pressure
- Grout discharge rate
- Velocity of rotation and retraction
- Total volume of the injected mixture
- Depth data

Documenting these factors is essential for quality assurance and subsequent assessment.

3.7 OPERATIONAL PARAMETERS IN THE JET GROUTING METHOD

In jet grouting applications, a crucial aspect in attaining the desired column quality and performance is the set of operating parameters utilized during execution. The parameters encompass regulated factors like injection pressure, withdrawal rate, rotational speed, cement dose, and mixing ratios. Each of these parameters directly affects the column's diameter, strength, and uniformity. Consequently, meticulous planning, oversight, and enhancement of these variables are important during the jet grouting procedure.

3.7.1 Injection Pressure And Injection Time

In jet grouting applications, injection pressure is one of the most critical parameters affecting the formation and quality of the column. It usually varies between 200 and 600 bar. Increased injection pressure improves grout penetration into the soil, resulting in a bigger column diameter and enhanced

homogeneity (Karahan, 2015). Qian et al. (2022) noted that an injection pressure of 20 MPa (about 200 bar) produced 1.4-meter diameter columns with markedly enhanced strength properties. Excessively high pressure may result in earth heave or damage to nearby structures (Güler & Seçilen, 2021).

The duration of injection is a critical element influencing column shape. Figure 3.10. demonstrates a distinct correlation among injection time, pressure, and column diameter. At a steady pressure, an increase in injection time results in a proportionate enlargement in column diameter, particularly at intermediate pressures. For example, columns subjected to pressures between 400 and 600 bar exhibit considerable diameter expansion when the injection duration is increased from 4 to 12 seconds. In contrast, brief injection durations typically provide narrower columns, irrespective of the exerted pressure.

This interaction illustrates that both injection pressure and injection time must be concurrently tuned to achieve the requisite column dimensions and mechanical performance. Inadequate management of length may lead to inconsistent columns, diminished grout-soil interaction, and excessive material usage.

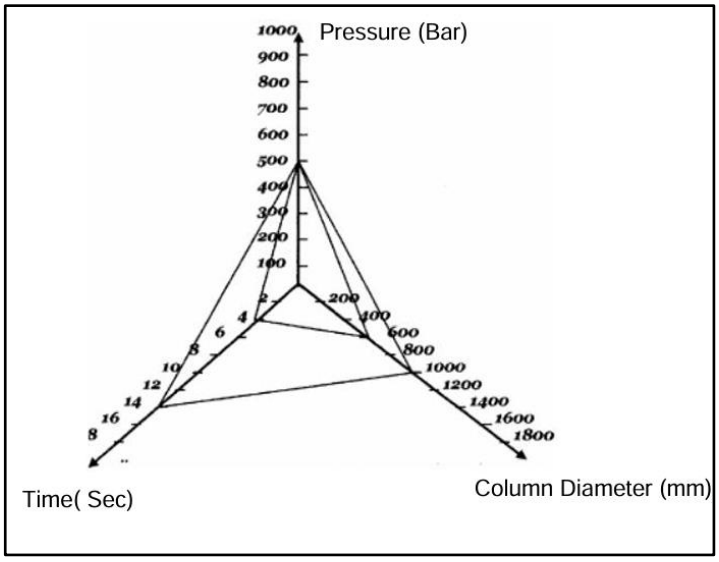

Figure 3.9 Pressure - Dwell Time - Column Diameter Relationship (Melegary and Garassino, 1997)

3.7.2 Withdrawal Rate

The withdrawal rate of the drilling equipment, indicating the upward movement velocity during the grouting operation, directly influences the homogeneity and axial uniformity of the column. A reduced withdrawal rate facilitates the development of thicker and more resilient columns by permitting enough interaction and mixing between the grout and the adjacent soil. A rapid withdrawal may cause inadequate grout dispersion, perhaps leading to weak zones in the column (Erkan & Tan, 2016).

The literature normally defines the optimal withdrawal rate as ranging from 10 to 60 cm/min. Qian et al. (2022) indicated that a withdrawal rate of 0.2 m/min (20 cm/min) produced high-quality columns with superior structural integrity. The withdrawal rate should not be assessed in isolation; it must be analyzed with rotation speed and injection pressure, since these factors are interrelated and together affect the final column shape and strength.

3.7.3 Angular Velocity

Rotation speed is crucial for the uniform distribution of cement grout in the soil and for attaining a constant cross-sectional geometry of the jet grout column. Typically, advised values fluctuate between 5 and 20 revolutions per minute (rpm). Inadequate rotation speed can cause suboptimal mixing and non-uniform columns, whereas too high speeds may decrease column diameter due to insufficient contact time between grout and soil (Ichihashi et al., 1992).

In an experimental investigation, Qian et al. (2022) utilized a constant rotation speed of 10 rpm, which they found to provide an excellent column form and quality. Moreover, it is essential to set an appropriate ratio between rotation speed and withdrawal rate to ensure column continuity and uniformity throughout its depth.

3.7.4 Dosage (Cement Content)

The quantity of cement utilized in jet grouting applications directly affects the strength and impermeability of the resultant column. The research indicates that standard cement doses vary from 350 to 700 kg/m³ (Altun, 2018). Although elevating the dose often enhances compressive strength, exceeding a specific limit may diminish the pumpability of the grout mixture and may not be economically feasible (Karadeniz, 2014).

In loose soils, adequate performance may frequently be attained with reduced cement concentrations, but high plasticity clays typically need increased cement quantities to obtain the appropriate mechanical qualities. Güler and Seçilen (2021) indicated that a dose of 650 kg/m³ achieved an excellent equilibrium between strength growth and workability.

3.7.5 Proportion Of Mixture (Water/ Cement Ratio)

The water-to-cement (W/C) ratio influences both the flowability of the injection mixture and the ultimate strength of the grout column. An elevated water-to-cement ratio enhances the pumpability and injectability of the grout, whereas a reduced ratio yields stronger and denser columns. Literature often reports values between 0.8 and 1.5 (Yilmaz, 2016).

Qian et al. (2022) indicated that a W/C ratio of 1.0 attained an optimal equilibrium between grout flow properties and setting duration, yielding effective performance in field applications. Excessive water content may elevate porosity in the column, thereby diminishing its mechanical strength and long-term durability.

3.7.6 Duration Of Injection

The duration of injection determines the period of grout interaction with the soil, directly affecting the diameter and homogeneity of the resultant column. Extended injection durations enable the jet to influence a broader soil volume, leading to increased column diameters. Nonetheless, prolonged injection may

result in economic inefficiency owing to excessive cement usage and might potentially change the column shape (Shen & Wang, 2013).

The injection duration for an individual jet grout column generally varies from 5 to 20 minutes, contingent upon soil classification and design specifications. If the withdrawal process begins early, the grout may inadequately engage with the surrounding earth, resulting in incomplete columns. Consequently, the injection period must be meticulously adjusted according to site conditions, grout mixture characteristics, and intended column performance.

3.7.8 Injection Flow Rate

The injection flow rate denotes the volume of grout mixture injected into the ground per unit of time, usually measured in liters per minute (L/min). This parameter influences both the rate of column production and the ultimate diameter and strength. In practical applications, injection flow rates typically range from 100 to 250 L/min (Rahmani & Ahangari, 2010).

An increased flow velocity facilitates expedited building and the formation of broader columns. Excessively high flow rates may jeopardize the system's stability, particularly in poor or wet soils. Qian et al. (2022) established that a flow rate of 40 L/min yielded excellent outcomes for column strength and diameter.

Evaluating flow rate alongside injection pressure and grout viscosity is crucial, as these factors are interrelated. Optimizing flow rate based on site-specific variables enhances control over column formation and material efficiency.

3.8 GROUT INJECTION TECHNIQUES IN JET GROUTING APPLICATION

Jet grouting is a soil enhancement method that involves the injection of high-pressure cementitious mixes into the ground, resulting in the creation of

high-strength soil-cement columns by in-situ mixing. The efficacy of the injection procedure is not exclusively dictated by the grout mixture but is also profoundly affected by the injection technique employed. Injection techniques are chosen and modified according to the application's objective, soil characteristics, and local environmental circumstances.

The quality, diameter, continuity, and strength of jet grout columns are primarily influenced by the injection method utilized, along with associated factors and the operational sequence. The primary injection strategies utilized in jet grouting applications are delineated below.

3.8.1 Descending Stage Technique

The descending stage method involves the injection of grout beginning at the borehole's apex and advancing downward in increments. Each phase is grouted prior to advancing drilling to the subsequent depth. This enables the application of elevated grout pressures at greater depths, resulting in improved penetration and increased column diameters in cohesive soils (Choi, 2005; Warner, 2004). A primary advantage of this approach is the capacity to regulate grout dispersion and minimize grout loss. Nonetheless, it necessitates halting the drilling procedure at each phase, potentially resulting in extended building timelines.

3.8.2 Progressive Stage Method

In the ascending stage approach, the borehole is excavated to its entire depth prior to the injection of any grout. The drill string is progressively retracted as grout is injected from the bottom to the top. This guarantees thorough backfilling of the borehole with grout and aids in sealing any cracks created during drilling (Choi, 2005). The benefit is in the upward advancement, which diminishes the likelihood of cavities developing near the surface. Nevertheless, the column height necessitates elevated pressure to transport grout to the top levels, which may prove ineffective in deep or coarse-grained soils (Ismail, 2002; Warner, 2004).

3.8.3 Sequential Injection Technique

Sequential injection denotes the systematic administration of grout in many stages or layers to enhance uniformity or mitigate ground heave. This method is especially advantageous in applications related to ground lifting or settlement remediation, as incremental injections mitigate the danger of abrupt ground displacement (De Mello & Fernandes, 2007). This approach involves for grout to partially cure between injections, resulting in layered soil-grout formations. This procedure improves the overall stability and efficacy of the treated column (Amano & Shibata, 1988).

3.8.4 Circulatory Injection Technique

The circulation injection technique utilizes a closed-loop system that recirculates the grout mixture to avert blockage or solidification within the pipeline. This technique guarantees a steady flow and uniform pressure, which is especially crucial for low-viscosity grouts like silicates or polymer solutions. Circulation facilitates the monitoring of flow rates and the detection of leaks or returns at the surface (Gallavresi, 1992; Bruce et al., 2013). This technology improves operational control, however it is mostly a characteristic of injection logistics rather than a separate grouting process.

3.8.5 Tube-A-Manchette Technique

The tube-à-manchette (TAM) technique employs a perforated pipe equipped with unidirectional valves (manchettes) to execute several injections at different depths within a borehole. Injection is executed using loaders that separate particular sections of the TAM pipe, allowing aimed grout application under regulated pressure (Bello, 1995; Warner, 2004). This technique offers superior control over grout application and is frequently employed in permeation grouting or in broken areas requiring precise sealing.

3.8.6 Silicate Influsion

Silicate injection utilizes low-viscosity sodium silicate solutions, frequently catalyzed by acids or salts to promote gelation. Silicates may infiltrate fine-grained soils because to their superior flow qualities, unlike cement grouts (Karol, 2003). These grouts are economical and non-toxic, rendering them appropriate for transitory uses like as seepage management. Nonetheless, their long-term endurance is constrained by syneresis, leaching, and shrinking (Clough & Kramer, 2006; Gallavresi, 1992). Consequently, silicate grouting is often confined to temporary or non-structural stabilizing activities.

3.8.7 Injection Apparatus And Application Specifications

Jet grouting apparatus generally comprises a high-pressure pump, a revolving drill rig, and a rod fitted with jet nozzles. Pressures ranging from 400 to 600 bar are often utilized, facilitating the creation of soil-cement columns with diameters of up to 2 meters, contingent upon the soil type and employed methodology (Terashi, 2003). Three primary systems are employed: single-fluid (cement slurry alone), double-fluid (cement combined with air), and triple-fluid (water, air, and cement). These changes provide enhanced control over soil excavation and column configuration (Bello, 1995; Warner, 2004). Automated systems regulate rotation and withdrawal rates during jetting, while instrumentation documents grout volume, flow, and pressure for quality assurance (Ismail, 2002). Precise regulation of these parameters is essential for attaining the requisite strength, geometry, and longevity of the treated columns.

3.9 CONTROLS AND TESTS APPLIES IN JET GROUT METHOD

In ground improvement applications performed using the jet grout method, various control and testing procedures are carried out to ensure that the designed columns meet the targeted criteria such as strength, geometry, and continuity. These controls are critically important both for monitoring the quality of the

application and for verifying its compliance with the design. The frequency and method of the tests may vary depending on the characteristics of the application area, the type of soil, and the diameter and length of the columns. The following section presents the most commonly used control and testing methods in jet grout applications.

3.9.1 Jet Grout Field Control

A field test program for jet-grouted trial columns is essential prior to full-scale operations. This experiment involves testing several parameter sets to calibrate the design and establish viability.

During the trial phase, columns are frequently excavated completely or partially (if practicable) to enable direct measurement of diameter and continuity. Croce et al. assert that trial columns should be dug wherever feasible to assess column diameter and verify material continuity. The trial columns undergo sampling and laboratory testing to ascertain their strength; the recorded diameters and strengths thereafter become standards for the production phase (Schneider, 2019). During production, some projects further incorporate confirmatory columns or "monitoring" columns, which are regularly dug or probed to verify that the actual column shape aligns with the design specifications. Saglamer et al. (2002) detail a scheme in which every 20th production column underwent integrity testing, and a sequence of confirmatory 7 m columns was excavated for visual diameter assessments. During column building, builders frequently assess supplementary performance measures. In waterproof applications, monitoring systems may incorporate water pressure and temperature sensors within the excavation throughout the curing of the column (Croce et al., 2014), or utilize vibration and moisture sensors on the drill rod (“rover” approach) to ascertain diameter in real time (Schneider, 2019). Most systems further document ruin volume (returned cuttings) and juxtapose it with the predicted soil volume displaced; a diminished spoil return may suggest inadequate mixing. In summary, field quality control depends on both physical testing of finished columns and ongoing monitoring of execution parameters.

3.9.2 Laboratory Testıng Of Jet-Grout Materıal

Laboratory analyses of jet-grout samples (derived from cores or cast specimens) measure strength and other characteristics. The unconfined compressive strength (UCS) serves as the principal index: cores or molded cylinders undergo uniaxial compression testing following a designated curing period, typically 28 days. Saglamer et al. (2002) extracted cores from every 50th column and conducted ASTM C42 unconfined compression tests on three samples per core, revealing design strengths ranging from 4 to 20 MPa. Gurpersaud et al. similarly describe that spoils and samples from test columns were placed into cylinders for UCS and permeability assessments. Besides UCS, the static elastic modulus (E_{50}) may be obtained from the stress-strain curve, with certain standards defining E_{50} as the secant at 50% of UCS. Direct shear or triaxial tests are seldom conducted because to sample variability, however they may be executed on large laboratory-fabricated specimens when necessary. Cores are assessed visually and by length recovery to evaluate uniformity. Certain standards specify a Uniformity Index as the proportion of the core run that is completely homogenized, eliminating any unmixed soil aggregates. Cores can be photographed or subjected to CT scans to identify interior voids or flaws. Non-destructive testing of cores is occasionally employed; for instance, ultrasonic pulse velocity (UPV) studies on field cores can identify interior cavities or differences in density. Permeability testing is conducted on cured specimens to confirm low conductivity, particularly for barrier applications. Occasionally, laboratory immersion or freeze-thaw durability experiments evaluate the long-term stability of soil-cement; however, these are seldom employed in standard quality control. Laboratory tests primarily aim to verify that jet-grouted soil satisfies the designated strength, stiffness, and homogeneity criteria outlined in the design (Saglamer et al., 2002; Gurpersaud et al., 2013).

3.9.3 In-Situ Testing Of Jet Grout Columns

Multiple in-situ tests are employed to validate column design, continuity, and performance without significant excavation. The most straightforward method is the extraction and measuring of test columns: upon curing, columns may be dug or removed at the surface (if they are shallow) to assess diameter and examine visual quality. When excavation is unfeasible (such as with deep columns or underwater), alternative approaches are required. Conventional instruments comprise caliper logs or mechanical probes (e.g., the "inverted umbrella" or Rover devices) that extend from the column center to measure radius in many directions. Contemporary geophysical techniques are being utilized with growing frequency. Electrical Resistivity Tomography (ERT) in downhole or crosshole seismic applications can delineate column extent. Galindo-Güerros et al. (2015) illustrated the application of crosshole and downhole seismic tomographic imaging to ascertain column diameter, emphasizing that excavation is the most dependable albeit expensive technique. Similarly, Schneider (2019) characterizes vibration monitoring of the drilling rod as a quality-control instrument to deduce column dimensions. Ultrasonic Pulse Velocity (UPV) measurements conducted on drilled cores or permanently placed transducers can identify voids or heterogeneity. As Cinar (2023) observes, UPV serves as a non-destructive method for evaluating grout homogeneity and detecting delaminations inside columns. Column integrity testing, similar to pile integrity testing, is occasionally utilized: Pile Dynamic Analysis or Impulse-Echo tests are utilized on jet columns to detect fractures or vacancies. Nonetheless, results may be challenging to interpret, as jet-soil columns frequently exhibit acoustic qualities like to soil, while toe reflections are feeble. Packer permeability tests are conducted in permeable barriers, where an inflatable packer separates a part of the column, and flow and pressure are recorded to calculate hydraulic conductivity. For instance, Gurpersaud et al. performed in-situ packer testing in test columns to confirm that permeability conformed to design specifications (e.g. $\mathbf{1 \times 10^{-7}}$ cm/s).

3.9.4 Regulated Variables And Their Impact On Quality

The grouting parameters significantly affect column quality. Injection pressure and fluid flow regulate the energy available for soil erosion and mixing; elevated pressure and flow often enhance column diameter and strength (within certain limits). Rotation speed and lift rate dictate the form and consistency: slower rotation combined with faster lifting often results in thicker, more uniform columns, whereas higher lift rates and rotation may provide thin or irregular forms. The design of grout mix (cement content, additives, water/cement ratio) determines the matrix strength: more concentrated mixtures provide stronger soil-cement but may be more difficult to pump. Due to the interaction of these characteristics with soil type, field experiments must optimize them for each location (Bayesteh & Sabermahani, 2019). Contractors systematically measure and document all essential parameters for each column, while the quality control tool links this execution data with the observed outputs (diameter, strength, uniformity).

3.9.5 Homogeneity And Performance Verification

Achieving uniformity of the treated column is a primary quality control objective. Alongside the core-recovery Uniformity Index, non-destructive testing yield valuable insights: UPV and crosshole seismic methods can disclose differences in density or stiffness both longitudinally and transversely inside the column.

Electrical techniques, such as downhole resistivity probes or tomography, are experimental yet hold promise for delineating column geometry and identifying abnormalities (Cinar, 2023; Schneider, 2019). Permeability is essential for performance in several tasks. Alongside the aforementioned packer tests, comprehensive water drawdown tests of excavation pits including jet grouted foundation slabs can verify water-tightness by conducting pressure tests on the barrier. Load-bearing performance is often assessed by settlement or load testing on structures rather than on individual columns; nonetheless, bearing-

capacity calculations are based on column strength and spacing. Quality control ultimately verifies that the grout columns conform to the design parameters for strength, diameter, continuity, and permeability. Croce et al. assert that the attributes of all prototype columns diameter, alignment, strength, etc. must be meticulously monitored to quantify statistical variability, and, if feasible, overall functionality (water tightness, bearing capacity) should be evaluated.

3.10 PREVIOUS STUDIES

Fontanella et al. (2011) investigated the effects of jet grout columns on lateral earth pressure in deep excavations using field observations. The study found that jet grout applications resulted in outward wall displacements rather than the typical inward movements observed in diaphragm walls during excavation. This indicates that jet grout columns may cause distinct behaviors in surrounding structures.

Wong and Poh (2000) evaluated the impact of jet grouting on adjacent soil and structures through field measurements. Their findings showed that jet grouting induced significant bending moments exceeding 1000 kN·m/m' in nearby diaphragm walls, resulting in considerable increases in internal stresses.

Rabaiotti et al. (2015) studied the pre-stressing effects of jet grout slabs formed at excavation bases using field tests. They observed notable increases in soil pressure and internal forces within surrounding diaphragm walls following jet injections. The research demonstrated that jet grouting could transfer load to structures even before excavation begins.

Jiang et al. (2021) examined the impact of jet grout columns installed in groups around tunnel segments on lateral earth pressure. Their study indicated that numerous jet grout columns improved the soil-structure load-sharing mechanism and substantially reduced actual lateral pressures.

Feizi et al. (2024) analyzed the influence of jet grouting parameters on ground movements in soft clay through three-dimensional numerical modeling. They found limited lateral displacements in flat terrain, whereas inclined

surfaces exhibited significantly increased deformation. The importance of injection pressure control was also emphasized.

Yao et al. (2024) compared the "super jet" (SJT) technique with the classical Rodin Jet Pile (RJP) method in terms of lateral soil deformation using field experiments. Results showed that SJT caused notably less deformation, particularly advantageous in group implementations due to minimal impact on surrounding soils.

Brown et al. (1988) conducted full-scale experiments to investigate load-sharing factors within pile groups. The research demonstrated that front-row piles carried a significantly higher load, whereas subsequent rows experienced considerably lower load distribution.

Rollins et al. (1998) conducted full-scale field tests to evaluate the lateral load behavior of pile groups in soft clay. Results indicated that grouped piles experienced higher lateral displacements and bending moments ranging from 50% to 100% greater than individual piles.

Rollins et al. (2006) analyzed the effects of pile spacing on load distribution, finding that increased spacing reduced group interactions significantly. They concluded that group effects become negligible when the spacing exceeds approximately 6–8 times the pile diameter.

CHAPTER 4

4. MATERIALS AND METHOD

In geotechnical engineering, understanding soil behavior and soil-structure interaction commonly requires integrating analytical, empirical, and numerical approaches. Soil exhibits complex mechanical characteristics due to its inherently heterogeneous, anisotropic, nonlinear, multiphase, and porous nature. Within the scope of this thesis, soil parameters were determined from site-specific field investigations and laboratory tests.

Recent advances in computational tools have significantly enhanced the application of numerical methods in geotechnical analyses. Initially, this research presents analytical and empirical formulations addressing the bearing capacity of jet grout columns, group effects, group bearing capacity, block behavior, and settlement characteristics. Furthermore, analytical approaches are employed to evaluate lateral earth pressures acting on diaphragm walls, vertical displacement (settlement), and structural bearing capacity. These analytically derived results serve as benchmarks to verify and validate numerical simulations conducted with the PLAXIS software. Particularly, this verification targets numerical predictions concerning the lateral earth pressures generated by jet grout columns under group interactions. Consequently, the reliability and consistency of numerical findings obtained from PLAXIS, widely adopted in complex soil-structure interaction problems, have been thoroughly assessed through comparison with established analytical solutions from the existing literature.

4.1 ANALYTICAL METHODS FOR JET GROUT COLUMNS

Accurately determining the bearing capacity of jet grout columns is crucial for evaluating their ability to safely transfer loads to the soil under field

conditions. Although several calculation methods are proposed in the literature for determining this bearing capacity, there is currently no universally accepted standard method in geotechnical engineering practice. To accurately estimate the bearing capacity of jet grout columns, a detailed investigation of site-specific soil conditions is essential. This investigation typically includes soil classification (e.g., clay, sand, gravel, silt, rock, etc.), the depth at which the columns will be constructed, and relevant soil strength parameters. Within the scope of this thesis, the bearing capacity of jet grout columns was calculated using the method proposed by Garassino (1997), a widely recognized and accepted approach in the literature. Calculations for soil improvement generally follow two main approaches. The first approach focuses on the bearing capacity of the columns, while the second aims to control settlements within allowable limits. Furthermore, bearing capacity calculations are subdivided into two categories: group bearing capacity of structural elements and block behavior analysis.

4.1.1 Determination Of Bearing Capacity In Group Jet Grout Columns

Jet grout columns exhibit strong interaction with the surrounding soil due to their construction via high-pressure injection techniques. Particularly when implemented in soft or loose soil conditions, these columns typically have higher structural stiffness compared to the native soil. As a result, jet grout columns can effectively bear a substantial portion of the loads imposed on them. Analytical methods similar to those commonly used for pile foundations can be adopted for calculating the bearing capacity of jet grout columns (Garassino, 1997).

$$Q_u = Q_s + Q_b \tag{4.1}$$

Here, Q_s is the bearing capacity derived from the skin friction along the column, while Q_b is the bearing capacity at the base (tip) of the column.

- Calculation of Skin Friction Resistance (Q_s)
- The skin friction resistance (Q_s) is calculated differently depending on thesoil type:

For cohesive soils,

$$\boldsymbol{Q_s = \pi D_{jg} \int_{l_1}^{l_2} a c_u \, dz} \quad (4.2)$$

where:

$\boldsymbol{D_{jg}}$: Diameter of the jet grout column (m)

$\boldsymbol{c_u}$: Undrained shear strength of the soil (kPa)

α : Adhesion factor between soil and column (dimensionless)

$\boldsymbol{l_1}$, $\boldsymbol{l_2}$: Upper and lower depth boundaries of the column (m)

For cohesionless soils,

$$Q_s = \boldsymbol{\pi D_{jg} \int_{l_1}^{l_2} \gamma z K_s} \tan(\delta)\, dz \quad (4.3)$$

where:

$\boldsymbol{\gamma}$: Unit weight of soil (kN/m³)

z: Depth (m)

$\boldsymbol{K_s}$: Coefficient of lateral earth pressure (dimensionless)

δ: Interface friction angle between soil and column surface (°)

Calculation of Tip (End-Bearing) Resistance (Q_b)

- The tip bearing capacity of the column (Q_b) is calculated differently according to the type of soil:

For cohesive soils,

$$Q_b = 9 c_u A_{Jg} \quad (4.4)$$

For cohesionless soils,

$$Q_b = \frac{(1+2K_0)}{2} \sigma'_{v0} N_q \xi A_{Jg} \quad (4.5)$$

A_{Jg}: Base area of the jet grout column

K_0: Coefficient of lateral earth pressure at rest

σ'_{v0}: Effective vertical stress at the base of the column (kPa)

N_q: Bearing capacity factor

ξ: Shape factor

These formulas allow analytical calculation of the bearing capacity of jet grout columns based on site-specific soil conditions and column characteristics (Garassino, 1997).

Jet grout columns, formed by high-pressure injection methods accompanied by vibration, result in compaction of the natural soil surrounding the column. Columns produced by this method typically have irregular cross-sectional shapes with wavy and rough surfaces. This rough surface texture significantly increases the interface contact area between jet grout columns and the soil, particularly in cohesive (clay) or cohesionless soils, resulting in stronger and denser interaction compared to conventionally constructed driven or bored piles.

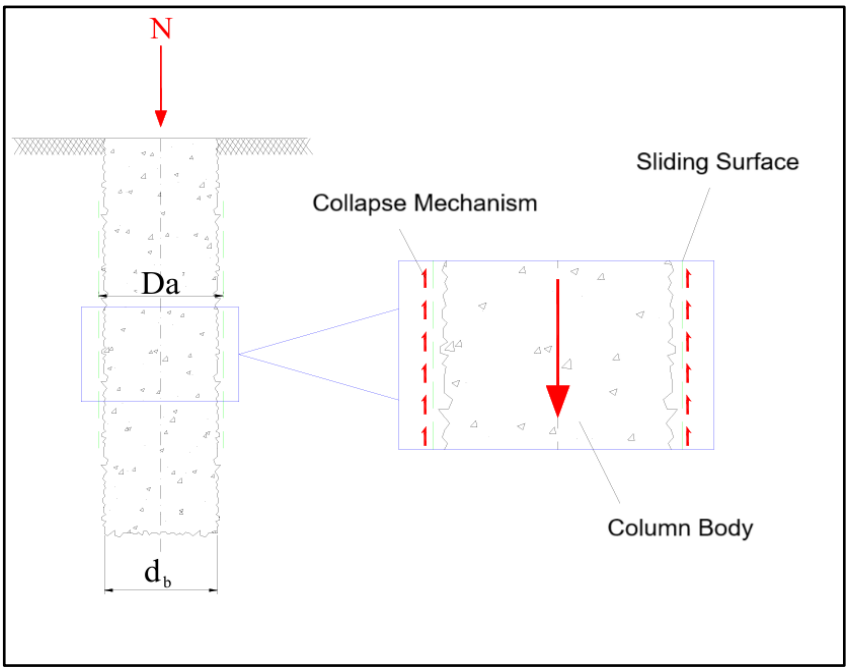

Figure 4.1 Behaviour of the Jet grout column (Garassino, 1997)

Adhesion reduction factor related to the slip surface;

In cohesive soils:

α=1 for normally consolidated soils

α=0.45 for over-consolidated soils

In granular soils:

$Ks > 1$

Determining the column diameter is a critical design parameter and must therefore be approached with great care. The column diameter value used during the design stage should be selected lower than the expected diameter in the field to remain on the safe side. This approach helps reduce uncertainties arising from variations in field conditions, thereby increasing the reliability of the design.

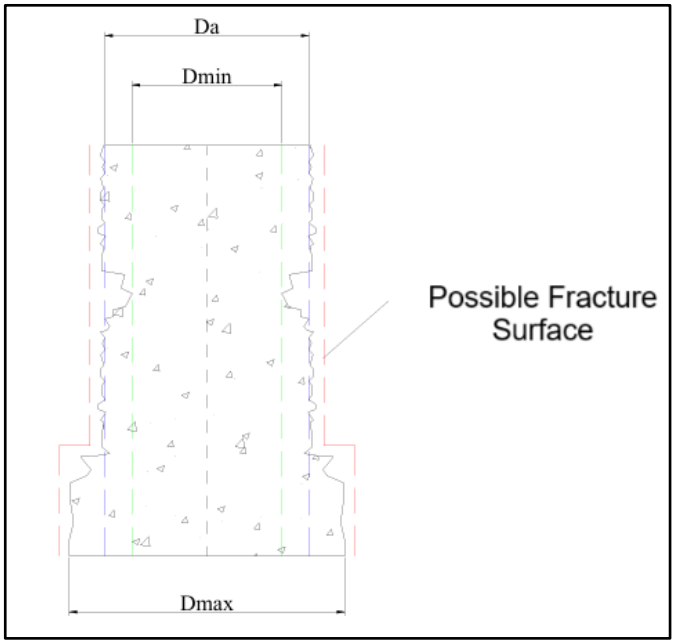

Figure 4.2 Possible slip surface in the Jet grout column manufactured in the ground (Garassino, 1997)

The bearing capacity of jet grout columns is determined by selecting an appropriate column diameter, choosing an adhesion reduction factor (α) of either 0.45 or 1 for cohesive soils, or selecting a lateral earth pressure coefficient (Ks) ranging from 1 to 1.4 for granular soils (Garassino, 1997).

Similar to pile foundations, negative skin friction should also be considered for jet grout columns. As in deep foundations, jet grout columns exhibit strong contact between the column tip and the soil, resulting in a high end-bearing capacity comparable to that of pile foundations.

In properly executed applications, the strength of improved soils can reach values as high as 4 MPa in clays and up to 12 MPa in sandy gravels. By employing pre-washing techniques, particularly in clay soils, even higher strength values can easily be achieved (Garassino, 1997). The settlement required for full mobilization of skin friction in jet grout columns is negligible, and the settlement necessary for complete mobilization of tip resistance is also relatively low (Garassino, 1997).

Table 4.1 Limit Values Used For Column Design In Granular Soils (Garassino, 1997)

Pile Type	Creep Force Reduction Factor		Limit Values for Unit Wall Friction	Tip Power Reduction Factor
	δ/φ	Ks	τ (kPa)	ξ
Bored Pile	0,6	0,5-0,65	100-200	0,33-0,5
Drive Pile (Open End)	2/3	0,65-0,95	100-200	0,7-0,8
Drive Pile (Closed End)	0,75	1,0-1,5	120-180	1
Drive Pile (Closed End)	0,75	1,0-1,5	120-180	1
Jet Grout Cloumn	1	1,0-2	≥180	1

Table 4.2 Limit Values Used For Jet Grout Column Design In Cohesive, I.E. Fine-Grained Soils

Pile Type	Creep Force Reduction Factor		Limit Values for Unit Wall Friction	Tip Power Reduction Factor
	α (Normal Consolidated)	α (Over Consolidated)	τ (kPa)	ξ
Bored Pile	0,9	0,35	275	0,66
Drive Pile (Open End)	0,95e- 0,80i	0,4e-0,35i	200	0,7
Drive Pile (Closed End)	0,95	0,45	200	0,8
Jet Grout Cloumn	1	0,45	280	1

4.1.2 Ground Improvement With Columns Formed In The Ground

Soil improvement is the process of altering the behavioral characteristics of a large soil mass through various techniques. The calculations performed for soil improvement generally involve two fundamental approaches. The first approach focuses on determining the bearing capacity of the improved soil, while the second approach involves block analysis aimed at limiting settlements within acceptable levels.

Bearing capacity calculations are further divided into two sub-categories: group bearing capacity, which evaluates the collective behavior of improvement elements, and block analysis, which considers the overall behavior of the improved soil mass. Through these calculation methods, the general performance and stability of the soil under applied loads can be comprehensively assessed.

4.1.2.1 Group Bearing Capacity Calculation Of Load- Bearing Elements

The bearing capacity of the group is calculated as the sum of the individual bearing capacities of the jet grout columns within the group.

$$P_{ul(grup)} = \beta\, n\, m\, P_{ul\,(column)} \tag{4.6}$$

In the expression above:

$P_{ul(grup)}$: Bearing capacity of the jet grout column group

β : Reduction factor depending on column spacing, column lengths, soil type, and other similar characteristics

n : Number of columns in the horizontal direction

m : Number of columns in the vertical direction

$P_{ul(column)}$: Bearing capacity of a single jet grout column

4.1.2.2 Block Analysis Method

The bearing capacity of the block is determined by treating the group of jet grout columns as a cohesive unit and considering both the frictional forces developed along its side surfaces and the bearing resistance at its bottom surface. Thus, the performance of the column group under loading can be analyzed comprehensively through this holistic approach.

$$P_{ul(grup)} = B.L.Q_b + 2(B+L).(h_2.Q_{12(ort)} - h_1 Q_{11(ort)}) \tag{4.7}$$

In the above expression:

B : Width of the block

L : Length of the block

Q_b : Unit tip bearing capacity at depth H

$P_{ul(grup)}$: Bearing capacity of the jet grout column group

$Q_{12(ort)}$: Average lateral friction value at depth h_2

$Q_{11(ort)}$: Average lateral friction value at depth h_1

h_1 : Thickness of the soft soil layer where negative skin friction may develop

h_2 : Depth of the competent bearing layer into which the columns are fully embedded

If negative skin friction is not present, then it should be assumed that h_1 = 0 and h_2 = H.

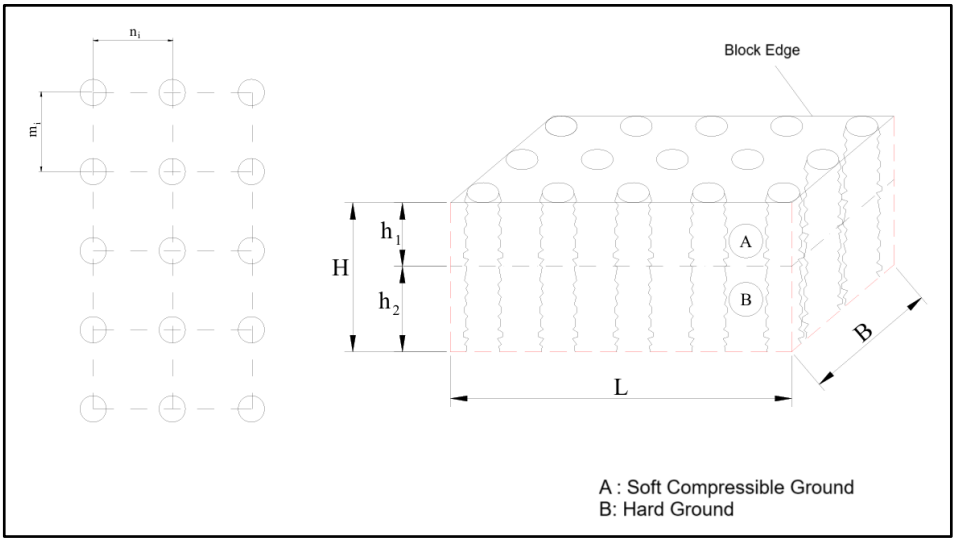

Figure 4.3 Total/block bearing capacity of the soil improved with jet grout columns (Garassino, 1997)

4.1.3 Settlement Analysis Of Jet Grout Columns

The jet grouting technique is an effective ground improvement method widely used to reduce settlement issues by enhancing the mechanical properties of the soil (Melegari and Garassino, 1997). Accurate analysis of the bearing capacity and deformation behavior of soils improved with jet grout columns is crucial. In settlement analysis, elastic settlement and consolidation settlement are generally evaluated (Uzuner, 1985).

Possible scenarios for settlement analysis are presented below;

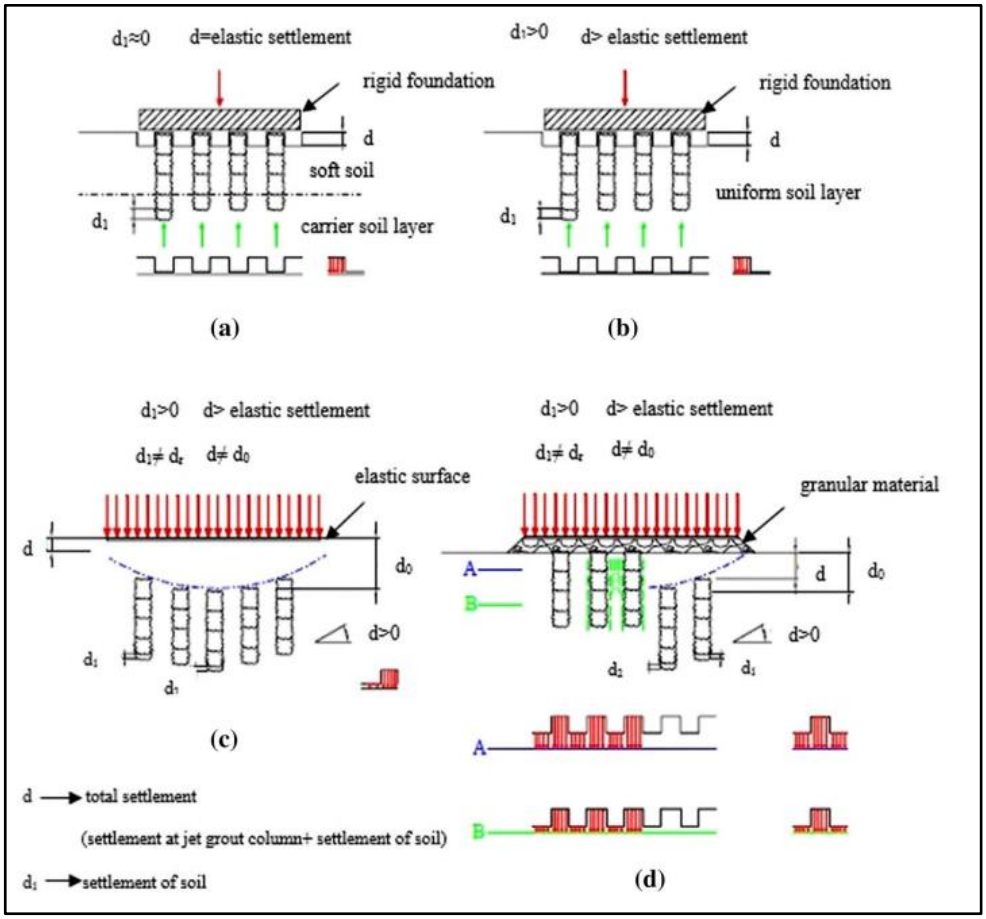

Figure 4.4 Settlements That Can Occur At The Soils Improved By Jet Grout Columns (Garassino 1997)

Based on the studies conducted by Garassino (1997) and Erdil (2008), various possible scenarios that may be encountered during settlement analyses of jet grout columns are presented in Figure 4.4.

As shown in Figure 4.4.A, in cases where the load is transferred to the jet grout columns through a rigid foundation and the tips of these columns are embedded into a competent bearing layer, the entire load is transmitted to this underlying layer by the columns. In such cases, settlements are limited solely to the elastic deformation of the jet grout columns, thus maintaining the potential soil settlements at relatively minimal levels.

As shown in Figure 4.4.B, if the loads are transferred to the jet grout columns through a rigid foundation, but the column tips are not embedded into any bearing stratum, the columns behave like floating piles. In this situation, a significant portion of the load is carried by the jet grout columns, while a smaller portion is transferred to the soil. When the column tips are not seated on a bearing layer, the settlements occurring in the soil exceed the elastic deformation of the columns.

As shown in Figure 4.4.C, if loads are uniformly transferred to jet grout columns through a flexible foundation surface and the column tips are not embedded into a bearing stratum, a large portion of the loads will be carried by the columns, while a certain portion is supported by the soil. In this scenario, settlements occurring within the soil are not homogeneous and vary across different regions, due to the distribution of the load between the columns and the soil.

As shown in Figure 4.4.D, if a granular material layer is present between the load and the foundation system, a significant portion of the load is carried by the jet grout columns, while the remaining portion is supported by the soil. The presence of granular material results in more uniform and consistent behavior of the columns under loading. However, as depth increases, soil stresses are predominantly transferred to the columns, causing the columns to bear loads more effectively compared to the surrounding soil.

4.1.3.1 Elastic Settlement

Elastic settlement refers to the immediate deformation occurring in the soil upon the application of a load, which is largely reversible once the load is removed. Methods employed to calculate this deformation are categorized into three main groups: empirical and semi-empirical methods based on field observations and experimental data, and theoretical methods grounded in analytical principles. These methods are utilized to evaluate soil behavior under loading and to predict potential settlements.

4.1.3.1.i Semi- Empirical Methods

Semi-empirical methods are analysis techniques developed by combining theoretical foundations with field or laboratory test results. In calculating the settlement of jet grout columns or piles using these methods, the total settlement is determined by combining the elastic shortening of the column, deformation occurring in the soil at the column tip, and the frictional effects along the column surface. Particularly in the approach proposed by Poulos and Davis, soil stiffness parameters are directly obtained from field tests such as CPT, SPT, and pressuremeter, resulting in more reliable and realistic assessments that closely represent actual site conditions.

4.1.3.1.ii Empirical Methods

Empirical methods rely entirely on experimental data and field observations. The empirical approach developed by Vesic (1970) calculates the settlement of jet grout columns using the following formula (Melegari and Garassino, 1997).

$$St = \frac{D}{100} + \frac{(Q_{va} L)}{(A_p \, E_p)} \tag{4.8}$$

In the above expression:

St : Total elastic settlement of the jet grout column (m)

D : Column diameter (m)

Q_{va} : Vertical load applied to the column (kN)

L : Column length (m)

A_p : Cross-sectional area of the column (m²)

E_p : Modulus of elasticity of the column (kN/m²)

4.1.3.1.iii Theoretical Methods

Theoretical methods calculate settlement by assuming the soil behaves elastically under loading, based on Hooke's law. The elastic settlement beneath jet grout columns can be theoretically determined using the formulas provided

below. This approach allows for the analytical calculation of settlement values based on the elastic properties of both the column and the soil.

$$\Delta h_e = \frac{\sigma}{E_{JGC}} L \tag{4.9}$$

$$\sigma = \frac{Q_v}{\pi \frac{D^2}{4}} \tag{4.10}$$

Δh_e : Elastic shortening of the column (m)

σ : Stress acting on the column (kN/m²)

L : Length of the column (m)

A: Cross-sectional area of the column (m²)

E_{JGC} **:** Modulus of elasticity of the jet grout column (kN/m²)

4.1.4 Group Effect In Jet Grout Columns

Jet grout columns demonstrate the "group effect," a notion initially recognized in experimental investigations of traditional pile groups (Converse & Labarre, 1932) and later modified for various soil conditions and ground enhancement methods (Tan et al., 2014). The group effect refers to the alterations, either beneficial or detrimental, in the total load-bearing capacity or settlement performance when individual columns function collectively in a grouped arrangement. The presence and extent of the group effect are often assessed by empirical formulations and sophisticated numerical modeling techniques, enabling a thorough evaluation of group interaction processes across diverse geotechnical situations.

4.1.4.1 Area Replacement Ratio

The first dimensionless parameter commonly used to evaluate the effectiveness of column groups beneath a foundation is the area replacement ratio. This parameter is defined as follows:

$$AF = \frac{\sum Ac}{A_f} \tag{4.11}$$

where;

Ac = cross-sectional area of a single jet grout column,

$\sum Ac$ = total cross-sectional area of all columns,

A_f = area of the foundation.

An increase in the area replacement ratio generally indicates a higher degree of ground improvement and a more pronounced group effect (Tan et al., 2014).

4.1.4.2 Group Efficiency

The aggregate load-bearing capacity of pile or column groups, relative to the cumulative capabilities of individual elements under equivalent conditions, is measured by the group efficiency (η). The concept initially suggested by Converse & Labarre (1932) is articulated as follows:

$$\eta = \frac{Q_{group}}{n \times Q_{single}} \tag{4.12}$$

where;

Q_{group} = Total load-bearing capacity of the column group,

Q_{single} = Load-bearing capacity of a single column,

η= Number of columns in the group.

A more practical version of this formula, frequently used in engineering applications, is given by:

$$\eta = 1 - \left[\frac{(n_1-1)n_2+(n_2-1)n_1}{90\ x\ n_1 x n_2}\right] \times Q \tag{4.13}$$

$$Q = \tan^{-1}(\frac{D}{S}) \tag{4.14}$$

where:

n_1, n_2 = Number of columns in each row and column, respectively,

D = Diameter of each column,

S = Center-to-center spacing between columns.

If the group efficiency η is significantly less than 1, a negative group effect is present; if it is close to 1, the group effect can be considered negligible; and if it exceeds 1, a positive synergy within the group is indicated (Pratama et al., 2023).

4.1.4.3 Settlement Improvement Factor (N)

The group effect can also be assessed based on the improvement in settlement (vertical displacement) performance. The settlement improvement factor (n) is defined as follows (Tan et al., 2014):

$$\eta = \frac{s_0}{s_1} \tag{4.15}$$

where:

s_0 : Settlement of the unimproved soil,

s_1 : Settlement of the soil improved with a group of columns.

If the value of n is close to 1, the group effect is limited; as n increases, the columns are seen to reduce settlement more significantly. In practice, a value of n > 1.1 is considered to indicate a meaningful group effect.

4.2 ANALYTICAL METHODS FOR RETAINING WALLS

4.2.1 Lateral Earth Pressures

One of the most critical parameters to consider in the engineering design of soil-structure interaction systems is lateral earth pressure. Lateral earth pressure is defined as the horizontal stress exerted by a soil mass and plays a decisive role particularly in the design of retaining walls, excavation support systems, basement walls, and similar structures.

The total lateral earth pressure acting on a structure generally consists of two components: static and dynamic. Static pressures develop under natural conditions due to the self-weight of the soil and the movement of the structure; whereas dynamic lateral earth pressures are mostly caused by transient effects such as earthquakes, traffic loads, or machine vibrations, and can directly influence the seismic performance of the structure. Static lateral earth pressures are evaluated under three different conditions depending on the horizontal displacement between the soil and the structure:

- At-rest condition (K_0 state): The soil mass does not exhibit any horizontal deformation. In this case, the lateral pressure is expressed as a proportion of the vertical stress only.
- Active condition (K_a state): When the wall moves away from the soil mass behind it, the soil starts to relax and mobilizes its shear strength, resulting in the minimum lateral pressure.
- Passive condition (K_p state): When the wall moves towards the soil, the soil becomes compressed and, with full mobilization of shear resistance, the maximum lateral pressure is developed.

These circumstances are schematically depicted in Figure 4.1. In the illustration, when a stiff wall shifts to the right, an active zone emerges on the left surface, while a passive zone forms on the right side owing to soil resistance. The orientation of wall movement is a critical factor that directly influences the distribution of soil stresses.

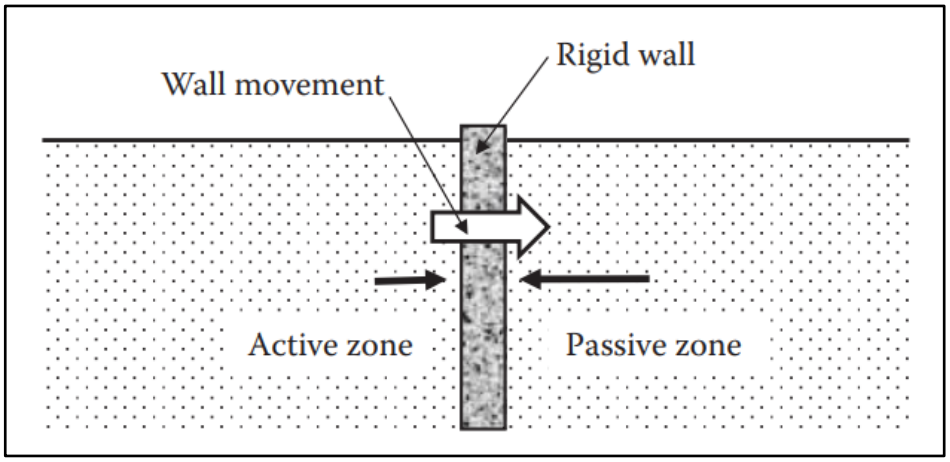

Figure 4.5 Lateral Earth Pressure Conditions

To accurately use lateral earth pressure theories in engineering design, it is crucial to comprehend the interaction mechanisms and the conditions that give rise to these stresses. This section will first elucidate the essential principles of lateral earth pressure, followed by a detailed presentation of the classical theories

developed by Rankine (1857) and Coulomb (1776). Given that these theories were formulated on assumptions applicable specifically to cohesionless, homogeneous, and isotropic soils, the engineering ramifications of these assumptions will also be assessed in the pertinent parts. The objective is to evaluate lateral earth pressure using both analytical theories and contemporary numerical methods, so creating a theoretical basis for the safer and more realistic design of soil-structure interaction systems.

4.2.1.1 Lateral Earth Pressure At Rest (K_0)

Lateral earth pressure at rest occurs when no horizontal deformation takes place in the soil, meaning there is no relative movement between the soil and the structure. In this case, the horizontal stress in the soil is evaluated as a proportion of the vertical stress. The horizontal stress is expressed as follows:

$$\sigma'_h = K_0 \cdot \sigma_v \tag{4.11}$$

Here, σ_v is the vertical stress, and K_0 is the coefficient of lateral earth pressure at rest. The empirical relationship proposed by Jaky (1944) for cohesionless and drained soils is given below:

The formulas used for normally consolidated sands and consolidated clays are presented in Equations 4.2 and 4.3, respectively.

$$K_0 = 1 - \sin(\phi) \tag{4.12}$$

$$K_0 = 0.19 + 0.233 + \log(PI) \tag{4.13}$$

The formulas used for overconsolidated soils are provided in Equation 4.4.

$$K_0 = (1 - \sin\phi)(OCR)^{\sin\phi'} \tag{4.14}$$

In these equations, ϕ represents the internal friction angle of the soil. The at-rest condition is particularly valid in cases where the wall does not exhibit any horizontal movement. (Jaky, J., 1944).

4.2.1.2 Rankine's Active And Passive Earth Pressure Theory

One of the most widely used theories in lateral earth pressure analysis is Rankine's Theory, first introduced by William John Macquorn Rankine in 1857.

This approach is based on the assumption that soil behaves in a non-elastic (plastic) manner and allows the analytical calculation of lateral earth pressures through a set of simplifying assumptions related to stress conditions.

Although the Rankine theory was initially developed only for cohesionless soils (where c = 0), it was later expanded to include the effects of cohesion in the formulations. In this way, the theory became applicable to both homogeneous and cohesive soils from an engineering perspective.

The method developed by Rankine provides a practical approach particularly for the calculation of active (Pa) and passive (Pp) earth pressure conditions. According to this theory, it is assumed that the minimum lateral stress in the soil occurs under active conditions, while the maximum lateral stress occurs under passive conditions. Rankine reached this conclusion by analyzing the stress distribution within the soil using Mohr's circle.

4.2.1.2.i Rankine Theory-Active Earth Pressure

For the calculations made using the Rankine method to be valid, the following conditions must be satisfied:

The soil mass must be homogeneous and isotropic, meaning that the cohesion, internal friction angle, and unit weight of the soil are constant throughout the entire mass. The wall surface is assumed to be smooth and rigid, and the back of the wall is vertical and planar. No wall-soil interface friction is considered ($\delta = 0$).

The ground surface is horizontal, and due to loading, only normal stresses are generated; shear stresses are neglected. If the wall moves away from the soil, active earth pressure develops; if it moves toward the soil, passive pressure develops.

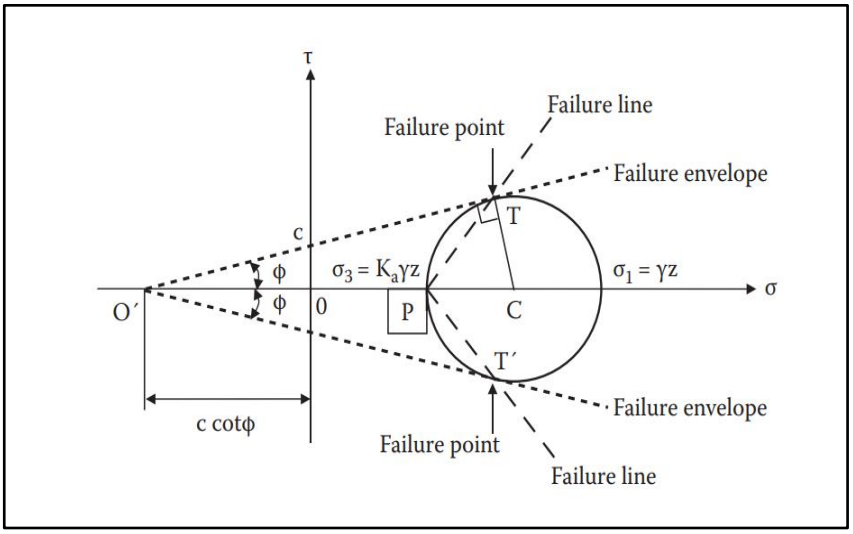

Figure 4.6 Explanation of Rankine Active Earth Pressure with the help of Mohr's Circle

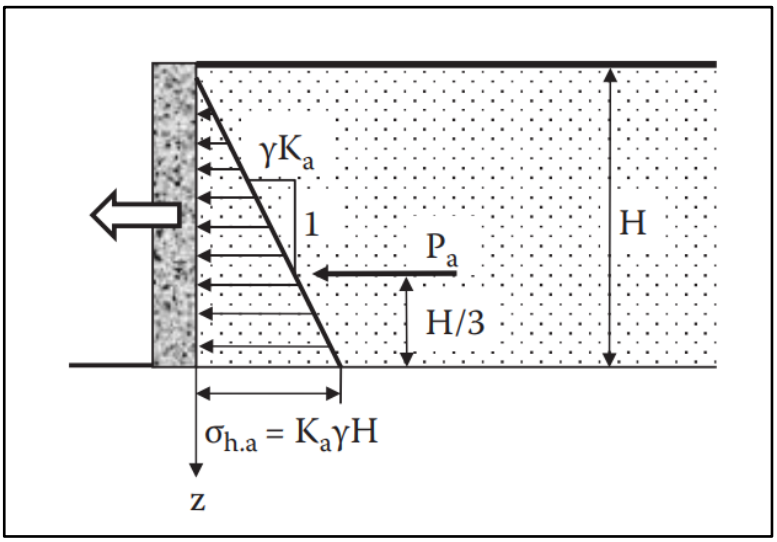

Figure 4.7 Rankine's Theoris Distribution and Composition of Active Lateral Earth Pressure

The stress distribution is defined using the Mohr-Coulomb failure envelope.

Rankine's theory, based on the plastic behavior of soil, allows for the analytical calculation of lateral earth pressure. In this theory, stress analysis is carried out using Mohr's circle, and the active failure plane formed within the soil mass is considered. As shown in Figure (4.6), active lateral stress develops at the point where the Mohr circle becomes tangent to the failure envelope, indicating that the shear strength of the soil has been mobilized. This condition occurs when the wall moves away from the soil mass behind it (i.e., when it displaces outward).

Determination of the failure plane angle;

The inclination of the active failure plane within the soil is theoretically defined as follows:

$$\boldsymbol{\theta_a = 45^0 + \frac{\emptyset}{2}} \tag{4.15}$$

This expression is derived from the geometric relationship between Mohr's circle and the shear strength plane of the soil (Figure 4.2). Shearing that occurs along this plane mobilizes the shear strength of the soil, leading to the development of active conditions.

In cohesive soils, the active lateral earth pressure can be calculated using the following general equation, derived through analysis on the Mohr's circle:

$$\boldsymbol{\sigma_a = \gamma.z \cdot tan^2\left(45^o - \frac{\phi}{2}\right) - 2c\,.tan^2\left(45^o - \frac{\phi}{2}\right)} \tag{4.16}$$

In this equation:

- γ: Unit weight of the soil (kN/m³),
- z: Depth (m),
- ϕ: Internal friction angle (°),
- c: Soil cohesion (kPa)

As shown in the expression above, when the cohesion ccc is greater than zero, an additional resistance develops against lateral pressure, which leads to a reduction in active pressure. Equation (4.16) can also be expressed in its more common form as follows:

$$\boldsymbol{\sigma_a = \gamma.z \cdot k_a - 2c.\sqrt{K_a}\ \ ile\ \ K_a = tan^2\left(45^o - \frac{\phi}{2}\right)} \tag{4.17}$$

This formula represents the classical form of Rankine's theory developed for cohesive soils.

4.2.1.2.ii Tension Crack Zone

Since soil exhibits limited resistance to tensile stress, negative pressures may develop near the surface (particularly at z=0) in cohesive soils. This condition is referred to as the tension crack zone, where active lateral pressure is assumed to be zero.

$$\boldsymbol{z_0} = \frac{\boldsymbol{2c}}{\boldsymbol{\gamma \cdot tan\left(45^0 - \frac{\phi}{2}\right)}} \tag{4.18}$$

In this zone, the soil cannot sustain tensile stresses; therefore, the active lateral pressure is considered zero, and the pressure distribution begins from a certain depth $\boldsymbol{z_0}$.

4.2.1.2.iii Total Active Lateral Force (Cohesive Soils)

Taking the tension crack zone into account, the effective pressure distribution is assumed to be triangular, and the total active force $\boldsymbol{P_a}$ is calculated as follows:

$$\boldsymbol{P_a = \frac{1}{2}[\gamma(H - z_0)K_a - 2c(H - z_0).\sqrt{K_a}]} \tag{4.19}$$

Here:

- H: Height of the wall
- $\boldsymbol{z_0}$: Depth of the tension crack zone

The resulting total force acts at a distance of $(\boldsymbol{H - z_0})/3$ from the base of the wall.

4.2.1.2.iv Passive Lateral Earth Pressure According To Rankie Theory

In soil-structure interaction, passive lateral earth pressure represents the maximum lateral resistance that develops when a structure is pushed into the soil. This condition typically occurs in scenarios where structural elements such as retaining walls move backward, i.e., toward the soil. In response to this

compressive movement, the soil fully mobilizes its internal shear strength to resist deformation.

Rankine's theory idealizes this behavior mathematically, enabling the estimation of lateral stresses in the passive state.

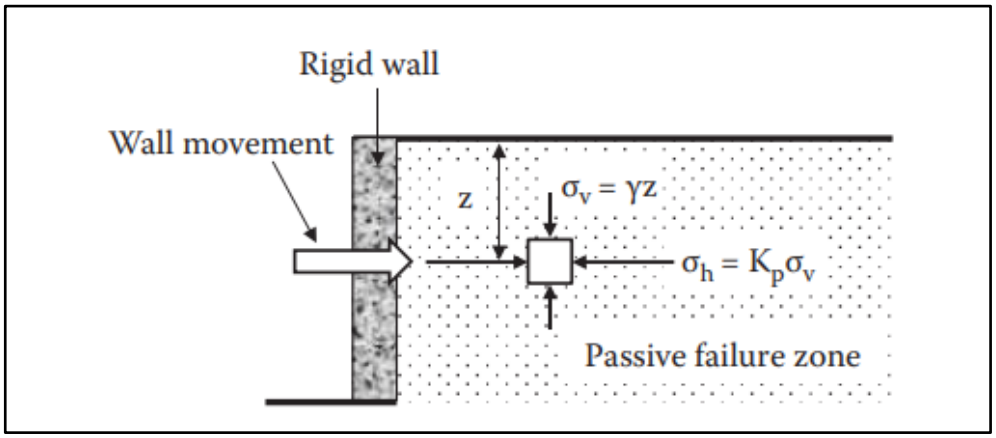

Figure 4.8 Passive Earth Pressure Distribution on a Rigid Wall According to Rankine's Theory

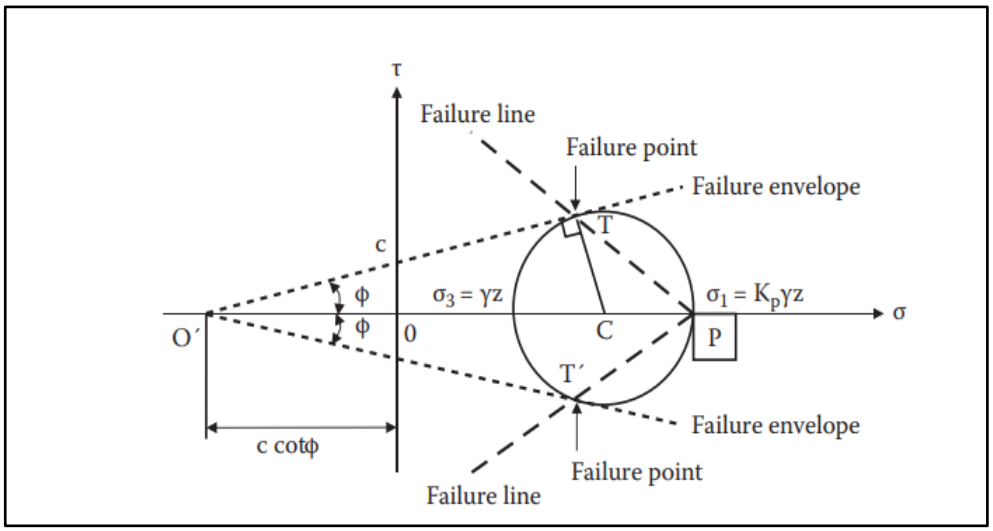

Figure 4.9 Mohr-Coulomb Failure Criterion for Passive Earth Pressure (Rankine's Theory)

Unlike active pressure, passive pressure represents a condition in which the soil is compressed rather than expanded. In this case, Rankine's theory assumes that the soil mass reaches a limiting state where the major principal stress occurs in the horizontal direction. According to this approach, the vertical stress $\boldsymbol{\sigma_a = \gamma.z}$ is taken as the minor principal stress (σ_3), while the horizontal stress $\boldsymbol{\sigma_a = \sigma_1}$ becomes the major principal stress.

Under these assumptions, the passive lateral earth pressure is expressed as:

$$\boldsymbol{\sigma_{h,p} = \gamma.z \cdot tan^2\left(45^o + \frac{\phi}{2}\right) = \gamma.z \cdot K_p} \quad (4.20)$$

This equation clearly reveals the relationship between the soil's internal friction angle (ϕ) and its passive lateral resistance. An increase in the friction angle enhances the soil's ability to generate higher passive resistance.

Effect of Cohesion If the soil cohesion c is greater than zero, it contributes to the passive lateral pressure, and the equation is updated as follows:

$$\boldsymbol{\sigma_{h,p} = \gamma.z \cdot K_p + 2c.\sqrt{K_p}} \quad (4.21)$$

The contribution of cohesion is generally more pronounced near the surface. In practice, this implies a stronger bond between the wall and the soil, which is especially observable in piled systems. However, it should also be noted that under site conditions, the beneficial effect of cohesion can be significantly reduced if cohesive soils become saturated with water.

Passive pressure increases linearly with depth and is typically assumed to have a triangular distribution. The total passive force $\boldsymbol{P_p}$ is calculated as the area of this triangular pressure distribution:

$$\boldsymbol{P_p = \frac{1}{2} K_p.\gamma.H^2} \quad (4.22)$$

The point of application of this force is located at a distance of H/3 from the base of the wall.

When cohesion is present, the passive pressure distribution consists of both triangular and rectangular components. In such cases, the total passive force $\boldsymbol{P_p}$ is calculated as the sum of these two components:

$$\boldsymbol{P_p = P_{p,1} + P_{p,2}} \quad (4.23)$$

$$\boldsymbol{P_{p,1} = 2c \cdot \tan\left(45^o + \frac{\phi}{2}\right).H}\text{(quadrilateral area)} \quad (4.24)$$

$$\boldsymbol{P_{p,2} = \frac{1}{2}.\gamma.H^2(tan^2 45^o + \frac{\phi}{2})}\text{ (triangle area)} \quad (4.25)$$

The points of application of the passive pressure components are determined based on the geometry of the pressure distribution: the rectangular component acts at a distance of H/2 from the base of the wall, while the triangular component acts at H/3 from the base.

4.2.1.3 Coulomb' s Lateral Earth Pressure Theory

In lateral earth pressure calculations, another classical method based on equilibrium analysis along a potential failure plane is Coulomb's theory. This theory was developed in 1776 by Charles-Augustin de Coulomb and is based on modeling the soil as a sliding wedge. The Coulomb approach offers more realistic results compared to Rankine's theory, particularly by taking into account the wall-soil interface friction (δ) and the inclination of the backfill surface (β).

The main assumptions of Coulomb's theory are as follows: the soil is homogeneous, isotropic, and generally cohesionless; however, the effect of cohesion can be included when necessary. Soil-structure interaction is assumed to be undrained (instantaneous loading). The soil mass behind the wall is modeled as a triangular sliding wedge, with the base of the wedge extending from the base of the wall at a certain angle into the soil. Both the interface friction (δ) between the wall and the soil and the inclination (β) of the backfill surface are considered in the analysis. (Yildiz, M. C., 2015).

4.2.1.3.i Coulomb Active Lateral Earth Pressure

In Coulomb's active pressure approach, when the wall moves sufficiently away from the soil, an active wedge (ABC) forms within the soil mass (see Figure 4.6). Only three forces act on this wedge: the self-weight of the soil (W), the horizontal reaction force exerted by the wall on the soil (Pa), and the resisting force (R) developed along the failure plane.

The equilibrium of these three forces is represented by the closure of the force polygon, indicating that the wedge is in a limit state of stability. This graphical representation is essential in determining the magnitude and direction of the active earth pressure.(Ishibashi & Hazarika, 2005).

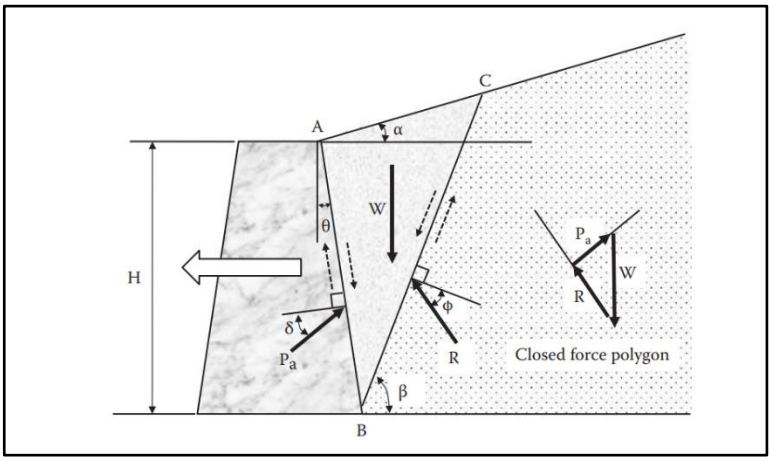

Figure 4.10 Formation of Active Lateral Earth Pressure and Sliding Wedge Model According to Coulomb's Theory. Coulomb's active earth pressure (Ishibashi & Hazarika, 2005

Coulomb assumes that the direction of the maximum resisting force, which prevents movement along the failure plane, aligns with the soil's internal friction angle ϕ. On the other hand, the direction of the active force applied to the wall surface is defined by the wall-soil interface friction angle δ. Under these conditions, the active earth pressure can be expressed as follows:

$$\boldsymbol{P_a = \frac{1}{2}\gamma.H^2.Ka} \tag{4.26}$$

$$\boldsymbol{K_a = \frac{cos^2(\phi-\theta)}{cos^2\theta\cdot\cos(\delta+\theta)\left[1+\sqrt{\frac{\sin(\delta+\phi).\sin(\phi-\beta)}{\cos(\delta+\theta)\cos(\theta-\beta)}}\right]^2}} \tag{4.27}$$

Here, $\boldsymbol{K_a}$ is the Coulomb active earth pressure coefficient, which is determined based on parameters such as the backfill slope (β), wall inclination (θ), soil internal friction angle (ϕ), and the wall-soil interface friction angle (δ).

According to Ishibashi & Hazarika, in Coulomb's analysis, the point of application of the active force $\boldsymbol{P_a}$ is located at one-third of the wall height (H/3) from the base. However, the authors describe this as "merely an assumption proposed by Coulomb" and emphasize that this assumption is valid only under specific wall movement conditions.

4.2.1.3.ii Coulomb Passive Lateral Earth Pressure

In the passive case, the wall is pushed toward the soil, and the soil wedge is compressed backward. In this scenario, the forces R (resisting force) and $\boldsymbol{P_p}$ (passive pressure) act on opposite sides of the wedge surface, as the soil is being compressed by the wall. Similar to the active case, Coulomb derived the solution for passive earth pressure using a closed force polygon and a failure plane approach.

The passive lateral earth pressure is expressed as follows:

$$\boldsymbol{P_p} = \frac{1}{2}\boldsymbol{\gamma}.\boldsymbol{H^2}.\boldsymbol{Kp} \tag{4.28}$$

$$\boldsymbol{K_P} = \frac{\boldsymbol{cos^2(\phi - \theta)}}{\boldsymbol{cos^2\theta \cdot cos(\delta - \theta)\left[1+\sqrt{\frac{\sin(\delta+\phi).\sin(\phi+\beta)}{\cos(\delta-\theta)\cos(\beta-\theta)}}\right]^2}} \tag{4.29}$$

Here, $\boldsymbol{Kp}$ is the passive earth pressure coefficient, and similar to the active case, it is influenced by various angles such as the backfill inclination (β), wall inclination (θ), internal friction angle (ϕ), and wall-soil friction angle (δ). According to the definition by Chang-Yu Ou, this force is also determined using the closed force polygon principle, and different values of β are tested to identify the minimum value of $\boldsymbol{P_p}$. This ensures that the maximum passive pressure acting on the wall is conservatively estimated.

In both active and passive cases, the point of application of the total lateral force obtained through Coulomb's theory is commonly assumed to be at one-third the height of the wall (H/3). However, this is not a fixed physical reality but rather an engineering assumption. Particularly in the passive case, the reversed movement of the failure wedge and the influence of surface inclinations can alter the distribution and application point of this force.

4.2.1.4 Comparative Analysis Of Rankie And Coulomb Lateral Earth Pressure Theories

The two primary classical methodologies for assessing lateral earth pressure in the construction of retaining structures are Rankine's theory (1857) and Coulomb's theory (1776). While both methods seek to quantify lateral stresses within the soil mass, they markedly diverge in their assumptions, calculation techniques, and areas of applicability.

4.2.1.5 Conceptual Framework

Rankine's hypothesis is founded on stress analysis. The allocation of stresses in the soil is shown using Mohr's circle and stress planes. This methodology presumes the absence of friction at the wall-soil contact and considers the earth as a free body devoid of structural support behind it. Consequently, Rankine's hypothesis is best applicable to vertical walls featuring smooth surfaces and horizontal backfills.

Coulomb's theory, in contrast, relies on force equilibrium and is regarded as an energy-based approach. The soil behind the wall is represented as a sliding wedge, with the vectorial equilibrium of all forces acting on this wedge preserved. The Coulomb method clearly considers wall inclination, backfill slope, and wall-soil contact friction, rendering it more applicable to constructions with intricate geometry. A fundamental distinction between the theories is to their treatment of soil-structure friction. Rankine's hypothesis entirely disregards the contact friction angle (δ). This simplification may compromise accuracy, particularly when the wall surface is uneven. Coulomb's theory directly integrates contact friction into its calculations, producing more realistic outcomes. A significant divergence emerges in the management of backfill slope. Rankine's methodology presupposes a horizontal backfill and possesses restricted capacity to simulate sloped surfaces. Coulomb's hypothesis, by accommodating diverse backfill inclinations (β), demonstrates more adaptability to actual site circumstances.

The two theories diverge in their assumptions on wall geometry. Rankine's theory is applicable just to vertical and smooth walls, while Coulomb's theory accommodates inclined and uneven surfaces, rendering it a more favored approach in the construction of inclined retaining structures. From an analytical perspective, the two methodologies vary fundamentally. Rankine's technique employs stress-based analysis through Mohr's circle to assess the major stresses in the soil and ascertain the lateral pressure. Coulomb's technique, conversely, relies on the idea of force equilibrium and assesses the stability of a soil wedge under the influence of three forces.

Rankine's theory is frequently employed in early designs or instructional contexts because to its simplicity, minimal parameter requirements, and efficiency. Coulomb's theory, because to its heightened sensitivity to diverse factors, is favored under intricate field settings, facilitating more precise and dependable evaluations. Ultimately, although both models presuppose a triangular distribution of lateral pressure, elements such as backfill tilt, wall roughness, and interface friction in the Coulomb model might modify the configuration of this distribution. This underscores the necessity for more meticulous evaluation when employing Coulomb's technique in design.

The selection of an appropriate theory for engineering practice should be contingent upon the project's geometry, the characteristics of the soil profile, and the anticipated deformation behavior. Rankine's theory presents a rapid solution under ideal circumstances, but Coulomb's theory delivers a more thorough solution that accurately mirrors field conditions.

4.2.2 Stability Anaylsis Of Retaining Walls

Retaining walls must satisfy several stability criteria to safely retain the soil behind them under various load conditions. In the design of retaining walls, the initial step involves identifying the loads acting on the wall, followed by preliminary dimensioning. After this initial dimensioning, internal and external stability analyses must be performed to ensure the wall's safety and performance. External stability analyses include checks against overturning, sliding, bearing

capacity of the foundation soil, and excessive settlement. Internal stability analyses verify whether the shear forces, normal forces, and bending moments within the wall body and foundation produce stresses that can be safely resisted by the construction materials. These analyses utilize well-established geotechnical principles, including formulas, safety factors, and methods recommended by national and international standards (Eurocode, ACI, TS500/TS7994, TBDY). Ultimately, these checks ensure that the retaining wall remains stable and safely performs its intended function throughout its lifespan.

4.2.2.1 Safety Check Against Overturning In Retaining Wall

Overturning refers to the tendency of retaining walls to rotate forward around the toe (the front-bottom edge) under lateral earth pressures and other external loads (Figure 4.11). The wall's safety against overturning is assessed by comparing the sum of resisting moments around the toe to the sum of overturning moments acting around the same point. Overturning moments arise primarily from the active horizontal earth pressures behind the wall. In contrast, resisting moments originate from the wall's self-weight, the weight of soil above the heel, the vertical component of active earth pressure, and passive earth pressure acting in front of the wall toe. Many national and international standards specify a minimum overturning safety factor of 1.5 for static conditions. For example, Turkish Standard TS 7994 (1990) sets this value as the basic requirement for cantilever retaining walls. Meeting or exceeding this safety factor indicates that the retaining wall has adequate stability against overturning throughout its service life.

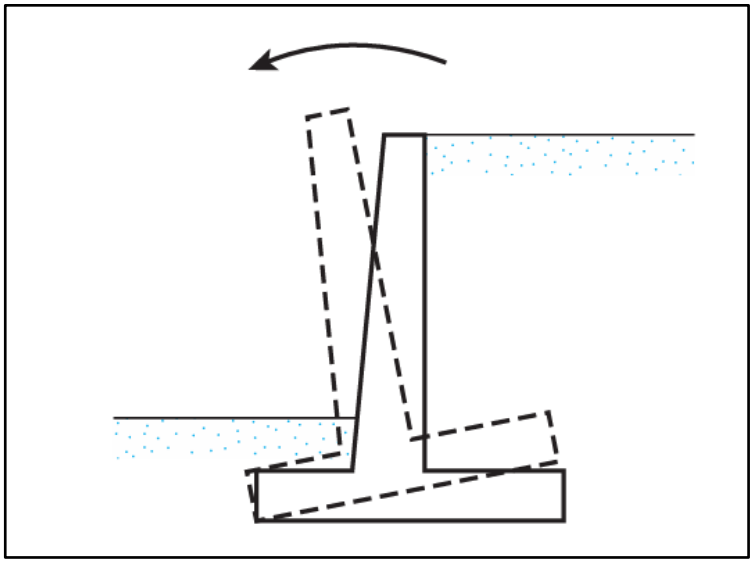

Figure 4.11 Overturning Stability Failure of Retaining Wall (Das, 2011)

The factor of safety (FS) against overturning is calculated using the following formula:

$$FS_{overturning} = \frac{\sum M_R}{\sum M_O} \tag{4.30}$$

Where:

$FS_{overturning}$: Factor of safety against overturning,

$\sum M_R$: Sum of resisting moments generated by the wall's self-weight, soil weight over the heel, and passive earth pressure, which stabilize the wall,

$\sum M_O$: Sum of overturning moments created by active horizontal earth pressures and water pressures acting behind the wall.

Although the acceptable limit for this ratio depends on the specific design standards used, a factor of 1.5 is generally considered acceptable in practice. A calculated safety factor greater than this value indicates that the retaining wall is adequately secure against overturning and ensures a conservative and safe design.

4.2.2.2 Sliding Safety Check For Retaining Walls

Sliding stability analysis aims to prevent the retaining wall from sliding horizontally as a rigid block along its base. The active earth pressure acting on the wall and additional horizontal loads tend to push the wall forward. Resistance against sliding primarily arises from the frictional forces developed at the wall base and the cohesion of the foundation soil; additionally, passive resistance from the soil in front of the wall may theoretically contribute. However, in practice, passive resistance is generally neglected due to the uncertainty of soil availability and adequacy of resistance at the front of the wall (Das, 2011).

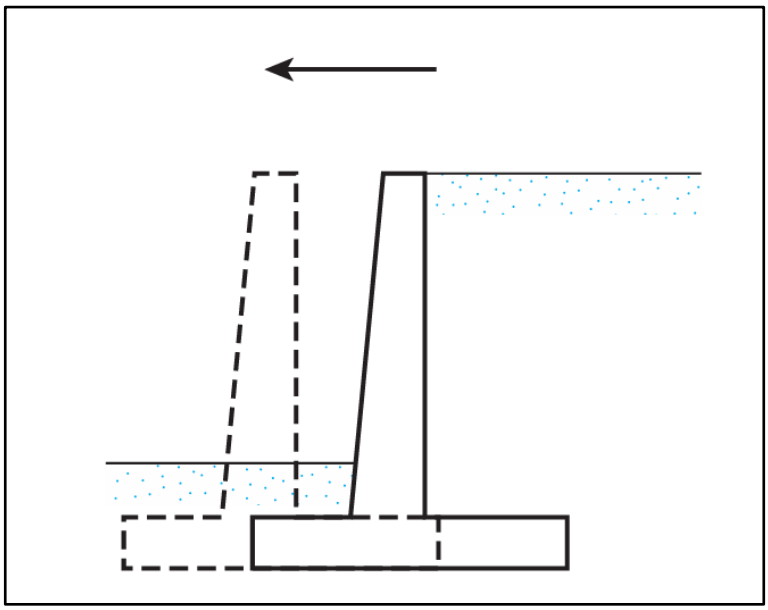

Figure 4. 12 Sliding Stability Failure of Retaining Wall (Das, 2011)

Sliding stability is assessed by taking the ratio of the total horizontal resisting force at the wall base to the total horizontal driving force causing sliding. The factor of safety (FS) against sliding is defined by the following formula:

$$FS_{(sliding)} = \frac{\sum F_{R'}}{\sum F_d} \tag{4.31}$$

Where;

$\sum F_d$: Total horizontal force driving the wall forward (active earth pressure and additional horizontal loads).

$\sum F_{R'}$: Total horizontal resisting force at the wall base, generally calculated using frictional resistance and passive soil resistance.

The horizontal resisting force of the retaining wall against sliding depends on the frictional force developed at the base, and this frictional force is calculated using the following equation:

$$\sum F_{R'} = \sum V \tan\delta \quad (4.32)$$

$\sum V$: Total vertical load acting on the wall base (weight of the wall, surcharge load, etc.).

δ : Interface friction angle between the base of the foundation and the soil.

The friction angle varies depending on factors such as the type of soil behind the retaining wall, soil density, cohesion, and surface roughness of the wall's rear face. It can be directly obtained from tables provided in the literature, or typically estimated to range between one-third ($\phi/3$) and two-thirds ($2\phi/3$) of the soil's internal friction angle (ϕ).

In practice, accurately determining the friction angle is crucial for ensuring a safe design against sliding. The calculated factor of safety (FS) against sliding is expected to be 1.5 or higher. If this safety factor is not achieved, measures such as widening the base of the wall, reducing pore water pressures, or improving soil conditions through various ground improvement techniques can be employed to enhance frictional resistance.

4.2.2.3 Bearing Capacity Safety Check For Retaining Walls

The bearing capacity safety check for retaining walls aims to evaluate whether the foundation soil can safely support the stresses transferred by the wall. This assessment is critical in preventing shear-type soil failures (Bowles, 1996). Because loads acting on the wall base are generally eccentric, a non-uniform stress distribution occurs under the footing. Maximum and minimum soil stresses are calculated using the following formulas (Das, 2011):

$$q_{max} = \frac{\sum V}{B}(1 + \frac{6e}{B}) \quad (4.33)$$

$$q_{min} = \frac{\sum V}{B}(1 - \frac{6e}{B}) \quad (4.34)$$

Where;

$\sum V$: Total vertical load at the base of the wall

B : Width of the footing

e : Eccentricity of the resultant load from the center of the footing

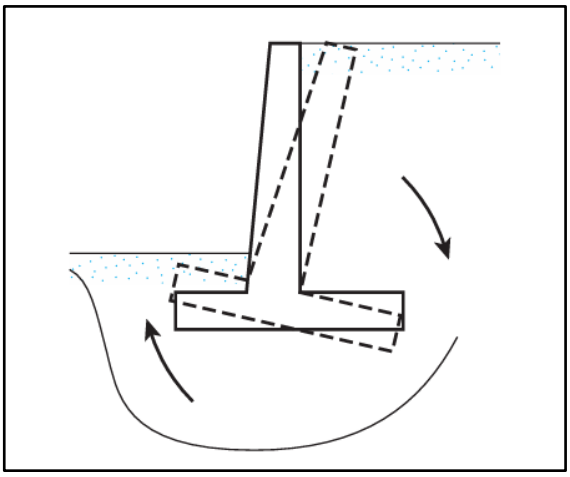

Figure 4.13 Bearing Capacity Stability Failure of Retaining Wall (Das, 2011)

If the eccentricity exceeds one-sixth of the footing width (B/6), negative stresses may occur at the footing edge, causing the footing to lose contact with the soil. Therefore, the design criterion $|e| \leq B / 6$ is typically required (Bowles, 1996). The ultimate bearing capacity of the soil (q_{ult}) can be computed using Terzaghi's classical bearing capacity equation (Terzaghi, 1943):

$$q_{ult} = c' N_c + \gamma' D_f N_q + \frac{1}{2}\gamma' B N_\gamma \quad (4.35)$$

Where;

c' : Effective cohesion of the soil

γ' : Effective unit weight of the soil

D_f : Depth of footing embedment

N_c, N_q, N_γ : Bearing capacity factors related to the soil friction angle (∅).

The calculated maximum footing stress (q_{max}) should not exceed the allowable bearing capacity of the soil (q_{allow}). Typically, allowable bearing capacity is obtained by dividing the ultimate bearing capacity (q_{ult}) by a safety factor of approximately 2 to 3 (Das, 2011).

The factor of safety (FS) against bearing capacity failure is evaluated as:

$$FS = \frac{q_{ult}}{q_{max}} \tag{4.35}$$

Generally, it is recommended that the factor of safety for retaining wall foundations should be at least FS ≈ 3 (Bowles, 1996; Das, 2011). If the calculated FS is insufficient, solutions such as widening the foundation or applying soil improvement techniques are suggested (Bowles, 1996).

4.2.2.4 Deep-Seated Shear Failure Safety Check For Retaining Walls

In designing retaining structures, ensuring only local stability (such as overturning, sliding, and bearing capacity) is not sufficient. Even though local stability conditions around the wall might be safe, there still remains a risk of deep-seated shear failure involving larger soil masses behind the wall. Therefore, slope stability analyses should be conducted around retaining walls to assess potential global instability (Clayton et al., 2014). Particularly for cantilever and counterfort retaining walls, a minimum factor of safety (FS ≥ 1.5) is generally required against deep-seated shear failure (TS 7994, 1990).

Various methods are available for slope stability analyses, among which the Swedish Slice Method (also known as the Fellenius Method) is widely used in engineering practice. This method is based on dividing the soil mass above the assumed circular slip surface into vertical slices (Uzuner, 2014).

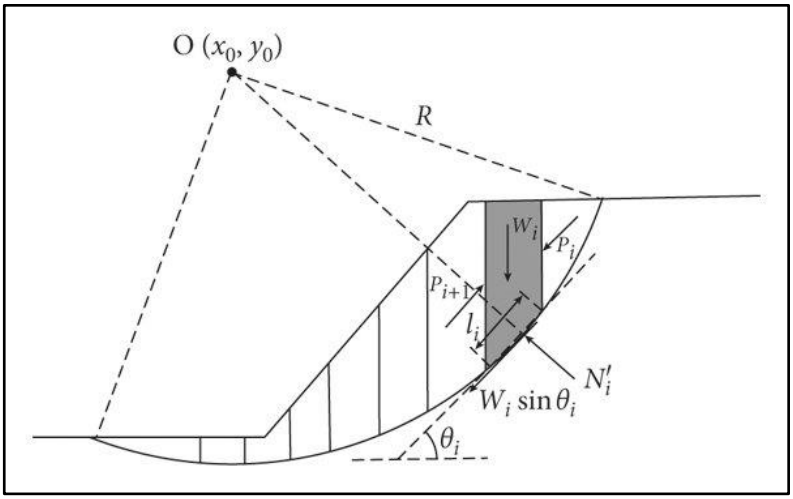

Figure 4.14 Analysis Of Circular Slip Surface Using Swedish Slice Method (Gong Et Al., 2017; Ravichandran & Shrestha, 2020; Zhou Et Al., 2020)

The average normal stress (σ_n) at the base of each slice is calculated using the vertical component of the slice weight (N_i) and the length of the slice base (ΔL_i) as follows:

$$\sigma_n = \frac{N_i}{\Delta L_i \, x \, 1} \tag{4.36}$$

Using this calculated normal stress, the shear strength ($\boldsymbol{T_{f_i}}$) of each slice is determined according to the Mohr-Coulomb criterion.

$$T_{f_i} = c + \sigma_n \, tan\emptyset \tag{4.37}$$

Where;

$\boldsymbol{c}$ **;** Cohesion of the soil

$\emptyset$; Internal friction angle

Subsequently, the total shear resistance at the base of each slice (R_i) is calculated using the following formula:

$$R_i = \Delta \, L_i \, x \, T_{f_i} \tag{4.38}$$

The factor of safety (FS) is calculated by taking the ratio of the sum of shear resistances of all slices to the sum of the driving forces. Considering the radius (r) of the circular slip surface, this relationship can be expressed as follows (Uzuner, 2014):

$$FS = \frac{\sum_{i=1}^{n}(c\Delta L_i + N_i \tan\emptyset)\mathrm{r}}{\sum_{i=1}^{n} T_i} \quad (4.39)$$

Where;

T_i : Horizontal components of the slice weights driving the slope to slide

n : Number of slices.

If the calculated safety factor is below the target value, measures such as revising wall dimensions, improving soil properties, or embedding the foundation deeper must be implemented. Consequently, while retaining walls may provide sufficient local stability, they alone may not prevent deep-seated shear failures. Therefore, comprehensive slope stability analyses must be conducted (Uzuner, 2014).

4.3 NUMERICAL METHODS

With the advancement of technology, numerical methods have become increasingly prevalent in solving complex geotechnical engineering problems. Numerical methods offer significant advantages, particularly in analyzing complex soil-structure interactions that are difficult to solve using analytical approaches. In this thesis, the bearing capacity and behavior of jet grout columns and diaphragm walls have been analyzed using the Finite Element Method (FEM) via PLAXIS 2D software. The soil parameters utilized in the modeling were derived from data obtained through field investigations.

4.3.1 The Finite Element Method

The Finite Element Method (FEM) is a numerical technique developed to solve complex engineering problems. FEM involves dividing continuous media (such as soils or structural elements) into smaller segments, known as finite elements, and generating equations that approximate the behavior of the entire system (Elgamal, 2021). This approach is highly effective for solving engineering problems that involve complex geometries, heterogeneous materials, or nonlinear behaviors, particularly when classical analytical methods

are insufficient or impossible. The widespread adoption of FEM in geotechnical engineering is primarily due to its capability to effectively model the complex, nonlinear, and time-dependent stress-strain behavior of soils and rock masses. Traditional analytical methods typically fall short in adequately representing such intricate soil characteristics (Keseroğlu et al., 2025).

In this thesis, PLAXIS software, which is based on finite element analysis, has been utilized. Various specialized software has been developed to bridge the theoretical advantages of the finite element method with practical applications. Among these is PLAXIS, a FEM-based software specifically designed for addressing geotechnical engineering problems.

PLAXIS offers an extensive library of material models to simulate the nonlinear and time-dependent behaviors of soils, such as plastic deformation, creep, and consolidation (Bentley Systems, 2021). The software includes several advanced material models ranging from the basic Mohr-Coulomb model to more sophisticated options like Hardening Soil and Soft Soil models.

The stress-strain behavior of materials under applied loads is defined through material models. According to Hooke's law, linear elastic stress-strain relationships can be described with fundamental parameters such as the elasticity modulus (E) and Poisson's ratio (ν). However, the behavior of soil materials often cannot be fully captured using linear elastic assumptions due to their complexity. Therefore, elastoplastic models are generally more suitable for various soil types. Conversely, elastic theory remains adequate for more rigid and elastic materials, such as rocks. Selecting the most suitable material model based on the soil properties and behaviors under investigation is crucial for obtaining accurate and realistic analysis outcomes.

4.3.2 Soil Models

The success of numerical analyses directly depends on the accuracy of the selected soil models. In this context, commonly adopted models in the literature, such as Mohr-Coulomb, Hardening Soil (HS), and Hardening Soil Small-Strain (HS-Small), were evaluated. However, considering the scope of the study and

practical applicability, the Mohr-Coulomb model was chosen as the primary model for the analyses.

4.3.2.1 Mohr-Coulomb Soil Model

The Mohr-Coulomb model is one of the most fundamental elasto-plastic models used to represent the shear strength behavior of soils. The model is based on the shear strength hypothesis proposed by Charles-Augustin de Coulomb in the 1870s, and on the Mohr's Circle approach developed by Otto Mohr in the early 1900s.

The key assumption of the model is that the maximum shear stress on a potential failure plane is linearly related to the normal stress acting on that plane. This leads to a linear failure envelope that characterizes the soil's resistance to shear failure.

The Mohr-Coulomb model is defined by the following failure criterion:

$$\boldsymbol{\tau = c + \sigma \cdot tan(\phi)} \tag{6.1}$$

In the Mohr-Coulomb model, the elastic behavior of the soil is characterized using the Young's modulus (E) and Poisson's ratio (ν), while the plastic behavior is defined by the shear strength parameters discussed earlier. Additionally, a dilatancy angle (ψ) is included to represent volumetric expansion behavior during shearing.

The Mohr-Coulomb model defines soil behavior using six fundamental parameters:

- E: Elastic modulus (kPa)
- ν: Poisson's ratio
- c: Cohesion (kPa)
- ϕ: Internal friction angle (°)
- ψ: Dilatancy angle (°)
- γsat, γunsat: Saturated and unsaturated unit weights (kN/m³)

The main advantage of this model is that its parameters can be easily determined through standard field and laboratory tests, and it offers rapid

computation in numerical analyses. However, it has limited capability in simulating complex behaviors such as strain hardening or softening after plastic yield.

4.3.2.2 Hardening Soil (Hs) Model

The Hardening Soil (HS) model was developed to simulate more realistic soil behavior, particularly under loading-unloading cycles and stress-dependent deformations. It is an advanced elasto-plastic model that accounts for soil stiffening and increased rigidity upon reloading.

This model uses three different elastic modul:

E_{50}: Secant elastic modulus (for primary loading)

$E_{oe}d$: Oedometer modulus (for one-dimensional consolidation)

E_{ur}: Unloading-reloading modulus (for stress reversals)

The main limitation of the HS model is the requirement for precise determination of these moduli through sophisticated laboratory testing. Since this study focuses on the short-term behavior and group effect of jet grout columns, the detailed elastic representation provided by the HS model was not deemed critical.

4.3.2.3 Hardening Soil Small-Strain (Hs-Small) Model

Conventional models often fail to capture the high stiffness behavior of soils under very small strains (typically in the range of $\mathbf{10^{-4} - 10^{-5}}$). To address this limitation, the HS-Small model was developed, incorporating the initial small-strain shear modulus (G_0) as a defining parameter. This model is particularly valuable for simulations involving soil vibrations, resonance behavior, or seismic effects.

However, since the primary focus of this study is on plastic deformations related to lateral earth pressure under the group effect of jet grout columns, the HS-Small model was not directly employed. Nevertheless, it is recommended for use in future advanced analyses where dynamic or small-strain behavior is of interest.

Following comprehensive evaluations, the Mohr-Coulomb model was deemed sufficient for representing the group effect on lateral earth pressure, which was the primary objective of the analysis. The compatibility of most field-derived parameters with this model, its computational efficiency, and its frequent use in similar studies in the literature were decisive in its selection.

CHAPTER 5

5. NUMERICAL ANALYSIS STUDIES

In this section, the numerical models developed using PLAXIS 2D finite element software are detailed to evaluate the contribution of jet grout columns to lateral earth pressure under group effects. Initially, the main objective was to establish a reliable numerical model based on actual field data. To achieve this, geotechnical parameters of the soil were determined through site-specific borehole investigations and laboratory tests, which were then directly integrated into the numerical model. Additionally, the geometric properties of jet grout columns, such as column diameter, length, and precise field positions, were accurately incorporated into the model. The model's accuracy and reliability were verified by comparing load-displacement behavior and lateral earth pressure values. After validating the numerical model, the effects of varying column arrangements, column spacing, and column diameters on lateral earth pressure were systematically investigated. Within this section, processes including geometric modeling, soil profile establishment, modeling of jet grout columns and diaphragm walls, definition of boundary conditions, assignment of displacement values, creation of the finite element mesh, and initialization of stress conditions are explained sequentially under separate subsections.

5.1 ESTABLISHMENT OF NUMERICAL MODEL

5.1.1 Creation Of Geometric Model

The numerical model established in PLAXIS 2D software had horizontal and vertical dimensions of 35 m and 25 m, respectively, ensuring adequate distance to minimize boundary effects and accurately represent soil-structure interaction conditions. The diaphragm wall modeled in the analyses had a constant height of 6 m and a thickness of 0.3 m, reflecting the actual dimensions

encountered on-site. Additionally, the raft foundation, modeled as a plate element with a thickness of 0.5 m, and the jet grout columns with a uniform diameter of 0.563 m and length of 6 m, were explicitly defined within the model. Furthermore, the caisson foundation was represented with a length of 7 m and also modeled as plate elements. These structural components were precisely positioned and dimensioned within the numerical domain, enabling an accurate and realistic evaluation of their interaction with the surrounding soil.

A uniform column diameter of 0.563 m and a fixed embedment depth of 6 m were maintained across all numerical models. To better investigate and analyze the group effect on lateral earth pressure, only the spacing between the jet grout columns was varied in the defined case studies, while all other parameters including soil properties, jet grout material parameters, foundation, diaphragm-wall characteristics, and boundary conditions were kept constant throughout the analyses. Five asymmetric spacing patterns were therefore established for the quintuple-column arrangement:

Case Study 1: 1.50 m – 1.50 m

Case Study 2: 1.50 m – 1.00 m

Case Study 3: 1.00 m – 1.50 m

Case Study 4: 1.50 m – 0.75 m

Case Study 5: 0.75 m – 1.50 m

Each case study was subjected to a full PLAXIS 2D staged-construction analysis under identical boundary conditions (horizontal extents $\geq 6 \times$ column diameter) and loading sequences. By holding all other variables constant, this systematic approach isolates the influence of spacing asymmetry on group interaction, enabling a clear quantification of its effect on lateral earth-pressure reduction and distribution around the jet grout cluster.

5.2 SOIL DATA

The soil profile used in this study was developed based on data obtained from a real construction site located in parcel number 7223, block number 15,

within the Sancaktepe district of Istanbul. The building project at this location consists of one basement floor and three standard floors. A cross-sectional view of the project is illustrated in Figure 5.1. Detailed field investigations have confirmed that there are no geological risks such as landslides, rockfalls, or liquefaction at the site. The geotechnical characteristics of the area were determined through drilling activities conducted on-site, supported by laboratory testing of collected soil samples.

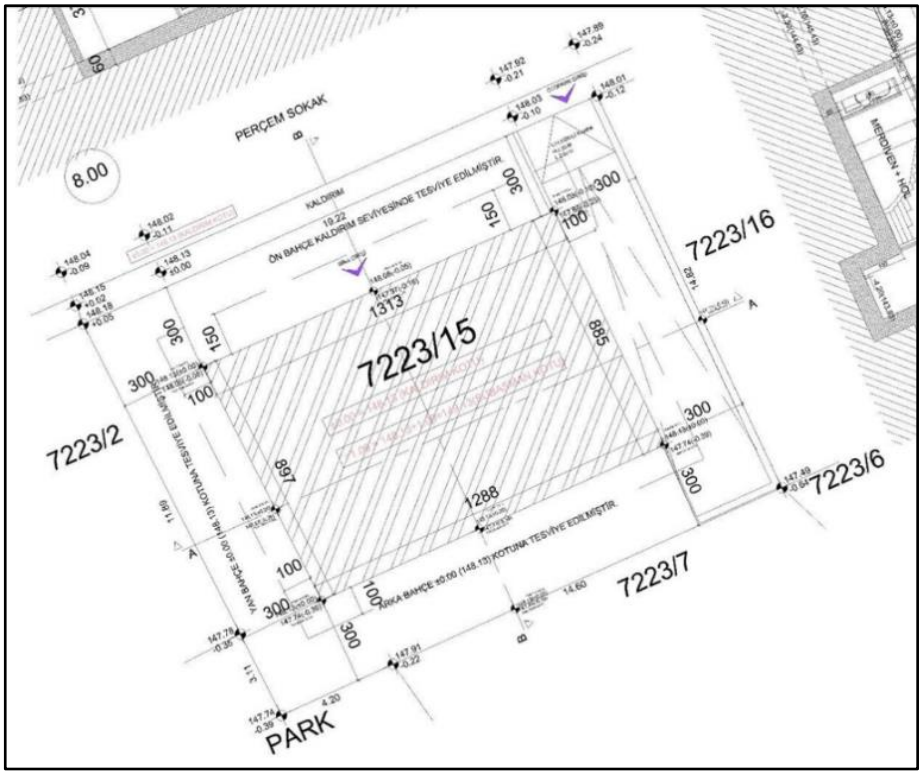

Figure 5.1 Section View of the Building

Figure 5.2 The Rotary Drilling Machine Used During The Borehole Operation.

5.2.1 Determination Of Soil Parameters Based On Field Data

The soil properties utilized in this study were derived from field data collected from parcel number 7223, block number 15, located in the Eyüp Sultan neighborhood of the Sancaktepe district in Istanbul.

At the site, three boreholes were drilled at depths of 30 m, 15 m, and 15 m respectively; two MASW (Multichannel Analysis of Surface Waves) tests, one Electrical Resistivity Tomography (ERT/DES) measurement, and pressuremeter tests were conducted. The locations of these field tests are shown in Figure 5.2. The rotary drilling machine and the site layout used during drilling operations are presented in Figure 5.3, while core samples extracted from the boreholes are illustrated in Figures 5.4, 5.5, and 5.6, respectively. These investigations provided critical data for identifying soil layers and defining their geotechnical characteristics.

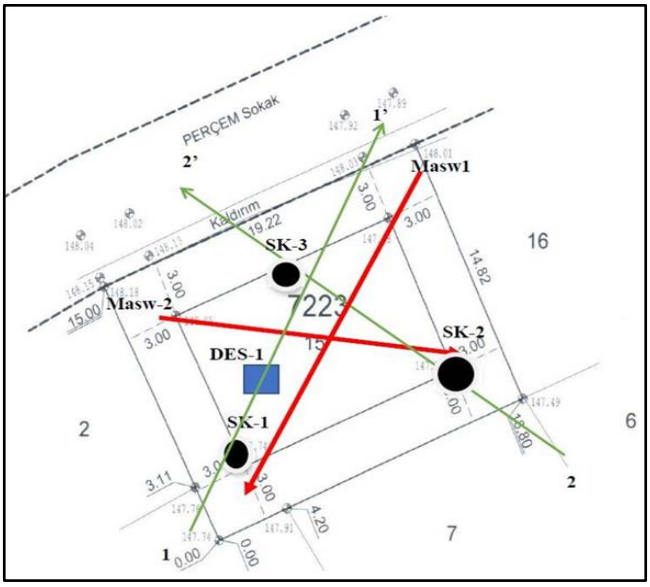

Figure 5.3 Locations of the Three Boreholes

Figure 5.4 Soil core samples obtained from Borehole SK-1

Figure 5.5 Soil core samples obtained from Borehole SK-2

Figure 5.6 Soil core samples obtained from Borehole SK-3

The study area is situated in the eastern part of Istanbul, near the western boundary of the Kocaeli Plateau. Geomorphologically, the site is located on sloping terrain surrounded by quartzite hills such as Aydos and Kayişdağı. Geologically, the region consists of alternating layers of quartzite, sandstone, and mudstone.

The soil samples obtained from the boreholes were subjected to extensive laboratory analyses. Based on these investigations, the determined soil profile (Table 5.1) starts from the surface with an approximately 1.5-meter-thick fill

layer, beneath which lie alluvial units and gravelly, sandy, silty clay layers belonging to the Sultanbeyli Formation. The alluvial unit is characterized as yellowish-brown in color, stiff in consistency, gravelly, sandy, and silty clay, occasionally containing gravel-sized rock fragments. During field measurements, no groundwater was encountered at the site.

Table 5.1 Soil Stratigraphy from Borehole Logs

Borehole	Elevation (m)	Depth Interval (m)	Soil Description
SK-1	147,74	0.00 - 1.50	Fill
SK-1	147,74	1.50 - 4.50	Alluvial unit; yellowish-brown, stiff, gravelly, sandy, silty clay with occasional boulders
SK-1	147,74	4.50 - 30.00	Stiff, gravelly, sandy, silty clay with occasional boulders
SK-2	147,74	0.00 - 1.50	Fill
SK-2	147,74	1.50 - 4.50	Alluvial unit; yellowish-brown, stiff, gravelly, sandy, silty clay with occasional boulders
SK-2	147,74	4.50 - 15.00	Stiff, gravelly, sandy, silty clay with occasional boulders
SK-3	147,97	0.00 - 1.50	Fill
SK-3	147,97	1.50 - 3.50	Alluvial unit; yellowish-brown, stiff, gravelly, sandy, silty clay with occasional boulders
SK-3	147,97	3.50 - 15.00	Stiff, gravelly, sandy, silty clay with occasional boulders

Table 5.2 summarizes the parameters adopted for the soil layers used in the numerical modeling. The parameters were interpreted on a layer-by-layer basis from data obtained through the Standard Penetration Test (SPT) conducted in the field and laboratory tests. In accordance with the drained Mohr–Coulomb model, the adopted values include natural and saturated unit weights (γsat), Young's modulus (E), Poisson's ratio (ν), internal friction angle (φ'), cohesion (c'), dilatancy angle (ψ), and the coefficient of permeability (k). For the clay unit, the undrained shear strength (cu) was also reported for reference; however, it was not used in the calculations since the analyses were performed under drained conditions. Layer thicknesses and depths were determined from the borehole logs, and this parameter set was transferred into the PLAXIS 2D environment as described in Section 5.1.2.3.

Table 5. 2 Geotechnical Parameters Used in the Numerical Analysis

Parameter	Alluvial Soil	Sand
Natural Unit Weight (γ) (kN/m³)	19	18.8
Saturated Unit Weight (γsat) (kN/m³)	20	19.8
Undrained Shear Strength (cu) (kPa)	25	–
Internal Friction Angle (φ) (°)	18	34
Cohesion (c) (kPa)	10	1
Young's Modulus (E) (kPa)	8000	20000
Poisson's Ratio (ν)	0.38	0.30
Permeability Coefficient (k) (m/s)	1×10^{-8}	1×10^{-6}
Dilatancy Angle (ψ) (°)	0	5
Model Type	Mohr-Coulomb	Mohr-Coulomb

5.2.2 Seismicity Of The Region

The study area is located within an active tectonic belt, and the most significant seismic threat for the region is the Marmara Fault Line (North Anatolian Fault Zone), situated approximately 16 km away. Based on the soil type identified at the site, the local soil class was determined as ZC according to the Turkish Building Earthquake Code (TBDY-2018), as shown in Table 5.3. This soil class includes very dense sand, gravel, stiff clay layers, and weathered or highly fractured weak rocks. Following the determination of the soil class, local soil amplification factors were initially obtained from the Turkish Building Earthquake Code (TBDY-2018), and these values are presented in Table 5.4.

Table 5. 3 Local Soil Amplification Factors (TBDY-2018)

Local Soil Class	Local Soil Effect Factor Fs for Short Period Region					
	Ss ≤ 0.25	**Ss = 0.50**	**Ss = 0.75**	**Ss = 1.00**	**Ss = 1.25**	**Ss ≥ 1.50**
ZA	0,8	0,8	0,8	0,8	0,8	0,8
ZB	0,9	0,9	0,9	0,9	0,9	0,9
ZC	1,3	1,3	1,2	1,2	1,2	1,2
ZD	1,6	1,4	1,2	1,1	1	1
ZE	2,4	1,7	1,3	1,1	0,9	0,8
ZF	Site-specific analysis required					
Local Soil Class ZC ve Ss = 0,838 for Fs = 1,200						

Local Soil Class	Local Soil Effect Factor Fs for Short Period Region					
	Ss ≤ 0.25	**Ss = 0.50**	**Ss = 0.75**	**Ss = 1.00**	**Ss = 1.25**	**Ss ≥ 1.50**
ZA	0,8	0,8	0,8	0,8	0,8	0,8
ZB	0,9	0,9	0,9	0,9	0,9	0,9
ZC	1,3	1,3	1,2	1,2	1,2	1,2
ZD	1,6	1,4	1,2	1,1	1	1
ZE	2,4	1,7	1,3	1,1	0,9	0,8
ZF	Site-specific analysis required					
Local Soil Class ZC ve Ss = 0,838 for Fs = 1,200						

Based on the data obtained from the table and according to the Turkey Earthquake Hazard Map Report provided by AFAD's official website, the earthquake ground motion level has been defined as DD-2. This level corresponds to seismic effects with a 10% probability of exceedance in 50 years (recurrence period of 475 years). The horizontal elastic design spectrum and vertical elastic design spectrum of the soil were determined using AFAD's report, along with building occupancy classes, building importance factors, building height classes, and seismic design coefficients. These are presented in Table 5.5 and 5.6.

Table 5.4 Soil Profile Table According to the Turkish Building Earthquake Code (TBDY-2018)

Local Soil Class	Soil Type	Average above 30 metres		
		(Vs)30 [m/s]	(N60)30 [blow/30 cm]	(cu)30 [kPa]
ZA	Hard, intact rocks	> 1500	-	-
ZB	Slightly weathered, moderately strong rocks	760 - 1500	-	-
ZC	Very dense sand, gravel, and stiff clay layers, or highly weathered, highly fractured weak rocks	360 - 760	> 50	> 250
ZD	Medium dense to dense sand, gravel, or stiff clay layers	180 - 360	15 - 50	70 - 250
ZE	Loose sand, gravel, or soft to firm clay layers, or profiles with soft clay layers thicker than 3 m satisfying conditions PI > 20 and w > 40% or with undrained shear strength (cu < 25 kPa)	< 180	< 15	< 70
ZF	Soils requiring site-specific investigation and evaluation: Soils susceptible to collapse and potential failure under seismic effects (liquefiable soils, highly sensitive clays, collapsible weakly cemented soils, etc.), Peat and/or highly organic clays with a total thickness greater than 3 meters, Highly plastic clays (PI > 50) with a total thickness exceeding 8 meters, Very thick (> 35 m) soft or medium-stiff clays.			

Table 5.5 Horizontal Elastic Design Spectrum

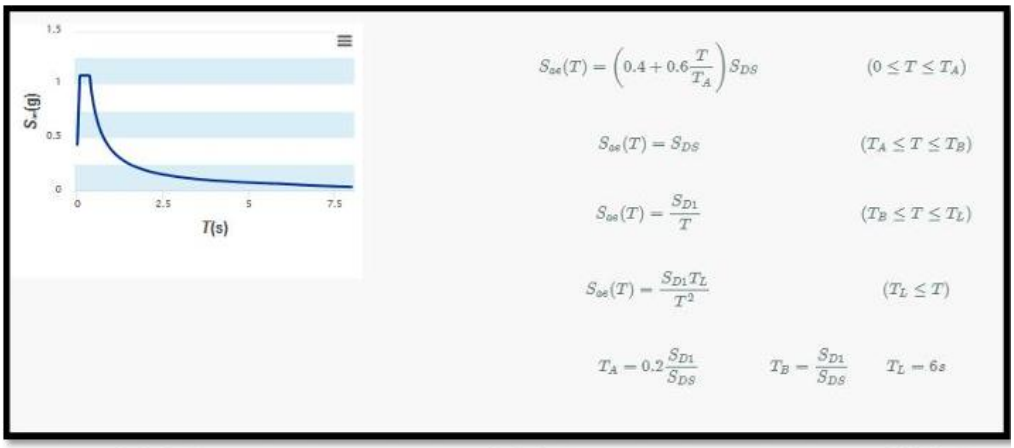

T_A = 0,070 (s) T_B = 0,352 (s) T_L = 6.000 (s)

Table 5.6 Horizontal Elastic Design Spectrum

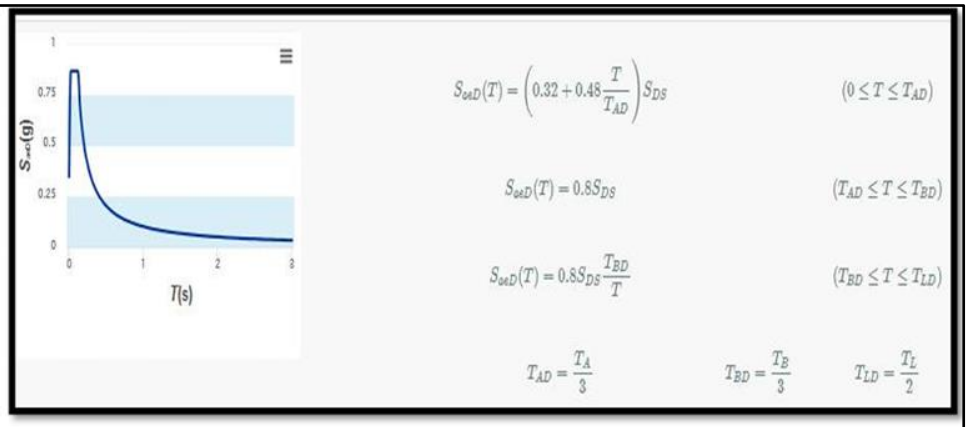

Table 5.7 Building Occupancy Classes and Building Importance Factor (TBDY, 2018)

Building Usage Class	Purpose of Building Usage	Building Importance Factor (I)
BKS = 1	Buildings required to be used after earthquakes, buildings heavily and frequently occupied by people, buildings storing valuable goods, and buildings containing hazardous substances. a) Buildings necessary immediately after earthquakes (Hospitals, dispensaries, healthcare centers, fire stations and facilities, PTT and other communication facilities, transportation stations and terminals, energy production and distribution facilities, provincial and district administrative buildings, first aid and emergency management stations) b) Schools, other educational buildings and facilities, dormitories and nurseries, military barracks, prisons, etc. c) Museums d) Toxic, explosive, flammable, and other hazardous substances production or storage facilities	1,5
BKS = 2	Buildings where people are present for short-term but intensively (Shopping malls, sports facilities, cinemas, theaters, concert halls, places of worship, etc.)	1,2
BKS = 3	Other buildings Buildings not falling under BKS=1 and BKS=2 definitions (Residential buildings, workplaces, hotels, industrial-type buildings, etc.)	1

The Building Occupancy Classes (BKS) and Building Importance Factors (I), essential for determining the earthquake design classes, have been defined in the table according to their intended use. Based on Table 5.7, the Building

Importance Factor was determined as I=1, and the Building Occupancy Class was identified as BKS=3

Table 5.8 Earthquake Design Classes (TBDY, 2018)

Short-Period Design Spectral Acceleration Coefficient s_{DS} at the DD-2 Earthquake Ground Motion Level	Building Occupancy Class	
	BKS = 1	BKS = 2, 3
s_{DS} < 0.33	DTS = 4a	DTS = 4
0.33 ≤ s_{DS} < 0.50	DTS = 3a	DTS = 3
0.50 ≤ s_{DS} < 0.75	DTS = 2a	DTS = 2
0.75 ≤ s_{DS}	DTS = 1a	DTS = 1

Based on the Building Occupancy Classes and the short-period design spectral acceleration coefficient (SDS) defined for the DD-2 earthquake ground motion level, the Earthquake Design Classes (DTS) to be adopted in seismic design according to TBDY will be determined according to the table below. According to Table 5.8, the Earthquake Design Class was identified as DTS=1.

Table 5.9 Building Height Classes (TBDY, 2018)

Building Height Class	Building Height Ranges [m] Defined According to Building Height Classes and Earthquake Design Classes		
	DTS = 1, 1a, 2, 2a	DTS = 3, 3a	DTS = 4, 4a
BYS = 1	H_N > 70	H_N > 91	H_N > 105
BYS = 2	56 < H_N ≤ 70	70 < H_N ≤ 91	91 < H_N ≤ 105
BYS = 3	42 < H_N ≤ 56	56 < H_N ≤ 70	56 < H_N ≤ 91
BYS = 4	28 < H_N ≤ 42	42 < H_N ≤ 56	42 < H_N ≤ 56
BYS = 5	17.5 < H_N ≤ 28	28 < H_N ≤ 42	28 < H_N ≤ 42
BYS = 6	10.5 < H_N ≤ 17.5	17.5 < H_N ≤ 28	17.5 < H_N ≤ 28
BYS = 7	7 < H_N ≤ 10.5	10.5 < H_N ≤ 17.5	10.5 < H_N ≤ 17.5
BYS = 8	H_N ≤ 7	H_N ≤ 10.5	H_N ≤ 10.5

Under seismic loading conditions, buildings are categorized into eight Building Height Classes (BYS) based on their heights. The defined height intervals for buildings belonging to these classes, depending on the Earthquake

Design Classes (DTS), are presented in the following table. For DTS=1, the Building Height Class was identified as BYS=6, as shown in Table 5.9.

5.2.3 Input Of The Soil Profile Into Plaxis

Based on Table 5.2, the layer-specific parameters were imported into PLAXIS 2D, and the analyses were conducted under drained conditions using the Mohr–Coulomb elasto-plastic model. Initial in-situ stresses were generated with the K_0-procedure ($K_0 \approx 1 - \sin\varphi$ for normally consolidated soils). Soil–structure interfaces were activated to represent realistic slip/bond behavior and were assigned $R_{inter} = 1.0$ in Rigid (automatic) mode. After defining the primary inputs (γ, γ_{sat} , E , ν , φ , ψ , k) the software automatically derived secondary quantities (G_{ref}, E_{oed}) and the small-strain wave velocities (V_s, V_p) from internal relations and reported them in the Alternatives panel. In this context, the undrained shear strength (c_u) reported for the clay unit in Table 5.2 was retained for reference only; it was not included in the calculations since the analyses were performed under drained conditions. These values were retained for completeness and internal consistency checks; because the study is static, V_s, V_p were not used in the calculations. To address the well-known small-strain stiffness limitation of the Mohr–Coulomb model, a limited, measurement-consistent calibration was applied: Young's modulus was moderately increased on a layer basis, strength parameters φ and c were kept within field/lab ranges, and dilatancy was bounded as $\psi = \max(\varphi - 30^o, 0)$ sand $\varphi = 0^o$ for clay. The resulting datasets were then used unchanged across all jet-grout spacing configurations to isolate the columns' group effect on lateral earth pressures.

Figures 5.7, 5.8, 5.9, 5.10 present the PLAXIS 2D input screens for the Alluvial (Silty Clay) and Fill layers. The images document the primary inputs entered on the General and Parameters tabs (γ, γ_{sat}, E, ν, c, φ, ψ, k) together with the secondary quantities (G_{ref}, E_{oed} , V_s, V_p) that the program automatically derives from its internal relations. The analyses were performed using the drained Mohr–Coulomb model with the K_0 procedure; soil–structure interfaces

were activated with $R_{inter} = 1.0$ in Rigid (automatic) mode. The values shown in the screenshots are consistent with the calibrated set reported in Table 5.2 and explained in Section 5.1.2.3. Small-strain wave velocities (V_s, V_p) are displayed for completeness and internal consistency checks but were not used in the static analyses.

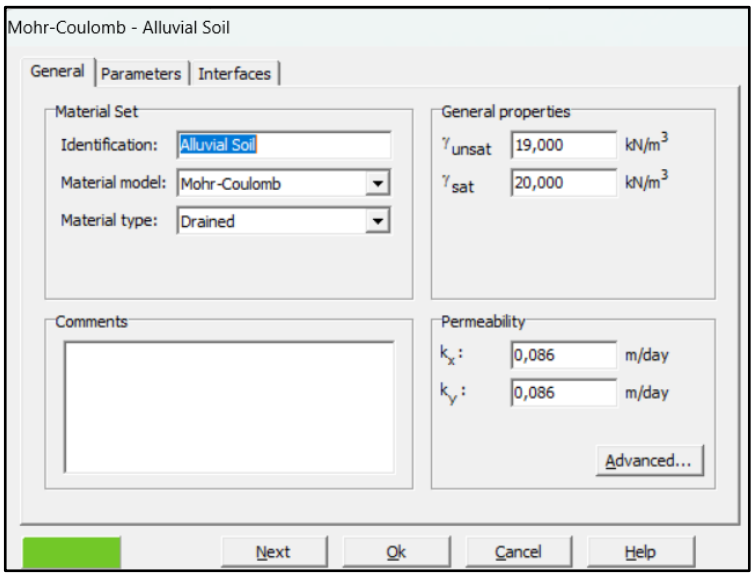

Figure 5.7 Parameters of the alluvial soil as defined in PLAXIS

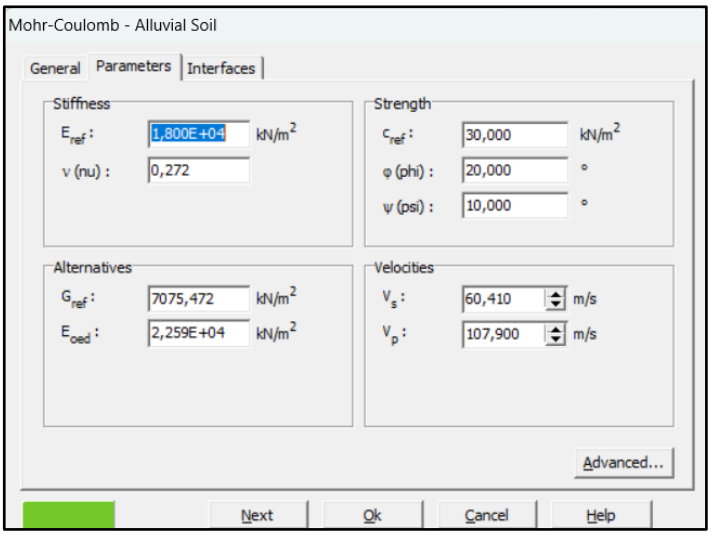

Figure 5. 8 Parameters of the alluvial soil as defined in PLAXIS"

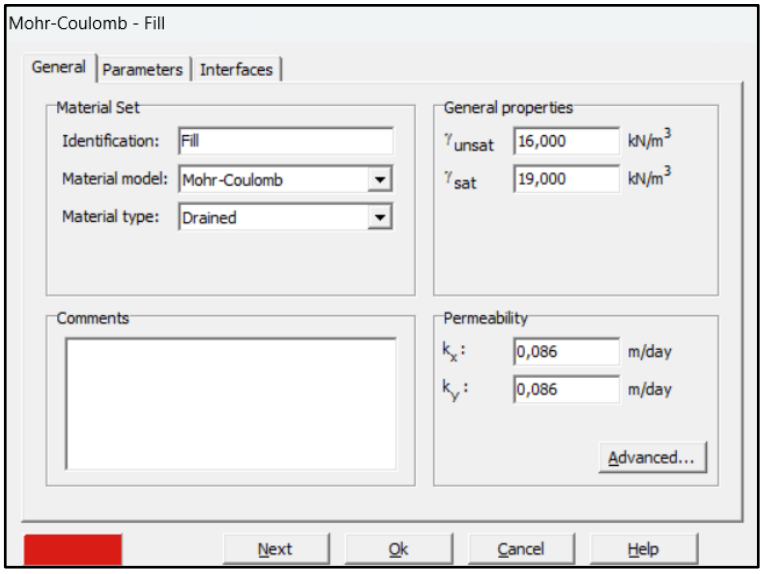

Figure 5.9 Parameters of the fill soil as defined in PLAXIS

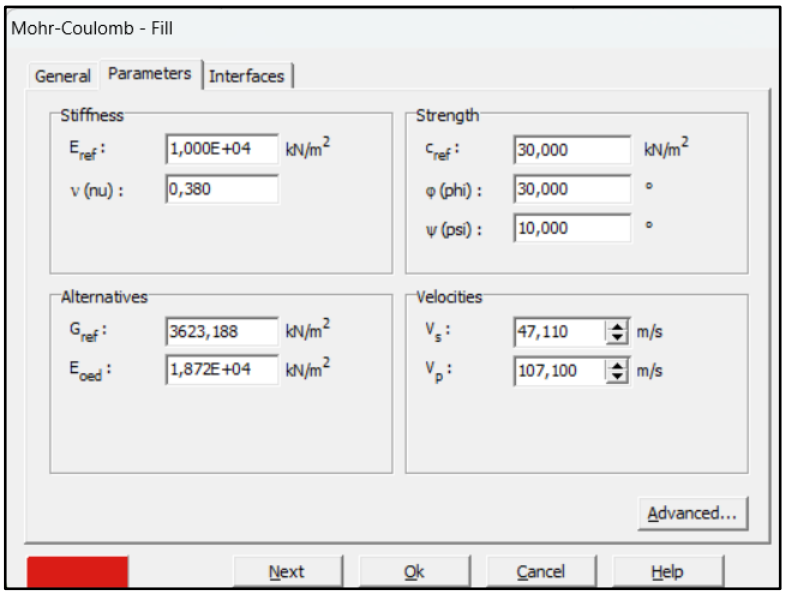

Figure 5. 10 Parameters of the fill soil as defined in PLAXIS

5.2.4 Implementation Of Structural Elements In Plaxis: Jet Grout Columns, Raft Foundation And Diaphragm Wall

The superstructure, being a rigid entity composed of reinforced concrete shear walls and frames, was represented with the Linear Elastic material model. This methodology depends on the premise that the structure will mostly exhibit elastic behavior under service loads, with plastic deformations remaining insignificant. The Linear Elastic definition accurately represents the stress-strain relationship between the structure and the ground during soil-structure interaction, maintaining computational efficiency due to its elevated elastic modulus and little deformation capacity.

The structure, composed of reinforced-concrete frames and shear walls, has a rigidity far greater than that of the adjacent earth. The Linear Elastic material model in PLAXIS was used, anticipating that it will remain within the elastic range under service loads. The literature indicates typical property ranges for reinforced-concrete structures as follows: $E = 20–35$ GPa, $\nu = 0.15–0.20$, and $\gamma \approx 24$ kN m^{-3} (ACI 318; Eurocode 2; Zhou et al., 2022). This study utilized $E = 20$ GPa, $\nu = 0.15$, and $\gamma = 24$ kN m^{-3} to accurately depict the rigid-block behavior of the building while avoiding the inclusion of superfluous plastic factors in the soil-structure interaction analysis. The comprehensive array of superstructure input values designated in PLAXIS is illustrated in Figure 5.10 and Figure 5.11, displaying the material properties precisely as inputted in the software interface.

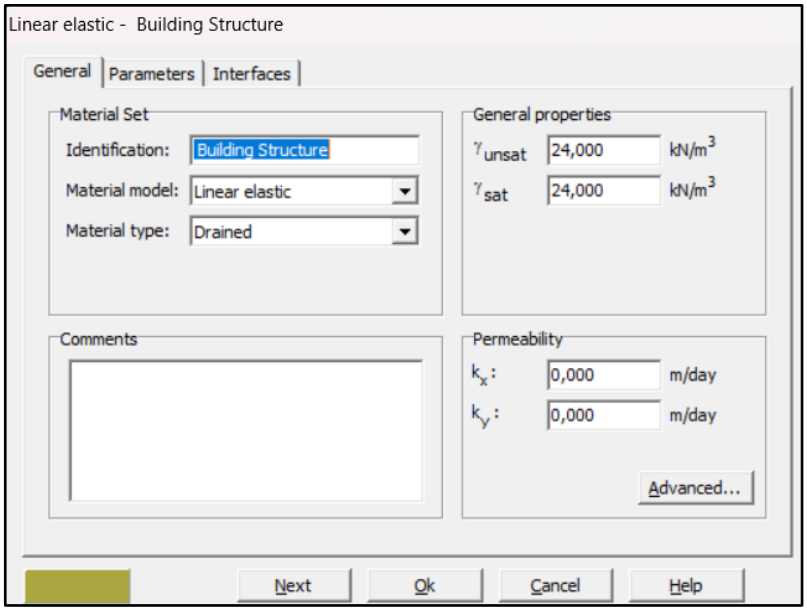

Figure 5.11 Superstructure material parameters as entered in PLAXIS

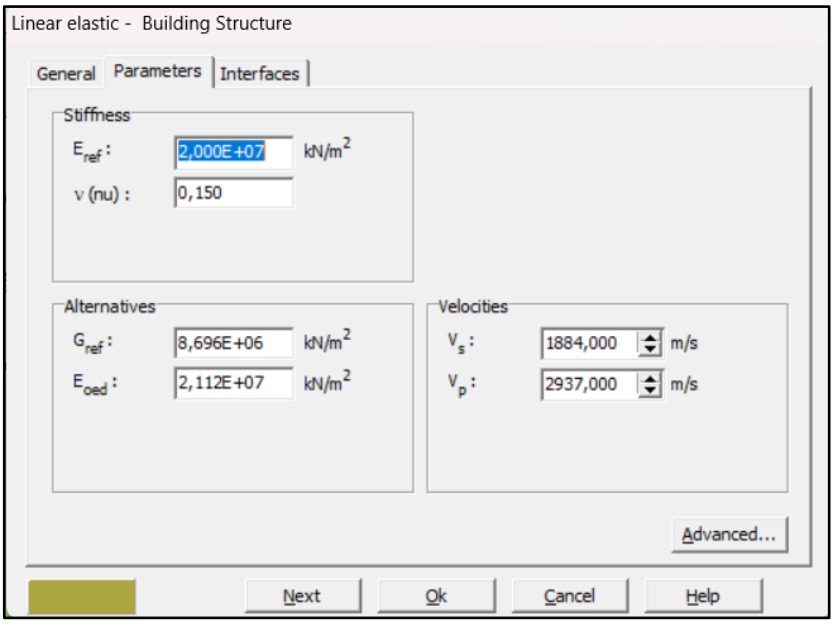

Figure 5.12 Superstructure material parameters as entered in PLAXIS

These elements are also made of high-strength reinforced concrete; however, because their primary function is either to improve the ground (jet-grout columns) or to distribute loads to the soil (raft foundation and diaphragm

wall), a simple Elastic material model is sufficient. Elastic parameters were determined by combining the section geometry (thickness/diameter) with a concrete Young's modulus of E ≈ 28 GPa. The axial rigidity (EA) and bending rigidity (EI) values assigned in PLAXIS are summarised in Table 5.10.

Table 5.10 Material Parameters Of The Raft Foundation, Diaphragm Wall, And Jet-Grout Columns Used In The Numerical Model

Element	EA (kN m^{-1})	EI (kN m^2 m^{-1})	Poisson v	Self-weight w (kN m^{-1} m^{-1})
Raft Foundation	15000000	313100	0,15	5
Diaphragm Wall	9000000	67100	0,15	5
Jet Grout Column (plate equivalent)	88500	2340	0,25	5

The EA and EI values were obtained from the Plate properties window in PLAXIS (see Figures 5.13, 5.14, 6.15). These rigidities were calculated using a concrete Young's modulus of E = 28 GPa and correspond to a jet-grout column diameter of 0.563 m, a raft-foundation thickness of 0.50 m, and a diaphragm-wall thickness of 0.299 m.

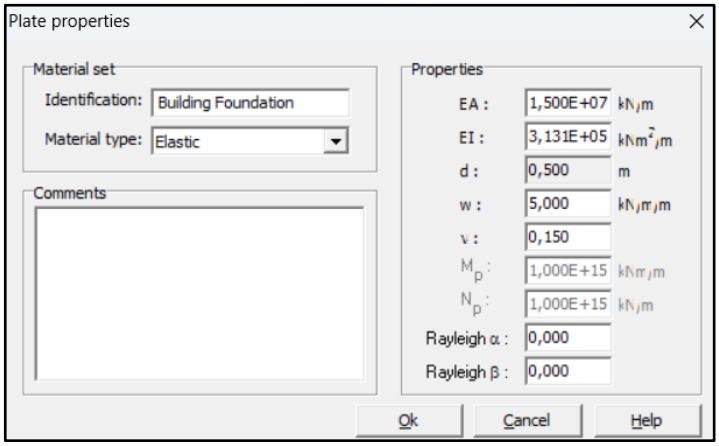

Figure 5.13 Diaphragm (Slurry) Wall Material Parameters As Entered In PLAXIS

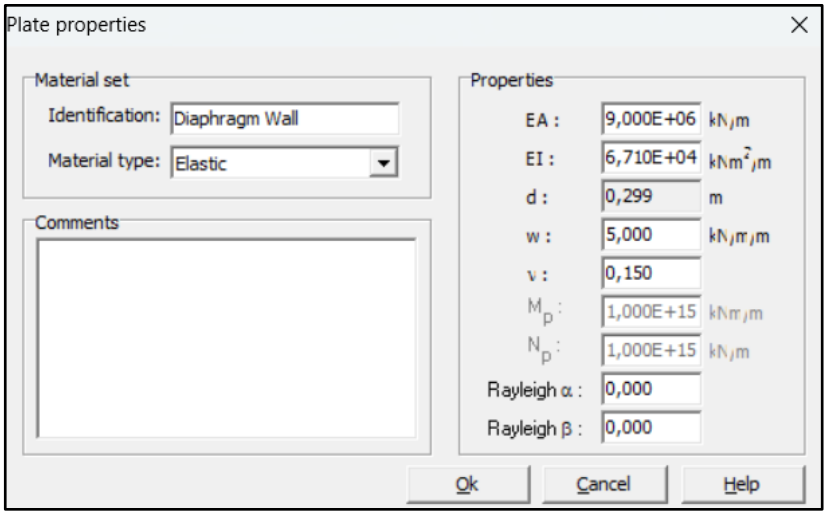

Figure 5.14 Diaphragm (Slurry) Wall Material Parameters As Entered In PLAXIS

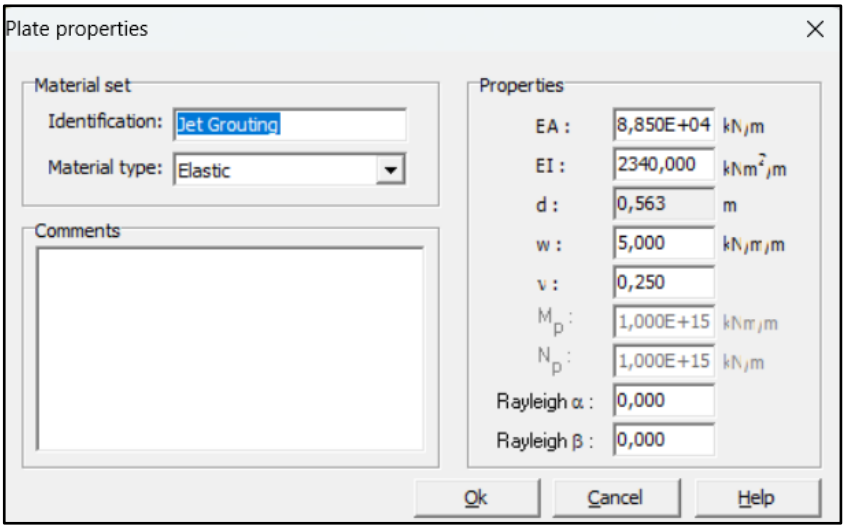

Figure 5.15 Jet-grout column material parameters as entered in PLAXIS

5.3 MESH GENERATION AND BOUNDARY CONDITIONS IN PLAXIS

The finite element mesh was generated in PLAXIS software using 15-node triangular elements to accurately represent the stress and deformation behavior

of the soil and structural elements. To enhance the accuracy of the analysis, the mesh was refined and made finer, particularly around critical regions such as jet grout columns, diaphragm walls, and foundations.

In the numerical model, standard boundary conditions (Standard Fixities) were applied to accurately represent real site conditions. Horizontal movements were restricted at the lateral boundaries of the model, while both horizontal and vertical movements were fixed at the bottom boundary. Thus, the soil behavior and the soil-structure interaction were realistically simulated.

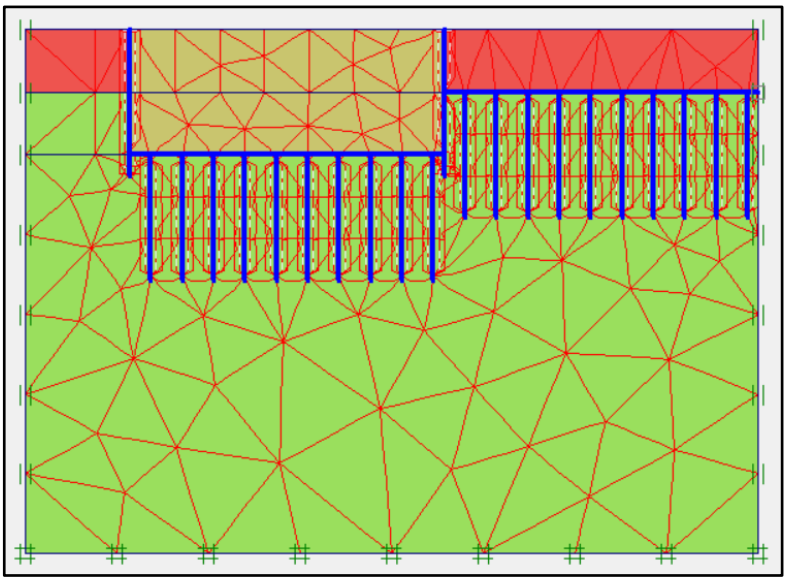

Figure 5.16 Finite-Element Mesh And Boundary Conditions In PLAXIS 2D

5.4 PHASE DEFINITIONS AND ANALYSIS SETUP

In this study, identical construction stages consisting of initial stress generation, excavation, installation of jet grout columns, activation of the diaphragm wall, and application of superstructure load were simulated for all case studies using the "Staged Construction" feature of PLAXIS 2D. The only parameter varied among the case studies was the spacing between the jet grout columns; all geometric, material, and boundary conditions were kept constant. The chronological order of all construction phases is presented in detail using

Case Study 1 as an illustrative example. This framework allows for a systematic evaluation of the spacing effects on lateral earth pressure independently from other influencing variables.

The phase sequence defined in the Staged Construction window is presented in Figure 5.17. In Phase 0, initial stresses were generated using the K_0-procedure based on the Jaky equation. During Phase 1 Figure 5.18, the raft foundation and linear-elastic superstructure block of Building 1 were activated. In Phase 2 Figure 5.19, the fill material in the Building 2 area was excavated and equilibrium was re-established. Phase 3 Figure 5.20 involved activating the raft foundation of Building 2 followed-within the same phase-by the installation of the jet-grout column group. Finally, in Phase 4 Figure 5.21, the superstructure of Building 2 was introduced and a uniform surcharge of 100 kPa was applied to its raft foundation. With all geometric, material and boundary conditions held constant apart from column spacing, this staged approach realistically captures the incremental effects of excavation and construction on soil–structure interaction.

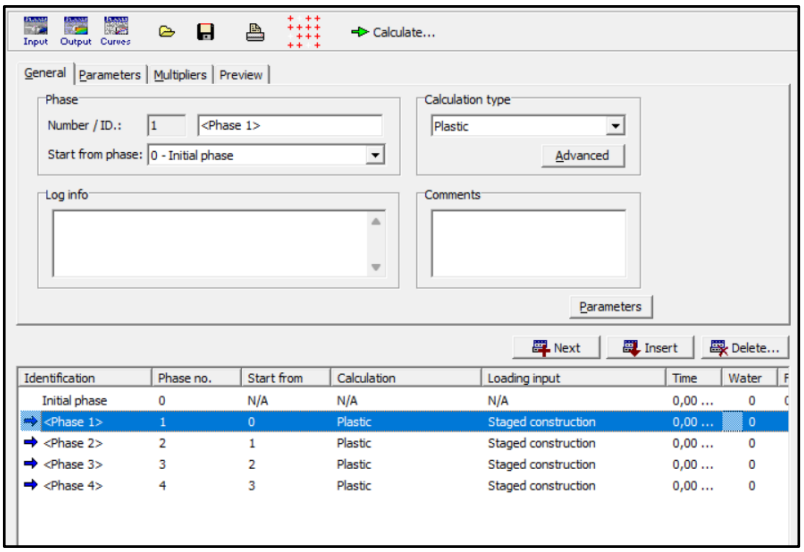

Figure 5.17 Phase Sequence As Defined In The Staged Construction Window

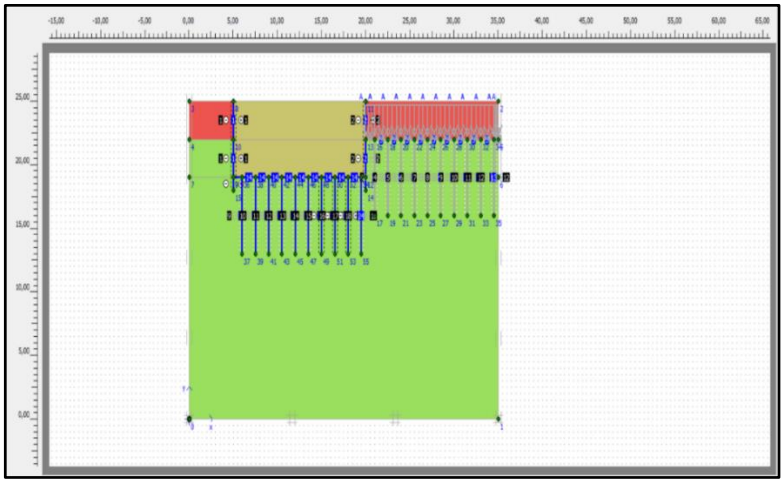

Figure 5.18 Phase 1 – Activation Of Building 1 Raft Foundation And Superstructure

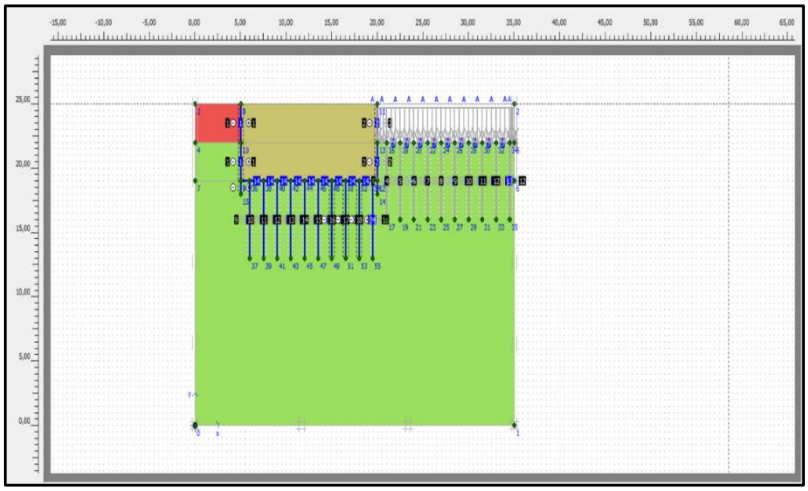

Figure 5.19 Phase 2 – Excavation Of The Fill Material In The Building 2 Area

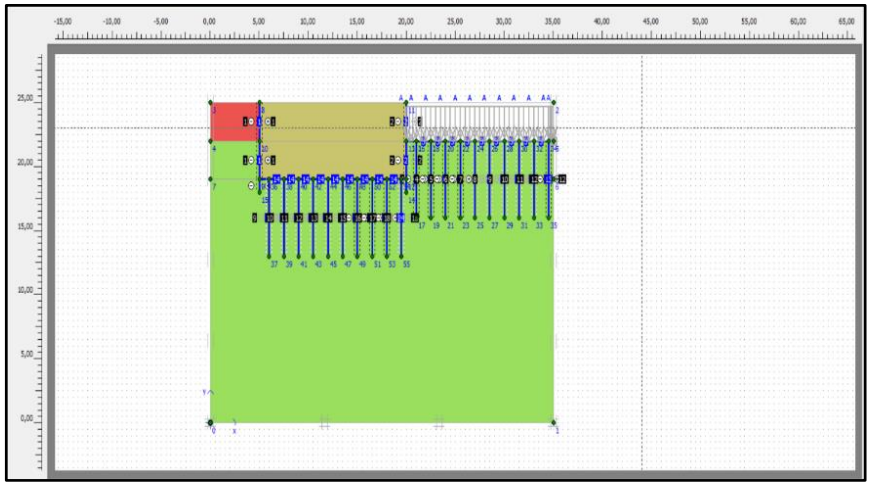

Figure 5.20 Phase 3 – Activation Of The Building 2 Raft Foundation Followed By Installation Of The Jet-Grout Column Group

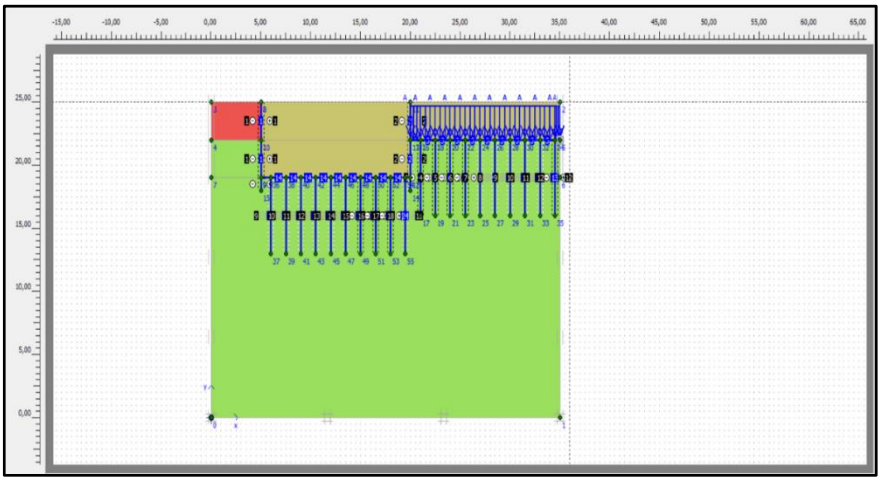

Figure 5.21 Phase 4 – activation of the Building 2 superstructure and application of a 100 kPa uniform surcharge

CHAPTER 6

6. ANALYSES AND EVALUATION OF RESULTS

This chapter examines the impact of jet-grout column group effects on lateral earth pressure, utilizing field data from an ENAK Construction project in Sancaktepe (Istanbul). Two structural configurations, designated as Structure 1 and Structure 2, are analyzed herein. In each instance, just the inter-column spacing is modified; foundation loads, soil profile and characteristics, and boundary conditions remain unchanged to isolate the group impact to the column arrangement. Initially, we examine the distributions of shear force and bending moment inside the columns, along the horizontal (total) stress in the adjacent earth, utilizing characteristics obtained from in situ research. Secondly, we assess the settlement (vertical displacement) characteristics of the column groupings. We also evaluate the horizontal displacement of the retaining (diaphragm) wall subjected to lateral stress. All models are developed and analyzed in PLAXIS 2D utilizing the finite-element method, adhering to established protocols and standards outlined in Chapter 5. The outcomes for Structure 1 and Structure 2 are thereafter shown both individually and comparatively, followed by a discussion on the engineering implications of the group effect.

6.1 FINITE ELEMENT ANALYSIS OF CASE STUDY 1 IN PLAXIS

In this section, we present a comprehensive finite-element analysis for Case Study 1 to quantify how jet-grout columns affect horizontal stress, shear force, bending moment, and vertical displacement within the columns. In addition, we evaluate the horizontal displacement of the caisson foundation system. The analysis is based on soil parameters derived from in situ investigations at an ENAK Construction project in Sancaktepe (Istanbul).

Finite-element models are developed and evaluated in PLAXIS 2D under the boundary and loading conditions described in Chapter 5. In each case, only the inter-column spacing is varied, whereas foundation loads, soil stratigraphy and properties, and boundary conditions are held constant so that the group effect is isolated to the column layout. Each stage of the analysis is presented under the relevant subheadings, and the findings are interpreted in the context of international literature and engineering practice.

In Figure 6.1, the general view of the model geometry and setup for Case Study 1 is presented. Before initiating the analyses, a 1.5 m thick fill layer underlain by an alluvial soil stratum was modeled, and the geotechnical parameters obtained from field data were assigned to the respective layers. Jet grout columns were modeled at 1.5 m intervals for both Structure 1 and Structure 2. In the scope of the analysis, the building foundation and the caisson wall were defined for Structure 1, and the structural parameters were assigned as linear elastic. For Structure 2, the building foundation was first modeled, followed by the jet grout columns at 1.5 m intervals, and a distributed load of 100 kPa representing the superstructure was applied. Mesh generation was performed and standard boundary conditions were defined for all analyses. Additionally, as the soil water content was assumed to be zero, the groundwater level was not included in the model.

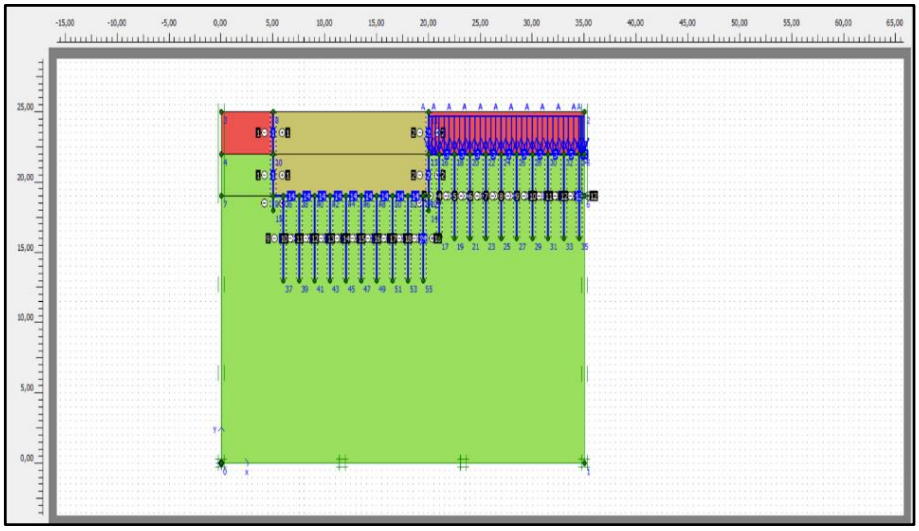

Figure 6.1 Presents The General View Of The Model Geometry And Setup For Case Study 1

To enhance the reliability of the analyses, appropriate interface definitions were specifically implemented between the jet grout columns and the surrounding soil, as well as between the caisson wall and the adjacent soil. Similarly, interface parameters for the caisson wall-soil contact were defined to realistically simulate the relative displacement and stress transfer between the structural elements and the ground. These interface definitions were assigned to the relevant elements in PLAXIS and activated in the model prior to analysis.

Regarding the analysis steps, in Phase 1, the caisson walls, building foundation, jet grout columns, and superstructure parameters of Structure 1 were activated, while no elements belonging to Structure 2 were activated at this stage. In Phase 2 (Figure 6.2), the excavation of the fill soil for Structure 2 was performed. In Phase 3, following the excavation, the foundation and jet grout columns of Structure 2 were activated at 1.5 m intervals in the model (Figure 6.3). In Phase 4, the distributed superstructure load was applied and the building parameters for Structure 2 were activated (Figure 6.4). After completing all phase steps, the model was run and the analyses were carried out.

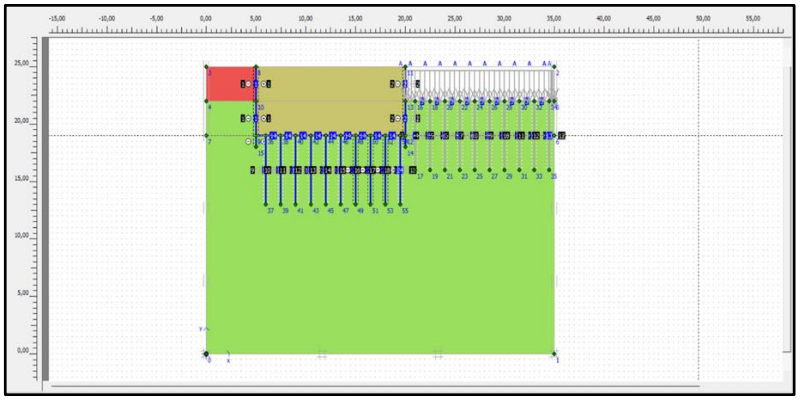

Figure 6.2 Model Representation of Phase 2

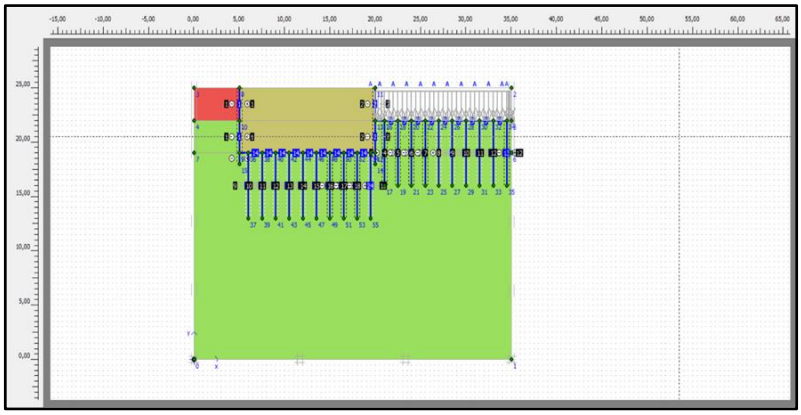

Figure 6.3 Model Representation of Phase 3

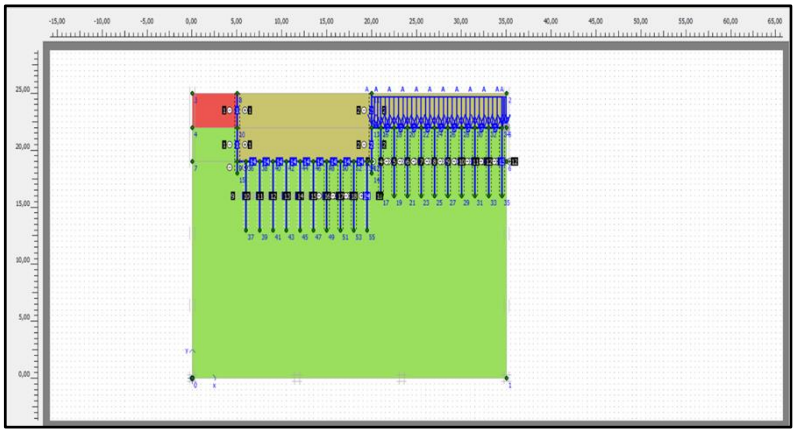

Figure 6.4 Model Representation of Phase 4

The examination of Structure 1 indicated substantial disparities in horizontal stress, bending moment, and shear force values, especially for the corner jet grout columns. The principal cause of these discrepancies is that the weight transmission processes at corner columns differ from those in center regions. According to the Horizontal Total Stress graph (Figure 6.5), corner columns exhibit higher negative horizontal stress values. This indicates that corner columns play a crucial role in horizontal load transfer between the structure and the soil, highlighting load concentration in these areas.

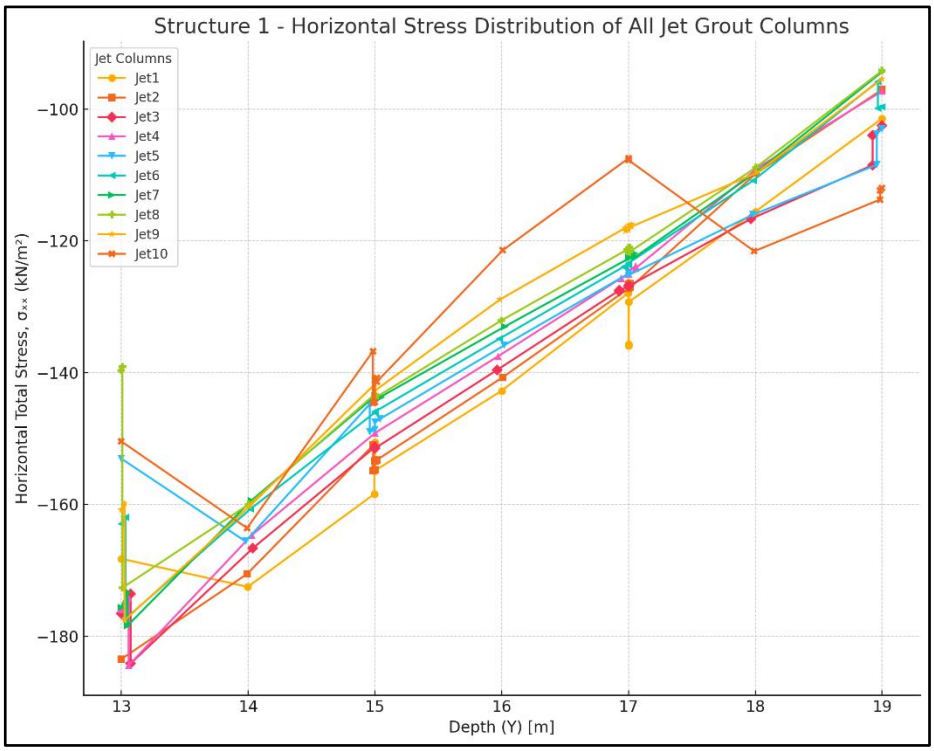

Figure 6.5 Horizontal Stress Distribution of Jet Grout Columns Case Study 1- Structure 1

In the Shear Force graph (Figure 5.6), it is observed that shear forces significantly increase with depth, particularly at the tips of the corner columns. This increase is associated with the maximum transfer of horizontal loads at the column tips.

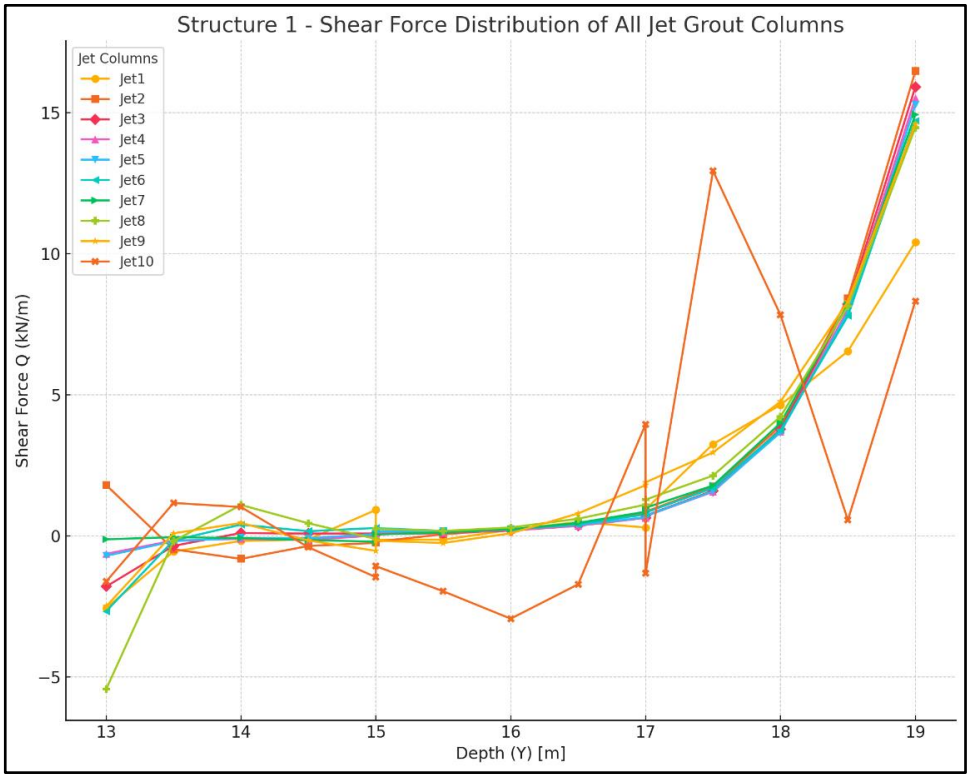

Figure 6.6 Shear Force Distribution of Jet Grout Columns Case Study 1-Structure 1

The Bending Moment graph (Figure 6.7) shows that negative moment values significantly increase with depth for the corner columns. This clearly indicates a more critical bending behavior in the lower regions of these columns.

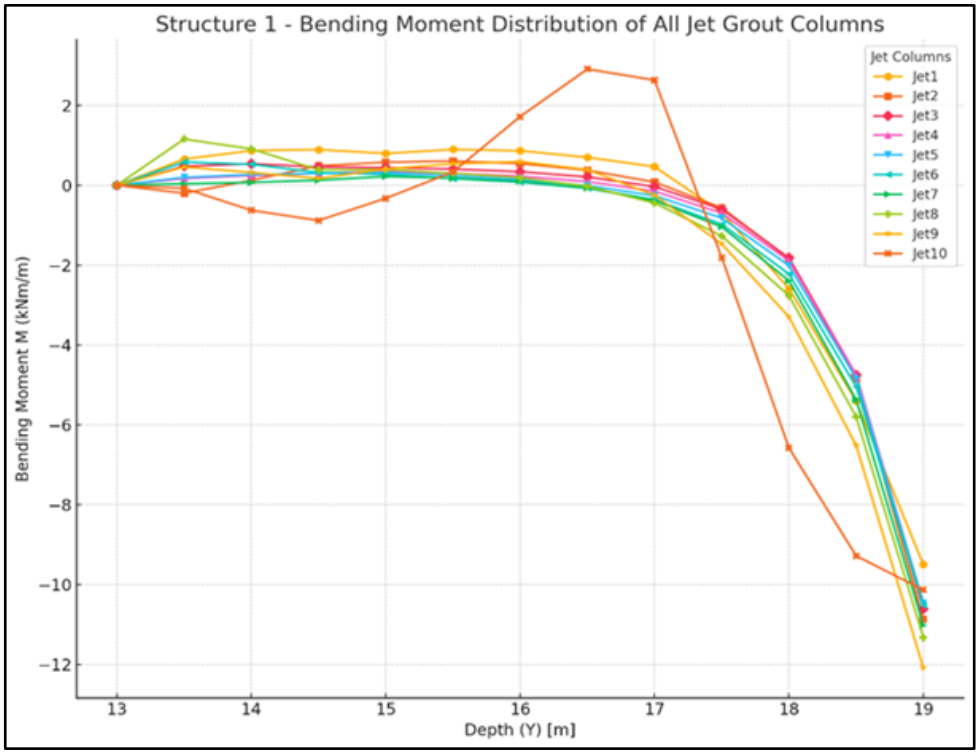

Figure 6.7 Bending Moment Distribution of Jet Grout Column Case Study 1-Structure 1

In the Plaxis model, the jet grout columns are modeled with upper levels at 19 m and lower levels at 13 m. This modeling approach ensures accurate analysis of stress, shear force, and bending moment distributions throughout the depth. Corner columns serve as boundary conditions in the load distribution between soil and structural systems. These columns experience higher horizontal stress, bending moment, and shear forces compared to other columns due to structural rigidity concentrating horizontal loads at these points. Additionally, corner columns receive less lateral support compared to interior columns and experience varied soil-column interactions, contributing to distinct load-bearing behavior. The absence of group effects has been explicitly stated in the analysis.

The column spacing (1.5 m) is sufficiently wide in this scenario, preventing overlap of effective soil interaction zones, thereby eliminating

negative group effects. Thus, columns behave independently but experience different loading conditions based on their geometric positions.

For Structure 2, jet grout columns were modeled with upper levels at 22 m and lower levels at 16 m, also at 1.5 m spacing. According to the Horizontal Total Stress graph (Figure 6.8), stress values significantly increase negatively towards the lower sections of the columns, indicating heightened horizontal load transfer at the tips of the columns.

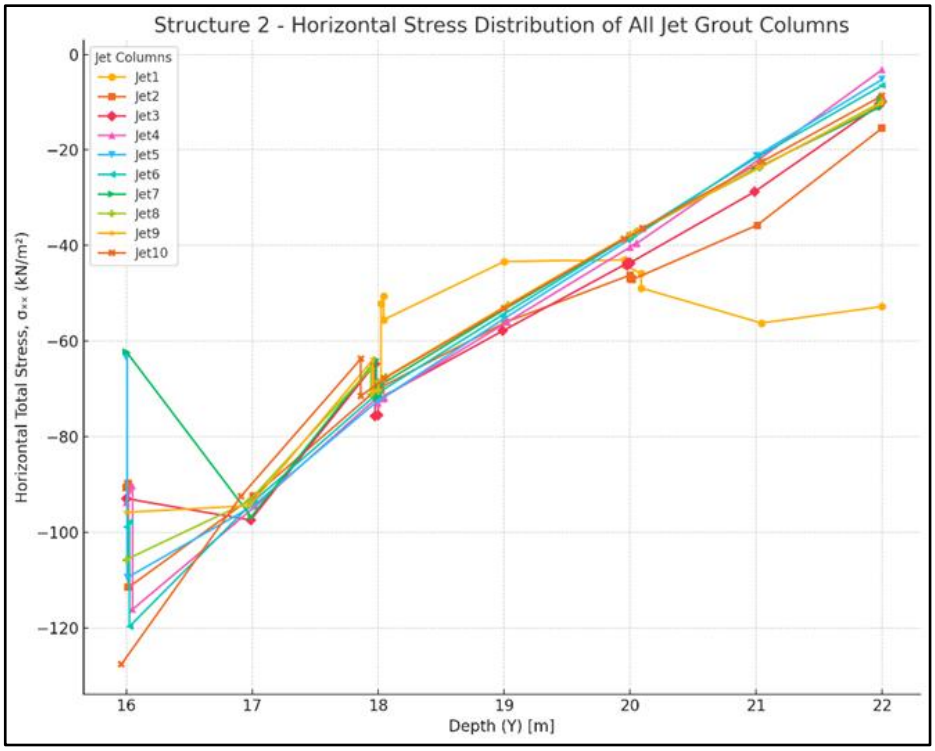

Figure 6.8 Horizontal Stress Distribution of Jet Grout Columns Case Study 1 - Structure2

The Shear Force graph (Figure 6.9) similarly demonstrates a noticeable increase in shear forces at lower depths, specifically at the tips, where load concentrations are evident.

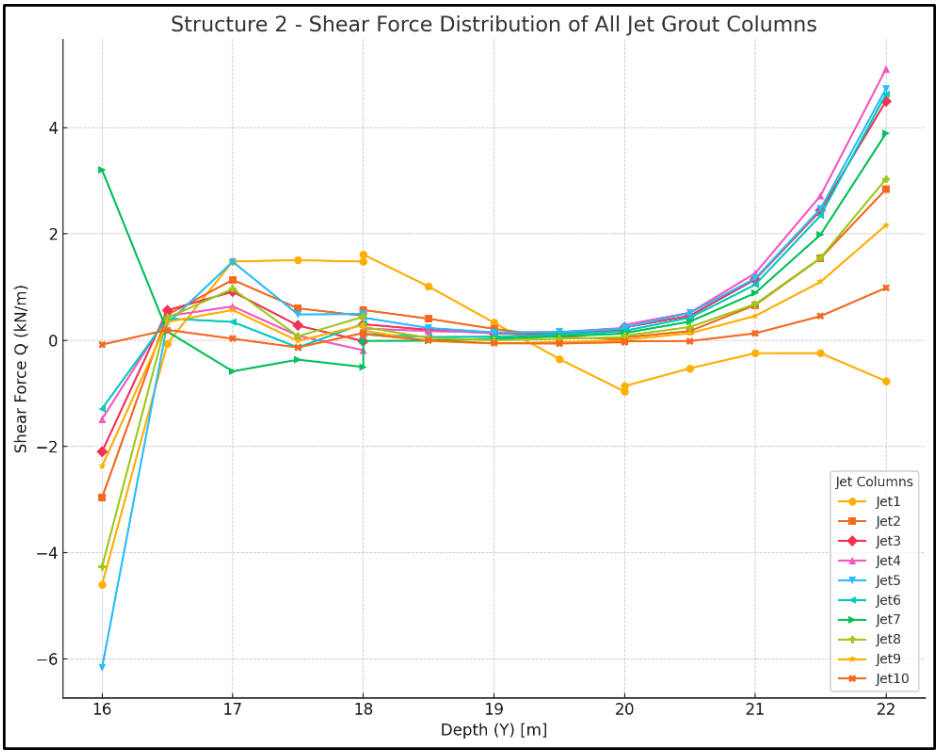

Figure 6.9 Shear Force Distribution of Jet Grout Columns Case Study 1- Structure 2

The Bending Moment graph (Figure 6.10) further confirms this trend, revealing substantial increases in negative bending moments towards the lower depths, underscoring critical bending behavior at the column tips.

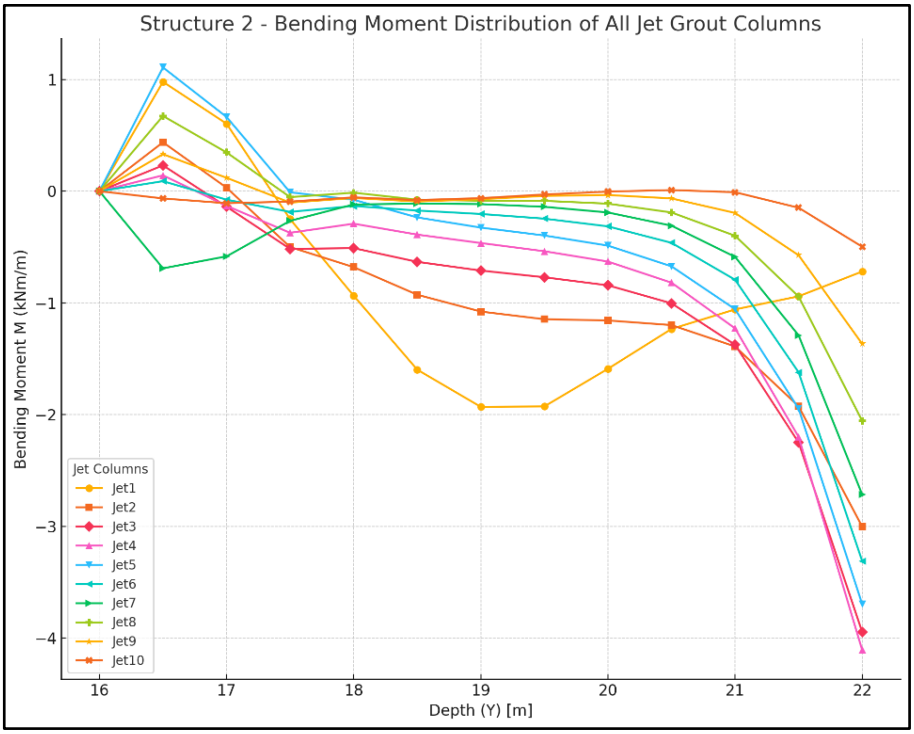

Figure 6.10 Bending Moment Distribution of Jet Grout Columns Case Study 1-Structure 2

The analysis clearly shows no group effects in Structure 2 as well, as the jet grout columns behave independently without load transfer interactions due to adequate spacing. Thus, the observed variations are attributed to individual loading conditions and local soil-column interactions rather than group influences.

Vertical displacement profiles of jet grout columns indicate consistent settlement behavior for Structure 1 (Figure 6.11) and Structure 2 (Figure 6.12). In Structure 1, vertical displacements show a uniform and linear increase towards the bottom, with slight differences between columns. In contrast, Structure 2 shows greater variability, particularly higher displacement values in corner columns. These findings emphasize the influence of column positioning and load distribution patterns, confirming the absence of group interactions.

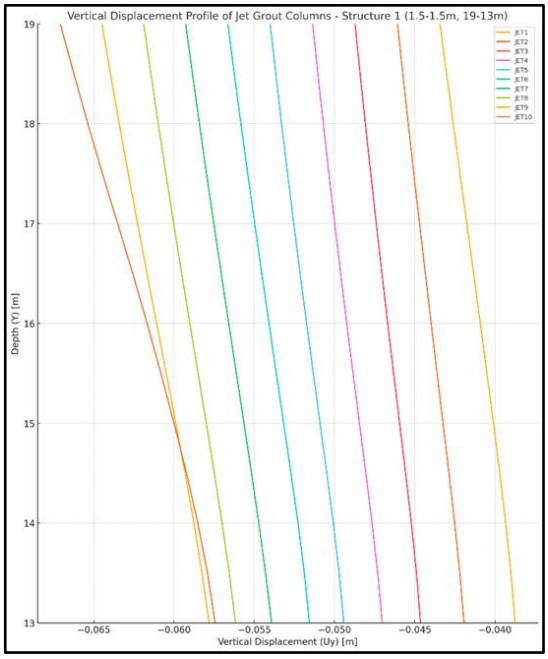

Figure 6.11 Vertical Displacement Profile of Jet Grout Columns Case Study1- Structure 1

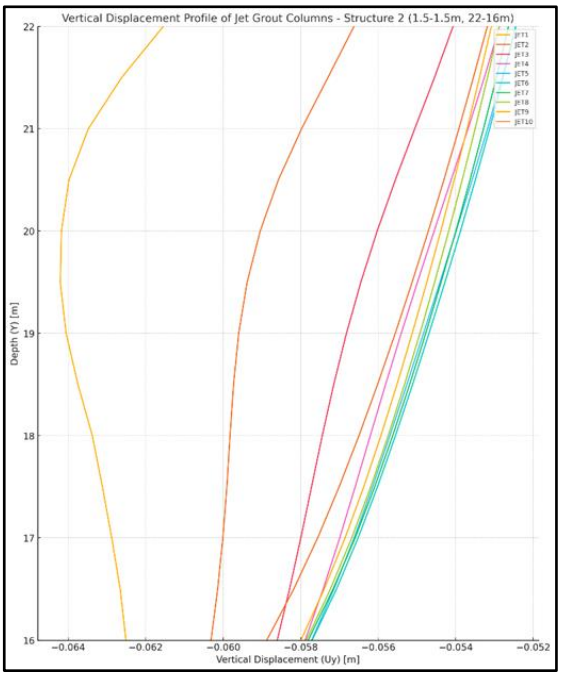

Figure 6.12 Vertical Displacement of Jet Grout Columns of Case Study 1 - Structure 2

Horizontal displacement analyses performed for Phase 2 and Phase 4 indicate substantial variations between these two phases. In Phase 2, the maximum horizontal displacement is approximately -4.92 × 10^{-3} m (Figure 6.13), with displacement values steadily increasing towards lower sections. However, in Phase 4, horizontal displacement significantly increases to approximately -10.31 × 10^{-3} m (Figure 6.14).

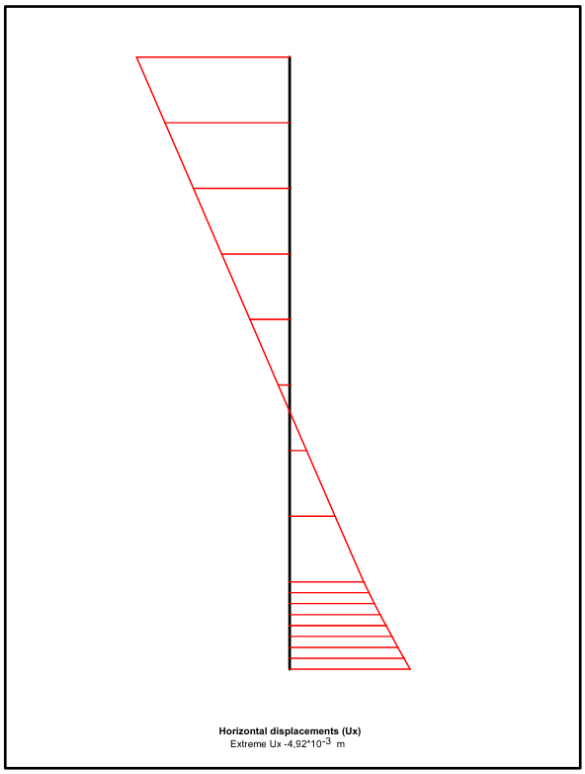

Figure 6.13 Horizontal Displacement of Diaphragm Wall at Case Study1 Phase 2

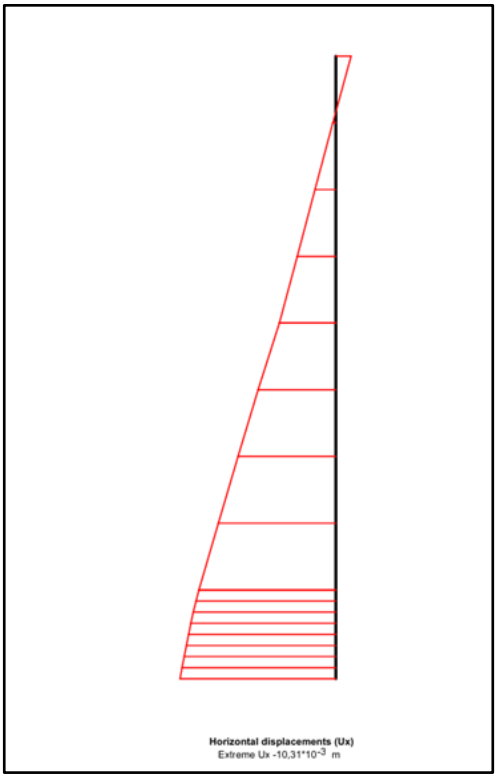

Figure 6.14 Horizontal Displacement of Diaphragm Wall at Case Study1 Phase 4

This pronounced increase underscores the impact of additional loading conditions, excavation scenarios, or structural modifications between phases. High displacement values at the lower sections demonstrate critical regions for horizontal load transfer, suggesting necessary reinforcement and stabilization measures at these depths to enhance structural integrity and performance.

Additionally, the transition from Phase 2 to Phase 4 resulted in significant changes in lateral earth pressures. Phase 2 reflects post-excavation conditions dominated by active earth pressures, leading to lower lateral pressure values on columns. Conversely, Phase 4 represents the fully loaded system, resulting in increased lateral earth pressures and the development of passive pressure zones around columns. The increase in horizontal stresses and corresponding lateral pressures at the lower sections indicates enhanced horizontal load transfer capacity, emphasizing improved stability and increased soil bearing capacity.

In conclusion, the case study clearly demonstrates that jet grout columns behave independently without significant group effects due to adequate spacing. Variations observed in horizontal stress, bending moment, shear force, and displacement analyses strongly emphasize the importance of structural positioning and local soil-column interactions. These findings provide valuable insights for optimizing design strategies and ensuring structural stability and performance.

6.2 FINITE ELEMENT ANALYSIS OF CASE STUDY 2 IN PLAXIS

In Case Study 2, the modeling approach largely followed the procedure described in Case Study 1, with some modifications made to the spacing of jet grout columns. Specifically, the column spacing for Structure 1 was maintained at 1.5 m, identical to Case Study 1, whereas the spacing for Structure 2 was reduced to 1.0 m to clearly illustrate the impact of increased group interactions. The phases and loading steps applied in the analyses remained identical to those used in Case Study 1, with the only difference being the reduced column spacing for Structure 2. This adjustment aimed to evaluate potential changes in lateral earth pressure, internal forces (shear forces and bending moments), horizontal stress distributions, settlement behaviors, and lateral displacements of the caisson foundation resulting from closer-spaced columns. The general geometry and column arrangement for this case are presented in Figure 6.15.

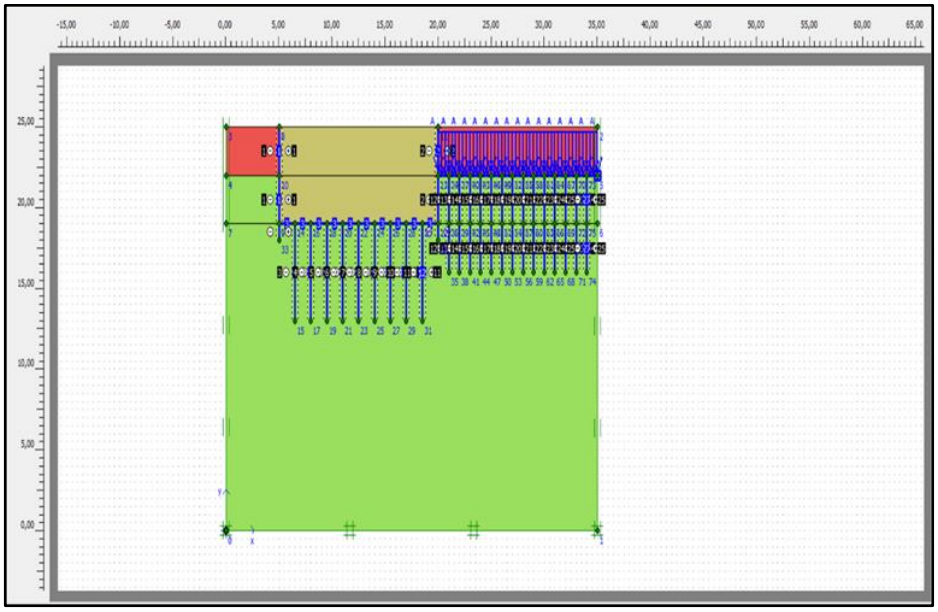

Figure 6.15 General view of finite element model showing geometry, stratification, and structural components for Case Study 2 in PLAXIS

Upon examining the internal force and stress distributions for the jet grout columns of Structure 1, it was observed that maximum values occurred near the lower tips of the columns (approximately between 13–14 m depth) and gradually decreased, approaching zero at the upper levels (around 19 m depth). Notably, the columns located at the corners and those positioned between Structures 1 and 2 exhibited significant variations and higher values compared to the other columns. The primary reasons for these variations include proximity to boundary conditions, complex load distributions resulting from structure-to-structure interactions, internal stress concentrations at the soil-column interfaces, and unbalanced lateral loading conditions induced by nearby excavations and external loads. These findings clearly emphasize the importance of the spatial arrangement and column spacing in the design of jet grout columns. The bending moment distributions of the columns are presented in Figure 6.16, shear force distributions in Figure 6.17, and horizontal total stress distributions in Figure 6.18.

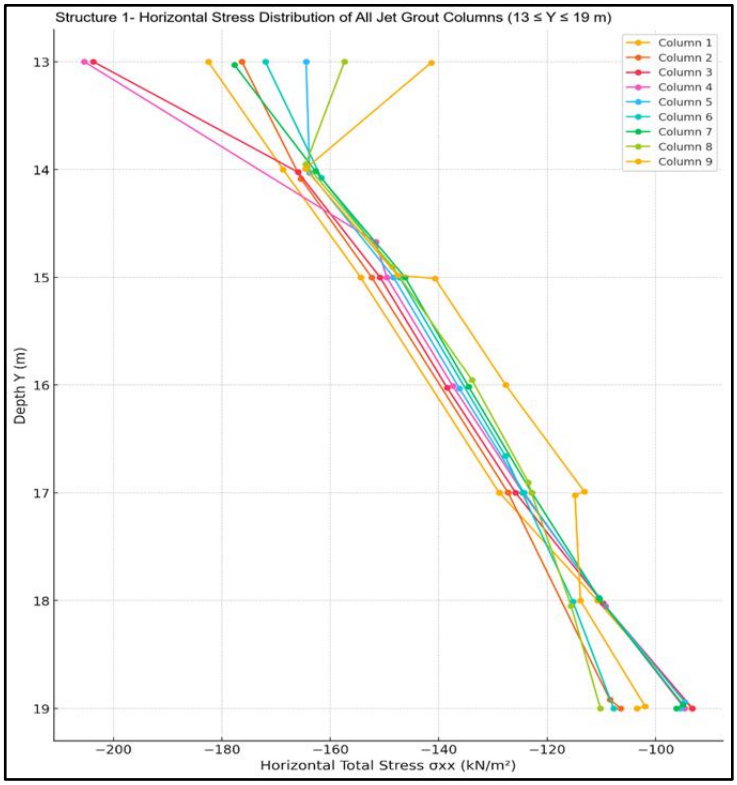

Figure 6.16 Horizontal Stress Distribution of Jet Grout Columns Case Study 2 - Structure 1

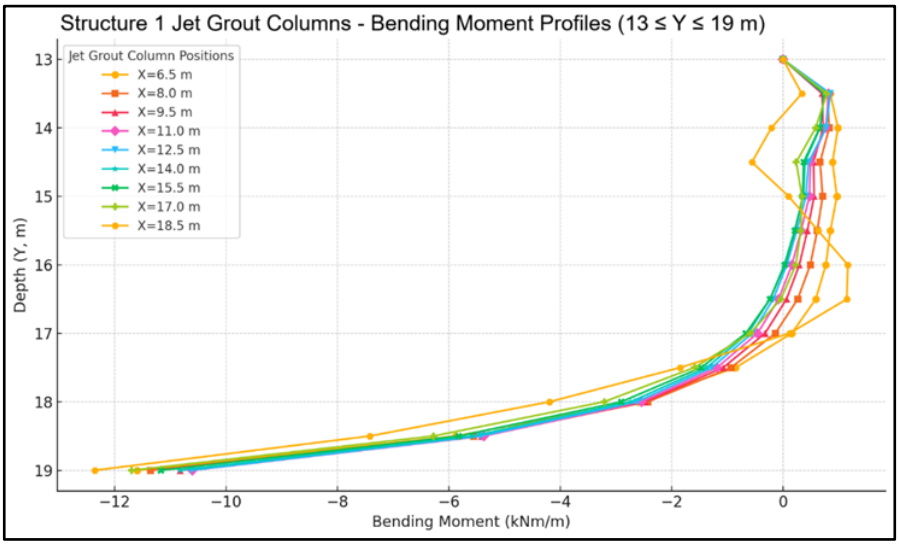

Figure 6. 17 Bending Moment Distribution of Jet Grout Columns Case Study 2 - Structure 1

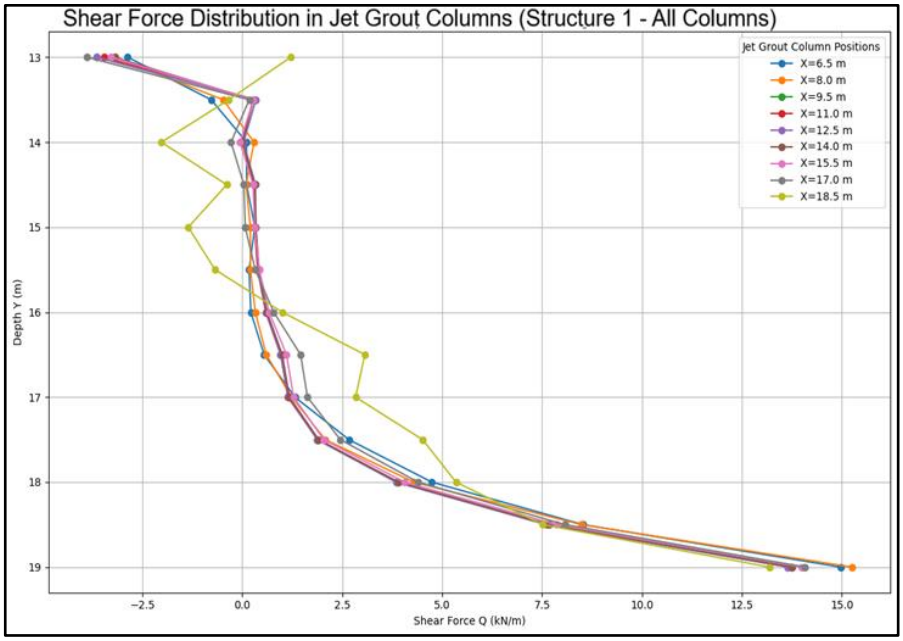

Figure 6.18 Shear Force Distribution of Jet Grout Columns Case Study 2 - Structure 1

With the reduction of jet grout column spacing to 1.0 m for Structure 2, significant variations in internal force distributions and horizontal stresses within the columns were observed. The reduced spacing between columns intensified the group effect by increasing the interaction zones, thereby directly influencing the loading conditions experienced by each column. The analyses indicated notable increases in shear forces (Figure 6.19), bending moments (Figure 6.20), and horizontal total stresses (Figure 6.21), particularly within the middle and lower sections of the columns (approximately between 16 and 19 m depth), accompanied by fluctuations toward the column tips. This behavior was especially pronounced at corner columns and columns positioned between Structures 1 and 2, primarily due to boundary conditions and structural interaction effects. These columns experienced higher stresses and internal force magnitudes. The outcomes clearly demonstrate that reducing the spacing between jet grout columns amplifies group interactions, significantly impacting the load-bearing capacity and overall performance of the columns. These

findings underline the critical importance of spatial arrangement and column spacing in geotechnical design involving jet grout columns.

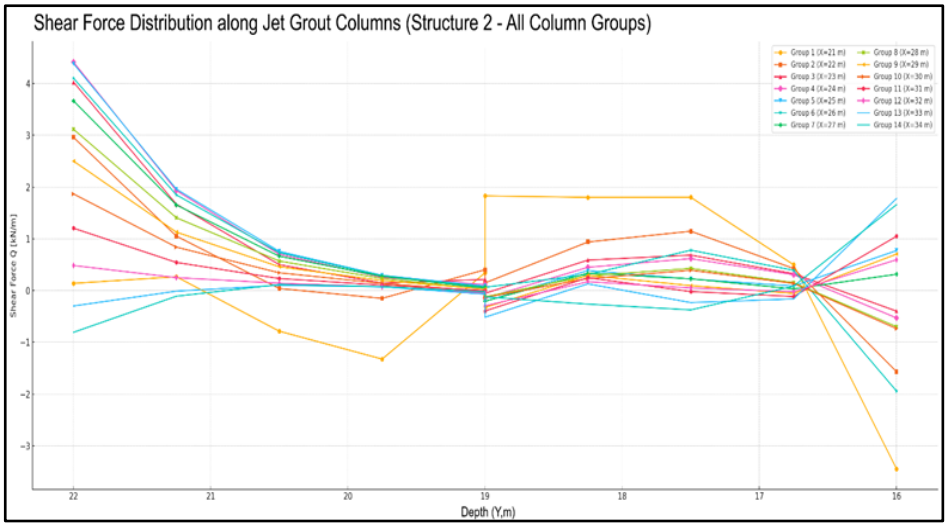

Figure 6.19 Bending Moment Distribution of Jet Grout Columns Case Study 2 - Structure 2

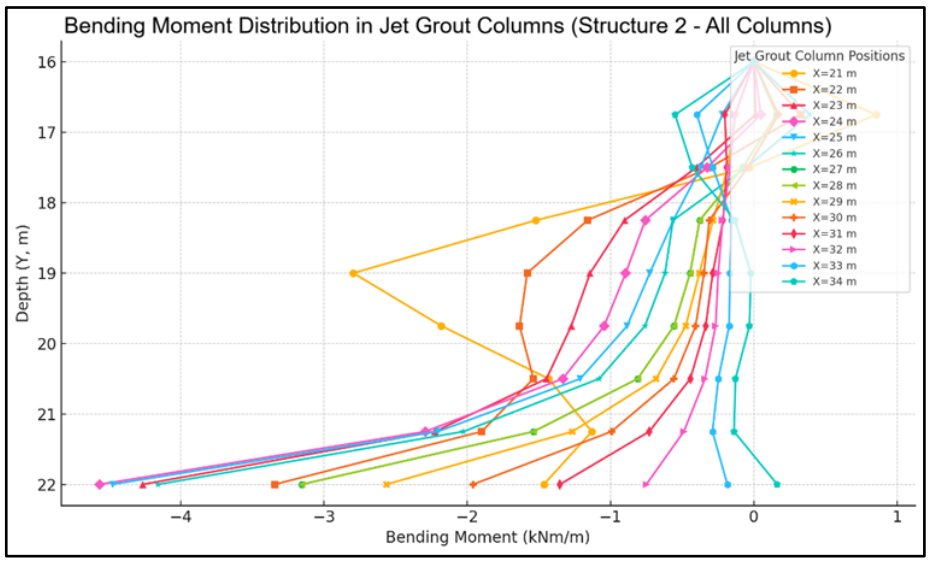

Figure 6.20 Shear Force Distribution of Jet Grout Columns Case Study 2 - Structure 2

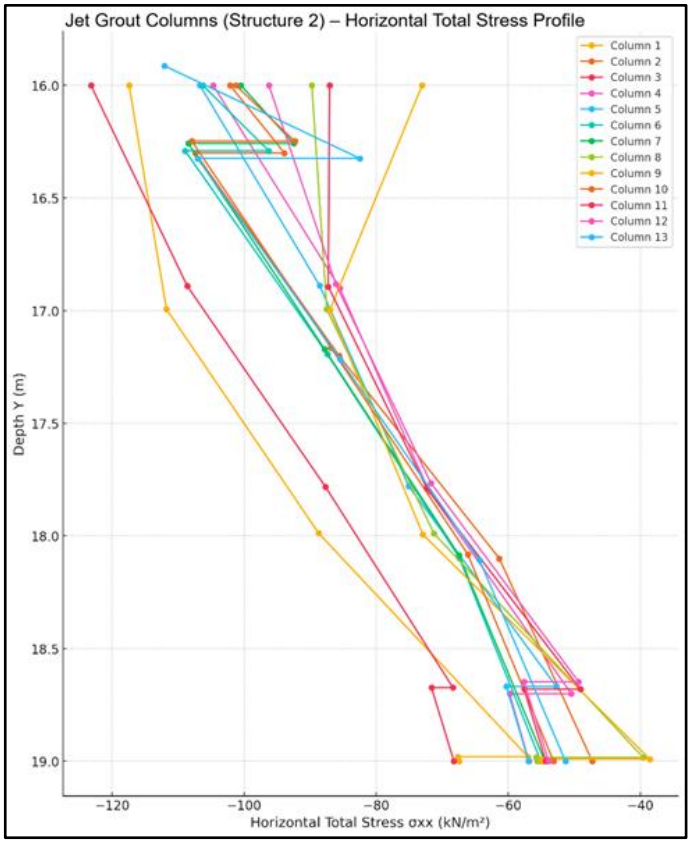

Figure 6.21 Horizontal Stress Distribution of Jet Grout Columns Case Study 2-Structure 2

When comparatively evaluating the effects of varying jet grout column spacing applied in Structure 1 and Structure 2, significant differences were observed in the internal force distributions and horizontal stress distributions. While columns were spaced at 1.5 m intervals in Structure 1, reducing the spacing to 1.0 m in Structure 2 notably increased the interaction zones among columns. This resulted in higher shear forces, bending moments, and horizontal total stress values in the jet grout columns of Structure 2 compared to those in Structure 1, particularly at the mid-to-lower depth regions (approximately between 16–19 m). Although reducing the spacing between columns decreased the individual load-bearing capacities due to heightened group interactions, it facilitated a more effective and integrated transfer of loads into the surrounding soil. This demonstrates that designing jet grout columns as groups can enhance

overall load-transfer performance, despite the reduction in individual column capacities. Notably higher internal forces and stress concentrations observed in corner columns and those located between the two structures further emphasize the critical influence of column arrangement and structural interactions on column behavior. These findings highlight the importance of optimizing column spacing within geotechnical design.

Upon examining the vertical displacement behaviors of jet grout columns for Structure 1 and Structure 2, the impact of column spacing on settlement distributions was clearly demonstrated. In Structure 1, vertical displacement values ranged approximately between -0.040 m and -0.065 m, beginning at lower magnitudes near the upper portions of columns (around 19 m) and notably increasing towards greater depths (around 13 m) (Figure 6.22). Columns located near structural boundaries exhibited higher displacement values due to stress concentration effects. For Structure 2, reducing the column spacing to 1.0 m significantly increased the group effect, resulting in higher vertical displacement values, ranging approximately from -0.056 m to -0.065 m (Figure 6.23). Particularly at upper elevations (between 22–20 m depths), corner and boundary columns showed distinctly higher displacement values compared to others. Comparative analysis revealed that although decreasing column spacing increased individual column settlements, it positively contributed to a more uniform and efficient load transfer into the soil. These findings underscore the importance of optimizing jet grout column spacing in ground improvement designs.

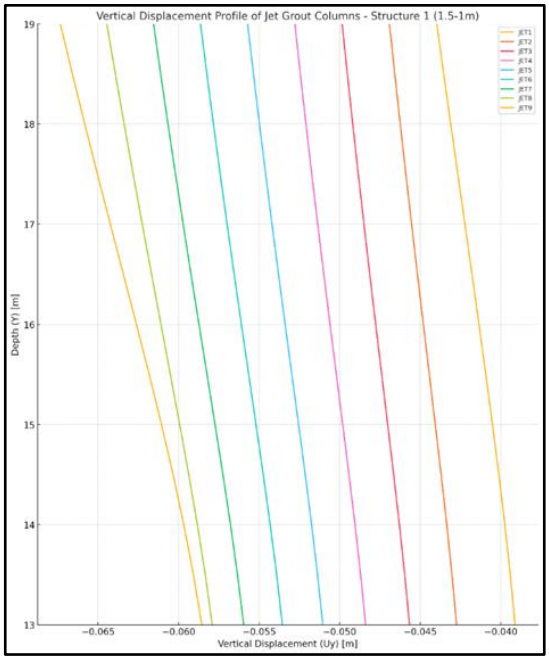

Figure 6.22 Vertical Displacement Profile of Jet Grout Column Case Study 2-Structure 1

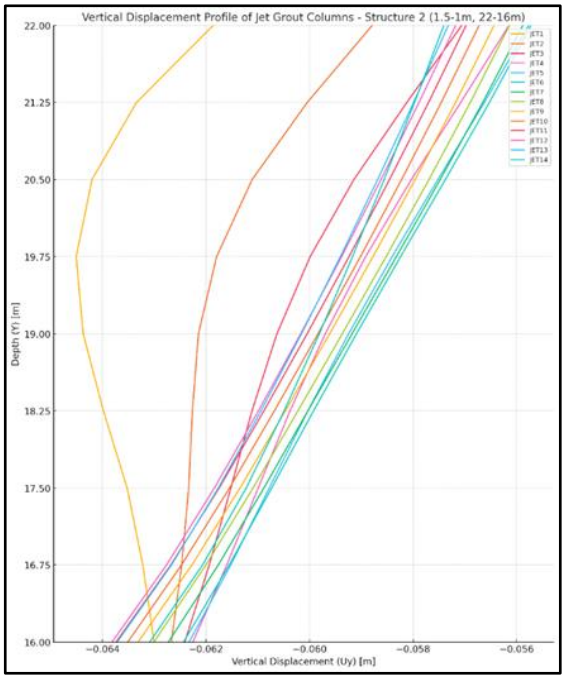

Figure 6.23 Vertical Displacement Profile of Jet Grout Columns Case Study 2-Structure2

It has been determined that reducing column spacing for Structure 2 significantly influences lateral earth pressures and associated lateral displacements due to the group effect. Analysis results indicate that lateral earth pressures, initially in a passive state (while Structure 1 was active), shifted towards an active state as interaction zones between columns increased. Particularly, the group effect present in Structure 2 reshaped the stress distribution within the soil, enabling passive pressures to be managed more effectively. This condition notably limited lateral movements of the columns, thereby helping control horizontal displacement values. In this context, it is clearly demonstrated that placing jet grout columns at closer spacing positively contributes to controlling lateral loads and stabilizing the ground due to enhanced group interactions. The horizontal displacement profiles illustrating this effect are presented in Figure 6.24 and for Phase 2 and Figure 6.24 for Phase 4.

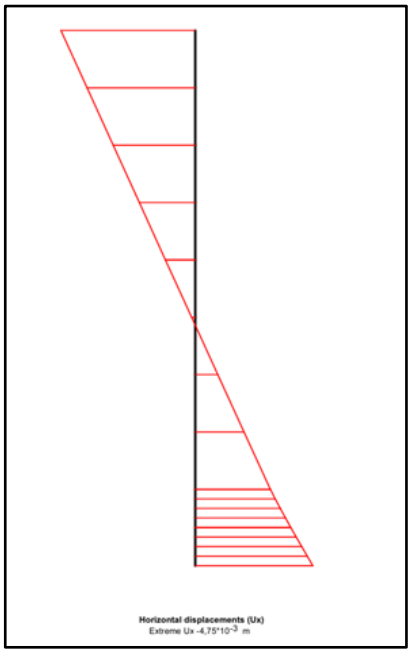

Figure 6.24 Horizontal Displacement of Diaphragm Wall at Case Study2 Phase 2

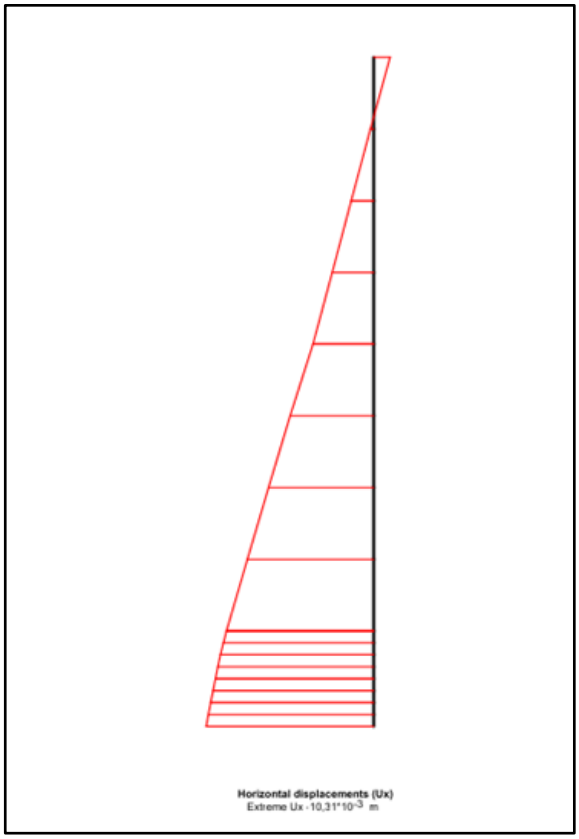

Figure 6.25 Horizontal Displacement of Diaphragm Wall at Case Study2 Phase 4

6.3 FINITE ELEMENT ANALYSIS OF CASE STUDY 3 IN PLAXIS

In this case study, the effects of modifying the spacing between jet grout columns are assessed by inversely adjusting the arrangements from the previous scenario. Specifically, jet grout columns in Structure 1 are placed at a closer spacing of 1.0 meter, while those in Structure 2 have an increased spacing of 1.5 meters. This alteration aims to clearly illustrate the influence of varying column spacing on lateral earth pressures, bending moments, shear forces, and vertical and horizontal displacements. Comparative analyses with the preceding cases will facilitate an enhanced understanding of group interaction phenomena and guide optimized design practices. The geometrical configuration and model setup for this scenario are illustrated in Figure 6.26.

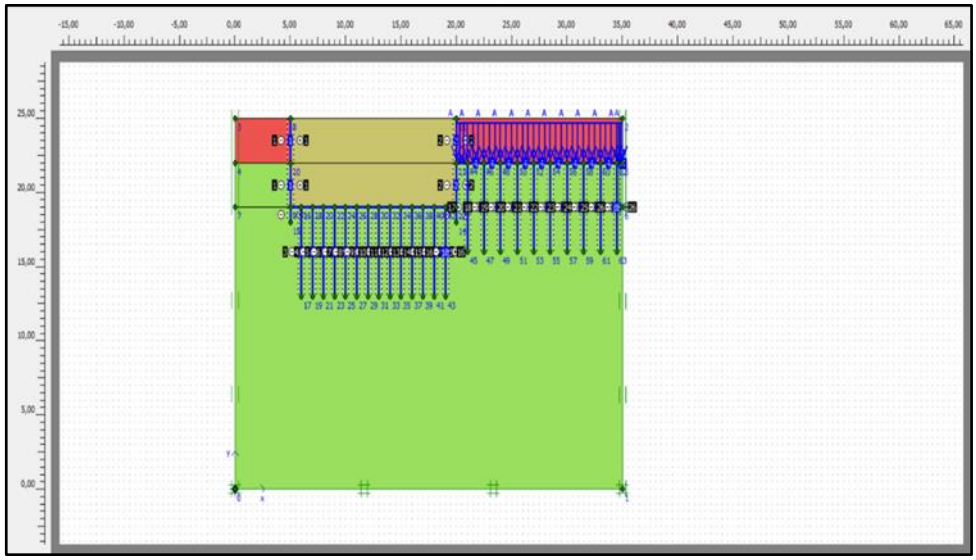

Figure 6.26 General View Of Finite Element Model Showing Geometry, Stratification, And Structural Components For Case Study 3 In PLAXIS

In the analyses conducted for Structure 1 within the scope of Case Study 3, the upper and lower levels of the jet grout columns were defined as 19 m and 13 m, respectively. Assessments considering these height ranges revealed that the horizontal total stresses increased steadily along the columns and that there were significant stress concentrations, particularly at the lower height of 13 m (Figure 6.27). Similarly, the bending moment analysis showed a marked increase in negative moment values as the lower height of the columns (13 m) was approached (Figure 6.28). The negative moment demand at the end region emerges as a critical design condition below the 1.0 m span; it requires special attention to the material strength and integrity in the end zone and to the edge/corner column details. Shear forces also showed an increasing trend from the upper height (19 m) to the lower height (13 m), reaching particularly pronounced concentrations in the lower region of the columns (Figure 6.29). These findings clearly demonstrate that the heights of the columns directly affect their behaviour due to group interactions and cause structural capacities to approach critical levels, particularly in the lower end zone.

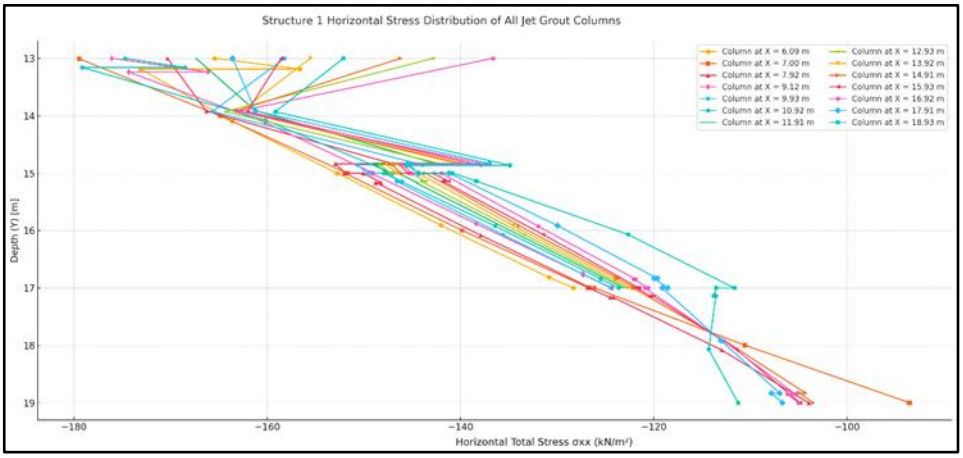

Figure 6.27 Horizontal Stress Distribution of Jet Grout Colum Case Study 3 Structure 1

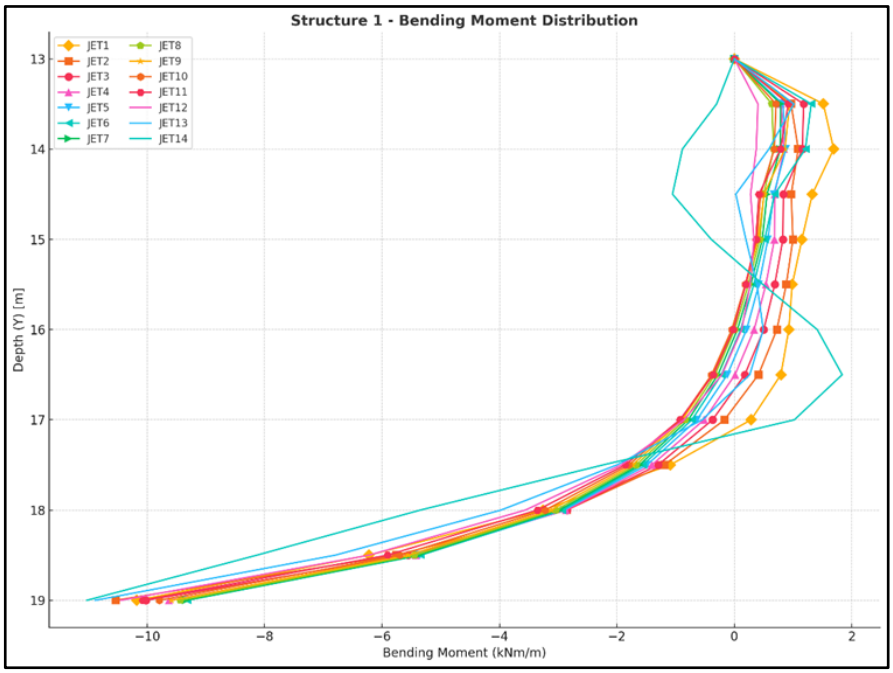

Figure 6.28 Bending Moment Distribution of Jet Grout Columns Case Study 3-Structure 1

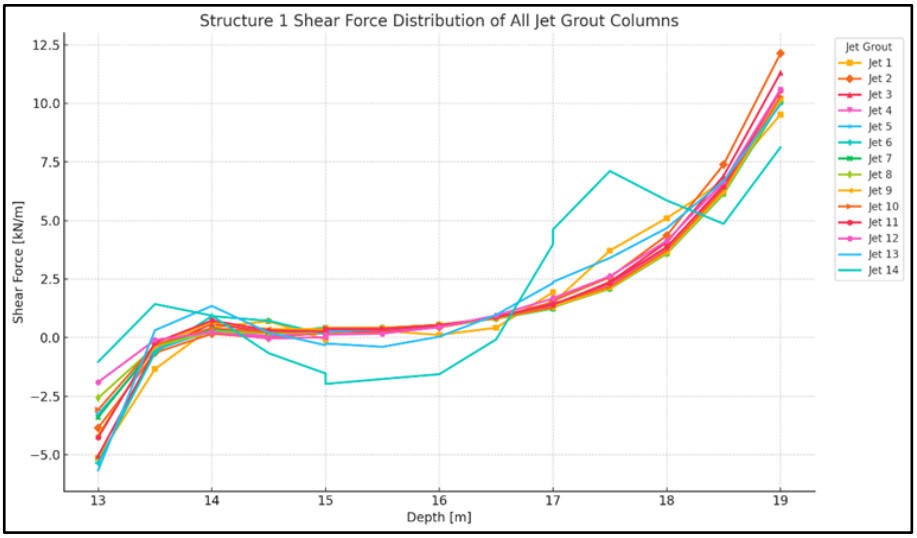

Figure 6.29 Shear Force Distribution of Jet Grout Columns Case Study 3 Structure 1

In the analyses conducted for Structure 2, evaluations were made considering that the upper elevation of the jet grout columns was at 22 meters and the lower tip at 16 meters. Upon examining the horizontal total stress distributions resulting from the columns being placed at 1.5 meter intervals, it was observed that a more balanced and controlled stress distribution occurred among the columns. However, irregular and notable increases in stress were evident at the lower tip region of the columns, particularly at a depth of 16 meters (Figure 6.30).

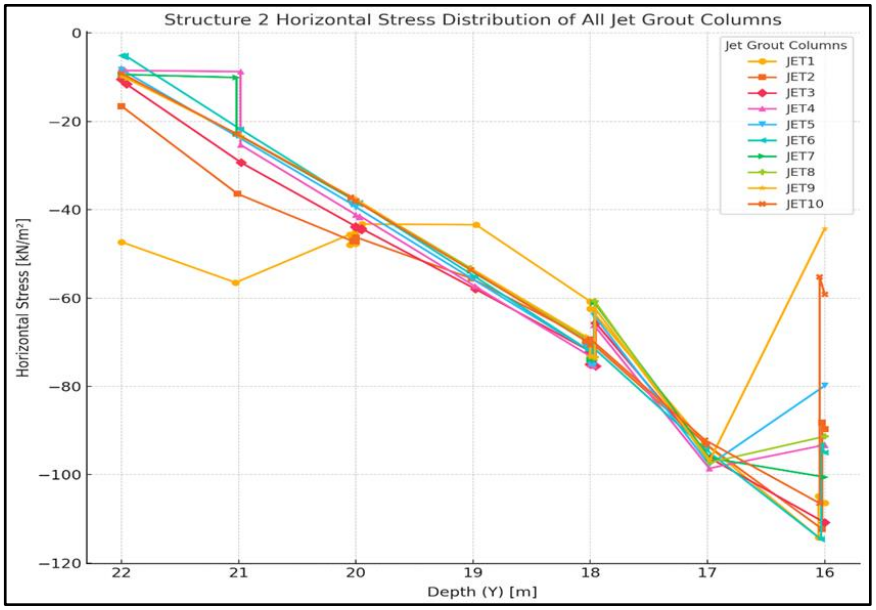

Figure 6.30 Horizontal Stress Distribution of Jet Grout Columns Case Study 3-Structure 2

In the bending moment analysis, columns exhibited stable and regular behavior in their middle sections, while significant and elevated bending moments were observed towards their upper and lower tip regions, especially around the lower tip region at 16 meters depth. This indicates that the interaction at the column tips reached critical levels, underscoring the need for special consideration in the structural design (Figure 6.31).

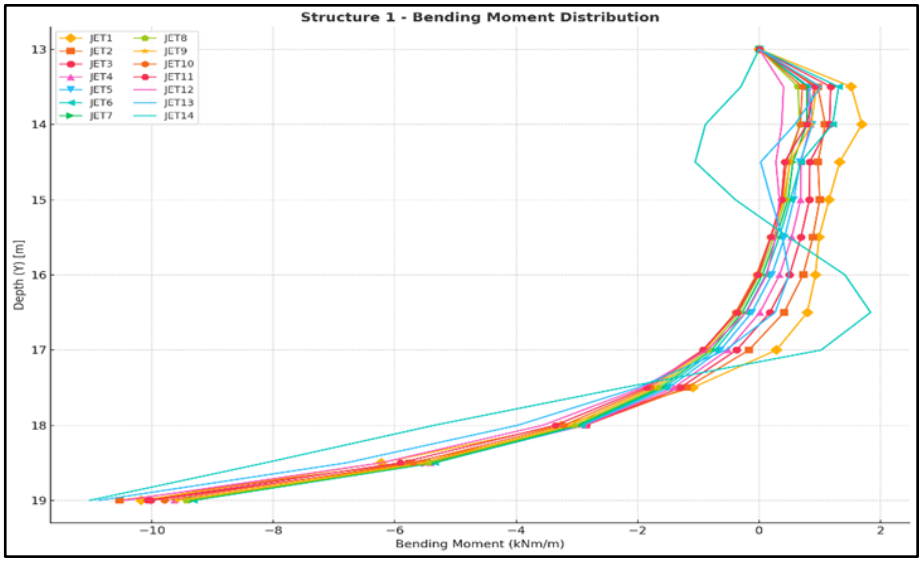

Figure 6.31 Bending Moment Distribution of Jet Grout Columns Case Study 3- Structure 2

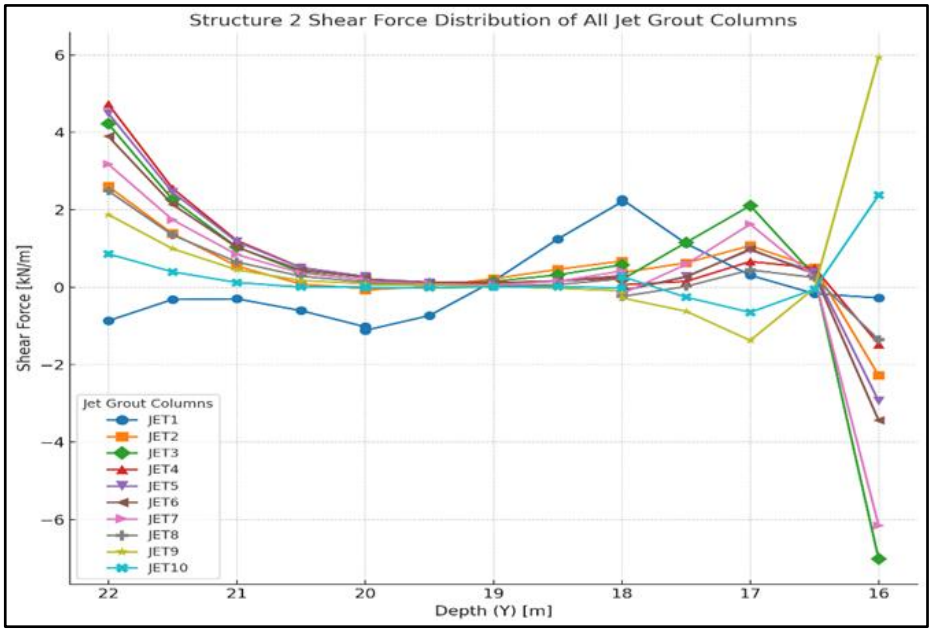

Figure 6.32 Shear Force Distribution of Jet Grout Columns Case Study 3- Structure 2

In the shear force analysis, although there was generally a consistent decreasing trend along the column depth, significant increases and irregularities were detected near the lower tip regions (at 16 meters depth). The notable increase in shear forces in this area clearly highlights that the column-soil interactions subjected the column tips to critical stress and forces (Figure 6.32).

Irregular distributions particularly observed at the column toes and along edge columns arise from unilateral support conditions and local stiffness constraints. These observations emphasize the critical importance of explicitly considering group effects in the toe regions and of selecting column spacing with care during design. Within Case Study 3, a comparative assessment was conducted for Structure 1 and Structure 2. In Structure 1 (spacing 1.0 m; head ≈ 13 m, toe ≈ 19 m), the close layout enlarges the interaction zone among adjacent columns, producing higher and more irregular horizontal total stresses, especially near the toe; bending moments reach critical levels at the toes and shear forces increase markedly along the column length with locally concentrated peaks toward the bottom. By contrast, in Structure 2 (spacing 1.5 m; head 22 m, toe 16 m), the wider spacing reduces inter-column interaction, leading to lower-magnitude and more uniform horizontal stress distributions; bending moments are lower and more evenly distributed, and shear forces remain controlled and stable over depth, with only localized variability near the toe (~16 m). Overall, the results demonstrate that increasing spacing mitigates group effects and promotes a more homogeneous lateral earth pressure response, whereas close spacing drives the system toward critical toe demands.

This comparative analysis demonstrates that reducing column spacing significantly increases group effects and pushes structural behaviour towards critical levels. Therefore, it emphasises that careful selection of column spacing during design and consideration of specific issues for corner and edge columns in closely spaced arrangements are critical for structural safety.

The analyses conducted demonstrate that the intensification of group effects due to reduced spacing between columns significantly affects the settlement behaviour of jet grout columns. In Structure 1, the closer arrangement

of columns (1 m spacing) increased the interaction zone between columns and led to markedly higher and more irregular settlement values, particularly at the column ends near the lower zone at a depth of 19 m (Figure 6.33 - Structure 1). Conversely, in Structure 2, the wider column spacing (1.5 m) allowed the columns to behave more independently, resulting in more controlled, homogeneous, and generally lower settlement values (Figure 6.34 - Structure 2)

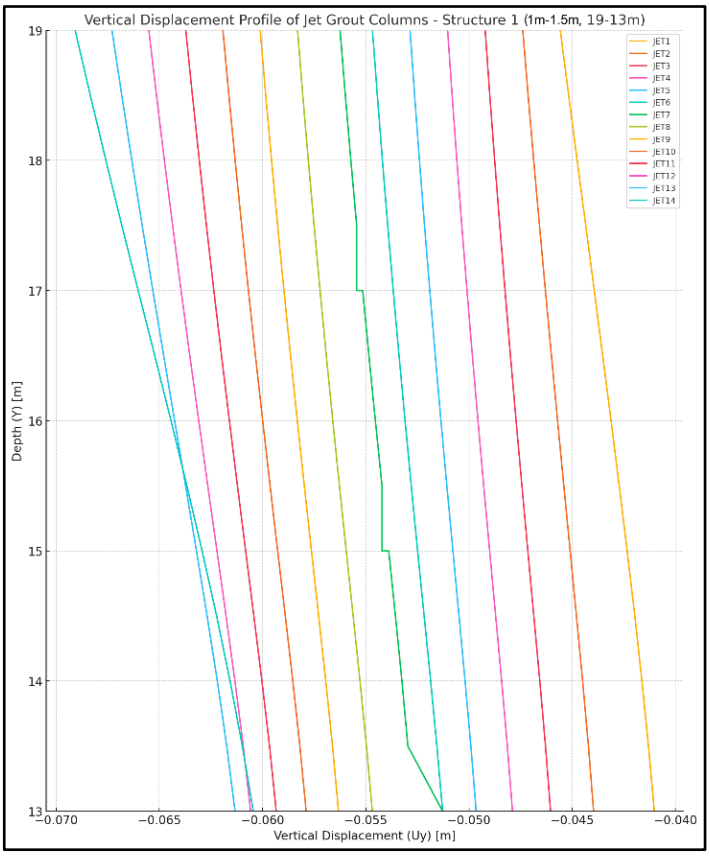

Figure 6.33 Vertical Displacement Profile of Jet Grout Columns Case Study 3-Structure 1

This clearly illustrates that under significant group effects, the expanded interaction zone near column tips leads to uneven load distributions, consequently increasing settlements. Therefore, careful determination of column spacing is crucial to minimize settlements at column tips and achieve more uniform settlement distributions.

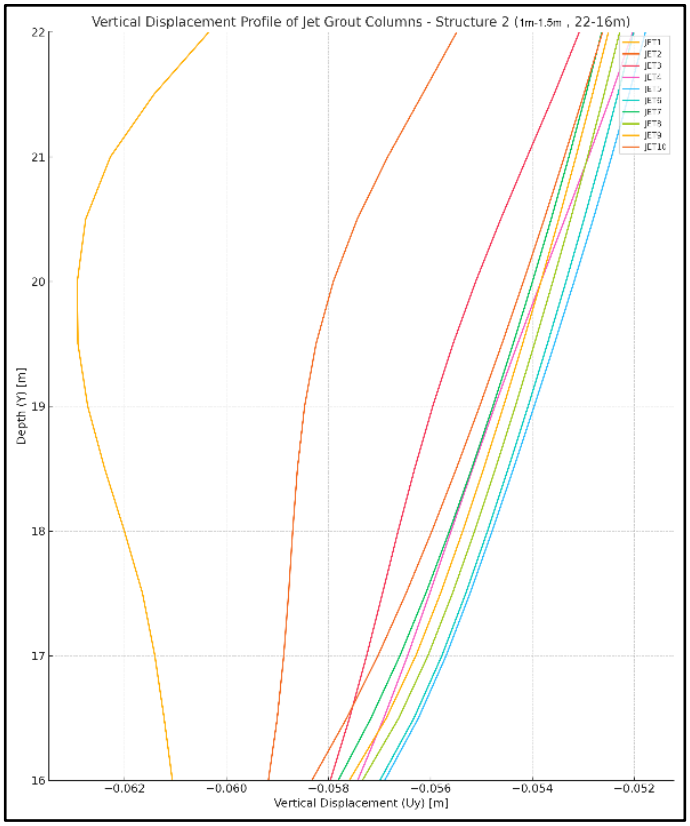

Figure 6.34 Vertical Displacement Profile of Jet Grout Columns Case Study 3-Structure 2

In Phase 2, horizontal displacement values of the diaphragm wall were relatively lower. Displacement decreased from the upper regions to the lower regions of the diaphragm wall, with the maximum displacement recorded as approximately 4.96 mm. This condition corresponds to a stage where loading conditions are limited and the structure is not yet fully loaded.

Moving to Phase 4, the maximum horizontal displacement value of the diaphragm wall increased significantly to 10.62 mm. This higher displacement occurred at the stage when structural loads were fully applied, resulting in increased loading on the columns. A noticeable increase in displacement was observed, particularly from the upper regions to the lower regions of the diaphragm wall. This is a direct result of stresses and deformations generated along the wall due to increased structural loads.

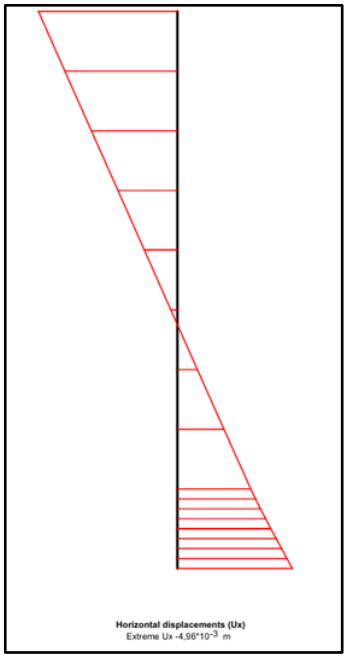

Figure 6.35 Horizontal Displacement of Diaphragm Wall at Case Study3 Phase 2

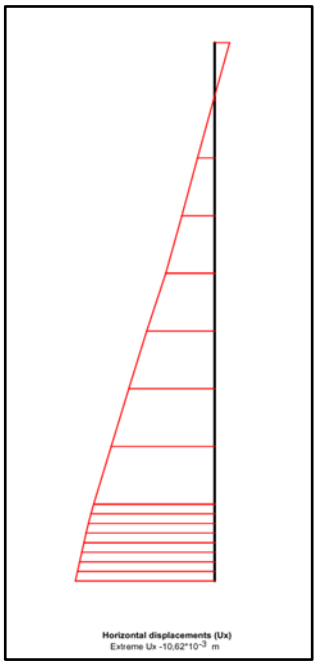

Figure 6.36 Horizontal Displacement of Diaphragm Wall at Case Study3 Phase 4

When comparing diaphragm wall displacements with horizontal total stress, bending moment, and shear force results obtained from jet grout columns, a similar behavior can be identified, particularly for Structure 1, which is under significant group effects. The lower regions of the jet grout columns experienced higher horizontal stresses, moments, and shear forces, which are analogous to the substantial displacements observed in the lower portion of the diaphragm wall.

In conclusion, increased loading during Phase 4 significantly heightened deformation and stress, especially at the lower regions of both the diaphragm wall and jet grout columns. Therefore, the impact of load increments on deformation and stress should be carefully assessed in structural design, and necessary strengthening measures and design considerations should be implemented, taking group effects into account.

6.4 FINITE ELEMENT ANALYSIS OF CASE STUDY 4 IN PLAXIS

In this case study, all model parameters remain consistent with previous analyses, except for the adjusted column spacings. Specifically, jet grout columns in Structure 1 are arranged at a spacing of 0.75 meters, whereas those in Structure 2 have a spacing of 1.5 meters. This strategic variation aims to intensify group interaction effects and provide clearer insights into how closely spaced columns influence lateral earth pressure distribution, bending moment responses, shear forces, and vertical and horizontal displacements. Comparative evaluations against earlier scenarios will enhance the understanding of spacing impacts on overall structural and geotechnical performance. The geometrical configuration and model setup for this scenario are illustrated in Figure 6.40. Structure 1 comprises 13 jet grout columns extending upwards from a bottom depth of 19 meters, while Structure 2 columns start at a depth of 22 meters and end at 16 meters. These findings clearly indicate that reducing column spacing enhances the group effect, substantially decreasing the resistance capacity of the columns in the surrounding soil.

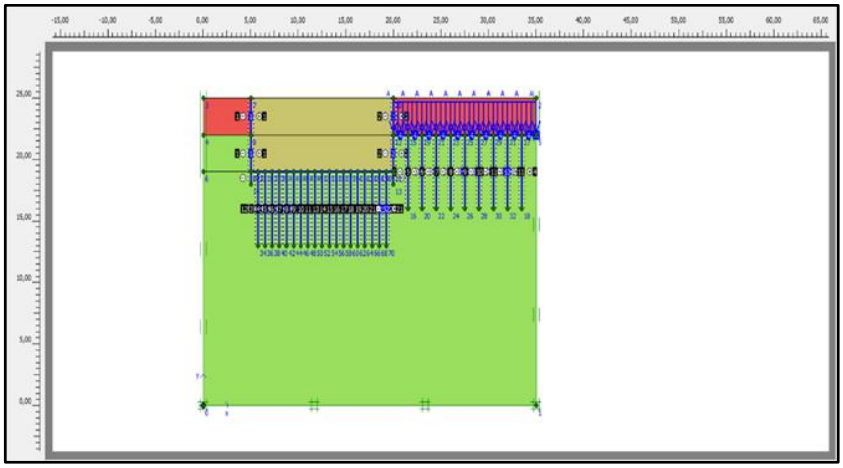

Figure 6.37 General View Of Finite Element Model Showing Geometry, Stratification, And Structural Components For Case Study 4 In PLAXIS

Within Structure 1, the arrangement of jet grout columns at closer intervals of 0.75 meters significantly enhances the group effect. Detailed analyses demonstrate that horizontal total stress (σ_{xx}) distributions presented in Figure 6.38

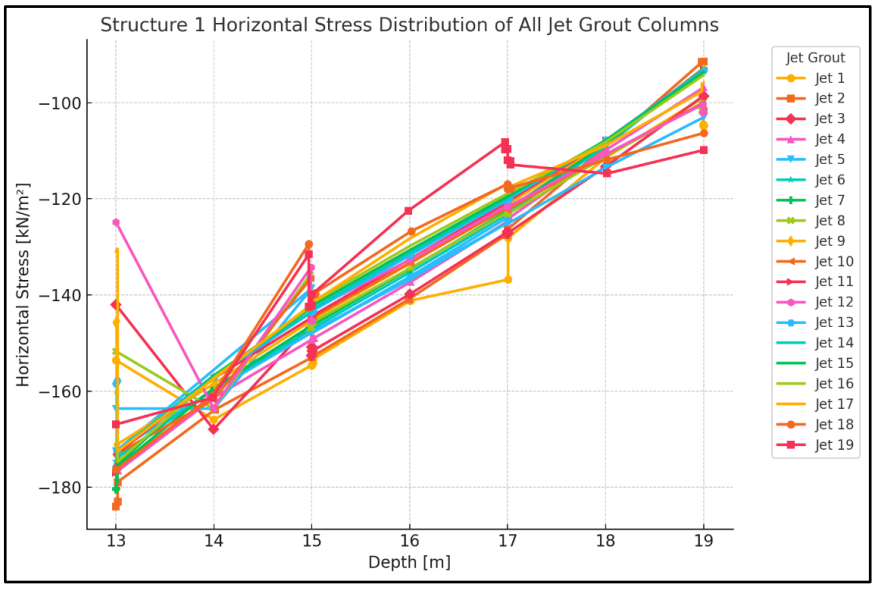

Figure 6.38 Horizontal Stress Distribution of Jet Grout Column Case Study 4-Structure 1

Exhibit denser and more uniform stress fields due to the closely spaced columns. The reduction in column spacing increases stress concentrations, consequently elevating the surrounding soil stresses. Examination of bending moment distributions illustrated in Figure 6.39 indicates notably higher positive and negative bending moments, particularly at the upper and lower column ends. This observation highlights the substantial increase in bending moments caused by intensified group interactions resulting from closer column spacing, emphasizing the necessity for meticulous evaluation of column bending resistance during design.

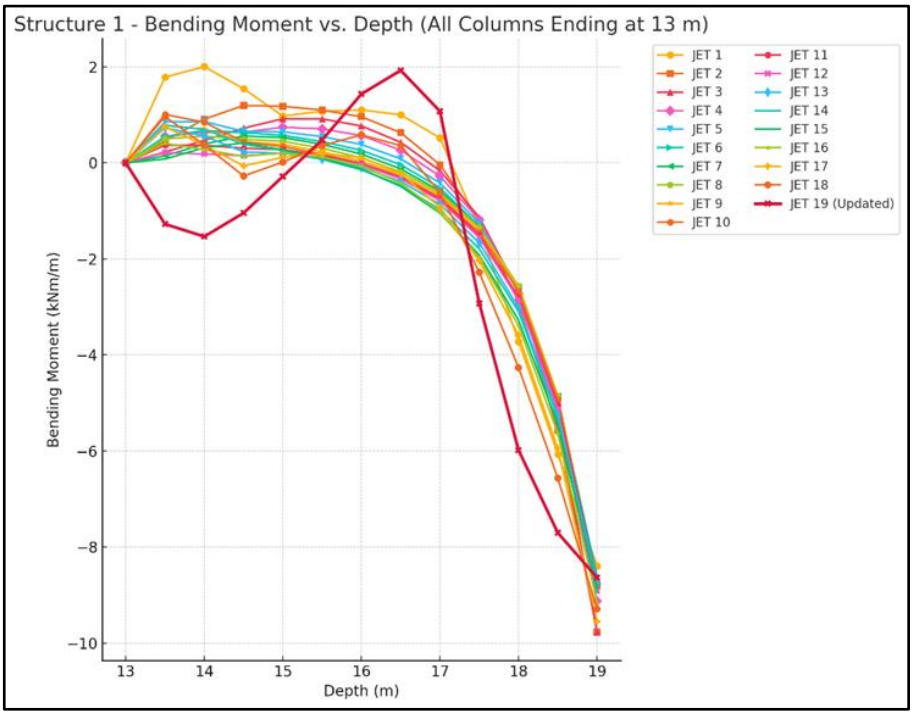

Figure 6.39 Bending Moment Distribution of Jet Grout Columns Case Study 4 - Structure 1

Lastly, shear force analyses shown in Figure 6.40 reveal a clear increase in shear forces along the column depth, particularly pronounced at lower sections. The intensified shear forces at these lower levels directly result from enhanced group effects due to reduced column spacing. Additionally, analyses

identify distinctly higher and irregular stress, bending moment, and shear force distributions specifically in edge columns. This anomaly arises because edge columns receive lateral support from only one side, lacking confinement and rigidity constraints. Conversely, centrally positioned columns, benefiting from mutual interaction, distribute loads more symmetrically and uniformly, resulting in comparatively lower and more homogeneous stress values. This atypical stress escalation observed in edge columns underscores the critical importance of carefully assessing rigidity and support conditions, as well as highlighting the significance of strategic placement of jet grout columns in design considerations. Consequently, these findings conclusively demonstrate that reduced jet grout column spacing under group effects substantially elevates horizontal total stresses, bending moments, and shear forces, necessitating careful consideration in the structural and geotechnical optimization process.

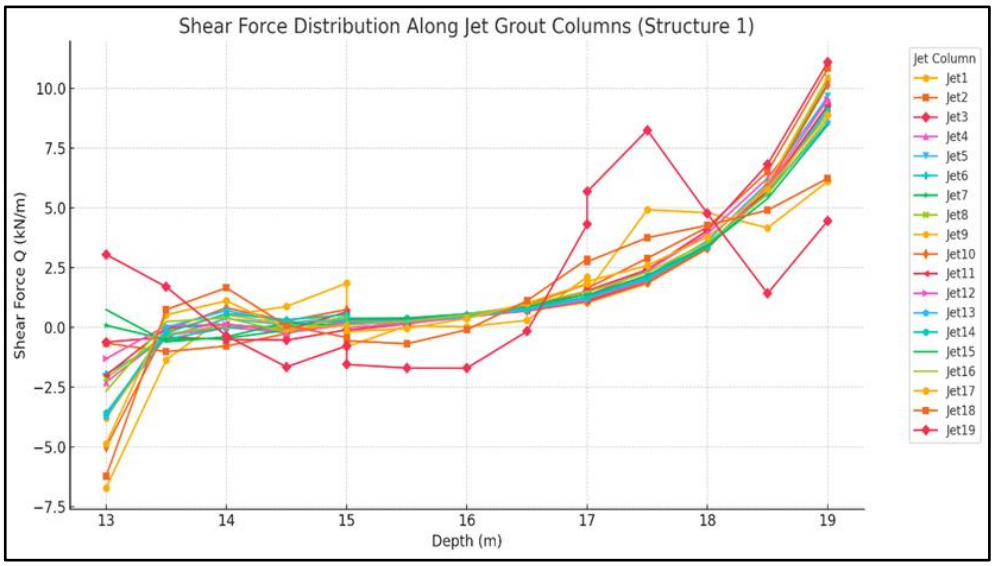

Figure 6.40 Shear Force Distribution of Jet Grout Columns Case Study 4-Structure 1

The analyses performed for Structure 2, where jet grout columns were arranged at 1.5-meter spacing, indicate significantly reduced group interaction effects compared to Structure 1, in which columns were spaced at 0.75 meters

and exhibited pronounced group behavior. In Structure 2, horizontal total stress (σ_{xx}) distributions appeared more regular and homogeneous (Figure 6.41), bending moments, although concentrated at the column tips, generally exhibited lower magnitudes (Figure 6.42). Additionally, shear forces, despite increasing with depth, were notably lower than the elevated levels observed in Structure 1 (Figure 6.43). These findings clearly demonstrate that increasing column spacing substantially mitigates group effects, yet attention must still be paid to critical stress and force regions, particularly at the tips and edges of the columns.

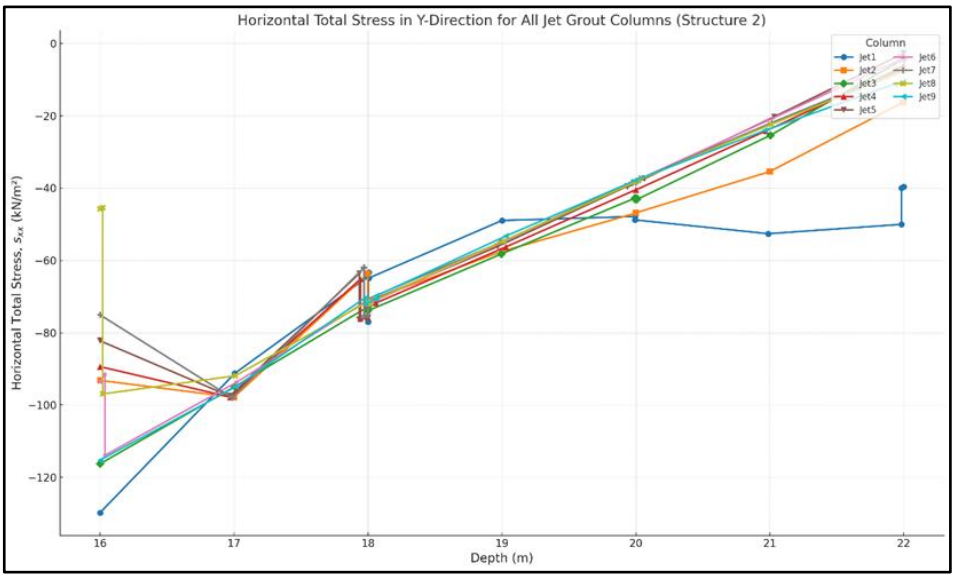

Figure 6.41 Horizontal Stress Distribution of Jet Grout Columns Case Study 4 - Structure 2

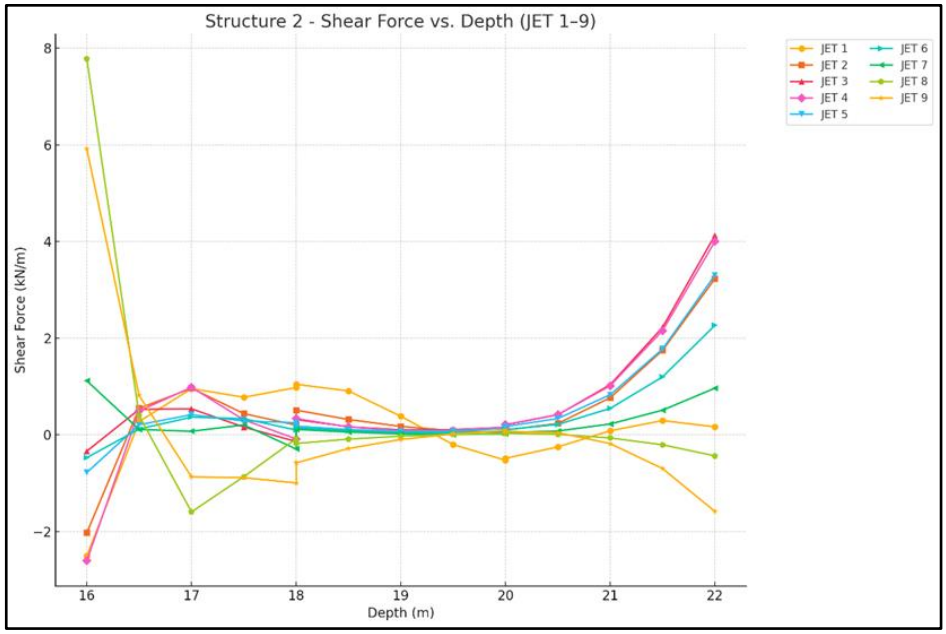

Figure 6.42 Shear Force Distribution of Jet Grout Columns Case Study 4- Structure 2

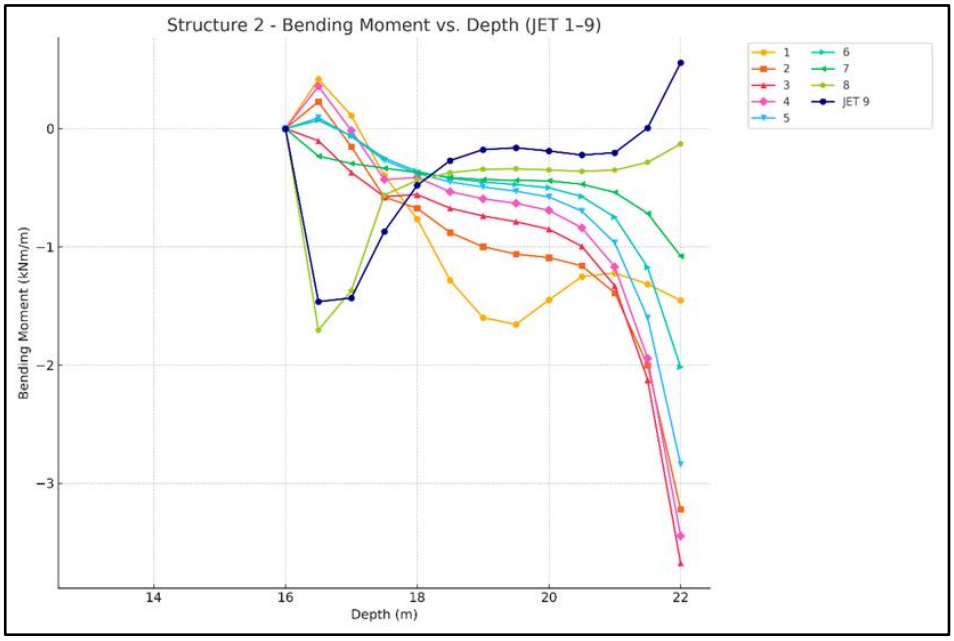

Figure 6. 43 Bending Moment Distribution of Jet Grout Columns Case Study 4- Structure 2

In vertical displacement analyses, it was observed that Structure 1, with closely spaced columns (0.75 m), exhibited generally higher and more pronounced vertical displacement values (Figure 6.44). Conversely, Structure 2, with wider column spacing (1.5 m), displayed reduced vertical displacements (Figure 6.45). Particularly noteworthy in Structure 1 are the differences observed in vertical displacements of edge and corner columns. This variation arises because edge and corner columns are supported by surrounding soil on only one side and lack the stabilizing confinement provided by adjacent columns. Central columns, benefiting from mutual interactions with surrounding columns, exhibited more uniform and lower displacement levels. These findings clearly demonstrate that the arrangement and spacing of columns significantly influence the group effect, directly affecting their vertical deformation performance.

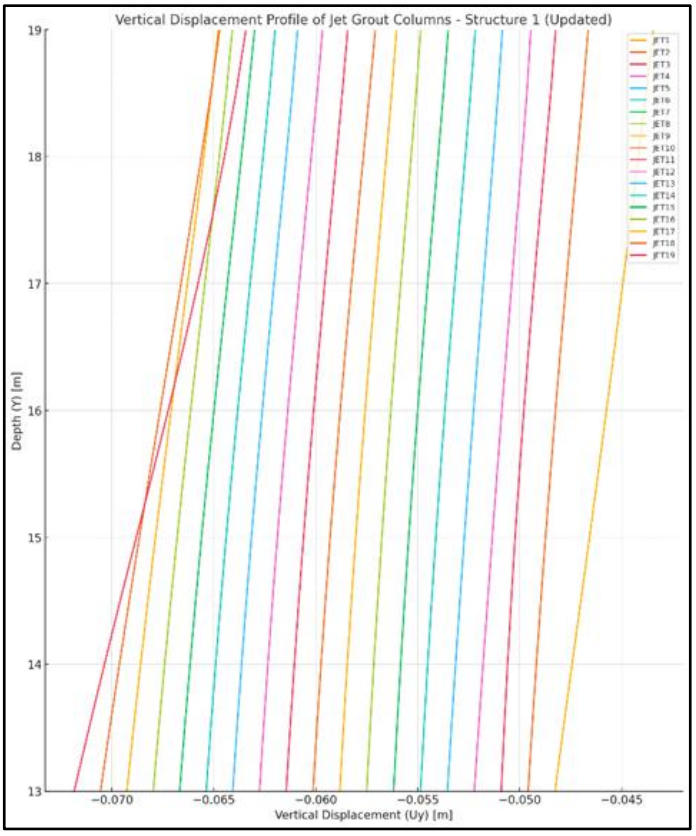

Figure 6.44 Vertical Displacement Profile of Jet Grout Columns Case Study 4-Structure 1

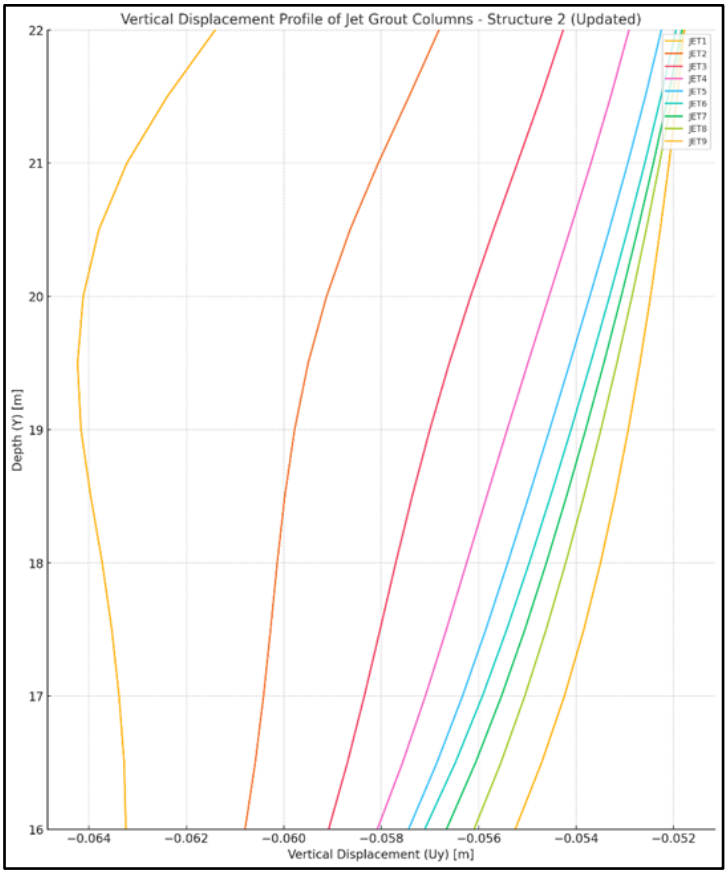

Figure 6. 45 Vertical Displacement Profile of Jet Grout Columns Case Study 4- Structure 2

In the horizontal displacement analyses conducted by comparing Phase 2 (Figure 7.49) and Phase 4 (Figure 6.46), the influence of diaphragm wall horizontal movements on the behavior of jet grout columns within the soil was examined. In Phase 2 (Figure 6.47), relatively low horizontal displacement values indicated a predominantly passive state, wherein columns effectively resist lateral soil pressures. However, in Phase 4 (Figure 6.48), the significant increase in horizontal displacements led to a transition from a passive to an active pressure condition, resulting in elevated horizontal total stresses, bending moments, and shear forces within the jet grout columns. This shift toward active conditions caused a critical redistribution of stresses at the soil-column interface, particularly at the column tips, thereby reducing column-soil interaction and

structural rigidity, and increasing the risk of deformation. Consequently, it was demonstrated that increased horizontal displacement of the diaphragm wall induces a clear shift from passive to active lateral earth pressure states, critically affecting jet grout column performance and emphasizing its importance in safe and optimal design practices.

In the horizontal displacement analyses conducted by comparing Phase 2 (Figure 7.49) and Phase 4 (Figure 7.50), the influence of diaphragm wall horizontal movements on the behavior of jet grout columns within the soil was examined. In Phase 2 (Figure 7.49), relatively low horizontal displacement values indicated a predominantly passive state, wherein columns effectively resist lateral soil pressures. However, in Phase 4 (Figure 7.50), the significant increase in horizontal displacements led to a transition from a passive to an active pressure condition, resulting in elevated horizontal total stresses, bending moments, and shear forces within the jet grout columns. This shift toward active conditions caused a critical redistribution of stresses at the soil-column interface, particularly at the column tips, thereby reducing column-soil interaction and structural rigidity, and increasing the risk of deformation. Consequently, it was demonstrated that increased horizontal displacement of the diaphragm wall induces a clear shift from passive to ctive lateral earth pressure states, critically affecting jet grout column performance and emphasizing its importance in safe and optimal design practices.

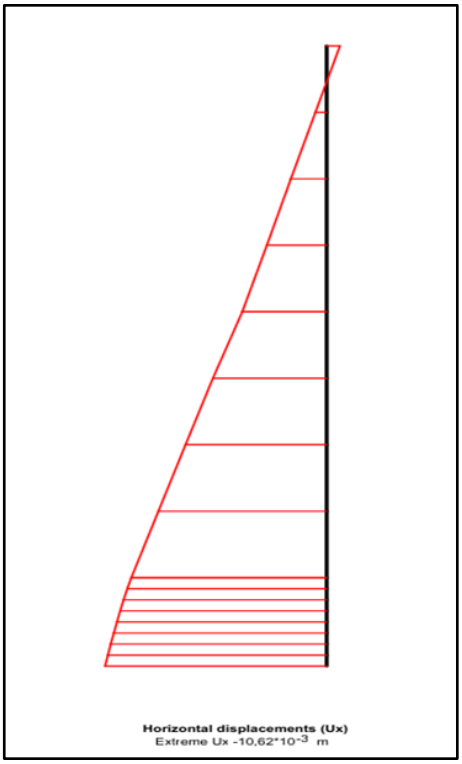

Figure 6.46 Horizontal Displacement of Diaphragm Wall at Case Study4 Phase 2

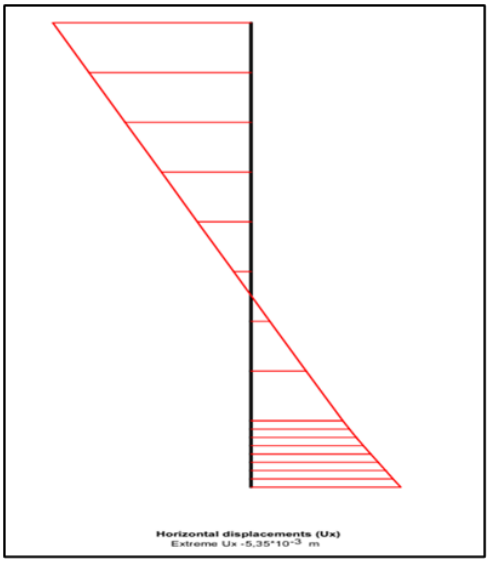

Figure 6.47 Horizontal Displacement of Diaphragm Wall at Case Study4 Phase 4

6.5 FINITE ELEMNT ANALYSIS OF CASE STUDY 5 IN PLAXIS

In Case Study 5, the analyses were repeated with the jet grout column spacing reversed compared to Case Study 4. All other model parameters remained unchanged; only the column spacing configurations were modified. Specifically, Structure 1 columns were placed at a spacing of 1.5 m, while Structure 2 columns were arranged at 0.75 m intervals. These findings clearly demonstrate that decreased spacing enhances group interactions and reduces the resistance capacity of columns, highlighting the importance of spacing arrangements in the optimization of structural and geotechnical designs. The geometrical configuration and model setup for this scenario are illustrated in Figure 6.48.

Before proceeding with the analyses, it should be noted that the positioning of the jet grout columns in Structure 1 starts from a depth of 19 m and ends at a depth of 13 m, whereas in Structure 2, the columns start at a depth of 22 m and terminate at a depth of 16 m. These column positions will be considered during the evaluation and interpretation of the analyses.

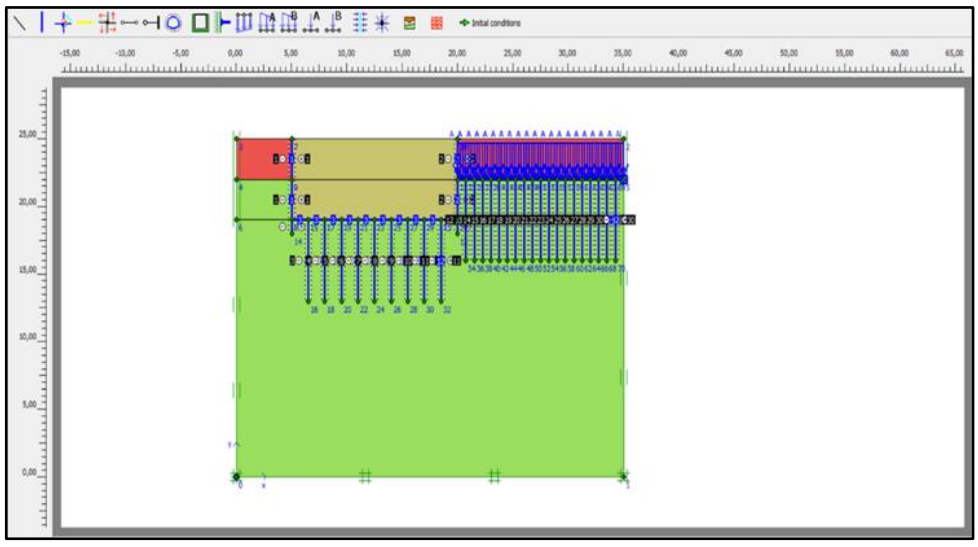

Figure 6.48 General View Of Finite Element Model Showing Geometry, Stratification, And Structural Components For Case Study 5 In PLAXIS

In Case Study 5, analyses performed for Structure 1 investigated the effects of arranging jet grout columns at a wider spacing of 1.5 meters. This arrangement resulted in generally lower and more homogeneous distributions of horizontal total stresses (Figure 6.49).

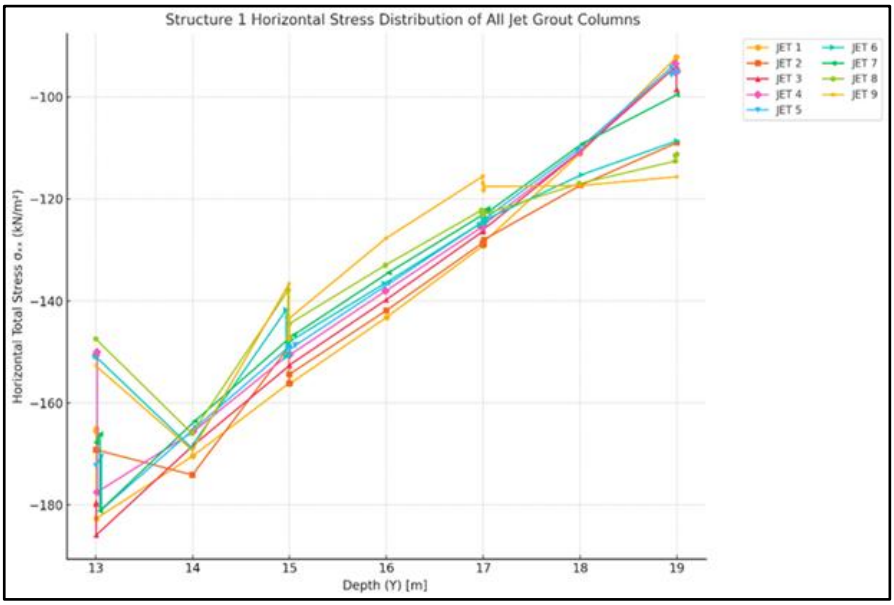

Figure 6.49 Horizontal Stress Distribution of Jet Grout Columns Case Study 5-Structure 1

Increasing the spacing between columns reduced group interaction effects, leading to more controlled stress concentrations. In terms of bending moment distributions, notable concentrations occurred particularly at the lower ends of the columns, but overall bending moment magnitudes remained lower compared to cases with narrower spacing (Figure 6.50).

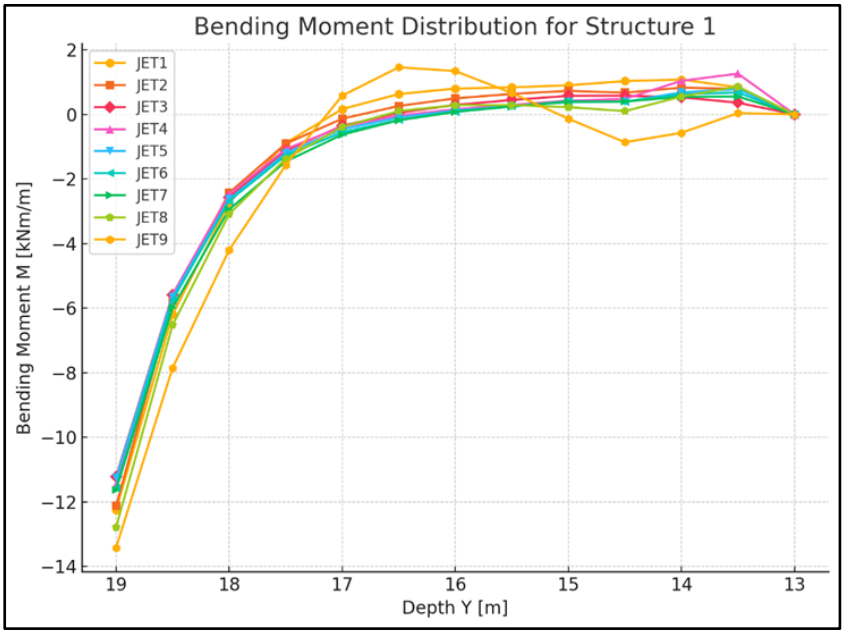

Figure 6.50 Bending Moment Distribution of Jet Grout Columns Case Study 5- Structure 1

Shear force analyses similarly showed a decreasing and more balanced shear force distribution along the column depth (Figure 6.51). Nevertheless, notably abnormal stress and force distributions appeared particularly in the edge and corner columns. These anomalies are attributed to the limited lateral support and rigidity conditions of edge columns, resulting in unilateral stress concentrations. Consequently, while wider column spacing positively impacts overall column performance by reducing group effects, careful consideration of stiffness and support conditions for edge columns remains essential in the design process.

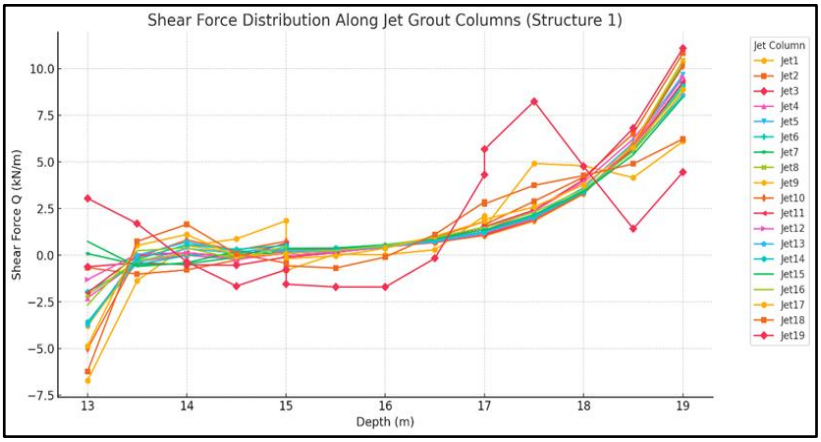

Figure 6.51 Shear Force Distribution of Jet Grout Columns Case Study 5- Structure 1

In the analyses conducted for Structure 2 within the scope of Case Study 5, evaluations were performed considering that the top region of the jet grout columns is located at a depth of 22 m, and the bottom tip region at 16 m. As a result of placing the columns at close intervals of 0.75 meters, noticeable increases and concentrations in horizontal total stress values were observed (Figure 6.52).

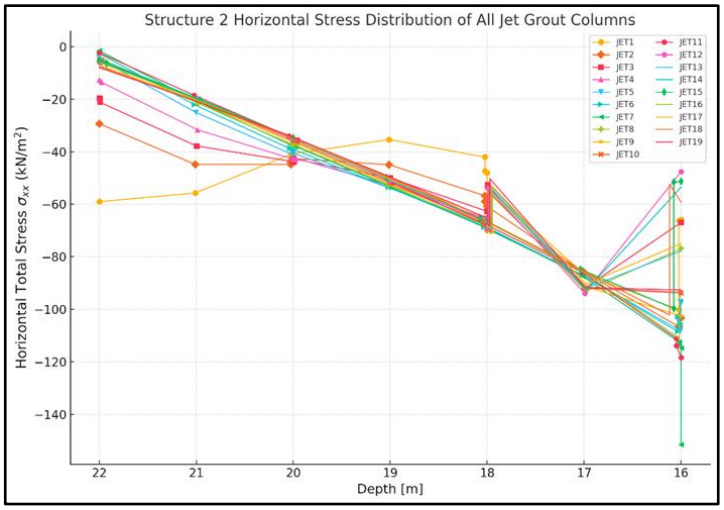

Figure 6. 52 Horizontal Stress Distribution of Jet Grout Columns Case Study 5 - Structure 2

Particularly towards the bottom tip region (at 16 m depth), significant rises and intensifications in stress values were evident. In the bending moment analysis, high moment values were clearly observed, especially towards the column tip regions (at around 16 m depth), demonstrating that the group effect arising from closely spaced columns brings structural capacities to critical levels (Figure 6.53).

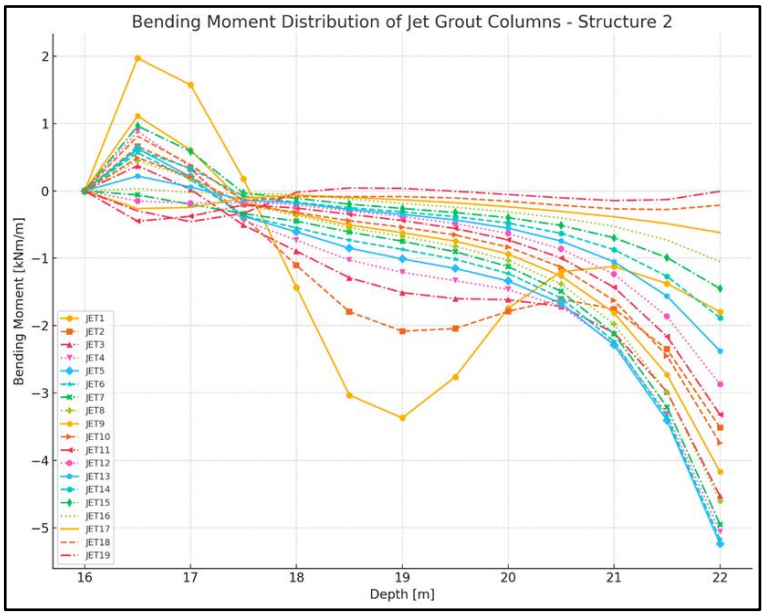

Figure 6.53 Bending Moment Distribution of Jet Grout Columns Case Study 5- Structure 2

Furthermore, shear force analyses revealed distinct increases in shear forces along the column depths (from 22 m down to 16 m), particularly resulting in high and irregular distributions near the bottom tip regions (Figure 6.54). These irregularities appeared notably pronounced in peripheral and corner columns due to their unilateral support conditions and rigidity constraints. These findings clearly emphasize the necessity of carefully determining column spacings during design and underscore the critical importance of group interactions in structural design, particularly when columns are positioned at close intervals.

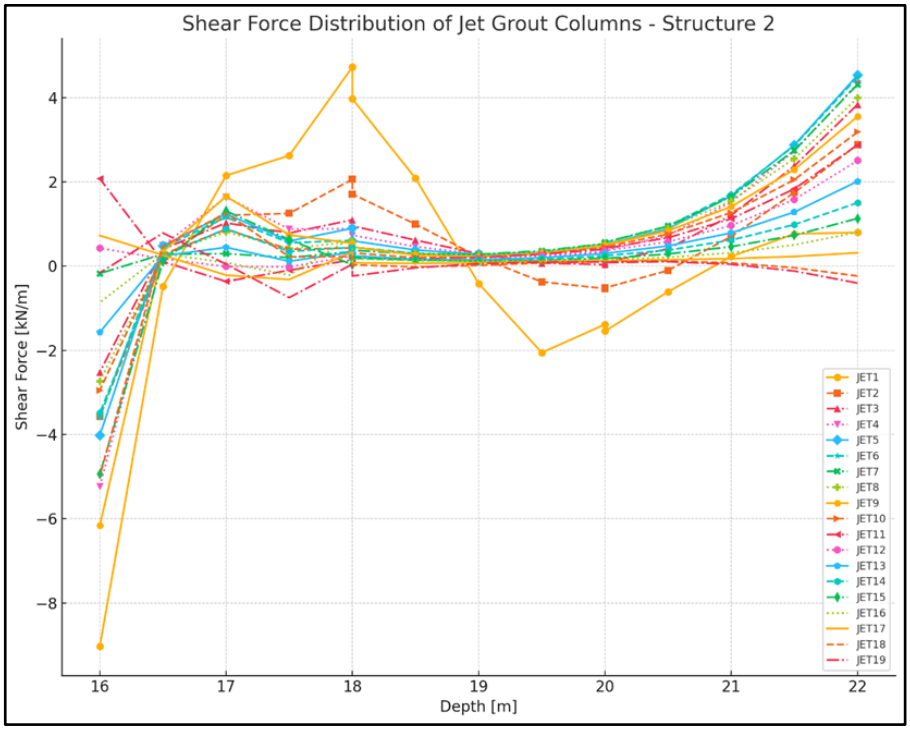

Figure 6.54 Shear Force Distribution of Jet Grout Columns Case Study 5-Structure 2

The comparative analysis results of Structure 1 and Structure 2 clearly demonstrate that the spacing of jet grout columns has significant effects on structural and geotechnical performance. In Structure 1, the column spacing of 1.5 meters reduced group interactions among columns, resulting in lower and more controlled values of horizontal total stress, bending moments, and shear forces (Horizontal Stress, Bending Moment, and Shear Force Figures - Structure 1). In contrast, the closer spacing of 0.75 meters in Structure 2 markedly increased group interactions, leading to higher, more intense, and irregular distributions of stress, bending moments, and shear forces. Particularly noticeable were the significant stress concentrations and bending moments observed near the lower tip regions of columns in Structure 2, critically approaching the structural capacities of the columns. Additionally, the distinctly higher shear force values in Structure 2 indicate that narrower column spacing substantially increases interactions between columns and the surrounding soil.

Irregular behaviors observed especially in peripheral and corner columns in Structure 2 clearly highlight the influence of lateral support conditions and stiffness constraints. Consequently, increasing the column spacing positively affects overall structural performance; however, when narrower spacings are employed, special precautions must be considered in designing peripheral and corner columns.

Settlement analyses of jet grout columns indicate significant differences between Structure 1 and Structure 2. For Structure 1, where columns extend from a depth of 19 meters at their top regions to 13 meters at their bottom tips, the wider column spacing of 1.5 meters resulted in relatively lower and uniform vertical displacement (settlement) values (Figure 6.55). In contrast, Structure 2, whose columns are positioned more closely at 0.75-meter intervals and extend from a depth of 22 meters at the top to 16 meters at their bottom tips, exhibited notably higher vertical displacement values due to increased column interaction. Specifically, significant and irregular displacement patterns were observed, particularly in the corner and peripheral columns, arising from unilateral support conditions and stiffness constraints (Figure 6.56). These findings emphasize that careful evaluation of soil-column interactions, particularly considering the specific top and bottom depth of columns, is critical when closely spaced columns are utilized, and highlight the need for specialized design measures, especially for peripheral regions.

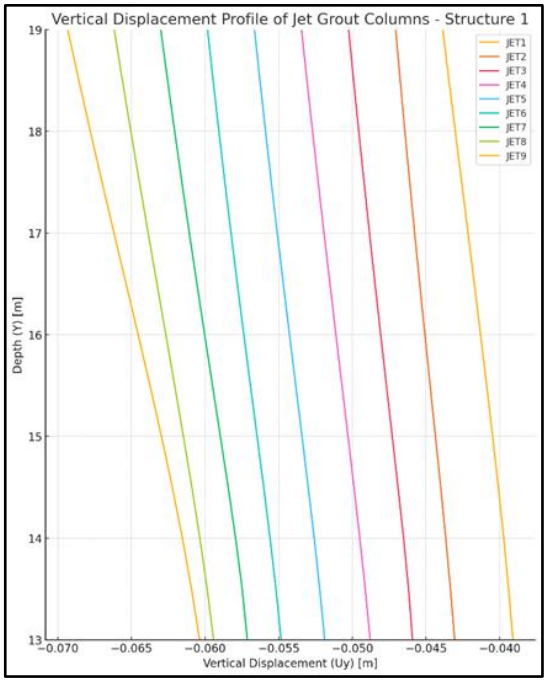

Figure 6.55 Structure 1 Vertical Displacement Profile of Jet Grout Columns Case Study 5 -Structure 1

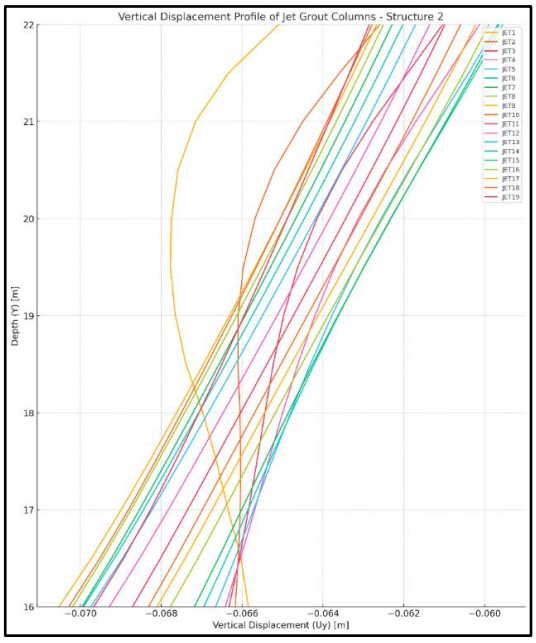

Figure 6.56 Vertical Displacement Profile of Jet Grout Columns Case Study 5- Structure 2

In the comparative evaluation of Phase 2 and Phase 4 for Case Study 5, significant differences were observed in horizontal displacements and their impacts on the jet grout columns. In Phase 2, characterized by excavation conditions and the absence of certain structural supports, horizontal displacements reached up to 4.78 mm, as illustrated in Figure Phase 2. This phase demonstrated initial passive earth pressures and moderate displacement values. In contrast, Phase 4, which involved additional excavation and activated structural elements, exhibited increased horizontal displacements, with maximum values rising notably to approximately 11.44 mm, as shown in Figure Phase 4. This transition from passive to active conditions markedly influenced the behavior of jet grout columns. The columns, initially stable and moderately stressed in Phase 2, experienced intensified bending moments, shear forces, and stress distributions under active earth pressure conditions in Phase 4. Particularly, the lower tip regions of the columns demonstrated elevated stress concentrations and critical bending moment values, underscoring the necessity for careful consideration of structural support arrangements and column spacing. This analysis emphasizes the critical impact of transitioning from passive to active conditions, significantly affecting the structural integrity and geotechnical performance of closely spaced jet grout column systems.

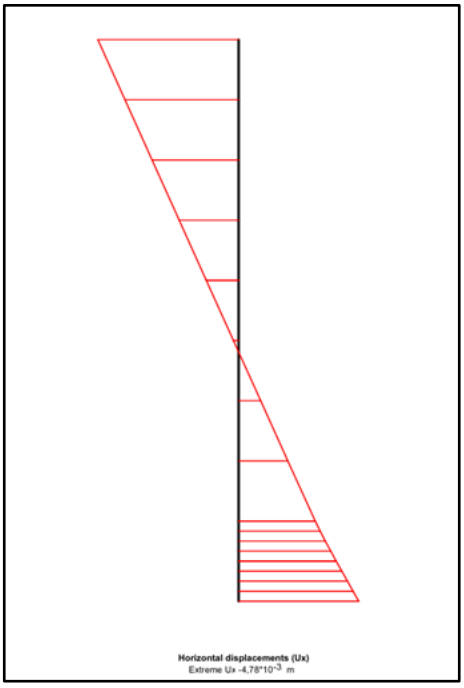

Figure 6.57 Horizontal Displacement of Diaphragm Wall at Case Study 5 Phase 4

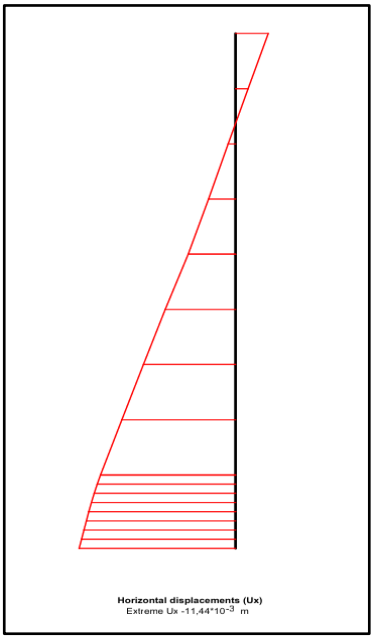

Figure 6.58 Horizontal Displacement of Diaphragm Wall at Case Study 5 Phase 4

CONCLUSION AND SUGGESTIONS

The main objective of this study is to investigate the effects of jet grout columns with varying spacings under group interaction conditions on lateral earth pressures, as well as the horizontal and vertical deformations of diaphragm walls, by employing numerical models based on geotechnical parameters obtained from the field, and to provide effective recommendations for structural design. In this context, numerical analyses were conducted for five different column spacing configurations using the PLAXIS 2D finite element software, and the impacts of reduced column spacing on stresses and deformations within diaphragm walls and columns were comprehensively evaluated. Based on the analysis results, significant insights regarding the behavior of column groups, soil-structure interactions, and design considerations are presented below. Five distinct case studies were examined within the scope of this research, where shear forces, bending moments, and vertical displacements of jet grout columns were analyzed in detail, with the detailed outcomes interpreted in Chapter 6. Additionally, vertical and horizontal displacements and horizontal stresses of diaphragm walls were evaluated, and comprehensive comparisons among case studies were conducted.

ANALYSIS RESULTS : JET GROUT COLUMNS UNDER GROUP EFFECT

The numerical analyses conducted in this study revealed that decreasing the spacing between columns significantly influenced the load-bearing capacities of the jet grout columns by increasing horizontal stresses, bending moments, and shear forces. Notable increases in both horizontal and vertical displacements were observed when column spacing was reduced, emphasizing the importance of interactions between columns. Furthermore, advanced-phase analyses (Phase 4) exhibited higher stresses and deformations compared to early-

phase analyses (Phase 2), clearly indicating the necessity of incorporating preventive measures for advanced stages into the design process.

Reducing column spacing resulted in enhanced horizontal load sharing, particularly among Structure 2 columns, leading to more regular and controlled horizontal displacements. Additionally, diaphragm wall horizontal stresses and horizontal displacement values remained controlled and low under tighter column arrangements, demonstrating that the columns effectively absorbed most of the loads, thus relieving and protecting the diaphragm wall.

However, narrower column spacing led to increased structural stress within the columns, notably higher bending moments and shear forces, necessitating enhanced structural strength in column design. Moreover, closer column spacing intensified vertical soil compaction and increased vertical displacement values, which raised critical considerations regarding soil stability.

In conclusion, the group effect of closely spaced jet grout columns positively contributes to the distribution and reduction of horizontal loads, thereby enhancing overall structural stability. Nonetheless, the increases in structural stresses within columns and vertical soil deformations must be carefully considered when determining optimal design parameters. The findings obtained from this study provide essential recommendations for effective jet grout column design in engineering applications.

EFFECTS OF JET GROUT COLUMN GROUP INTERACTION ON LATERAL EARTH PRESSURE ACTING ON THE DIAPHRAGM WALL

In order to evaluate the lateral earth pressure acting on diaphragm walls, numerical models were developed to assess the behavior of jet grout columns under group effects across five different column spacing configurations (case studies). In Phase 2 of the models, only Structure 1 was activated, while in Phase 4, both Structure 1 and Structure 2 were included. This enabled a comparative

analysis of the group effect on diaphragm wall stresses and deformations between early and advanced construction stages.

The numerical analyses clearly revealed the significant influence of jet grout column group effects on both lateral earth pressure and deformation behavior of diaphragm walls. In all case studies, the lateral earth pressures acting on the diaphragm wall significantly decreased from approximately 150–180 kN/m² in Phase 2 to as low as 0.003 kN/m² in Phase 4. This dramatic reduction indicates that, in densely spaced group configurations, the jet grout columns effectively absorbed the lateral loads, preventing them from being transferred to the diaphragm wall. In other words, the increased group effect between columns redistributed the stresses within the shared interaction zones of the soil, alleviating the pressure on the wall. These results are presented in the table below.

Phase-to-phase variation of horizontal stress acting on the diaphragm wall

Case	Phase 2 (kN/m²)	Phase 4 (kN/m²)
Case Study 1	-156.45	-0.00296
Case Study 2	-184.33	-0.00314
Case Study 3	-131.38	-0.00306
Case Study 4	-161.67	-0.00315
Case Study 5	-134.98	-0.00303

A same trend was noted in horizontal displacements. In scenarios with reduced column spacing, particularly in Case Study 4, the wall demonstrated a net alteration of -0.01597 mm between Phase 2 and Phase 4 (from +0.00535 mm to -0.01062 mm), indicating a directional reversal. The phase-wise displacement values for all examples are consolidated in the table below . In Phase 2, the wall receded from the backfill (active state), whereas in Phase 4, it advanced toward the backfill (mobilizing passive resistance). This directional shift signifies enhanced group effects, leading to increased confinement and lateral resistance. Horizontal displacement of the diaphragm wall between Phase 2 and Phase 4

Case Study	Phase 2 (m)	Phase 4 (m)	Difference (m)
Case Study 1	-0.00492	-0.01031	-0.00539
Case Study 2	-0.00496	-0.01062	-0.00566
Case Study 3	-0.00475	-0.01078	-0.00603
Case Study 4	0.00535	-0.01062	-0.01597
Case Study 5	-0.00478	-0.01144	-0.00666

Significant changes were also recorded in vertical displacements. For instance, in Case 5, the vertical displacement increased by 75.65 mm between Phase 2 and Phase 4. This substantial increase shows that closely spaced columns caused a more intense vertical compression in the soil, leading to higher settlement. The columns, working collectively due to group interaction, not only affected lateral load sharing but also played a crucial role in vertical stress transfer. Therefore, vertical deformation becomes a critical aspect in evaluating soil stability under such configurations. These findings are detailed in the table below.

Vertical displacement of the diaphragm wall between Phase 2 and Phase 4

Case Study	Phase 2 (mm)	Phase 4 (mm)	Difference (mm)
Case Study 1	0,00267	-0,06798	70,65
Case Study 2	-0,0002795	-0,07089	70,6105
Case Study 3	0,00311	-0,07025	73,36
Case Study 4	-0,00356	-0,07316	69,6
Case Study 5	0,00315	-0,0725	75,65

In this study, short column spacing was observed to amplify group effects, increase vertical deformation and settlements, disrupt the lateral earth-pressure distribution, and drive internal forces in the columns particularly at the toe and corner regions to critical levels; to mitigate these effects, designs should avoid excessive group action by providing adequate spacing and by increasing column diameter and embedment length (jet grout length). In addition, increasing the column-soil stiffness ratio and optimizing the ground-improvement mix design help balance load sharing and reduce

settlements. Finally, the excavation/fill construction sequence and staging should be planned to prevent the uncontrolled mobilization of passive resistance; taken together, these measures enable safer and more efficient solutions.

RECOMMENDATIONS FOR FUTURE STUDIES

Future studies should focus on several critical technical aspects to deepen the understanding and enhance practical implementation of jet grout column technologies. Comprehensive analyses considering diverse soil conditions and soil-structure interaction behaviors under varying groundwater conditions would provide valuable insights. Further investigation into dynamic loading conditions, including seismic responses of jet grout column groups, would greatly contribute to safer and more resilient designs. Additionally, research into the long-term durability and performance of jet grout columns, supported by field monitoring and experimental validations of numerical models, would strengthen the reliability of simulation tools used in design processes. Detailed cost-benefit analyses assessing economic viability under different scenarios and investigating innovative materials or additives to enhance column strength and durability are also recommended. Lastly, systematic studies into environmentally sustainable construction methods and comprehensive lifecycle assessments will significantly advance the sustainability and ecological footprint of jet grout column applications.

REFERENCES

Adams, J.I. (1972). Soil Nailing Practice in Europe.

Akagi, Y., Terashi, M., & Fukue, M. (1994). Jet Grouting Method and Design Considerations. Japanese Geotechnical Society.

Altun, S. (2018). Jet Grout Kolonlarinin Geoteknik Performansinin Arazi Deneyleri ile İncelenmesi. Yayınlanmamış Yüksek Lisans Tezi, Yildiz Teknik Üniversitesi.

Amano, K., & Shibata, T. (1988). "Field Tests on Layered Jet Grouting." Soil and Foundation Journal, 28(1), 81–90.

Andavan, S., & Kumar, B. M. (2020). Case study on soil stabilization by using bitumen emulsions – A review. Materials Today: Proceedings, 22, 1200-1202.

Andersland, O. B., & Ladanyi, B. (2004). Frozen ground engineering (2nd ed.)

Ayan, E. (2016). Zayif Zeminlerin Taş Kolonlarla İyileştirilmesi, Yayınlanmamış Yüksek Lisans Tezi, Dokuz Eylül Üniversitesi.

Ayesteh, H. & Sabermahani, M. (2019). Field study on performance of jet grouting in low water content clay. Engineering Geology, 264, 105314

Azat, E. (2019). Zeminlerde Taş Kolon Uygulamalari ve Performans Analizi, Yüksek Lisans Tezi, Karadeniz Teknik Üniversitesi.

Babu, G. L. S. (2004). Ground Improvement Techniques.

Bauer Maschinen GmbH. (2017). Jet Grouting (HDI) – Technical Brochure

Bell, F. (1993). Engineering treatment of soils. CRC Press.

Bell, F. G. (1996). Lime stabilization of clay minerals and soils. Engineering Geology, 42(4), 223-237

Bello, M. A. (1995). Grout Control for Jet Columns. DFI Technical Report No. 56.

Bergado, D. T., Anderson, L. R., Miura, N., & Balasubramaniam, A. S. (1991). Soft ground improvement via vertical drains and preloading. Journal of Geotechnical Engineering, 117(10), 1504–1533.

Bo, M. W. (2011). Vertical drains. CRC Press.

Bogati, K. (2019). Ground Improvement by Jet Grouting Techniques, Bachelor's thesis, Hämeenlinna University of Applied Sciences.

Brown, D. A., Reese, L. C., & O'Neill, M. W. (1988). Cyclic lateral loading of a large-scale pile group. *Journal of Geotechnical Engineering, 114*(11), 1261–1276.

Bruce, D. A. (2005). The Basics of Deep Mixing Methods as Used in Geotechnical

Bruce, D. A., & Sterling, R. L. (2002). Grouting techniques for soil improvement. Proceedings of Geo-Tech Conferences, 147–156.

Bruce, D. A., Gallavresi, F., & Bruce, M. E. C. (2013). "State of Practice Review of Micropile Design and Construction." DFI Journal, 7(2), 92–121.

Bruce, D.A. (2005). The Practical Use of Jet Grouting in North America. Grouting and Ground Treatment, ASCE.

Bruce, D.A., Gallavresi, M., & Siedel, J.P. (1987). The Development of Jet Grouting: A Historical Review. Grouting in Geotechnical Engineering.

Bulgaria Engineering. (n.d.). *Jet grouting technology*. Bulgaria Engineering. https://bulgaria-engineering.com/tehnologiya_jet_grouting

Carvajal, E., Vukotic, G., Sagaseta, C., & Wehr, W. (2013). Column supported embankments for transportation infrastructures: Influence of column stiffness, consolidation effects and cyclic loading. In Proc. 18th Int. Conf. on Soil Mech. and Geotech. Eng.

Ceylan, G. (2020). Design and Performance of Stone Columns in Soft Soils, Yayınlanmamış Yüksek Lisans Tezi, Yildiz Teknik Üniversitesi.

Choi, Y. (2005). Jet Grouting Methods and Applications in Soft Ground Improvement. Non- Unpublished Master's Thesis.

Chu, J., Yan, S. W., & Yang, H. (2000). Soil improvement by the vacuum preloading method for an oil storage station. Geotechnique, 50(6), 625-632.

Chun, B. S., Choi, J. K., Joung, Y. K., Yeoh, Y. H., "A Case on the Plan for Settlement Restraint by Compaction Grouting System", 12th Asian Regional Conf. On Soil Mechanics & Geotechnical Engineering, Volume 1, p:469-472.

Chung, M. Y., & Carson, J. L. (2002). Ground freezing and its application in tunnel construction. Tunnelling and Underground Space Technology, 17(3), 289–294.

CIRIA, 2000. "Grouting for grouting engineering". CRIRIA press, U. K., ISBN 0 86017 514 6. pp: 17-22

Cinar, M. (2023). Investigation of Mechanical and Physical Features of Cementitious Jet Grout Applications for Various Soil Types. Buildings, 13(11), 2833.

Cinar, M. (2023). Investigation of mechanical and physical features of cementitious jet grout applications for various soil types. Buildings, 13(11), 2833

Clough, G. W., & Kramer, S. L. (2006). Soil Improvement Techniques and Applications in Civil Engineering. ASCE Press.

Cokca, E. (2001). Use of Class C fly ashes for the stabilization of an expansive soil. Journal of Geotechnical and Geoenvironmental Engineering, 127(7), 568-573.

Converse, J.D. & Labarre, P.C. (1932). “Capacity of Pile Groups.” Transactions ASCE.

Croce, P., Flora, A., & Modoni, G. (2014). Jet grouting: Technology, design and control. CRC Press (Ground Improvement Series)

Croft, J. B. (1967). The influence of soil mineralogical composition on cement stabilization. Géotechnique, 17(2), 119-135.

De la Guardia, F., Stoehr, B., & Schaeuber, P. (2019). Vibro-replacement for challenging soil conditions in port structures – Recent cases from the Caribbean area. Keller Group.

De Mello, V. F. B., & Fernandes, R. B. (2007). “Ground Improvement by Jet Grouting.” Soils and Rocks, 30(3), 205–214.

Ehsanzadeh, B., & Ahangari, K. (2014). A novel approach in estimation of the soilcrete column’s diameter and optimization of the high pressure jet grouting using adaptive neuro fuzzy inference system (ANFIS). Open Journal of Geology, 4(8), 386-398.

Elkamash, I. M. (2016). Micropile Foundations for Infrastructure Projects.

Erkan, İ., & Tan, Ö. (2016). Jet Grout Uygulamalarinda Karakteristik Parametrelerin Etkinliği. Zemin Mekaniği ve Geoteknik Mühendisliği 17. Ulusal Kongresi Bildirileri.

Estabragh, A. R., Bordbar, A. T., & Javadi, A. A. (2015). Improvement of clay soil by electro-osmosis technique. Applied Clay Science, 116–117, 14–22.

Feizi, S., Nilsen, E., Tsegaye, A. B., & Karlsrud, K. (2024). Effects of jet grouting on adjacent ground through numerical modelling. *Proceedings of the Institution of Civil Engineers: Ground Improvement, 177*(5), 357–369.

Fontanella, E., Callisto, L., Desideri, A., Sciotti, A., & Ottaviani, C. (2011, May). An interpretation of jet grouting effects on the retaining structures of a deep excavation and on adjacent buildings. In *Proceedings of Conference "Geotechnical Aspects of Underground Construction in Soft Ground",* 941-948.

Galindo-Güerros, J. C., Niederleithinger, E., Mackens, S., & Fechner, T. (2015). Quality assurance of jet grout columns with borehole seismic measurements. NDT in Civil Engineering, Proc. Int. Symp. Non-Destructive Testing in Civil Eng.,

Gallavresi, F. (1992). "Grouting Improvement of Weak Soils." Grouting in Geotechnics, ASCE Geotechnical Special Publication No. 30.

Gan, Q., Liu, Z., Cui, C., & Liu, H. (2022). Interfacial resistance model for electro-osmotic system. Géotechnique, 72(6), 506–519.

Geotextiles in Embankment Dams (April, 2008) "Status Report on the Use of Geotextiles in Embankment Dam Construction and Rehabilitation Federal Emergency Management Agency

GTM Geo. (n.d.). *Geogridler*. GTM Geo. https://www.gtmgeo.com/tr/urunler/geogridler

Gurpersaud, N., Bruce, J., & Montgomery, M. (2013). An extensive jet grout test program for a low permeability barrier. Canadian Geotechnical Society Geo-Ottawa Conference Paper

Güler, E. & Secilen, G. G. (2021). Jet grouting technique and strength properties of jet grout columns. Journal of Physics: Conference Series, 1928(1):012006

Güler, M., & Seçilen, A. (2021). Jet Grout Yönteminde Kolon Performansini Etkileyen Parametreler. Geoteknik Dergisi, 26(2), 145–160.

Han, J. (2006). Principles and Practice of Ground Improvement. John Wiley & Sons.

Hansbo, S. (1987). Design aspects of vertical drains. Ground Engineering, 20(2), 16–25.

Hird, C. C., Pyrah, I. C., & Russell, D. (1992). Finite element analysis of vertically drained embankments. Geotechnique, 42(1), 109–125.

Holtz, R. D., Christopher, B. R., & Berg, R. R. (2008). Geosynthetic Design and Construction Guidelines. FHWA NHI-07-092, Federal Highway Administration.

Ichihashi, T., Konishi, K., & Okada, M. (1992). Development of High Energy Jet Grouting Method and its Applications. Grouting in Geotechnical Engineering, ASCE, 1, 24–38.

Indraratna, B., Balasubramaniam, A. S., & Khan, M. D. H. (1994). Performance of embankments constructed on soft marine clay with and without vertical drains. Ground Improvement, 1(1), 3–16.

Indraratna, B., Rujikiatkamjorn, C., & Sathananthan, I. (2005). Analytical and numerical solutions for a vertical drain improved by vacuum and surcharge loading. International Journal of Geomechanics, 5(2), 114–124.

Ismail, A. (2002). Performance of Jet Grouted Columns in Sand and Clay. PhD Thesis, University of Oxford.

Jaky, J. (1944). "The coefficient of earth pressure at rest." Journal of the Society of Hungarian Architects and Engineers, 355–358

Jessberger, H. L. (1988). Artificial ground freezing in geotechnical engineering. Geotechnique, 38(2), 123–135.

Jiang, H., Zhang, H., Zhang, Q., & Xu, C. (2021). Mechanical properties and microstructure of cemented soils improved by jet grouting. *KSCE Journal of Civil Engineering, 25*, 4005–4017.

John Wiley & Sons. Applications. FHWA-RD-03-085, U.S. Department of Transportation.

Jones, M. (2010). Application of ground freezing in shaft and tunnel construction. Non- Unpublished Master's, University of Cambridge.

Juran, I. et al. (1999). Micropiles and Anchors in Engineering Practice.

Karadeniz, D. (2014). Jet Grout Kolonlarinin Dayanim Parametrelerinin Deneysel Olarak Belirlenmesi.Yayınlanmamış Doktora Tezi, İstanbul Teknik Üniversitesi.

Karahan, M. (2015). Jet Grout Kolonlarinin Mekanik Özelliklerinin Sayisal Yöntemlerle Belirlenmesi. Yayınlanmamış Yüksek Lisans Tezi, Gazi Üniversitesi.

Karol, R. H. (2003). Chemical Grouting and Soil Stabilization. 3rd Ed., CRC Press.

Kiersnowska, M., Nowak, R., & Rogowski, M. (2023). Application of geosynthetic drainage systems in transport infrastructure. Sustainability, 15(4), 3771.

Kimpritis, T. (2013). The control of column diameter and strength in jet grouting processes and the influence of ground conditions. Non- Unpublished Master's Thesis.

Kirsch, K., & Bell, A. (Eds.). (2012). Ground improvement. CRC Press.

Kirsch, K., & Kirsch, F. (2017). Ground improvement by deep vibratory methods (p. 252). Taylor & Francis.

Koerner, R. M. (2012). Designing with Geosynthetics (6th ed.). Xlibris Corporation.

Kramer, S. L. (1996). Geotechnical earthquake engineering, Prentice Hall Upper Saddle River. New Jersey, 07458.

Martin, L., Alizadeh, V., & Meegoda, J. (2019). Electro-osmosis treatment techniques and their effect on dewatering of soils, sediments, and sludge: A review. Soils and Foundations, 59(2), (407-418.)

Menard, L., & Broise, Y. (1975). Theoretical and practical aspect of dynamic consolidation. Geotechnique, 25(1), 3-18.

Mesri, G., Ajlouni, M. A., & Feng, T. W. (1997). Settlement of embankments on soft clay. Journal of Geotechnical and Geoenvironmental Engineering, 123(4), 370–378.

Mitchell, J. K., & Soga, K. (2005). Fundamentals of soil behavior (3rd ed.). Wiley.

Mori, S., Terashi, M., & Tanaka, H. (1981). Field Applications and Quality Control of Jet Grouting. Proceedings of the International Conference on Soil Improvement.

Mostafa, M. A. (2010). Numerical modeling of dynamic compaction in cohesive soils. [Master's thesis, University of Akron]. OhioLINK Electronic Theses and Dissertations Center.

Müller, W. W., & Saathoff, F. (2015). Drainage capabilities of geocomposites in landfill base liners. Geotextiles and Geomembranes, 43(1), 1–13.

Nakanishi, T. (1968). Chemical Churning Pile Method. Japanese Patent No. 431244.

Özdemir, A., & Mehmet , Ö. (2006). Zeminlerin İyileştirilmesi ve Son Yillarda. Sondaj Dünyasi Dergisi, 34-38

PORR. (n.d.). *Bored piles*. PORR Group. https://porr.de/en/wiki-special-civil-engineering/bored-piles/

Prasetya, H. et al. (2025). Soil Nailing Performance for Urban Excavation. IOP Conf. Series: Earth and Environmental Science, 1462.

Qian, X., Sun, Y., Zhang, R., Xu, C., & Chen, Y. (2022). Experimental investigation and field application of high-efficiency multi-fluid jet grouting. Advances in Civil Engineering, Article ID 8829397, 1–15.

Rabaiotti, C., Muir Wood, D., & Standing, J. R. (2015). The response of jet grouted soil to excavation. *Proceedings of the Institution of Civil Engineers – Geotechnical Engineering, 168*(4), 335–347.

Rahmani, I., & Ahangari, K. (2010). Effects of grouting parameters on jet grout column diameter. Geotechnical and Geological Engineering, 28(5), 565–572.

Randolph, M., & Hope, S. (2004). Effect of cone velocity on cone resistance and excess pore pressures. In Effect of cone velocity on cone resistance and excess pore pressures, 147-152, Yodogawa Kogisha Co. Ltd.

Rollins, K. M., Gerber, T. M., & Lane, J. D. (1998). Lateral resistance of a full-scale pile group in clay. *Journal of Geotechnical and Geoenvironmental Engineering, 124*(6), 468–478.

Rollins, K.M., et al. (2006). “Measured and Computed Lateral Response of a Pile Group in Sand.” Journal of Geotechnical and Geoenvironmental Engineering.

Saglamer, A., Duzceker, Y., Gokalp, M. A., & Yilmaz, E. (2002). Testing and evaluation of jet grout columns for power plant foundations. In Proc. 15th Intl. Conf. Soil Mechanics & Geotech. Eng. (ISSMGE), 1839–1842

Sağlamer, A., 2006, Zemin iyileştirme yöntemleri, Karadeniz Teknik Üniversitesi.

Saito, Y., & Yonekura, R. (2011). Development of the X-Jet Grouting Method. Proceedings of the International Symposium on Ground Improvement.

Sanger, F. J., & Sayles, F. H. (1979). Thermal and mechanical properties of frozen soils: A review. Cold Regions Science and Technology, 1(2), 201–219.

Schneider, N. (2019). New aspects of quality control for jet grouting. Proc. XVII Europ. Conf. Soil Mechanics Geotech. Eng. (ECSMGE), Reykjavik, 2, 50–55

Schorr, C.-P., Traegner, R., & Micciche, R. J. (2007). Evaluating in-situ jet grout column diameters utilizing wave analysis. Geo-Denver 2007, ASCE Geotechnical Special Publication 166,113–122

Shen, S. L., & Wang, C. Y. (2013). Analysis of jet grouting column based on cavity expansion theory. Geotechnical Engineering Journal of the SEAGS & AGSSEA, 44(3), 52–59.

Shukla, S. K. (2016). Handbook of Geosynthetic Engineering (2nd ed.). ICE Publishing.

Śpitalniak, A., Nowocień, T., & Chodakowska, E. (2019). Use of geocomposites in waste landfills—A review. Environmental Protection and Natural Resources, 30(3), 17–24. Stabilisation of Soils for Foundations of Structures. Dept. of Civil Engineering University of California

Stark, T. D., Axtell, P. J., Lewis, J. R., & Dillon, J. C. (2009). Soil inclusions in jet grout columns. DFI Journal, 3(1), 50–61.

Sugiarti, S. (2004). Japan International Cooperation Agency (JICA).

Şengezer, L. (2010). Granüler zeminlerde dinamik kompaksiyon uygulamasi, YayınlanmamışYüksek Lisans Tezi.

Tan, T.S., Ng, X.C., & Sun, D.A. (2014). “Settlement improvement of soft clay by sand and stone columns.” Computers and Geotechnics.

Tao, Y., Liu, Z., Wang, W., & Zhang, F. (2022). Study on the electro-osmosis-combined-preloading method in strengthening reclaimed sludge from the macroscopic and microscopic views. Journal of Marine Science and Engineering, 10(5), 646.

Taube.G & Martin, P.E., P.G.2002, Stone Columns for Industrial Fills, Nicholson Construction Company, Cuddy.

Terashi, M. (2003). “The State of Practice in Jet Grouting.” Proceedings of the 3rd International Conference on Grouting and Ground Treatment, ASCE, 25–46.

Trevi Group. (n.d.). *Micropiles*. Trevi Group. https://www.trevispa.com/en/Technologies/micropiles

Türkiye Bina Deprem Yönetmeliğinden (TBDY-2018)

V.N.S. Murthy, Principles and Practices of Soil Mechanics and Foundation Engineering

Vyalov, S. S. (1986). Rheological fundamentals of soil mechanics. Elsevier.

Wang, H., Liu, Q., & Zhang, L. (2019). Behavior of frozen clayey soil under artificial ground freezing. Cold Regions Science and Technology, 157, 34–41.

Wang, J., Chu, J., & Yan, S. W. (2016). Experimental study on the improvement of marine clay slurry by electroosmosis–vacuum preloading. Geotextiles and Geomembranes, 44(4), 615–622.

Warner, J. (2004). Practical Handbook of Grouting. Wiley.

Warner, J., Brown, D., & Masters, D. (2007). Practical Guide to Grouting of Structures. Thomas Telford.

Wong, I. H., & Poh, T. Y. (2000). Interface shear strength of cement-treated soil. *Journal of Geotechnical and Geoenvironmental Engineering, 126*(3), 247–256. https://doi.org/10.1061/(ASCE)1090-0241(2000)126:3(247)

Yahiro, K., & Yoshida, S. (1973). Development of High Pressure Jet Grouting Method. Journal of Civil Engineering

Yao, X., Zhang, Y., Li, J., & Chen, H. (2024). Experimental study on mechanical behavior of jet grouted soil under different curing conditions. *Buildings, 14*(11), 3587.

Yee, K., & Aun, O. T. (2010). Ground Improvement—a green technology towards a sustainable housing, infrastructure and utilities developments in Malaysia. Geotechnical Engineering, 41(1), 123.

Yildiz, M. C. (2015). İstinat Duvarina Etkiyen Dinamik Toprak Basinçlari.

Yilmaz, O. (2016). Jet Grout Yöntemi ile Oluşturulan Kolonlarda Karişim Oraninin Performansa Etkisi. Yayınlanmamış Yüksek Lisans Tezi, Dokuz Eylül Üniversitesi.

CURRICULUM VITAE